Electropositive Metal N-heterocyclic Carbene Complexes

Ian J. Casely

This thesis is submitted for the degree of

Doctor of Philosophy

at the

University of Edinburgh

March 2009

Declaration

Except where specific reference has been made to other sources, the work presented in this thesis is the original work of the author. It has not been submitted, in whole or in part, for any other degree.

Ian J. Casely

March 2009

Abstract

The first chapter is an introduction to the f-elements, with a focus on the synthesis and chemistry of tetravalent cerium complexes. The synthesis, characterisation and reactivity of carbenes, particularly N-heterocyclic carbenes (NHCs), and anionic-functionalised NHC ligands is discussed. The synthesis and reactivity of s-block, Group three and f-block NHC complexes is reviewed.

The synthesis of the alcohol-functionalised unsaturated imidazolium proligand, $[H_2L]I$ [H_2L = $HOCMe_2CH_2(1\text{-}CH\{NCHCHN^iPr\})$], is extended to saturated imidazolinium analogues, $[H_2L^R]X$, $[HOCMe_2CH_2(1\text{-}CH\{NCH_2CH_2NR\})]X$ (R = ^{i}Pr, abbreviated to P; R = Mes, abbreviated to M; R = Dipp, abbreviated to D, X = Cl, I). Mono-deprotonation results in the isolation of bicyclic imidazolidines HL^R, which can be ring-opened and silylated by treatment with Me_3SiI, to afford $[HL^{R,\ OSiMe_3}]I$, R = ^{i}Pr and Mes. Further deprotonation of HL^R with $MN"_2$ (M = Mg, Zn; N" = $N(SiMe_3)_2$) affords $L^RMN"$ (M = Mg and Zn) and ZnL^R_2. These complexes proved active for the polymerisation of *rac*-lactide at room temperature without the need for an initiator.

The third chapter focuses on cerium chemistry. Repetition of the literature synthesis of Ce^{IV} *tert*-butoxide compounds affords the unsolvated $Ce(O^tBu)_4$ and also the cluster $Ce_3(O^tBu)_{11}$. Treatment of $Ce(O^tBu)_4$ with HL did not yield a Ce^{IV}-NHC complex, but one bearing a tethered imidazolium group, $(O^tBu)_3Ce(\mu\text{-}O^tBu)_2(\mu\text{-}HL)Ce(O^tBu)_3$. The synthesis of a Ce^{III}-NHC complex, CeL_3, and the oxidation of this forms an unprecedented Ce^{IV}-NHC complex, CeL_4, *via* ligand redistribution; the complex contains two bidentate ligands and two alkoxide-tethered free NHC groups. Functionalisation of the free NHCs with boranes affords the adducts $Ce(L)_2(L\text{-}B)_2$, where B = BH_3 or 9-BBN (9-Borabicyclo[3.3.1]nonane). A number of cerium complexes of the saturated-backbone NHC, L^R, $L^RCeN"_2$ and $L^R_2CeN"$, have been synthesised and their oxidation chemistry and reactivity investigated.

The final chapter contains an NMR study of the synthesis of a series of yttrium L^R adducts, $L^P_xYN''_{(3-x)}$ (x = 1, 2 or 3), and of the synthesis of uranium complexes $L^RUN''_2$, R = Mes or Dipp, including a range of small molecule reaction chemistry. The uranyl NHC complexes, $UO_2L^R_2$, R = Mes or Dipp, have also been synthesised and characterised; these possess very high frequency carbene carbon chemical shifts.

Acknowledgements

I would like to thank my supervisor Dr. Polly Arnold for her guidance and boundless enthusiasm over the last three and a half years. My thanks also go to our group postdocs, Dr. Steve Liddle for his invaluable input in the early days at Nottingham, and Dr. Chris Carmichael and Dr. Sergey Zlatogorsky at Edinburgh.

The group, both past and present, deserve thanks for making my time with them such an enjoyable one, as well as the friends I have made along the way at Nottingham and Edinburgh. Also to J.C. for providing numerous excuses to sample Scottish culture.

I would like to acknowledge the help of everyone who has assisted me in my work, particularly with X-ray crystallography, NMR and elemental analysis.

My thanks also go to my family, for their constant support and encouragement throughout my PhD and beyond.

Finally, to Katy, whom I cannot imagine life without. Our big day will be here before we know it. This is just the beginning…

Abbreviations

Ln	lanthanide
NHC	N-heterocyclic carbene
CAN	ceric ammonium nitrate
COT	cyclooctatetraene
N"	hexamethyldisilyl amide
N"'	*tris*(trimethylsilyl) amide
Cy	cyclohexyl
Cp	cyclopentadienyl
Cp^*	pentamethylcyclopentadienyl
NMR	nuclear magnetic resonance
DMSO	dimethylsulfoxide
cat.	catalyst/ catalytic
THP	tetrahydropyran
thd	tetramethylheptanedioate
IR	infra red
EPR	electron paramagnetic resonance
UV-vis-NIR	ultra violet-visible-near infra red
OTf	triflate
THF	tetrahydrofuran
Mes	mesityl
Dipp	2,6-di-*iso*-propylphenyl
TMEDA	tetramethylethylene diamine
DME	dimethoxyethane
Ind	indenyl
Flu	fluorenyl
Tp	*tris*(pyrazolyl borate)
CT	charge transfer
Ad	adamantyl

coe	cyclooctene
nbd	norbornadiene
BINOL	1,1’-bi-2-naphthol
ORTEP	Oak Ridge Thermal Ellipsoid Plot
PLA	Polylactic acid
ROP	Ring Opening Polymerisation
PDI	Polydispersity index
LA	Lactic Acid
GPC	Gel Permeation Chromatography
tmu	tetramethyl urea
DCM	Dichloromethane

Table of Contents

1. Introduction

2. Ligand Development

3. Cerium Chemistry

Chapter 1

Introduction

1. Introduction

1.1 The f-Block metals

The lanthanides (La to Lu) constitute the first row of the f-block elements and possess considerable uniformity across the group with respect to their properties.[1-3] The limited radial extension of the 4f-orbitals and their poor screening ability affects all of the electrons, resulting in a gradual reduction of the lanthanide metal and Ln^{III} ionic radii across the group, a phenomenon known as the lanthanide contraction. As the nucleus is only poorly screened, when the nuclear charge and number of f-electrons increases across the group, the *effective* nuclear charge experienced by all of the valence f-electrons increases and results in the observed contraction. A further consequence of the 4f-electrons being mainly 'core-like' is that they do not extend out far enough to interact significantly with incoming ligands, hence any complexes formed are held together by mostly electrostatic forces. Due to the large size of the lanthanides, coordination numbers of up to 12 are possible and steric factors play a large role in the spatial arrangement of any ligands. A consequence of the larger radial extension of the 5f orbitals results in the bonding in actinide complexes possessing more covalent character. It is highly desirable to be able to exploit this property, to effect better separation of the actinide components from the lanthanides in nuclear waste, enabling treatment of these highly radioactive and long lived components. One approach to developing these separation techniques is to employ extractant ligands bearing soft donor groups, to exploit the increased covalency inherent in the 5f elements. A number of chelating ligands, including N-heterocyclic carbene (NHC) complexes, have shown selectivity for the softer actinides in the presence of lanthanide metals.[4-7]

The lanthanides form predominantly trivalent complexes, as a consequence of the fourth ionisation energy being larger than the first, second and third ionisation energies combined. In most cases, the fourth ionisation energy is so large it cannot be offset by

the formation of new bonds, explaining the inaccessibility of tetravalent oxidation states. The most notable exception to this rule is cerium, however, as the Ce^{IV} ion possesses a more stable closed shell electronic configuration, $[Xe]4f^0$, which, coupled with the high energy and therefore inherent instability of the 4f orbitals in the early lanthanides, renders Ce^{III} complexes vulnerable to the loss of the final electron. Predictably, tetravalent cerium complexes are strong oxidising agents, with numerous inorganic salts, among them ceric ammonium nitrate (CAN) and cerium(IV) sulphate, having found myriad applications in both organic[8, 9] and inorganic[10] oxidation reactions.

1.1.1 Tetravalent cerium complexes

Well authenticated examples of organometallic Ce^{IV} complexes, excluding O-donor compounds, are relatively sparse, and the outcome of oxidation reactions for all but a handful of porphyrin complexes,[11-13] is capricious and highly dependant upon judicious choice of the ligand, solvent and oxidant.

Since the first report by Cesca *et. al.* in 1976 of the neutral cerium cyclooctatetraene (COT) complex $Ce(\eta^8\text{-}COT)_2$, cerocene, **I** in Figure 1,[14] there has been much academic debate as to the validity of the assignment of the Ce^{IV} oxidation state.[15-18] The synthesis and stability of cerocene has been noted as being quite remarkable, as the Ce^{IV} ion is a strong oxidising agent and the cyclooctatetraene dianion $(COT)^{2-}$, a strong reducing agent. A severely limiting factor to the study of the reactivity of **I** is the poor solubility of this complex, prompting Edelmann *et. al.* to develop more soluble silylated cerocenes, such as **II** in Figure 1, which are also more stable and enable a more detailed study of the associated redox activity.[19, 20] Numerous spectroscopic and theoretical investigations have been performed on both of these cerocenes, attempting to definitively assign the cerium oxidation state. It is now widely accepted that cerocene actually contains mostly trivalent cerium, and is better described as $[Ce^{III}\{(COT)_2\}^{3-}]$, containing a $[Xe]4f^1$ electron configuration and only partially reduced $(COT)^{1.5-}$ ligands.[21-25] More recent work has utilised substituted pentalene ligands in tetravalent cerium complexes as interesting comparisons for the structure and bonding observed in cerocene. At almost the same time, O'Hare *et. al.* reported the permethylated variant **III**,

Figure 1, and Cloke *et. al.* the silylated analogue **IV**.[26, 27] Following structural, spectroscopic and theoretical investigation, it was determined that although both complexes contain a formally Ce^{IV} cation, the actual charge on the metal centre was closer to Ce^{III}, a similar situation to that observed in cerocene.

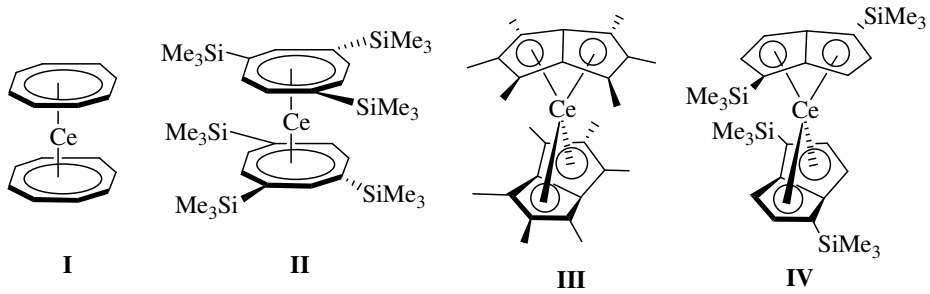

Figure 1. Tetravalent cerium COT and pentalene complexes.

1.1.2 Amides

There are currently only a handful of reported examples of Ce^{IV} amides in the literature, which highlights the inherent difficulties involved in preparing these compounds. The first, $CeN''_2(OBu^t)_2$ ($N'' = N(SiMe_3)_2$) was reported at a conference[28] and will not be discussed further here.

The second example is that reported by Scott and co-workers, involving the oxidation of a Ce^{III} triamidoamine $[N(CH_2CH_2NSiMe_2Bu^t)_3]^{3-}$ (NN'_3) with molecular halogens, Scheme 1.[29] Treatment of $Ce(NN'_3)$ with bromine or chlorine afforded the mixed valence $Ce^{III/IV}$ complexes **V** and **VI**, respectively, whereas treatment with iodine furnished the Ce^{IV} iodide **VII**. Two arguments for the observed reactivity are postulated by Scott. The first of these is that the ligands in $Ce(NN'_3)$ do not have to rearrange to accommodate the incoming group, and this rigorous 'facial' coordination enhances the Lewis acidity of the metal, helping to stabilise the Ce^{IV} centre. The second argument states that while the chloride and bromide in compounds **V** and **VI** form strong dative bonds to the Ce^{III} centre, the softer base iodide would only form a relatively weak dative bond, and that this would not be able to compensate for the dissociation energy of the

Ce^{IV}-I bond found in **VII**, thereby precluding the formation of an analogous mixed valence compound.

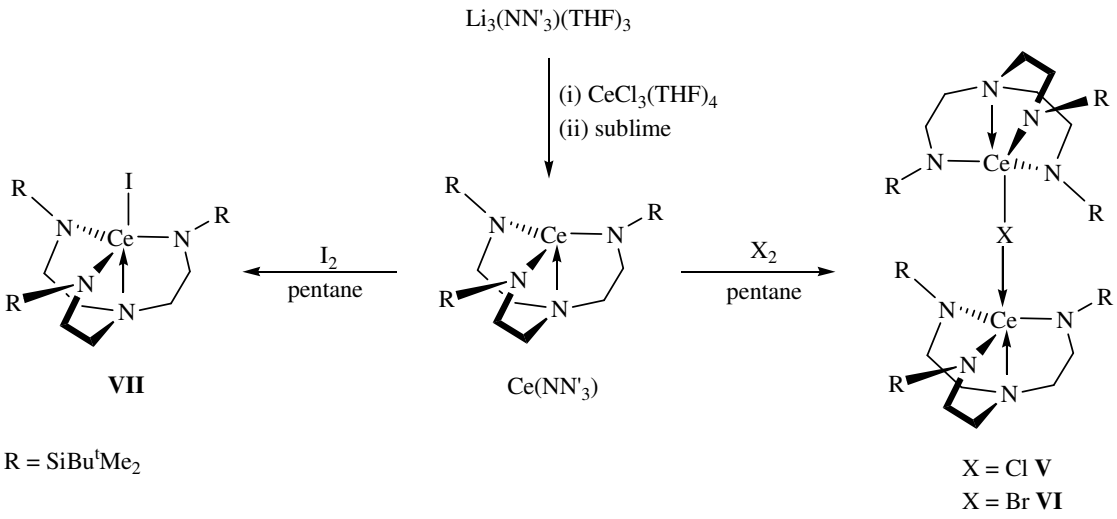

Scheme 1. Synthesis of tetravalent cerium amide complexes.

Subsequently, Lappert *et. al.* detailed the oxidation of the prototypical Ce^{III} amide $CeN"_3$ to the corresponding Ce^{IV} chloride and bromide complexes, Eq. 1.[30-32] Although $CeN"_3$ is resistant to oxidation by molecular halogens, application of the comparatively weaker oxidants $TeCl_4$ and PBr_2Ph_3 furnish **VIII** and **IX**, respectively. The authors postulate that the ability of these two oxidants to dissociate in coordinating solvents, to form the halogenonium ions $[TeCl_3]^+$ and $[PBrPh_3]^+$, may lower the energy barrier to electron transfer from cerium to the main group centre and allow the formation of **VIII** and **IX**.

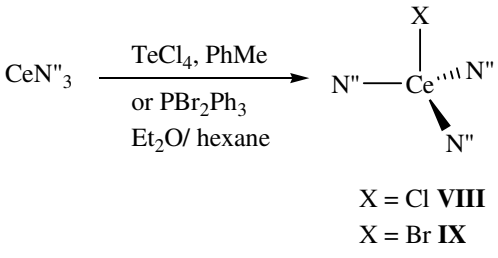

Eq. 1

More recently, Lappert has also reported the facile synthesis of a homoleptic Ce^{IV} amide *via* aerobic oxidation and concomitant ligand redistribution, **X** in Eq. 2.[33] Complex **X** displayed typically diamagnetic NMR spectra, and structural characterisation revealed the cerium to occupy a distorted tetrahedral geometry. The Ce^{IV}-N bond lengths in **X** lie within the range 2.238(5)–2.247(6) Å, predictably shorter than the Ce^{III}-N bond lengths in the starting material (range 2.299(2)–2.336(2) Å), but longer than the Ce^{IV}-N bond lengths in the less sterically hindered heteroleptic complexes **VIII** (2.217(3) Å) and **IX** (2.219(7) Å).

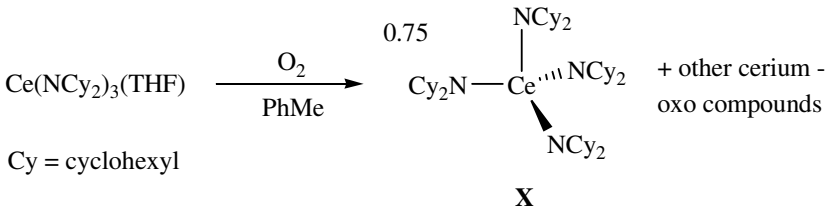

Eq. 2

1.1.3 Alkoxides

Unlike the cyclopentadienyl (Cp) derived ligands originally applied in lanthanide chemistry, which typically act as terminal η^5-ligands, the lone pairs on the oxygen of the alkoxide ligand means it has the potential to act as a one, three or five electron donor according to the hybridisation of the oxygen atom (a) sp^3, (b) sp^2, or (c) sp, Figure 2.[3]

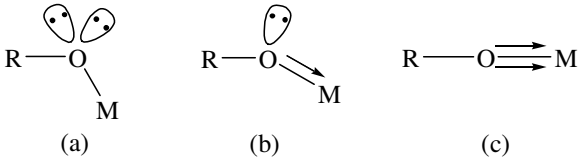

Figure 2. Possible alkoxide ligand binding modes.

Terminal lanthanide alkoxides most commonly contain linear or almost linear M-OR moieties, as a consequence of these metals forming largely ionic bonds and possessing

many orbitals with suitable symmetry to overlap with the ligand orbitals. It has also been argued by Kaltsoyannis and Sella that this linearity is due to a significant electrostatic repulsion occurring between the metal centre and the α-carbon atom.[34] The lone pairs also make it possible for alkoxide ligands to satisfy the higher degrees of steric and electronic saturation required at these large, electropositive metal centres, such that binding modes span terminal [(OR)-Ln], bridging [(μ-OR)-Ln_2], triply bridging [(μ_3-OR)-Ln_3] and occasionally quadruply bridging [(μ_4-OR)-Ln_4] interactions. An excellent review by Boyle and Ottley has recently been published, covering advances in this area.[35]

Although Ce^{IV} alkoxides have been known for many years, their preparation was laborious and time consuming,[36, 37] until the readily available and cheap tetravalent cerium reagent, ceric ammonium nitrate $(NH_4)_2Ce(NO_3)_6$ (CAN), was utilised in their synthesis, originally by Gradeff *et. al.*[38] and subsequently modified by Evans *et. al.*, Eq. 3.[39]

$$(NH_4)_2Ce(NO_3)_6 \text{ (CAN)} + n\ NaO^tBu \xrightarrow{THF} \begin{matrix} -\ 2\ NH_3 \\ -\ 2\ HO^tBu \\ -\ n\ NaNO_3 \end{matrix} \quad Ce(O^tBu)_{n-2}(NO_3)_{6-n}(THF)_2$$

$n = 2$, **XI**
$n = 3$, **XII**
$n = 4$, **XIII**
$n = 5$, **XIV**
$n = 6$, **XV**

Eq. 3

Evans demonstrated that it was possible to synthesise a range of Ce^{IV} nitrate, mixed nitrate-alkoxide and alkoxide complexes, **XI**–**XV**, by careful control of the reaction stoichiometry. The low cost, ease of synthesis and control of the functionalities present rendered this an appealing route into further Ce^{IV} chemistry for a number of groups. The same group subsequently utilised **XII** and three equivalents of NaCp in the synthesis of **XVI**, Figure 3, which represented the first structurally characterised example of a tetravalent cerium Cp complex.[40] More recently, Lappert *et. al.* reported the mixed valence cerium trinuclear cluster **XVII**, *via* treatment of a mixture of **XIV** and two

equivalents of **XV** with three equivalents of $Sn(C_5H_3{}^tBu_2\text{-}1,3)$.[41] Structural characterisation and a computational analysis of model compounds revealed the oxidation states of the metals as $Ce^{III}Ce^{IV}Ce^{IV}$, in which the single f electron is found to be localised on the NO_3-bearing cerium atom.

In contrast to the alkoxides, tetravalent cerium siloxides are considerably more scarce.[42, 43] In a recent report, Edelmann *et. al.* detailed the synthesis and structural characterisation of the heterobimetallic complex **XVIII**, from the reaction between **XIV** and two equivalents of the corresponding potassium siloxanediolate.[44]

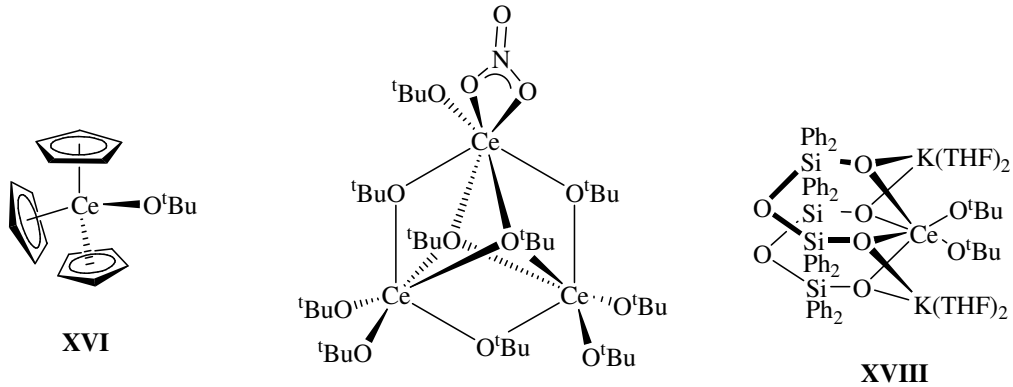

XVI **XVII** **XVIII**

Figure 3. Tetravalent cerium alkoxide complexes.

There is only one reported instance of a Ce^{IV} alkoxide being formed *via* an oxidation reaction, as detailed in the work of Sen *et. al.* from the reaction of cerium *tris*(tri-*tert*-butyl methoxide) with either an organic peroxide or benzoquinone.[45] This latter oxidation formed the hydroquinonediolate-bridging binuclear complex **XIX**, Eq. 4. The complex formed immediately upon mixing of the reagents, but decomposed over time, highlighting the instability of the Ce^{IV} state. Despite this, the diamagnetic NMR spectra were indicative of tetravalent cerium, and structural characterisation revealed *pseudo*-tetrahedral cerium centres, a consequence of the large steric profile of the alkoxide ligands restricting dimerisation.

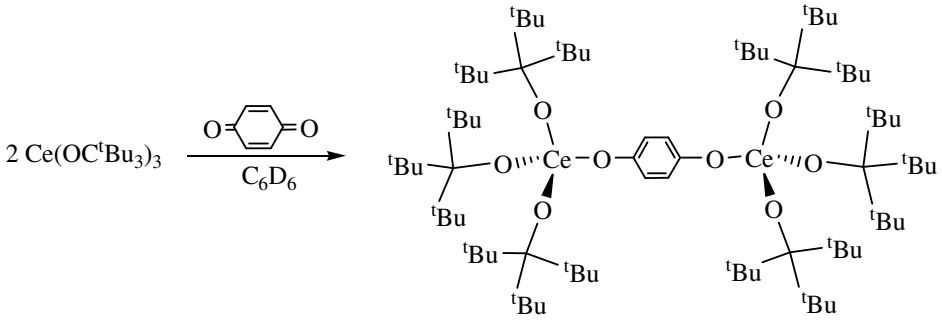

XIX

Eq. 4

1.2 Carbenes: Background

Carbenes are defined as neutral compounds that contain a divalent carbon atom which has only six valence electrons. They were first introduced into organometallic chemistry by Fisher in 1964,[46] and were for many years only considered as chemical curiosities. It was not until Arduengo isolated and characterised the first stable N-heterocyclic carbene (NHC) in 1991[47] that the interest of the scientific community was rekindled,[48-50] particularly into their properties and application as ligands in organometallic catalysis.[51-53]

1.2.1 Carbene ground state multiplicity and bonding

In the majority of cases, the geometry at the carbene carbon contains an sp^2-hybridised carbon with a bent geometry. This hybridisation has little effect upon the energy of one p orbital, conventionally called p_π, whereas the newly formed sp^2-hybrid orbital, described as a σ orbital, Figure 4, exhibits some s character and is therefore stabilised relative to the original p orbital. The two non-bonding electrons at the carbon centre can occupy these two empty orbitals with parallel spin (triplet state) or just the σ orbital with anti-parallel spin (singlet state), Figure 4.[54]

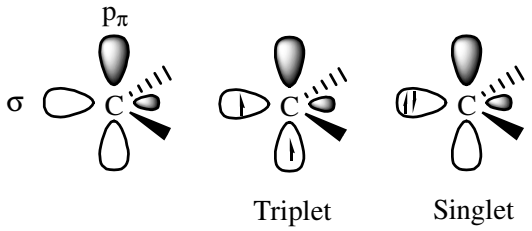

Figure 4. Carbene ground state spin multiplicity.

These different ground state multiplicities dictate the chemical properties of a carbene. Singlet carbenes show ambiphilic behaviour, due to the filled σ and empty p_π orbitals, which arises due to a large energy gap between the relative energies of these orbitals. This situation is found with more electronegative σ-electron withdrawing substituents, one of which should also be able to act as a good π-donor to stabilise the empty p_π orbital, and in complexes with late transition / low oxidation state metals the metal π-back donation is crucial to the stabilisation of the carbene centre. Triplet carbenes, however, behave as di-radicals due to the two unpaired electrons, and the necessary small energy difference between the two occupied orbitals is best attained by σ-electron donating substituents. Triplet carbene complexes containing metals with empty d-orbitals are most stable, typically early transition/ high oxidation state metals.[50, 55]

NHCs contain two nitrogen substituents and are particularly stable examples of singlet carbenes, due to the nitrogen lone pairs donating π-electron density into the empty carbene p_π orbital. NHCs act as excellent σ-donor ligands to metals, and it was widely believed as poor acceptors of metal to ligand π-back donation. This belief has been challenged in recent years by a number studies that support the existence of up to 30 % π-backbonding from electron rich, late transition metals into the carbene p_π orbital.[56-58]

The number of studies for more electropositive metal systems is limited, with a report by Arnold suggesting that the shorter Ti^{III}-NHC bonds observed in TiL_3 (L = $[OCMe_2CH_2(1\text{-}C\{NCHCHC^iPr\})]$), versus those observed in the analogous Y^{III}-NHC complex, YL_3, were more likely due to an increased electrostatic interaction caused by the smaller titanium centre, rather than a π-bonding contribution in this complex.[59, 60]

1.2.2 NHCs; Structural variations and effects

There are a number of possible variations in the basic structure of NHCs. The most common of these are the imidazole based imidazol-2-ylidine and the analogous saturated imidazolin-2-ylidine, **XX** and **XXI** in Figure 5. An extension of these is the six membered tetrahydropyrimid-2-ylidine, **XXII**.[61] The five-membered triazole derived NHCs, 1,2,4-triazol-(3,5)-ylidine, **XXIII** in Figure 5, can have carbenes located at the 3- and 5-positions, raising the possibility of binding to one or more metal centres.[62, 63] A number of other heterocyclic carbenes have been reported, based on; four-membered rings,[64] thiazole,[65] boron containing rings,[66, 67] P-heterocycles[68, 69] and cyclic alkyl(amino)carbenes (CAACs).[70, 71]

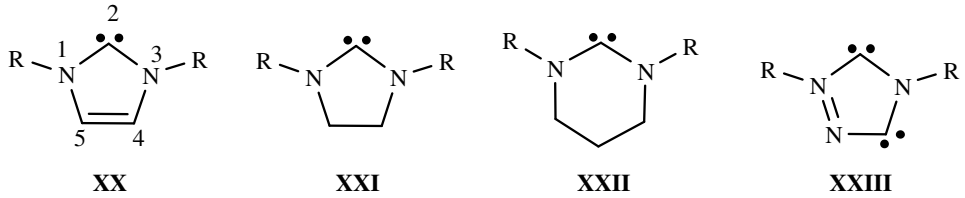

Figure 5. Types of N-heterocyclic carbenes.

The degree to which delocalisation of the 6 π-electrons in unsaturated NHCs, **XX**, contributes to the overall stability of the carbene centre has long been a contentious issue. Dixon and Arduengo initially reported that the stability of NHCs of this type was predominantly due to the inductive σ-charge transfer from the carbene carbon to the more electronegative nitrogen substituents, and that the mesomeric π-donation played a minor role.[72, 73] It has also been suggested that the C=C unsaturation would allow a delocalisation of electron density around the ring, providing a small but significant contribution to the overall stability of the NHC.[74-76] It was believed that this explained Arduengo's isolation of a free carbene, bearing an unsaturated backbone, when Wanzlick's initial work on saturated systems, **XXI** in Figure 5, yielded only dimers.[77] It was not until the first isolation of a free, saturated backbone NHC in 1995[78] that it became clear any delocalisation could only provide minimal overall stabilisation, and

that mesomeric π-electron donation from the nitrogen atoms to the carbene centre would be necessary and sufficient for stabilising the free carbene.[75]

The differences in donor capability between saturated and unsaturated NHCs has also been an issue of debate, and Nolan has endeavoured to answer some of these questions. By conducting experimental, spectroscopic and theoretical studies on analogous saturated and unsaturated ruthenium,[79] nickel[80] and platinum[81] NHC complexes, he has demonstrated that there is in fact little difference in the donor capacity between both types of ligand, although the saturated ligands can render some late transition metals marginally more electron rich.

The majority of NHC ligands possess the carbene located at the 2-position, between the two nitrogen substituents. As NHCs of the type **XX**, Figure 5, contain acidic backbone protons, there is the possibility of deprotonation at the 4-, **XXIV** in Figure 6, or 5-positions to yield an 'abnormal' carbene, and although small, the number of examples are growing.[82] A very recent example has been reported by Danopoulos *et. al.* of a 'pincer' C-N-C pyridine-dicarbene iridium complex which possesses three modes of NHC binding, namely at the normal C2 carbon, abnormal C5 carbon and a previously unknown binding mode with the unsaturated NHC backbone bonding to a second metal centre in a η^2-ethylene-like fashion, **XXV** in Figure 6.[83]

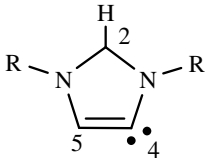

XXIV

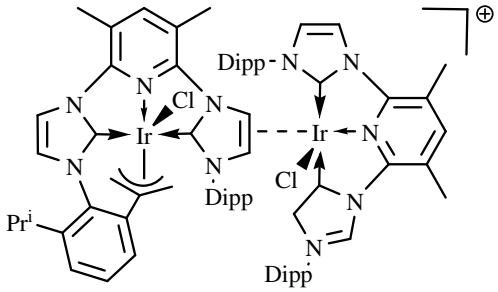

XXV

Figure 6. Abnormally bound NHCs.

The steric and electronic properties of NHC ligands can be modified either through the nitrogen or backbone substituents, and this has implications for the donor capability of the carbene centre. Several general backbone substitutions are known, some of which are shown in Figure 7. Benzimidazole substituted NHCs, **XXVI** in Figure 7, provide a ligand with no acidic backbone protons and the potential for a larger delocalised system.[84, 85] Other 4,5-substituted NHCs of the type **XXVII** have been reported with both electron withdrawing and donating groups, such as phenyl,[86, 87] chloride,[88, 89] cyano[90] and methyl.[91, 92] These substituents affect the donor strength of the carbene centre by withdrawing or donating electron density through the heterocyclic σ-framework. Fürstner *et. al*. have also reported asymmetrically substituted NHC ligands, bearing four different groups with previously inaccessible substitution patters, **XXVIII**.[93] Very recently, reports utilising more 'non-standard' NHCs have emerged, such as **XXIX** in Figure 7, which incorporates a d-block metal into the 6-membered heterocyclic ring.[94] Rhodium complexes of this redox-active ferrocene-containing NHC ligand demonstrated long-range, but significant, communication between the two metal centres.[95]

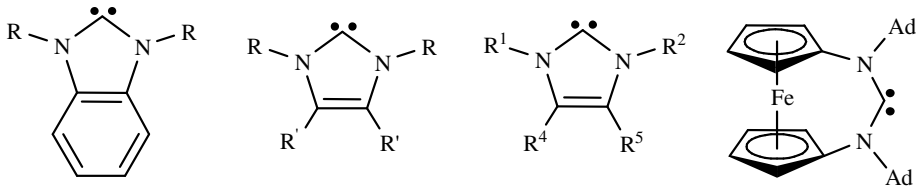

XXVI **XXVII** **XXVIII** **XXIX**

Figure 7. Backbone (4,5) substituted NHCs.

1.2.3 Synthetic routes to NHCs

Transition metal NHC complexes have been known for about 40 years. In 1968, Wanzlick treated an imidazolium salt with mercury(II) acetate to form **XXX** in Figure 8,[96] whilst in 1969 Öfele simply heated dimethylimidazolium hydridopentacarbonylchromate to form **XXXI** in Figure 8.[97]

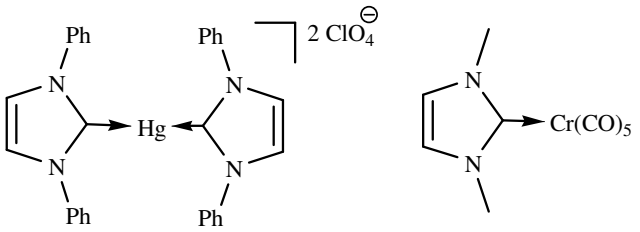

Figure 8. First metal NHC complexes.

Previous to this, Wanzlick had isolated the enetetraamine dimer **XXXII** in Scheme 2, instead of the target free carbene, by α-elimination of chloroform from an imidazolidine precursor. Subsequently, Lappert *et. al.* treated **XXXII** with a platinum complex and isolated **XXXIII**, the first saturated NHC metal complex.

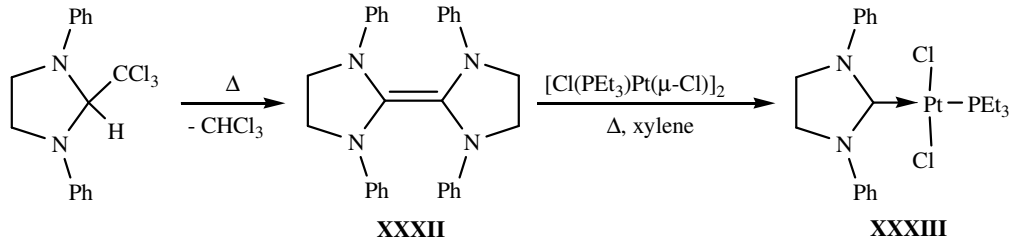

Scheme 2. First saturated NHC metal complex.

Research into this area stalled for the next 20 years, until in 1991 Arduengo *et. al.* isolated the first stable crystalline NHC, **XXXIV** in Eq. 5, *via* deprotonation of the corresponding imidazolium salt with sodium hydride in the presence of a catalytic amount of DMSO.[47]

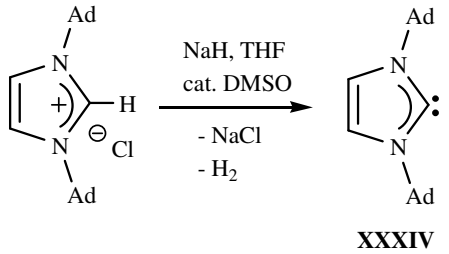

Eq. 5

The deprotonation of azolium salts is by far the most popular route into NHC chemistry, due to the clean, high yielding deprotonation step and the relative ease with which a range of saturated and unsaturated backbone precursor salts can be prepared, **XXXV** in Scheme 3. Two other routes are, however, worthy of mention. The first of these is reductive desulfurisation of an imidazol-2-thione, **XXXVI** in Scheme 3, by treatment with potassium metal in refluxing THF.[98] The second method is the thermal elimination of an alcohol from a 'masked' carbene; heating the alcohol adduct **XXXVII** forms the corresponding saturated backbone NHC *in situ*, ready for further chemistry.[99] Enders *et. al*. heated the methanol adduct of the 1,2,4-triazol-3-ylidine **XXXVIII**, Scheme 3, under reduced pressure to eliminate methanol and yield the free carbene. This method was necessary due to the difficulties encountered in directly deprotonating the triazolium salt.[62]

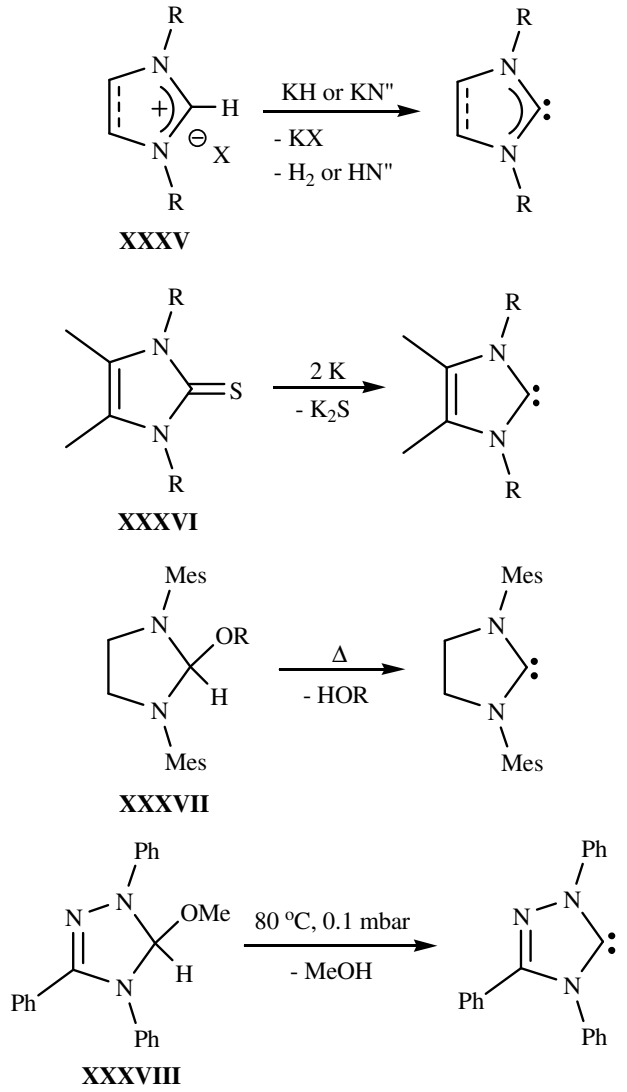

Scheme 3. Syntheses of NHCs.

1.2.4 Precursors to NHCs

Imidazolium salts can be synthesised either by nucleophilic substitution and subsequent alkylation of the imidazole heterocycle, or by a multicomponent reaction to produce ready substituted imidazoles which can be further alkylated. The first of these is shown in Scheme 4, although it is limited to the introduction of primary alkyl substituents, but can yield either symmetrically or unsymmetrically substituted imidazolium salts,

dependant upon how the reaction is conducted.[100, 101] A method for the introduction of aryl groups has also been reported.[102]

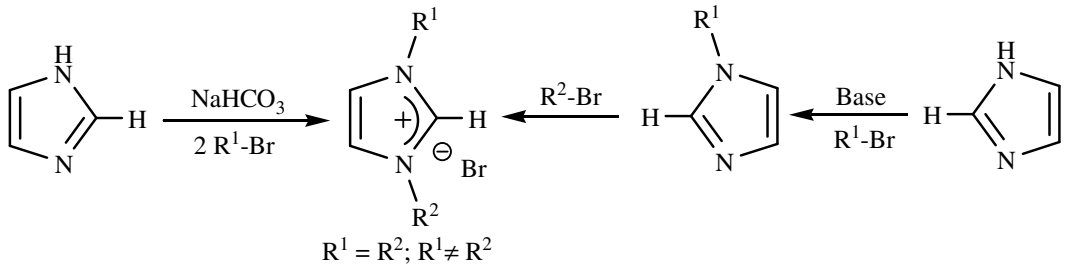

Scheme 4. Symmetrically and unsymetrically N, N'-substituted imidazolium salts.

The multicomponent reaction of primary amines, glyoxal and formaldehyde in the presence of an acid allows for the flexible synthesis of symmetrically substituted imidazolium salts, **XXXIX** in Scheme 5.[103] A combination of this multicomponent synthesis with an N-alkylation reaction can be used to readily synthesise unsymmetrically substituted variants, by isolation of the intermediate **XL**, Scheme 5.[104]

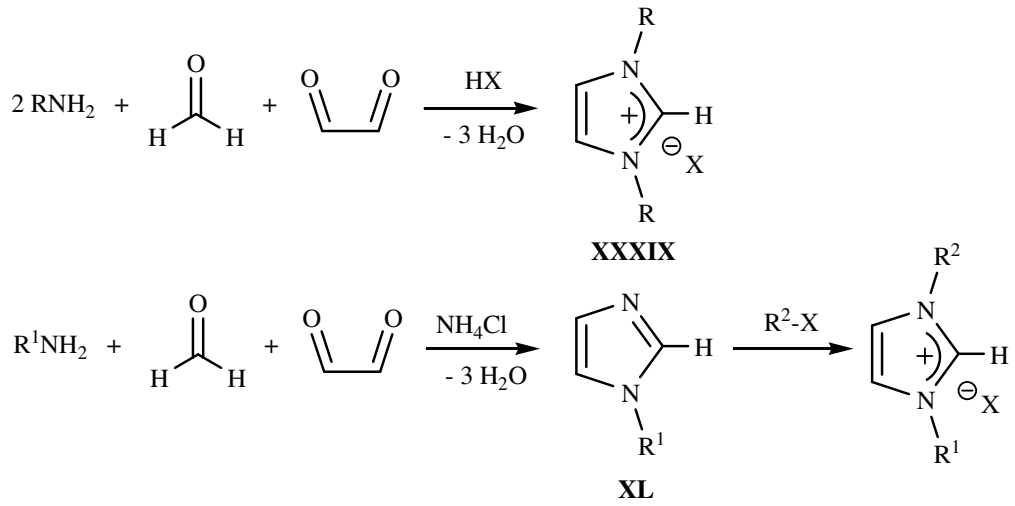

Scheme 5. Multicomponent imidazolium synthesis.

Intermediate **XL** can also be reacted with linker groups containing two or three alkyl halides, in the appropriate stoichiometry, to yield neutral bidentate *bis*-NHC[105] and tridentate *tris*-NHC ligands.[106]

Two methods for the synthesis of saturated backbone imidazolinium salts have proven to be useful, deriving from the simple ring closing of a substituted diamine, **XLI** in Scheme 6,[107] or a multicomponent synthesis using a primary amine, aldehyde or ketone, and an isocyanide with an acidic α-proton, which allows for substitution at every position around the heterocyclic ring, **XLII** in Scheme 6.[108] This method is very versatile and is only limited by the reactivity of the isocyanide used and the cost of the silver reagents.

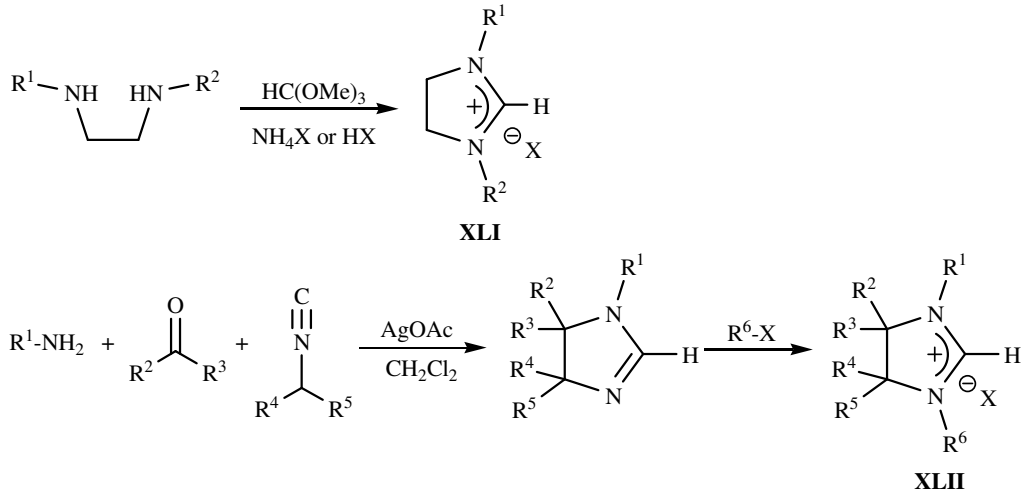

Scheme 6. Synthetic routes to imidazolinium salts.

1.2.5 Characterisation of NHCs

Imidazolium salts and the corresponding NHCs exhibit characteristic resonances in both the ^{1}H and ^{13}C NMR spectra. Both imidazolium and imidazolinium salts display a high-frequency singlet between δ = 8 and 10 ppm in the ^{1}H NMR spectrum, attributable to the proton on the central C2 carbon in the cationic ring. The ^{13}C NMR chemical shift range of the C2 carbon typically ranges from δ = 136 and 152 ppm for imidazolium salts and δ = 157 and 161 ppm for imidazolinium salts, Figure 9.[54] Upon deprotonation, and hence

carbene formation, the C2 resonance in the ^{13}C NMR spectrum is now observed at high frequency, and is typically of low intensity, between δ = 211 and 221 ppm for imidazol-2-ylidines and δ = 238 and 245 ppm for imidazolin-2-ylidines.

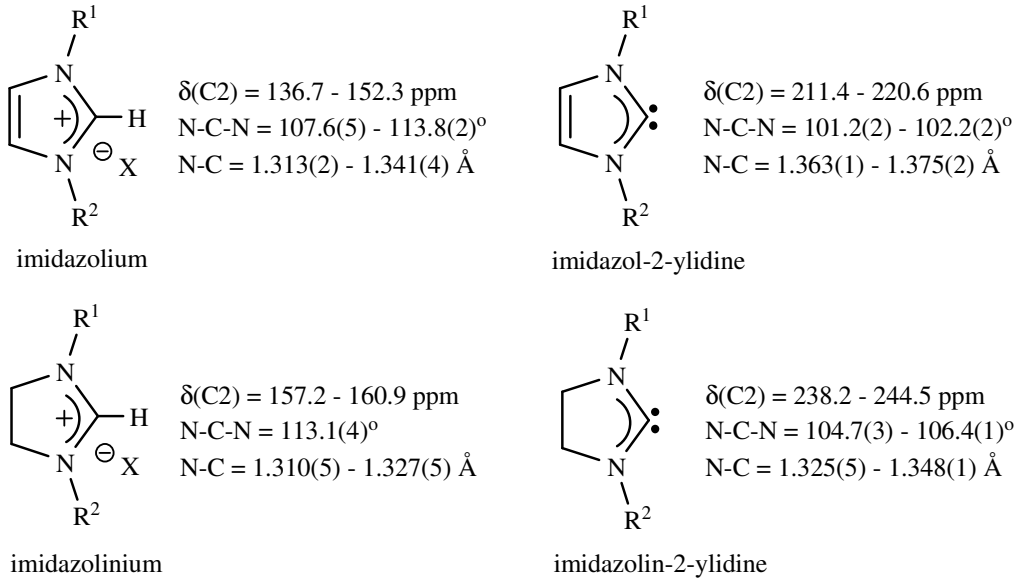

Figure 9. ^{13}C NMR chemical shift ranges and N-C-N bond angle and N-C bond length parameters for saturated and unsaturated NHCs and precursors.

There are also significant geometrical changes of the N-C2 bond length and N-C2-N bond angle within the heterocyclic ring upon formation of the free carbene from the corresponding imidazolium salt, as detailed in Figure 9. The N-C-N bond angles observed in imidazolium salts lie within the range 107–113°, although typically toward the lower end, and the N-C bond lengths within the range 1.31–1.34 Å. Upon formation of the free carbene, the N-C-N bond angle contracts to 101–103° due to the electronic repulsion of the lone pair centred at C2, and the N-C bond lengths elongate to 1.36–1.38 Å to accommodate the lone pair. The N-C-N bond angles observed for imidazolinium salts and the corresponding carbenes are larger than those seen in unsaturated variants, although a similar contraction is seen from ~113° to 104–106°, respectively. The N-C bond lengths again elongate upon carbene formation, but to a lesser degree, from 1.31–1.33 Å to 1.33–1.35 Å.

1.2.6 Reactivity of NHCs

As NHCs possess filled σ and empty p_π orbitals, they may be expected to show nucleophilic as well as electrophilic behaviour. Due to the mesomeric stabilisation of the empty p_π orbital by the substituent nitrogen lone pairs, NHCs in fact act as strongly Lewis basic electron donors, and metal NHC complexes are known for a majority of the metals in the periodic table.

The 1,2-alkyl migration reaction is a well known rearrangement of singlet carbenes, and occurs *via* a concerted uni-molecular process, Eq. 6. Although NHCs are examples of singlet carbenes, they do not undergo migration reactions due to the stabilisation imparted from the nitrogen substituents.

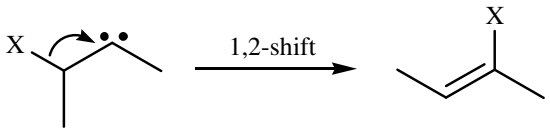

Eq. 6

Despite this, an example of a 1,2-silyl migration in the attempted formation of a series of 1,2,4-triazol-5-ylidines, by deprotonation of a triazolium salt, **XLIII** in Scheme 7, resulted in the isolation of the triazoles **XLIV**. This rearrangement occurs *via* an intermolecular process involving an electrophilic partner. The transient formation of the carbene was confirmed by conducting trapping experiments with benzaldehyde.[109]

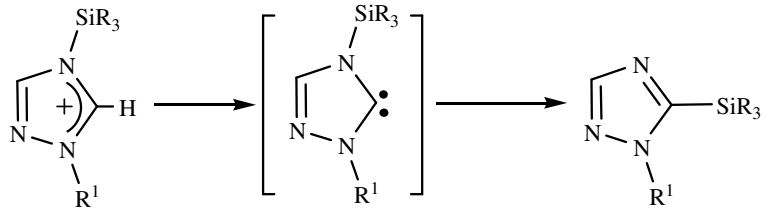

XLIII **XLIV**

R, R^1 = alkyl

Scheme 7. Triazole 1,2-silyl migration.

A fundamental aspect of NHC reactivity is dimerisation, a generic example **XLV** is shown in Eq. 7, which was first reported in some of the initial work by Wanzlick, see Scheme 2. This work was attempting to isolate free imidazolin-2-ylidines by thermal elimination of chloroform from the corresponding adduct, but the electron rich enetetramine **XXXII**, Scheme 2, was isolated.[110] It has since been established that saturated backbone imidazolin-2-ylidine dimerisation is controlled by the steric profile of the substituents, whereas unsaturated backbone imidazol-2-ylidines are thermodynamically stable towards dimerisation. The suggested mechanism of dimerisation does not involve the direct coupling of two NHCs, but rather the nucleophilic attack of one carbene upon its conjugate acid, with subsequent proton elimination.[111, 112]

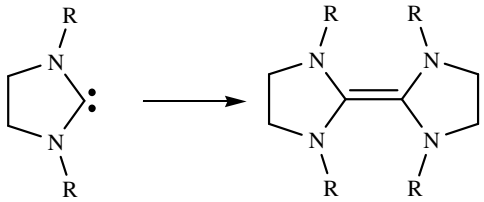

XLV

Eq. 7

1.3 Functionalised N-heterocyclic carbenes

The number of functionalised NHC ligands has grown very rapidly over the last few years, and a number of reviews have been published on this area.[113-116] These functionalised NHCs fall into one of two broad classes, i) those bearing a neutral donor, which have been reviewed previously and will not be discussed further here,[117] and ii) those bearing an anionic donor group.[118] These anionic tethers represent a method of covalently attaching the NHC ligand to early electropositive metal centres, helping to keep the NHC bound to, or in proximity to, the metal.

1.3.1 Oxygen donors

A convenient and flexible route into alkoxide tethered NHC ligands is through the ring opening of epoxides by imidazole, with subsequent quaternisation by an alkyl-halide to afford the corresponding imidazolium proligands, **XLVI** in Scheme 8.[119] This modular synthesis allows for the rapid formation of chiral and achiral ligands bearing a range of substituents, enabling straightforward tuning of the ligand steric and electronic profiles. Deprotonation of **XLVI** with either one or two equivalents of potassium hydride affords the zwitterionic compound **XLVII** or the potassium salt **XLVIII**, Scheme 8, respectively, which are applicable in subsequent metal amide protonolysis or metal halide salt elimination chemistry.[120, 121] The zwitterion **XLVII** can also be synthesised directly by the reaction of an epoxide with a substituted imidazole.

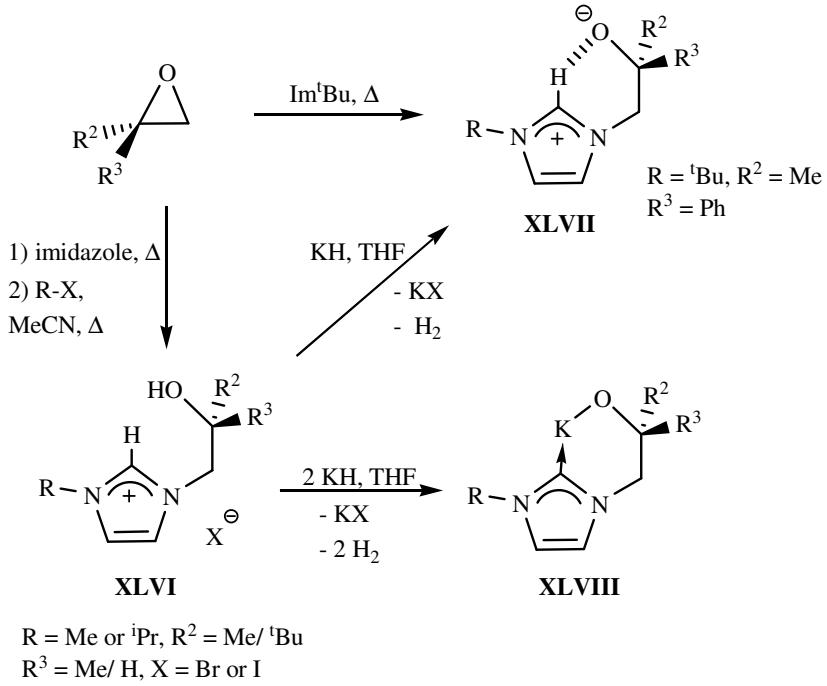

Scheme 8. Synthesis of unsaturated backbone alkoxy-carbene ligands and precursors.

Mauduit *et. al.* reported an alternative synthesis for saturated backbone alkoxy-NHC precursors, by the reaction of a primary amine with ethyloxalyl chloride. This was followed by coupling with a substituted amino-alcohol and reduction with lithium aluminium hydride, and was finally ring closed by condensation with trimethylorthoformate to yield **XLIX,** Figure 10.[122] A family of twenty proligands were synthesised and the copper complexes applied to the conjugate addition of diethyl zinc to a range of cyclic enones. The *bis*-alkoxide-NHC precursor, **L** in Figure 10, was synthesised by the coupling of two equivalents of a substituted amino-alcohol with 1,2-dibromoethane, followed by ring closure, and proved to be an effective proligand for the enantioselective addition of diethylzinc to aldehydes.[123]

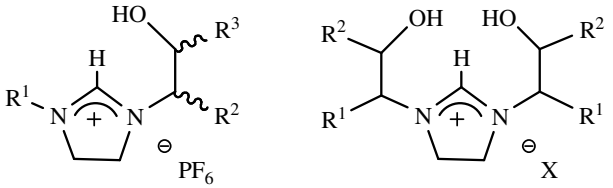

Figure 10. Alkoxy-carbene precursors.

Although there have been a number of alkoxide-tethered NHC ligands synthesised recently, the first deliberate synthesis was reported by our group in 2001.[124] Proligand **LI**, Eq. 8, was prepared in a one-pot reaction between two equivalents of *tert*-butyl imidazole (Im^{t}Bu) and a phenyl-substituted epichlorohydrin, and could easily be converted into the corresponding silver alkoxide *bis*-NHC complex, which proved to be an excellent ligand transfer agent to copper and ruthenium centres.[124, 125]

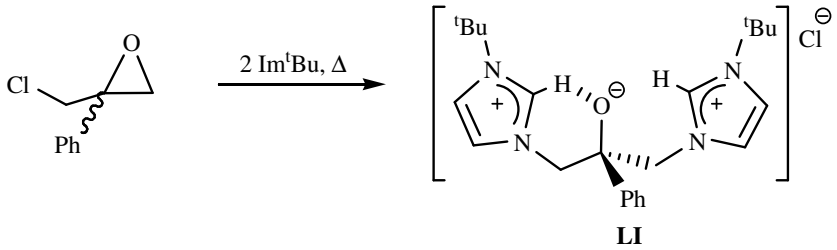

Eq. 8

A number of examples of aryloxo-functionalised NHC proligands have also been reported, as shown in Figure 11. Proligand **LII** was reported by Grubbs *et. al.* and was synthesised by a similar method to **XLIX**, with subsequent deprotonation and complexation to palladium and nickel.[126, 127] Hoveyda *et. al.* reported ruthenium complexes supported by chiral aryloxide NHCs based on proligands of the form **LIII**, Figure 11, which were found to be highly active and selective in cross metathesis reactions. The proligands were synthesised by the reductive amination between an optically pure binaphthyl amine alcohol and an aldehyde, followed by ring closure to the proligand.[128, 129] The *mono-* and *bis*-aryloxide NHC proligands **LIV** and **LV** respectively, Figure 11, were synthesised by the straightforward nucleophilic substitution of an alkyl halide with an imidazole.[130-133] Deprotonation of **LV** with two equivalents of NaN" affords the disodium salt, but this is unstable and decomposes by a 1,2-benzyl migration reaction if warmed to room temperature.

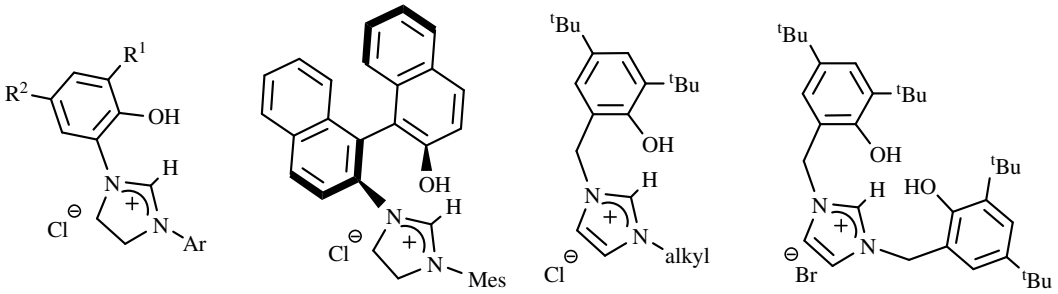

LII **LIII** **LIV** **LV**

Figure 11. Aryloxy-substituted NHC proligands.

Two further examples of oxygen-functionalised NHC precursors have been published, as part of a salicylaldimine group, **LVI** in Figure 12, reported by Shen *et. al.*,[134] and Waymouth's phenyl-ketone derivative **LVII**, which forms an enolate upon deprotonation and metal binding.[135] Both complexes were straightforwardly synthesised by quaternisation of a substituted imidazole with an appropriate alkyl halide and, following deprotonation and complexation to nickel, applied to styrene and ethylene polymerisation, respectively.

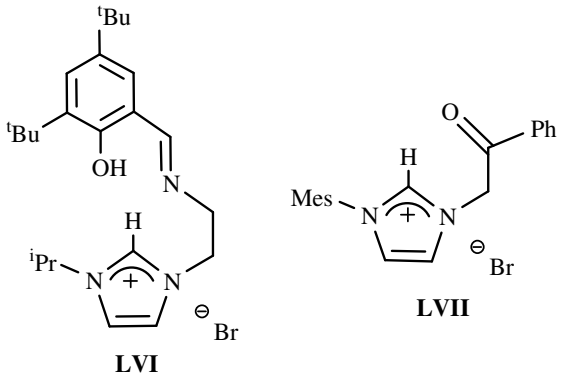

Figure 12. Salicylaldimine and enolate functionalised NHC proligands.

1.3.2 Nitrogen donors

The first amido-functionalised NHCs were reported by Arnold *et. al*., and proligand **LVIII**, Figure 13, was prepared by the alkylation of *tert*-butyl imidazole with $^{t}BuNHCH_2CH_2Br.HBr$ in high yield.[136] Subsequent deprotonation with potassium hydride affords the amine-carbene which can be utilised in protonolysis chemistry with metal amides, whereas treatment with a lithium base results in the amine-carbene as its lithium bromide adduct. Douthwaite *et. al*. reported the first amine-*bis*-imidazolium proligand, by coupling two equivalents of *tert*-butyl imidazole with a benzyl protected *bis*(chloroethyl)amine, which produced **LIX** after deprotection.[137] Subsequent deprotonation with silver oxide furnished a useful ligand transfer agent for the formation of amine *bis*-NHC palladium complexes. Arnold subsequently reported **LX**, *via* the more straightforward, one-pot reaction between two equivalents of mesityl imidazole and di(chloroethyl)ammonium chloride.[138] Fryzuk *et. al*. reported the first examples of *bis*-amine NHC ligands, **LXI** in Figure 13. These ligands are potentially tridentate, and were prepared from a borane-dimethylsulfide mediated reduction of a *bis*-amide-imidazolium chloride, followed by deprotonation with KN".[139] Subsequent treatment of **LXI** with group four metal amides or alkyls generated the metal *bis*-amide NHC complexes, which displayed a rich reaction chemistry.[140, 141]

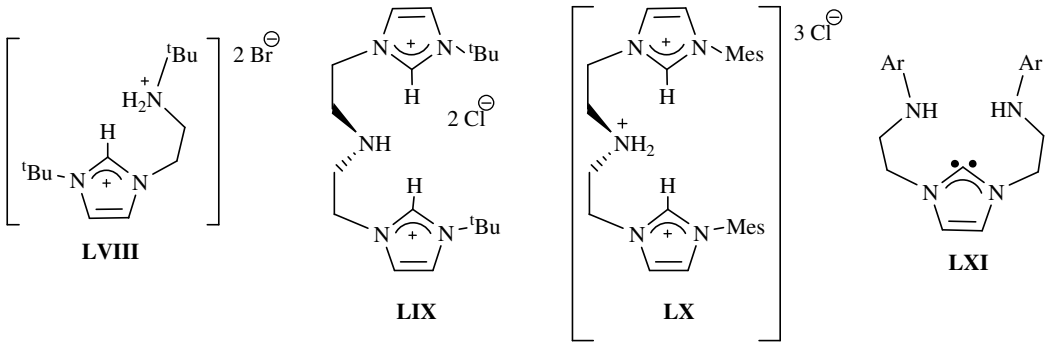

Figure 13. Amide functionalised NHC precursors.

1.3.3 Carbon donors

Despite the prevalence of cyclopentadienyl-substituted (Cp) ligands, as well as indenyl and fluorenyl variants, in organometallic chemistry, the first indenyl- and fluorenyl-tethered NHC proligands were only reported in 2006 by Downing and Danopoulos, represented by **LXII** in Figure 14.[142] These proligands were easily synthesised by the quaternisation of Dipp-imidazole with β-bromoethylindene or β-bromoethylfluorene, respectively, and could be easily deprotonated by a potassium base to afford the corresponding potassium salts. It was only very recently that the first Cp-functionalised NHC proligands have been reported by Muller,[143] and independently by Peris *et. al.*, **LXIII** in Figure 14.[144] This proligand was synthesised by deprotonation at the methylene group of benzyl-imidazole with Li^{n}Bu, followed by treatment with tetramethylfulvene, protonation with methanol and imidazole quaternisation with methyl iodide. A number of tautomers were formed, resulting from the different double bond positions in the Cp ring, of which **LXIII** is one example. Subsequent deprotonation in the presence of an iridium salt afforded a Cp*-NHC iridium complex, which was an active catalyst for a number of reactions.

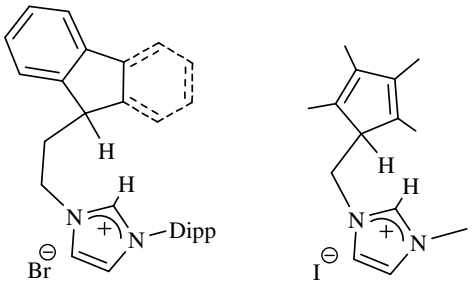

LXII **LXIII**

Figure 14. Anionic carbon-functionalised NHC precursors.

Tridentate CCC-pincer *bis*-NHC proligands have also been reported. Hollis and co-workers reported that proligand **LXIV**, Figure 15, could be formed by the copper-catalysed coupling of 1,3-dibromobenzene with imidazole and subsequent alkylation, which upon deprotonation with zirconium *tetrakis*(dimethyl amide) undergoes metallation of the aryl spacer group to afford the anionic ligand.[145] More recently, Cui and Lv reported the proligand **LXV**, formed from the quaternisation of two equivalents of mesityl-imidazole by 2,6-*bis*(bromomethyl)-1-bromobenzene in high yield.[146] Deprotonation of **LXV** with three equivalents of Li^{n}Bu in the presence of scandium trichloride afforded the unexpected scandium dibromides, in which the xylene-bridge has been metalated.

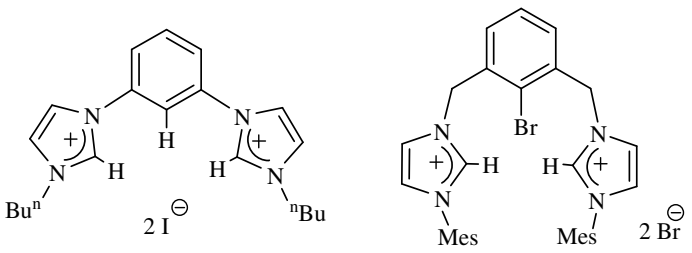

LXIV **LXV**

Figure 15. CCC-pincer *bis*-NHC precursors.

1.3.4 Sulfur donors

Sellmann *et. al.* reported the unexpected formation of a *bis*-thiolate NHC complex, **LXVI** in Scheme 9, initially by recrystallisation from DMF with insertion of CO into the Ni-N bonds of the corresponding nickel diamine dithiolate complex, with subsequent elimination of water and dimerisation. The same product could be isolated by the deliberate reaction with $HC(OEt)_3$.[147] Complex **LXVI** can be broken up into a neutral monomer, by reaction with Lewis bases such as phosphines and NHCs to afford **LXVII**.

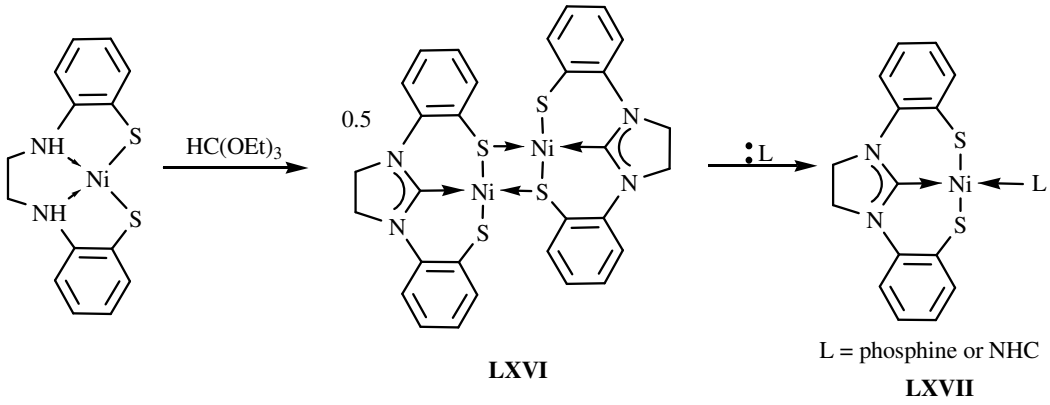

LXVI **LXVII**

Scheme 9. Synthesis of nickel *bis*-thiolate NHC complexes.

1.4 Group 1 NHC complexes

1.4.1 Lithium NHC complexes

The simple Li-NHC adduct, **LXVIII** in Figure 16, was reported by Arduengo *et. al.* in 1999, *via* the reaction of the corresponding free NHC with the lithium salt of a substituted Cp.[148] The ^{13}C NMR spectrum of **LXVIII** shows a $C_{carbene}$ resonance at δ = 190.7 ppm, comparable to literature values, and at higher frequency than the free carbene resonance. An X-ray structural determination revealed that the Li-$C_{carbene}$ bond length was 2.155(4) Å and that there is significant distortion associated with the lithium and carbene centre. The lithium cation is not symmetrically positioned with respect to

the Li-C-N bond vector, and is 8.9º away from the idealised imidazole C_2-axis. This distortion has been termed the 'yaw', Figure 17. The second distortion, the 'pitch', also in Figure 17, results in the imidazole and Cp planes deviating from the idealised orthogonal alignment by 21.4º.

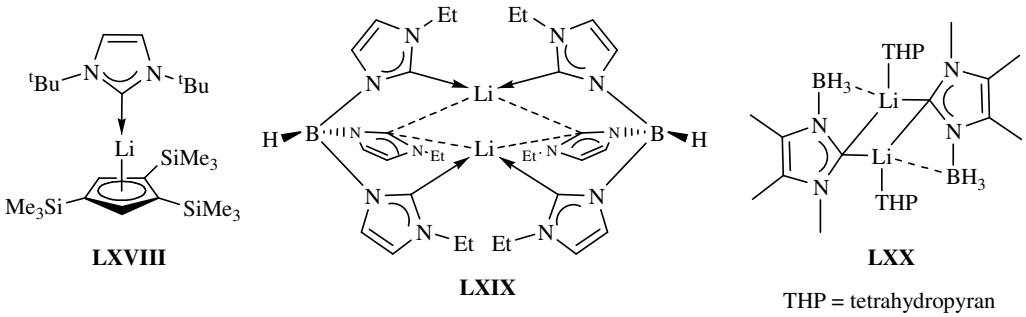

LXVIII **LXIX** **LXX**

THP = tetrahydropyran

Figure 16. Lithium NHC complexes.

Complex **LXIX** was formed by deprotonation of hydro-*tris*-(3-ethylimidazole)borate as the *bis*-tetrafluoroborate salt with Li^{n}Bu, and was structurally characterised with each lithium being unsolvated and coordinated to four NHC groups.[149] The coordination geometry at lithium is dramatically twisted, producing a triangular pyramid, in which the central C-Li-C angles are 111.8(2), 92.7(2) and 140.3(2)º, deviating from the idealised 120º angles. The lithium cations are coordinated by four NHC groups, through the terminal coordination of two NHCs to each lithium, with Li-$C_{carbene}$ bond lengths of 2.138(4) and 2.147(4) Å, comparable to those observed in **LXVIII**. The remaining NHC group from each ligand bridges both lithium centres and possesses significantly longer and very asymmetric Li-$C_{carbene}$ bond lengths of 2.201(4) and 2.311(4) Å. This asymmetry is akin to that observed in **LXX**, Figure 16, where it is even more pronounced with reported Li-μ-C bond lengths of 2.169(5) and 2.339(5) Å.[150]

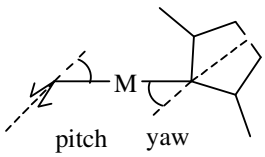

Figure 17. Diagram of metal-NHC bond deformation.

Lithium complexes bearing an amido-functionalised NHC ligand have been reported by our group,[136, 151] **LXXI** and **LXXII** in Scheme 10. Deprotonation of the alkylammonium imidazolium bromide proligand $^{t}BuNH_2CH_2CH_2[HC\{^{t}BuN(CHCH)N\}]Br_2$, **LVIII**, with two equivalents of Li^{n}Bu affords the lithium bromide adduct of the desired amine-carbene, **LXXI**, whereas treatment of **LVIII** with two equivalents of KH enables the isolation of the amine-carbene HL, and subsequent deprotonation with one equivalent of Li^{n}Bu affords complex **LXXII**. Both complexes have been structurally characterised, with **LXXI** possessing a Li-$C_{carbene}$ bond length of 2.196 Å, which is slightly longer than that observed in **LXVIII**. Complex **LXXII** exists as a discrete dimer, despite its unusually open coordination sphere, with Li-$C_{carbene}$ bond lengths of 2.124(4) and 2.162(4) Å being among the shortest so far reported. As previously observed, there is a dramatic distortion of the Li-NHC bond, such that the average pitch and yaw angles are 19º and 21º, respectively.

The ^{13}C NMR spectra of complexes **LXXI** and **LXXII** display a $C_{carbene}$ resonance at δ = 197.0 and 198.7 ppm, respectively, comparable to those previously observed.

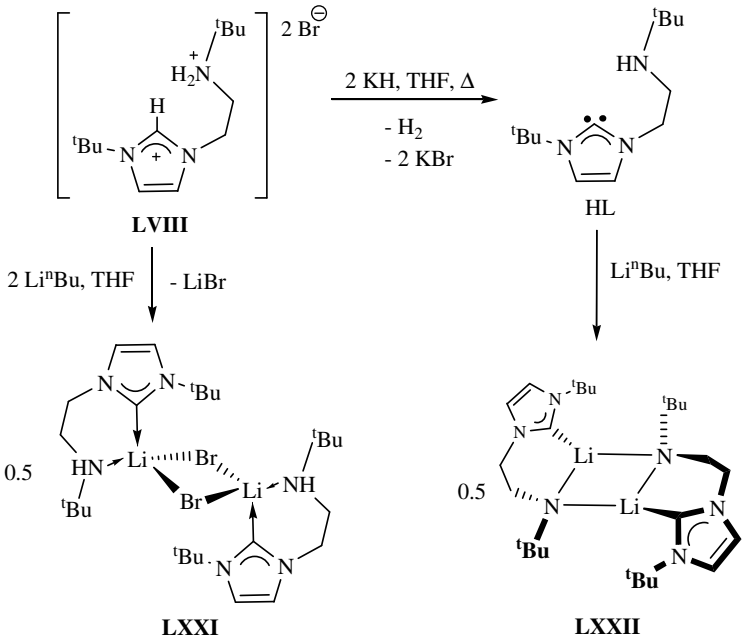

Scheme 10. Amide-tethered lithium NHC complexes.

Subsequently, our group also reported the lithium alkoxy-NHC [LiOC^{t}Bu(H)CH$_2${1-C(NCHCHNMe)}].LiI, **LXXIII**, which incorporated the lithium iodide by-product.[119] This complex is dimeric in the solid state and forms a tetrameric butterfly of lithium cations with the incorporated lithium iodide. The Li-$C_{carbene}$ bond length of 2.162(4) Å is short, and the distortion of the Li-NHC bond provides a pitch angle of 28º. Complex **LXXIII** has a $C_{carbene}$ resonance at δ = 200.0 ppm in the ^{13}C NMR spectrum.

Two other examples of lithium salts of functionalised NHCs have also been recently published, Figure 18, although neither example was structurally characterised. Complex **LXXIV** was synthesised by treatment of proligand **LX** with four equivalents of Li^{n}Bu in THF at -30 °C for 4 h, and is isolated with three equivalents of incorporated lithium chloride.[152] Attempts to remove this salt by solvent extraction in toluene or diethyl ether were successful, but resulted in ligand decomposition. The ^{13}C NMR spectrum displays a Li-$C_{carbene}$ resonance at δ = 203.4 ppm, commensurate with other examples. Complex **LXXV** was synthesised *via* treatment of the corresponding alcohol-imidazolium iodide salt with two equivalents of LiN" on an NMR scale, and was characterised by NMR spectroscopy, displaying a Li-$C_{carbene}$ resonance at δ = 186.3 ppm in the ^{13}C NMR spectrum.[153]

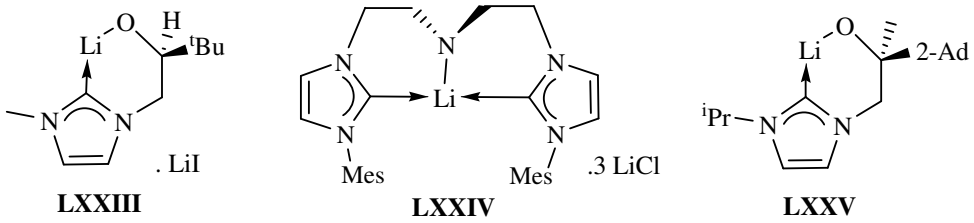

Figure 18. Further examples of lithium NHC complexes.

1.4.2 Potassium NHC complexes

The first example of a potassium-carbene complex was reported in 1999 as the adduct of a six-membered cyclic diaminocarbene and KN", **LXXVI** in Figure 19.[61] Structural determination found the molecule to be dimeric in the solid state, with bridging amide groups and a K-$C_{carbene}$ bond length of 3.0051(13) Å. The ^{13}C NMR spectrum shows a $C_{carbene}$ resonance at δ = 226.7 ppm.

Subsequently, our group reported the potassium-NHC complex **LXXVII**, which was straightforwardly synthesised *via* the deprotonation of the corresponding imidazolium salt, **XLVI** in Scheme 8, with two equivalents of KH, Figure 19.[154] The ^{13}C NMR spectra showed a high-frequency $C_{carbene}$ resonance at δ = 208.4 ppm. An X-ray diffraction study of **LXXVII** revealed the structure to be a polymeric network of $[KL]_4$ tetramers with cube-shaped K_4O_4 cores. Each metal is four-coordinate, binding three ligand alkoxides and a carbene C2, apart from one potassium in alternate cubes, which is also coordinated to a molecule of THF. All of the NHC groups bind potassium through the expected C2 carbon, but some also display additional close, and potentially bonding, contacts to backbone C4 and C5 carbons. Four of the ligands also bind to more than one cube through both the alkoxide and C2 carbon which completes the polymeric network. As with the Li-NHCs already discussed, the K-NHC bonds in **LXXVII** are significantly distorted and display pitch angles of between 9 and 52º, larger than those observed with Li-NHC complexes, and yaw angles in the range of 3 to 12º. The average K-C2 bond length is 3.048 Å which does not seem to be related to the degree of distortion of the K-NHC bond. Of the K-C4/ C5 close contacts, three are within the sum of the covalent radii of potassium and carbon, ranging from 3.083(4) to 3.161(4) Å, and are related to the growing number of 'wrong carbenes' that have been reported in recent years.[82]

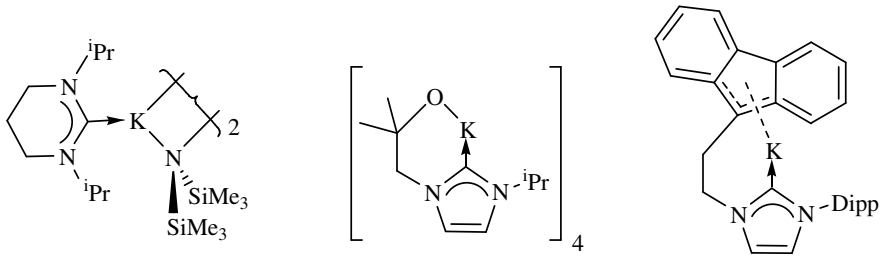

LXXVI **LXXVII** **LXXVIII**

Figure 19. Potassium NHC complexes.

Potassium salts of indenyl- and fluorenyl-functionalised NHCs have been reported by Danopoulos,[142, 155] and the fluorenyl- derivative has been structurally characterised, **LXXVIII** in Figure 19. It comprises polymeric potassium and bridging fluorenyl units in a 'zigzag' conformation, with two types of repeat unit. The first sees potassium ions sandwiched between two η^4-phenyl rings, whereas the second is sandwiched between one η^2- and one η^4-phenyl ring. The NHC binds to the potassium to complete the coordination sphere and displays K-$C_{carbene}$ bond lengths of 2.896–2.911 Å, which are considerably shorter than those observed in **LXXVII**. The pitch and yaw angles of 22-24º and 4-5º, respectively, are smaller than those seen in **LXXVII**.

1.5 Group 2 NHC complexes

1.5.1 Beryllium and Magnesium NHC complexes

Due to the particularly toxic nature of beryllium, there are a dearth of Be-NHC complexes, with the first of these being reported by Hermann *et. al.* in 1995.[156] This complex was formed by treatment of polymeric beryllium dichloride with a free carbene to yield the anionic complex $[ClBeL_3]^+Cl^-$ (L = C-($N^iPrCH)_2$), **LXXIX**, Figure 20, in high yield. The ^{13}C NMR spectrum shows a $C_{carbene}$ resonance in the expected region at δ = 174.8 ppm, and structural characterisation revealed that the beryllium exhibits a distorted tetrahedral geometry. There are two independent molecules per unit cell, which lie on a three fold axis rendering the three NHC ligands symmetry equivalent in each

molecule, although these pairs of molecules crystallise as a racemic mixture. Therefore, two Be-$C_{carbene}$ bond lengths of 1.807(3) and 1.822(3) Å are observed, and lie at the upper end of the range of single bond lengths. Complex **LXXX**, Figure 20, has been recently reported and was synthesised *via* treatment of diphenylberyllium with the corresponding free carbene.[157] Solid state structural analysis showed two unique molecules per unit cell, and the beryllium centres exhibit distorted trigonal planar geometry. The Be-$C_{carbene}$ bond lengths of 1.787(4) and 1.807(4) Å are slightly shorter than in **LXXIX**, due to the lower coordination number. The $C_{carbene}$ resonance of δ = 173.6 ppm in the ^{13}C NMR spectrum is also in good agreement.

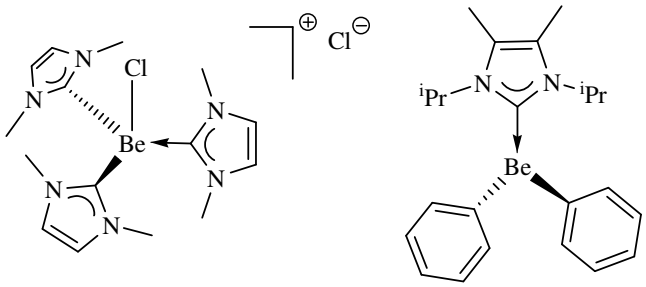

LXXIX **LXXX**

Figure 20. Beryllium NHC complexes.

The first magnesium NHC complexes were reported by Arduengo *et. al.* in 1993, and were NHC adducts of diethyl magnesium, **LXXXI** and **LXXXII** in Figure 21.[158] The ^{13}C NMR spectra demonstrated a $C_{carbene}$ resonance at δ = 180.1 and 194.8 ppm, respectively, and **LXXXII** was structurally characterised. The complex is dimeric in the solid state, formed through a bridging agostic interaction between one ethyl substituent and the opposing magnesium centre, and possesses a Mg-$C_{carbene}$ bond length of 2.279(3) Å. The same authors subsequently reported the metallocene derivative **LXXXIII**,[159] which was followed by Schumann *et. al.* publishing variations on this theme, **LXXXIV** and **LXXXV** in Figure 21.[160] Complex **LXXXIII** shows a Mg-$C_{carbene}$ bond length of 2.194(2) Å in the solid state, slightly shorter than seen in **LXXXII**, and a $C_{carbene}$ resonance at δ = 185.7 ppm in the ^{13}C NMR spectra. No ^{13}C NMR $C_{carbene}$ chemical shifts were reported for complexes **LXXXIV** and **LXXXV**, but **LXXXIV** was

structurally characterised and found to possess a Mg-$C_{carbene}$ bond length of 2.226(1) Å, longer than that in **LXXXIII,** which was postulated to be due to the larger steric profile of the N-substituents.

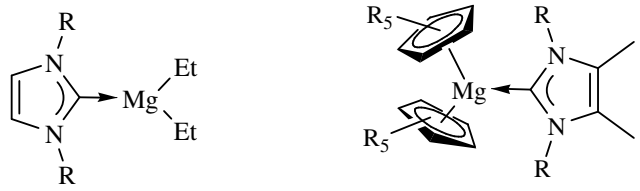

LXXXI, R = Mes
LXXXII, R = 1-adamantyl

LXXXIII, $R_5 = Me_5$, R = Me,
LXXXIV, $R_5 = Me_4H$, R = ^{i}Pr,
LXXXV, $R_5 = (^t BuSiMe_3)H_4$, R = ^{i}Pr

Figure 21. Magnesium-NHC adducts.

After this initial work examining simple Mg-NHC adducts, our group reported the synthesis of the amido-tethered Mg-NHC **LXXXVI**, Figure 22.[151] This complex was synthesised *via* deprotonation of the amine carbene precursor HL by dimethyl magnesium, and exhibits a $C_{carbene}$ resonance at δ = 185.4 ppm in the ^{13}C NMR spectrum. X-ray structural analysis revealed a mono-nuclear complex with a distorted-tetrahedral metal centre, and no coordinated solvent molecules. The Mg-$C_{carbene}$ bond lengths of 2.263(2) and 2.269(2) Å are average when compared to other Mg-NHC complexes, and the Mg-CN_2 fragment shows virtually no distortion from the anticipated trigonal planar geometry.

Complexes of an aryloxo-tethered NHC have been reported by Zhang *et. al.*,[161] and despite attempts to isolate sodium and potassium salts of these ligands only resulting in 1,2-migration of one of the N-alkyl substituents or ligand decomposition, *in-situ* deprotonation of the imidazolium precursor with a sodium base and subsequent addition of MesMgBr furnished **LXXXVII** in Figure 22. The ^{13}C NMR spectrum displayed a $C_{carbene}$ resonance at δ = 184.3 ppm, within the expected range, and structural characterisation showed the magnesium centres in a tetrahedral geometry with a dimeric structure containing bridging aryloxo groups. The Mg-$C_{carbene}$ bond length of 2.224(2) Å is within the range observed for other Mg-NHC complexes. A magnesium bromide

complex of a tripodal *tris*-(imidazol-2-ylidene)borate ligand has recently been reported, **LXXXVIII** in Figure 22, through the deprotonation of the ligand bromide precursor with MeMgBr, which represents the first use of a Grignard reagent in the formation of NHC complexes.[162] The solid state structure of **LXXXVIII** showed a four co-ordinate magnesium centre bound to the three NHCs, resulting in considerable distortion from ideal tetrahedral geometry and C-Mg-C angles closer to 90º. The bulky *tert*-butyl substituents resulted in a mononuclear complex with no coordinated solvent, and the average Mg-$C_{carbene}$ bond length of 2.21 Å is consistent with other Mg-NHC complexes, as is the $C_{carbene}$ resonance at δ = 185.0 ppm in the ^{13}C NMR spectrum.

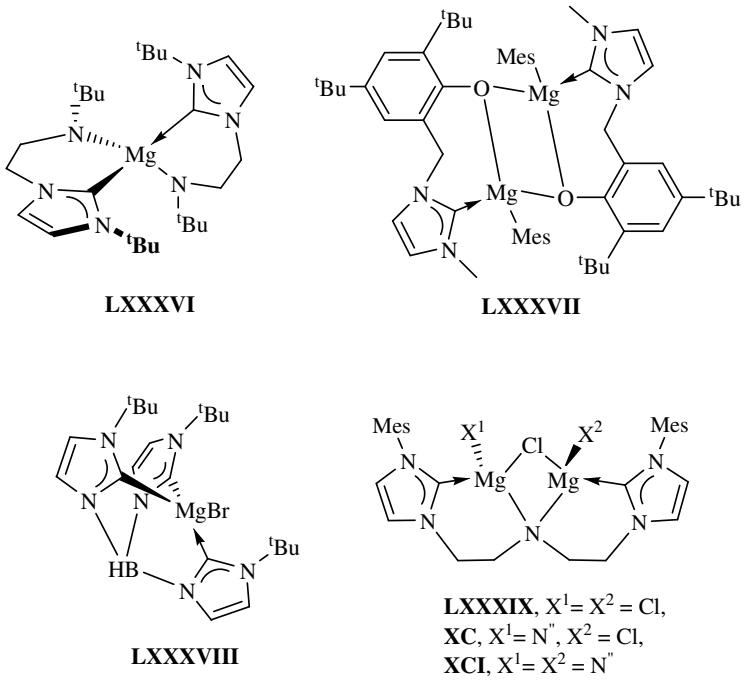

Figure 22. Anionic-NHC magnesium complexes.

Our group has very recently reported a series of magnesium complexes bearing a tridentate *bis*-NHC amide ligand, of which **LXXXIX**, **XC** and **XCI** are examples.[163] The proligand **LX**, $[H_2N\{CH_2CH_2(CHNCHCHNMes)\}_2]Cl_3$, is deprotonated by three equivalents of MeMgCl to yield the adduct of the amine-*bis*-carbene ligand and magnesium chloride $Mg_3(HL)Cl_6$, $[HN\{CH_2CH_2(MgCNCHCHNMes)\}_2]MgCl_6$. The

^{13}C NMR spectrum displayed a characteristic $C_{carbene}$ resonance at δ = 194.0 ppm, almost identical to **LXXXII**, and subsequent heating to 80 ºC for two hours produced **LXXXIX** as a dark purple compound, through elimination of $MgCl_2$ and deprotonation of the ligand with loss of HCl gas. The dark purple colour of this complex was thought to originate from either the formation of a ligand centred radical anion or through the non-innocence of the carbene π-heterocycle. An X-band EPR study of **LXXXIX** showed no resonances, so chemical reduction of $Mg_3(HL)Cl_6$ was attempted. Although treatment of $Mg_3(HL)Cl_6$ with one equivalent of potassium graphite resulted in deprotonation to form $Mg_3(KL)Cl_6$, treatment with a further equivalent of potassium graphite resulted in reduction of one of the NHC rings and formation of an organic radical, in which the electron resides in the NHC π-system, as identified by the *g* value obtained from the 10-line X-band EPR spectrum. The lack of strong colour associated with this organic radical compound further suggests that the dark purple colour of **LXXXIX** derives from a charge transfer process between adjacent π-systems. Complexes **XC** and **XCI** are formed by treatment of $Mg_3(HL)Cl_6$ with two and three equivalent of LiN", respectively, and both complexes have been structurally characterised. The ^{1}H NMR spectrum of **XC** suggests an asymmetric structure for the complex, due to the differing substituents bound to each magnesium, and the ^{13}C NMR spectrum shows two $C_{carbene}$ resonances at δ = 182.3 and 179.9 ppm, whereas **XCI** is a symmetric complex and only displays the one expected $C_{carbene}$ resonances at δ = 182.3 ppm in the ^{13}C NMR spectrum. The solid state X-ray structures of both complexes reveal that the magnesium centres are all four coordinate, with a distorted tetrahedral geometry. The asymmetric structure of **XC** suggested by NMR spectroscopy is confirmed, and large differences in the bond lengths from the bridging chloride to each magnesium centre of 2.5299(8) and 2.3767(8) Å can be observed. The Mg-$C_{carbene}$ bond lengths of 2.180(2) and 2.153(2) Å are shorter than previously reported examples and suggest that the ligand binds strongly to magnesium. Due to the symmetric structure of **XCI**, only one Mg-$C_{carbene}$ bond length of 2.199(2) Å is observed and lies within the typical range.

1.5.2 Calcium, Strontium and Barium NHC complexes

The known examples of heavier alkaline earth NHC complexes are all simple adducts. Arduengo *et. al.* first reported metallocene complexes based on pentamethylcyclopentadienyl (Cp^*) ligands as mono- and *bis*-adducts with tetramethylimidazol-2-ylidine [$C(NMeCMe)_2$], [$(Cp^*)_2M(C\{NMeCMe\}_2)_n$] (M = Ca, Sr, Ba, n = 1; M = Sr, Ba, n = 2).[159] This was followed up by Schumann and co-workers with examples of adducts of [$C(N^iPrCMe)_2$] with metallocenes of differing steric profiles, [$(C_5Me_4R)_2M(C\{N^iPrCMe\}_2)$] (M = Ca, R = H or ^{i}Pr; M = Sr, R = Me; M = Ba, R = ^{t}Bu).[160] All of these examples were synthesised via solvent displacement reactions. Very recently, Hill *et. al.* have reported a series of NHC adducts of heavier alkaline earth amide complexes [$MN"_2(C\{NRCH\}_2)$] (M = Ca, R = Mes or Dipp; M = Sr, R = Mes; M = Ba, R = Mes, and [MN"(Cl)$(C\{NRCH\}_2)$] (M = Ca, R = Mes), synthesised *via* treatment of the appropriate imidazolium precursor with the corresponding metal amide or addition of the free carbene to a solvent free metal amide.[164]

Data for M-$C_{carbene}$ bond lengths and ^{13}C NMR $C_{carbene}$ resonances, where available, for these complexes are collated in Table 1.

Table 1. Group 2 NHC complex metal-NHC bond lengths and ^{13}C NMR carbene chemical shift data.

Compound	M-$C_{carbene}$ bond length (Å)	$\delta\ ^{13}C\ C_{carbene}$ (ppm)[a]
$[(Cp^*)_2Ca(C\{NMeCMe\}_2)]$	2.562(2)	196.2
$[(C_5Me_4H)_2Ca(C\{N^iPrCMe\}_2)]$	2.593(4)	190.5
$[(C_5Me_4{}^iPr)_2Ca(C\{N^iPrCMe\}_2)]$	2.674(3)	195.9
$[CaN"_2(C\{NMesCH\}_2)]$	2.598(2)	193.3
$[CaN"_2(C\{NDippCH\}_2)]$	2.6259(2)[b]	195.4[b]
[CaN"(Cl)(C{NMesCH}$_2$)]	-	193.0
$[(Cp^*)_2Sr(C\{NMeCMe\}_2)]$	-	198.2
$[(Cp^*)_2Sr(C\{NMeCMe\}_2)_2]$	2.868(5), 2.854(5)	203.7
$[(C_5Me_5)_2Sr(C\{N^iPrCMe\}_2)]$	2.768(4)	-
$[SrN"_2(C\{NMesCH\}_2)]$	2.731(3)	199.0
$[(Cp^*)_2Ba(C\{NMeCMe\}_2)]$	2.951(3)	203.5
$[(Cp^*)_2Ba(C\{NMeCMe\}_2)_2]$	-	208.8
$[(C_5Me_4{}^tBu)_2Ba(C\{N^iPrCMe\}_2)]$	3.002(3)	200.4
$[BaN"_2(C\{NMesCH\}_2)]$	2.915(4)	-

[a] Spectra acquired in and referenced against C_6D_6. [b] Spectra acquired in d_8-toluene.

1.6 Group 3 NHC complexes

1.6.1 Scandium NHC complexes

Scandium NHCs were only recently reported by Cui *et. al.*, **XCIII** and **XCIV** in Figure 23.[165, 166] Both complexes were synthesised from the indenyl- or fluorenyl-functionalised free carbene ($C_9H_7CH_2CH_2(NCHCCHN)C_6H_2Me_3$-2,4,6 and $C_{13}H_7CH_2CH_2(NCHCCHN)C_6H_2Me_3$-2,4,6 respectively) made from a single deprotonation of the corresponding imidazolium bromide precursor HL, **XCII** in Figure 23, with $LiCH_2SiMe_3$. Subsequent treatment with the scandium *tris*-alkyl $Sc(CH_2SiMe_3)_3(THF)_2$ removed the remaining acidic cyclopentadienyl proton to furnish

the indenyl-NHC scandium *bis*(alkyl) complex **XCIII**, and the fluorenyl-substituted derivative, **XCIV**, respectively. The $C_{carbene}$ resonances in the ^{13}C NMR spectrum for both complexes of δ = 188.0 and 187.6 ppm, respectively, suggests the NHC is bound to the metal centre. Structural characterisation revealed a tetrahedral geometry at the scandium centre with Sc-$C_{carbene}$ bond lengths of 2.350(3) and 2.343(4) Å, respectively.

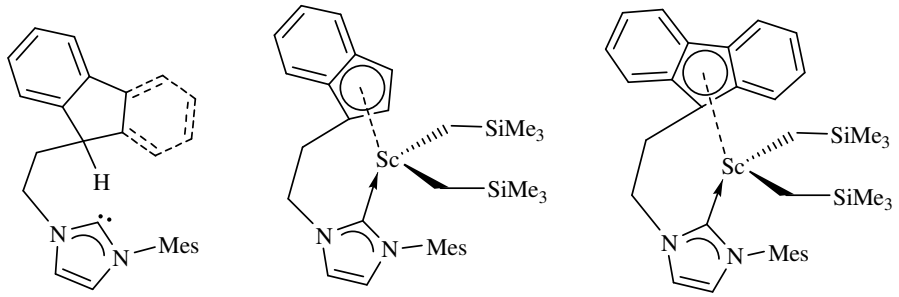

XCII **XCIII** **XCIV**

Figure 23. Indenyl- and fluorenyl-tethered NHC ligands and complexation to scandium.

The same authors have subsequently reported a scandium complex of a tridentate CCC-pincer *bis*(carbene) ligand, **XCV** in Eq. 9, as the dibromide THF solvate.[146] The synthesis of this complex is unusual, as the dibromide salt of the ligand precursor, **LXV**, was deprotonated *in situ* with three equivalents of Li^{n}Bu in the presence of $ScCl_3$; from this the scandium dibromide NHC complex **XCV** was isolated instead of the expected dichloride, Eq. 9. Complex **XCV** was structurally characterized by single crystal X-ray diffraction; the molecular structure contains a square-bipyramidal scandium geometry, the tridentate ligand adopts a *pseudo-meridional* conformation with average Sc-$C_{carbene}$ bond lengths of 2.390 Å. The ^{13}C NMR spectrum contains a $C_{carbene}$ resonance of δ = 193.1 ppm, which lies within the expected high-frequency region for a metal-bound NHC.

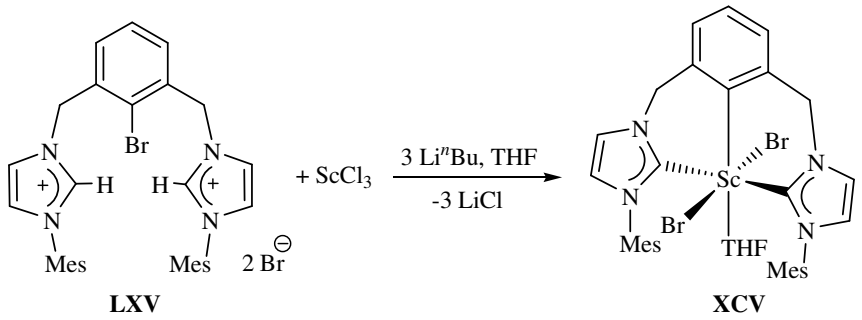

LXV **XCV**

Eq. 9

1.6.2 Yttrium NHC complexes

The first example of an yttrium-NHC complex was reported by Arduengo *et. al*. in 1994, as the mono-adduct [Y(thd)$_3$(C{NMeCMe}$_2$)], **XCVI** in Figure 24 (where thd = tetramethylheptanedioate).[167] The ^{13}C NMR spectrum showed a $C_{carbene}$ resonance at δ = 199.4 ppm as a doublet, due to coupling to the (I = 1/2) yttrium centre, with a coupling constant of $^1J_{YC}$ of 33 Hz.

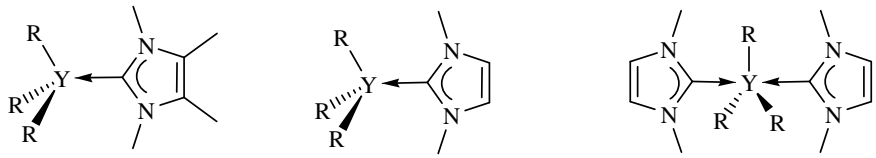

XCVI
R = Bu^{t}C(O)CHC(O)Bu^t

XCVII, R = N"
XCVIII, R = N(SiHMe$_2$)$_2$

IC
R = N(SiHMe$_2$)$_2$

Figure 24. Yttrium-NHC adducts.

A later report from Anwander *et. al*. examined mono-adduct formation of an NHC with yttrium *tris*(amido) compounds.[168] They initially examined the complex [YN"$_3$(C{NMeCH}$_2$)], **XCVII**, Figure 24, and characterised it by IR spectroscopy, elemental analysis and NMR spectroscopy, although the $C_{carbene}$ resonance in the ^{13}C NMR spectrum was not reported. They then investigated the mono-NHC complex [Y(N{SiHMe$_2$}$_2$)$_3$(C{NMeCH}$_2$)], **XCVIII,** and the *bis*-NHC complex

$[Y(N\{SiHMe_2\}_2)_3(C\{NMeCH\}_2)_2]$, **IC**, both shown in Figure 24, which were formed by treatment of the corresponding *bis*-THF adduct $Y(N\{SiHMe_2\}_2)_3(THF)_2$, with one or two equivalents of the free carbene, respectively. The ^{13}C NMR spectrum for **XCVIII** shows a $C_{carbene}$ resonance at δ = 190.3 ppm, resonating as a doublet, $^1J_{YC}$ = 49.6 Hz, which is larger than the value of 33 Hz previously reported, and indicates a strong bond between the yttrium and carbene group in solution. The $C_{carbene}$ resonance in **IC** was observed at δ = 194.0 ppm, although no coupling constant was given. Both complexes were structurally characterised. Complex **XCVIII** crystallises with two crystallographically independent molecules in the unit cell and the geometry at the yttrium centre is distorted tetrahedral, with an out-of-plane bending 'pitch' of the NHC plane from the Y-NHC plane of 8.7º, considerably smaller than those observed in group one metal complexes. The five-coordinate yttrium centre in **IC** is distorted trigonal bipyramidal, with the two NHC ligands diametrically opposed in this more sterically encumbered complex. The Y-$C_{carbene}$ bond lengths of 2.55(1) and 2.560(9) Å in **XCVIII** and 2.648(8) and 2.671(9) Å in **IC** are consistent with the higher coordination number in the latter complex.

The first N-functionalised NHC yttrium complex was reported by our group, **C** in Scheme 11, and was synthesised through treatment of $YN"_3$ with an equivalent of the lithium bromide adduct of the amine-carbene ligand precursor **LXXI**, accompanied by loss of HN".[136] Single crystal X-ray structural characterisation revealed the geometry at the yttrium centre as distorted tetrahedral with a Y-$C_{carbene}$ bond length of 2.501(5) Å. The ^{13}C NMR spectrum displayed an yttrium-coupled $C_{carbene}$ resonance as a doublet at δ = 186.3 ppm, with a coupling constant of $^1J_{YC}$ = 54.7 Hz, which was the largest yet reported value for an yttrium-NHC or even an yttrium-alkyl complex at the time. This large coupling constant possibly signifies a very strong σ-interaction between the two atoms.

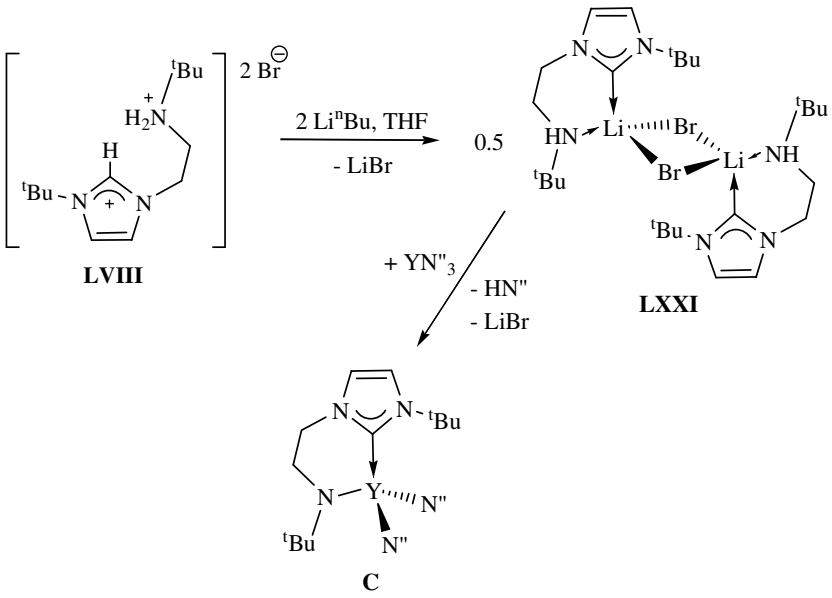

Scheme 11. Synthesis of a yttrium complex bearing an amide-functionalised NHC ligand.

A series of preliminary competition studies with potential donor ligands were undertaken with **C** in order to probe the lability of the Y-NHC bond. The addition of one equivalent of THF, Et_2O, PPh_3 or Me_3NO showed no reaction, but TMEDA or $OPPh_3$ successfully displaced the NHC group. These reactions were monitored by ^{13}C NMR spectroscopy, with the last two reagents resulting in the loss of $^1J_{YC}$ coupling and therefore the Y-NHC bond (*vide infra*).

Following these investigations, complex **C** was found to be an excellent bifunctional catalyst for the ring opening polymerisation of *rac*-lactide, producing highly heterotactic poly(*rac*-lactide) with low polydispersity. The bifunctional nature of the catalyst resulted from the lactide binding to the Lewis acidic yttrium centre, after which the labilized NHC functioned as a Lewis base to ring-open the monomer by a nucleophilic mechanism.[120]

Subsequently, our group reported that the treatment of **C** with potassium naphthalenide in DME/ diethyl ether at -78 ºC afforded complex **CI**, Scheme 12, formally as the product of deprotonation and subsequent migration of the C2 carbene from yttrium to the incorporated potassium cation, and represents the first example of a C,C-bridged NHC complex.[169] The ^{13}C NMR spectrum shows C2 and C4 carbene resonances at δ =

199.2 and 167.5 ppm, respectively, with the latter of these manifesting as a yttrium coupled doublet, $^{1}J_{YC}$ = 62 Hz. This is the largest coupling constant so far reported, and indicates a very strong interaction between yttrium and the C4 carbene. A solid state X-ray structure determination revealed that **CI** is dimeric in the solid state, with each four coordinate yttriate centre being N-bound to two N" ligands, one amide-N of the NHC tether and the newly formed C4 carbanion of the NHC backbone. The Y-C4 bond length of 2.447(2) Å is significantly shorter than the Y-C2 bond length in **C**, in agreement with the large observed $^{1}J_{YC}$ coupling constant, and is at the short end of the Y-C single σ-bond range. Changing the reducing agent to KC_8 resulted in no reaction. As complex **CI** is the product of a deprotonation reaction, treatment of **C** with a base was investigated. Although the use of KN" resulted in only trace amounts of **CI** being isolated, when KMe was used as the deprotonating reagent, the product could be isolated in high yield, 82 %.

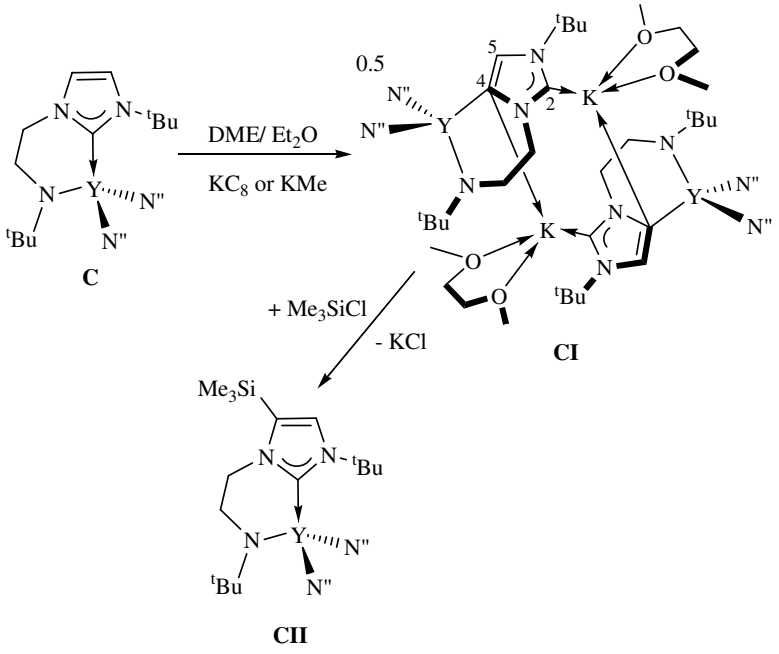

Scheme 12. Synthesis of a bimetallic Y/K amido-NHC complex and regioselective silylation.

Complex **CI** can be quenched with electrophiles, such that upon addition of Me_3SiCl, the regioselectively C4-silylated complex **CII** can be isolated in quantitative yield, with concomitant elimination of KCl, Scheme 12. The ^{13}C NMR spectrum shows a lower

frequency chemical shift for the Y-C2 resonance at δ = 172.7 ppm, which is again yttrium-coupled, $^{1}J_{YC}$ = 55.8 Hz with a very large coupling constant.

The yttrium complex **CIII**, Figure 25, was synthesised from the reaction of YN"$_3$ with one equivalent of the lithium chloride adduct of the aminodicarbene ligand, [(LiCl)$_3$HL], and the complexation of yttrium again confirmed by ^{13}C NMR spectroscopy, which showed an yttrium coupled doublet at δ = 194.3 ppm, $^{1}J_{YC}$ = 48 Hz.[152] This coupling is comparable to other yttrium-NHC complexes, but is smaller than that observed in the previously discussed bidentate amidocarbene complexes such as **C**. The molecular structure of **CIII** shows Y-$C_{carbene}$ bond lengths of 2.574(3) and 2.565(3) Å, which lie within reported values, although are longer than those observed in the bidentate amidocarbene complexes. The geometry at the yttrium centre is distorted trigonal bipyramidal with the tridentate ligand occupying a *meridional* configuration about the metal.

Complex **CIII** could be reliably isolated as the only product from this reaction, except upon one occasion when the dichloride **CIV** was isolated. All attempts at a rational synthesis of this complex from YCl$_3$(THF)$_3$ failed. This complex was characterised by NMR spectroscopy and elemental analysis, and showed a yttrium coupled $C_{carbene}$ resonance at δ = 192.8 ppm in the ^{13}C NMR, with a coupling constant $^{1}J_{YC}$ = 47 Hz. The lability of the Y-NHC bond was investigated *via* a series of competition experiments with triphenyl- and trimethyl-phosphine oxides. Although reactions of **CIII** only resulted in decomposition products, those of complex **CIV** yielded tractable precipitates from benzene which were formulated as the simple triphenyl- and trimethyl-phosphine oxide adducts. Both complexes showed yttrium coupled $C_{carbene}$ resonances in the ^{13}C NMR spectra at δ = 193.0 ppm, $^{1}J_{YC}$ = 38 Hz for the remaining bound carbene, indicating that only products of one NHC displacement could be isolated in these systems.

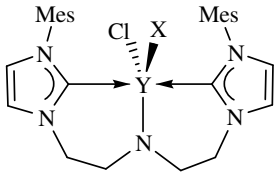

CIII, X= N"
CIV, X= Cl

Figure 25. Yttrium amido-*bis*-NHC complex.

Our group has very recently reported the synthesis of complex **CV**, Figure 26, through treatment of $YCl_3(THF)_3$ with three equivalents of the corresponding potassium ligand salt, **LXXVII**. Solutions of this complex exhibit a ^{13}C NMR spectrum with a $C_{carbene}$ resonance at δ = 197.3 ppm, at the high-frequency end of reported carbene chemical shifts, and with a $^{1}J_{YC}$ coupling constant of 31 Hz.[60] The solid state structure of **CV** revealed that the three *meridionally*-disposed ligands form a *pseudo*-octahedral geometry about the yttrium centre. Although the complex is not C_3-symmetric according to crystallography, at room temperature only one set of ligand resonances was measured in the ^{1}H NMR spectrum. However, cooling a solution of **CV** revealed the magnetic inequivalence of the three ligands, confirming that the structurally characterised single crystal was indeed representative of the bulk. The average Y-$C_{carbene}$ bond length of 2.588(12) Å is comparable to previously discussed examples.

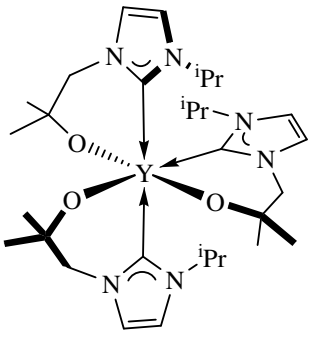

CV

Figure 26. Yttrium *tris*-alkoxy NHC complex.

Shen *et. al.* have reported the synthesis of aryloxy-functionalised NHC yttrium complexes, **CVI** and **CVII** in Scheme 13, through treatment of $[LiY(N^iPr_2)_4]$ with the corresponding ligand chloride salt and Li^{n}Bu in a 1:3:2 molar ratio.[131] Complex **CVI** was isolated when the reaction was conducted at -78 ºC. The ^{13}C NMR spectrum of **CVI** contained a very high-frequency $C_{carbene}$ resonance at δ = 199.9 ppm, although the magnitude of the expected yttrium coupling has not been reported. An X-ray diffraction study revealed the geometry at the yttrium centre to be distorted octahedral with an average Y-$C_{carbene}$ bond length of 2.621(3) Å, which is longer than in other Y-NHC examples.

When the same reaction is conducted at room temperature, the mono-NHC yttrium complex **CVII**, bearing a methylene-bridged *bis*(aryloxo) ligand instead of the expected ethyl-bridge, is isolated. This complex has a $C_{carbene}$ resonance at δ = 198.4 ppm in the ^{13}C NMR spectrum. The molecular structure shows a *pseudo*-octahedrally coordinated yttrium cation with a Y-$C_{carbene}$ bond length of 2.576(5) Å, closer to that in other examples. The mechanism involved in the formation of **CVII** remains unproven, although a reaction pathway proceeding *via* hydrogen transfer from the phenol to the carbene centre, breaking the benzylic N-C bond was proposed. This then requires an attack of the unsaturated ligand fragment by a metal-bound amido group to release a tertiary amine byproduct and allow the methylene-bridge coupled phenol to form.

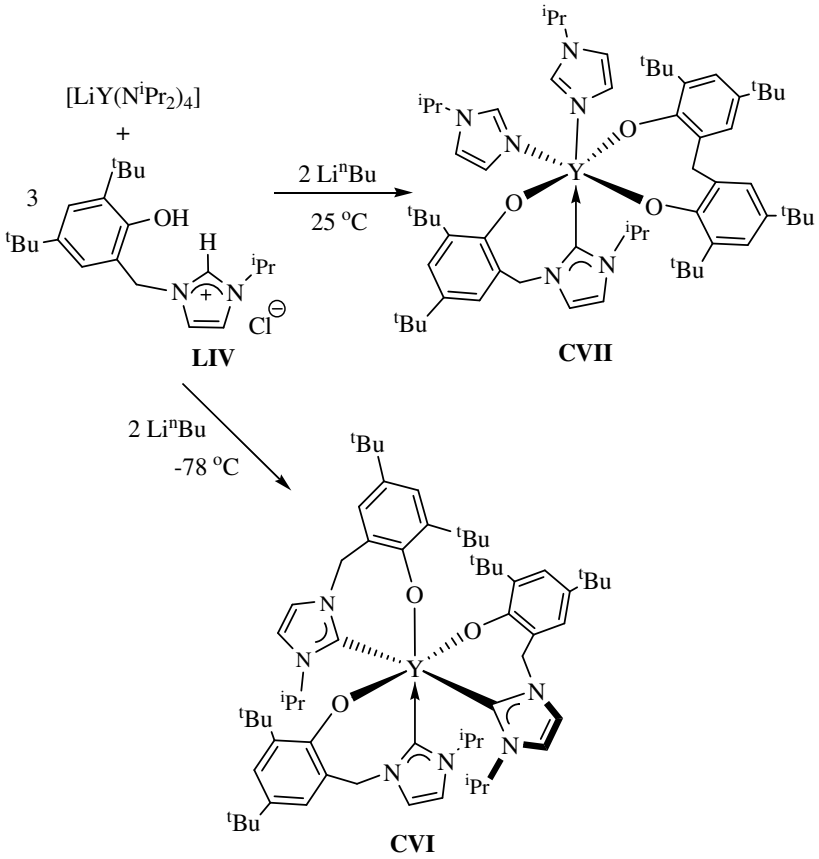

Scheme 13. Yttrium aryloxo-tethered NHC complexes.

Yttrium *bis*(alkyl) analogues of complexes **XCIII** and **XCIV**, Figure 23, bearing indenyl- and fluorenyl-functionalised NHC ligands, were reported at the same time by Cui *et. al.*, such that *in-situ* deprotonation of the corresponding imidazolium bromide precursor with $LiCH_2SiMe_3$, followed by addition of $[Y(CH_2SiMe_3)_3(THF)_2]$ furnished the indenyl-functionalised complex $[(Ind\text{-}NHC)Y(CH_2SiMe_3)_2]$**, CVIII,** and the fluorenyl-functionalised complex $[(Flu\text{-}NHC)Y(CH_2SiMe_3)_2]$, **CIX**, respectively (Ind-NHC = $C_9H_6CH_2CH_2(NCHCCHN)C_6H_2Me_3$-2,4,6, Flu-NHC = $C_{13}H_8CH_2CH_2(NCHCCHN)C_6H_2Me_3$-2,4,6).[165, 166] Both the indenyl and fluorenyl complexes exhibit yttrium-coupled $C_{carbene}$ resonances in the ^{13}C NMR spectra at δ = 191.2 ppm, $^1J_{YC}$ = 46.0 Hz, and δ = 190.8 ppm, $^1J_{YC}$ = 45.8 Hz, respectively, and in the solid state the former was proven to adopt a tetrahedral geometry at the yttrium centre with a Y-$C_{carbene}$ bond length of 2.501(3) Å. Both of these complexes were found to be

active catalysts for the 3,4-selective living polymerisation of isoprene to make syndiotactically enriched crystalline polymers, Eq. 10; complex **CIX** displays an enhanced selectivity and polymer polydispersity over complex **CVIII**.

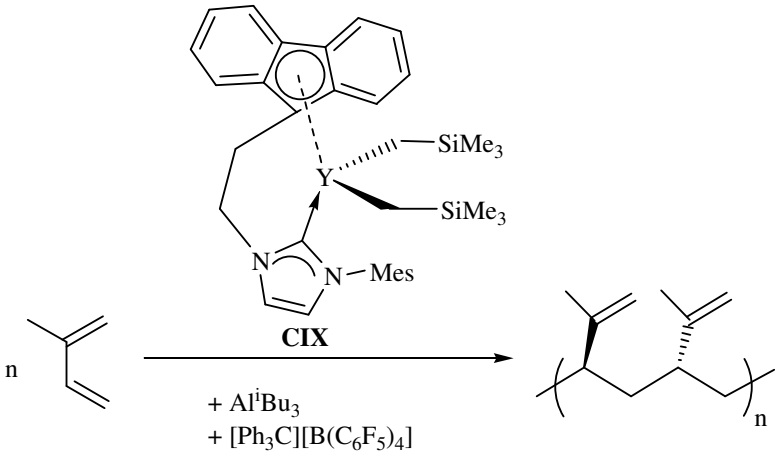

Eq. 10

Prior to these Ind-NHC and Flu-NHC reports, Danopoulos *et. al.* had reported early transition metal adducts of related ligands.[142] They subsequently reported an yttrium alkyl complex supported by the indenyl-functionalised NHC ligand, [1-(4,7-Me_2-C_9H_4)CH_2CH_2(C{NCHCHN(2,4,6-Me_3-C_6H_2)})Y(CH_2SiMe_3)(μ-Br)]$_2$, **CX**, which, despite being inaccessible from salt elimination routes, was successfully synthesised by treatment of [Y(CH_2SiMe_3)$_3$(THF)$_2$] with one equivalent of the corresponding imidazolium bromide ligand precursor, Figure 27.[155] The complex **CX** decomposes with time in solution, such that no ^{13}C NMR spectra could be obtained, but a structural analysis revealed the molecular structure as a centrosymmetric bromide-bridged dimer with the yttrium centre in a square-pyramidal geometry, and a Y-$C_{carbene}$ bond length of 2.547(5) Å.

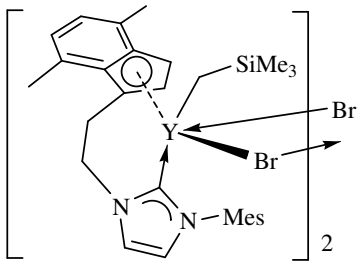

CX

Figure 27. Indenyl-functionalised NHC yttrium bromide complex.

1.6.3 Lanthanum NHC complexes

The only reported lanthanum-NHC complex is that of the simple adduct [LaN"$_3$(C{NMeCH}$_2$)], **CXI**, which was characterised by IR and NMR spectroscopies and elemental analysis. No further details have been reported.[168]

1.7 Lanthanide NHC complexes

1.7.1 Cerium(III) NHC complexes

The first Ce-NHC complexes, reported by our group in 2005,[170] contained an anionic, amido-functionalised NHC ligand. Thus, complex **CXII**, Figure 28, was synthesised *via* a transamination reaction between CeN"$_3$ and one half equivalent of the amine-NHC lithium bromide adduct **LXXI**, shown in Scheme 11. Structural analysis showed the complex to possess a Ce-$C_{carbene}$ bond length of 2.670(2) Å in the solid state, comparable to that seen in the four-coordinate U^{III} NHC complex **CLVII**, and long Ce-$N_{silylamide}$ bond lengths of 2.418(2) and 2.404(2) Å, a consequence of the sterically congested metal centre. On one occasion, complex **CXIII** was isolated from the above reaction, which subsequently proved to be unrepeatable, and formed *via* a ligand exchange reaction between the eliminated LiBr from the starting material and the product **CXII**.

Structural analysis of **CXIII** revealed a slightly longer Ce-$C_{carbene}$ bond length of 2.699(2) Å than observed in **CXII**, possibly attributable to the larger coordination number of the metal centre. The Ce-$N_{silylamide}$ bond length of 2.376(2) Å is again towards the higher end of reported values, although shorter than in **CXII**, and the two Ce-Br bond lengths of 3.026(2) and 3.056(2) Å are predictably long due to their bridging nature.

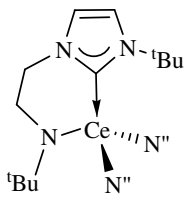

CXII

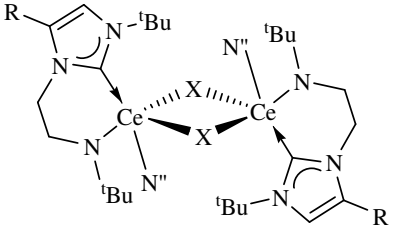

CXIII, X = Br, R = H
CXIV, X = I, R = H
CXV, X = I, R = $SiMe_3$

Figure 28. Cerium amido-NHC complexes.

Although complex **CXIII** is a potentially useful starting point to investigate further metathesis chemistry, the synthesis was not ideal and obviated its possible utility. As the bromide originated from the LiBr incorporated in the starting material, **CXII** was treated with LiI in a rational route to target the iodide anologue, **CXIV**. An X-ray diffraction study of **CXIV** revealed it to be isomorphous with **CXIII**.

Treatment of **CXII** with an equivalent of Me_3SiI afforded the regioselectively C4-silylated iodide-bridged dimer **CXV** and structural characterisation shows a Ce-$C_{carbene}$ bond length of 2.728(8) Å; it is isostructural with the neodymium compound **CXIX**, below.

Complexes **CXIII–CXV** are rare examples of heteroleptic lanthanide complexes of the type $LnL^1L^2L^3$ due to the prevalence of redistribution reactions for these metals with no orbital constraints on their bonding. The isolation of such kinetically inert heteroleptic complexes is normally limited to the smaller, heavier, lanthanides.

Soon after the report of complexes **CXII–CXV**, Ephritikhine published complexes **CXVI** and **CXVII**, Figure 29.[171] These are both adducts of the simplest two-electron donor NHC, C-$(NMeCMe)_2$, and can be synthesised by mixing the free NHC with the corresponding Ce^{III} starting material. Structural characterisation of both **CXVI** and **CXVII** confirmed the *pseudo*-tetrahedral geometry at each metal centre and Ce-$C_{carbene}$ bond lengths of 2.724(4) and 2.768(5) Å, respectively, which are longer than in **CXII** (in agreement with the higher coordination number at Ce).

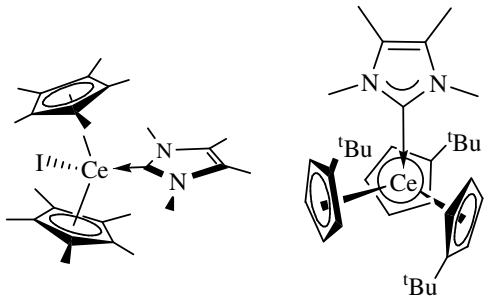

CXVI **CXVII**

Figure 29. Cerium Cp complexes with an NHC donor.

1.7.2 Neodymium NHC complexes

There are no reported praseodymium NHC complexes.

Our group has recently reported a series of neodymium NHC complexes synthesised from complex **CXVIII**, Scheme 14, which was synthesised in an analogous manner to the cerium congener, **CXII** in Figure 28, *via* the reaction of $NdN"_3$ with **LXXI**, shown in Scheme 11.[172] Subsequent treatment of **CXVIII** with Me_3SiI afforded **CXIX**, as the C4-silylated iodide-bridged dimer, in an analogous fashion to **CXV**. Both complexes were structurally characterised; **CXVIII** is isomorphous with **CXII**. In **CXVIII** the neodymium centre has a distorted tetrahedral geometry with a Nd-$C_{carbene}$ bond length of 2.609(3) Å. Complex **CXIX** is dimeric in the solid state with a central *transoid* Nd_2I_2 four membered ring, with five-coordinate neodymium centers in a distorted trigonal bipyramidal geometry. The Nd-$C_{carbene}$ bond length of 2.656(5) Å is longer than that in

CXVIII, and reflects the higher coordination number as well as the softer nature of the silylated NHC. In an attempt to probe the reduction chemistry of complex **CXIX**, with the possibility of isolating an activated dinitrogen complex, it was treated with potassium graphite under a dinitrogen atmosphere, but the reaction yielded **CXX** in low yield as the only isolable product. This results from ligand redistribution/ disproportionation, and demonstrates the subtle electronic requirements for reductive activation at these metal centers. In the solid state structure of complex **CXX**, the neodymium centre adopts a distorted tetrahedral geometry with a Nd-$C_{carbene}$ bond length of 2.648(3) Å, which is longer than that observed in **CXVIII** but the same as in **CXIX**, despite the larger coordination number of the metal centre in this complex. The only difference between complexes **CXVIII** and **CXX** is the silylated C4 position in the latter, and this allows for a direct probe of the effect of incorporation of an electropositive silicon atom into the NHC σ-framework. The elongation of the Nd-$C_{carbene}$ bond length between **CXVIII** and **CXX** is commensurate with this.

Despite the reduction of **CXIX** proving unsuccessful, salt elimination chemistry is facile, so that a reaction between **CXIX** and two equivalents of NaN_3 furnishes **CXXI**, Scheme 14. The solid state structure reveals a Nd-$C_{carbene}$ bond length of 2.672(3) Å, longer than in the other five-coordinate complex **CXIX**, while the average N-N bond distances of 1.16 Å are consistent with double bonds.

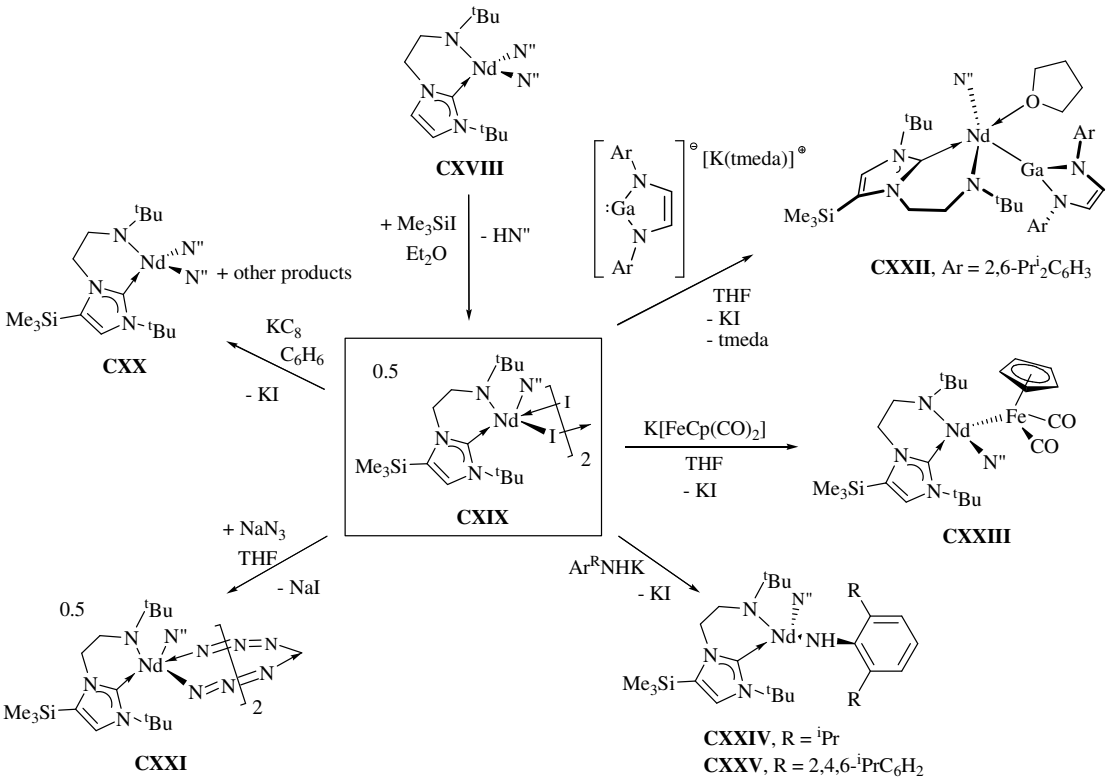

Scheme 14. Neodymium amido-NHC complexes and reactivity studies.

In pursuance of the utility of **CXIX** in salt elimination chemistry, a reaction between **CXIX** and the anionic gallium heterocycle $[Ga(NArCH)_2][K(tmeda)]$ (Ar = 2,6-$^{i}Pr_2C_6H_3$), which is valence isoelectronic with an NHC, was undertaken and yielded **CXXII**, Scheme 14, which is the first example of an f-element-gallium bond.[173] X-ray structural characterisation revealed the neodymium centre to be in a distorted trigonal bipyramidal geometry, with an unprecedented Nd-Ga bond length of 3.2199(3) Å and a Nd-$C_{carbene}$ bond length of 2.669(2) Å, which is at the higher end of reported Nd-NHC bonds and reflects the presence of the nucleophilic, anionic gallium heterocycle. A DFT study on a model of complex **CXXII** suggested a Nd-Ga bond with a small degree of covalent character.

Our group has also very recently reported complex **CXXIII**, synthesised by treatment of **CXIX** with one equivalent of $K[CpFe(CO)_2]$ (K[Fp]) in THF, Scheme 14, in which the product contains an unsupported Nd-Fe bond.[174] The ^{1}H NMR spectrum of **CXIII**

contains a set of paramagnetically shifted ligand resonances between δ = 70 and -6 ppm and possesses a solution magnetic moment of 3.41 BM. Structural analysis reveals the geometry at the Nd cation to be distorted tetrahedral, with a Nd-Fe bond length of 2.9942(7) Å and a Nd-$C_{carbene}$ bond length of 2.606(4) Å, comparable to that observed in the parent unsilylated **CXVIII**. Computational analysis indicated that the Nd-Fe bond is principally ionic in character, supported by FTIR measurements which showed a shift of the asymmetric $\nu(CO)_{as}$ stretch from 1770 cm^{-1} in K[Fp] to 1845 cm^{-1} in **CXXIII**. The magnitude of this shift ($\delta\nu_{as}$) of 75 cm^{-1} is smaller than the ($\delta\nu_{as}$) of 146 cm^{-1} observed in [$Me(CH_2SiMe_3N)_3$Ti-Fp], in which a significant Ti-Fe π-backbonding component was ascribed.[175]

Subsequently, treatment of **CXIX** with potassium aryl-amides afforded complexes **CXXIV** and **CXXV**, Scheme 14, which display dichroic behaviour in solution; dilute solutions (or samples viewed through a short path length) appear pale blue, whereas more concentrated (or longer path length) solutions appear dark red.[176] The solid-state structures of **CXXIV** and **CXXV** exhibit a neodymium centre with distorted tetrahedral geometry and similar Nd-$C_{carbene}$ bond lengths of 2.612(4) and 2.603(6) Å, respectively, which lie at the shorter end of reported Nd-NHC bonds. The Nd-NHC bond in **CXXV** is considerably more distorted from idealised trigonal planar geometry than in **CXXIV**, as a consequence of the much greater steric profile of the terphenyl ligand compared to the Dipp group. The 'pitch' angles, Figure 17, in **CXXIV** and **CXXV** are 6.5º and 18.0º, respectively, whilst the 'yaw' angles are 4.3º and 0.9º, respectively. Attempts to effect a second deprotonation of the primary amide moiety to afford anionic imido species yielded only ligand exchange or decomposition products.

Very recently, Shen *et. al.* have reported the use of a salicylaldimine-functionalised NHC ligand in the synthesis of a neodymium *bis*(NHC) mono-bromide complex, L_2NdBr, **CXXVI** in Eq. 11, (L = [3,5-$^tBu_2$-2-(O)C_6H_2CH=NCH_2CH_2(C{NCHCHN^{i}Pr})].[177]

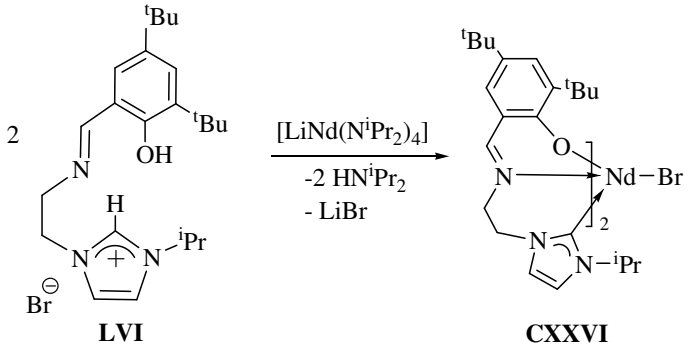

Eq. 11

This complex was accessed *via* a synthetically straightforward and useful protonolysis route involving a lanthanide amide $[LiNd(N^iPr_2)_4]$ and two equivalents of the imidazolium bromide ligand precursor **LVI**, and afforded **CXXVI** in good yield. This complex was structurally characterised and found to be monomeric and coordinatively saturated in the solid state, precluding the formation of bromide-bridged dimers that have been seen previously. The authors describe the geometry at the neodymium centre as a capped octahedron with equal Nd-$C_{carbene}$ bond lengths of 2.717(3) Å, longer than other neodymium-NHC complexes. But if the higher coordination number of Nd is taken into account the ligand is deemed to enforce stronger binding of the NHC group to the Nd cation.

1.7.3 Samarium(II) NHC complexes

Divalent samarium NHC complexes were amongst the first examples of lanthanide-NHC complexes; all those reported to date are simple adducts of substituted samarocenes, Figure 30.

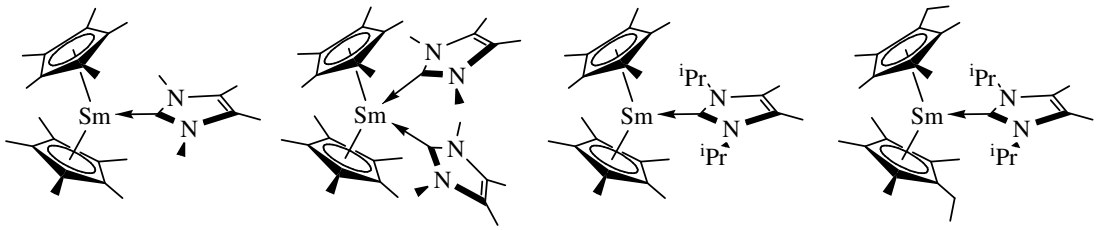

CXXVII **CXXVIII** **CXXIX** **CXXX**

Figure 30. Samarium NHC adducts.

The complexes were synthesised by displacement reactions of solvated samarocenes with free carbenes, some of which were structurally characterised. A comparison of the range of complexes and the Sm-$C_{carbene}$ bond lengths observed in the solid state are displayed in Table 2.

Table 2. Samarium NHC metal carbene bond lengths.

Compound	M-$C_{carbene}$ bond length (Å)	Reference
CXXVII	-	[178]
CXXVIII	2.837(7), 2.845(7)	[178]
CXXIX	2.782(3)	[179]
CXXX	-	[180]

1.7.4 Samarium(III) NHC complexes

The trivalent NHC adduct, $[(C_5H_4\text{-}^tBu)_2SmCl(C\{N^iPrCMe\}_2)]$, **CXXXI**, was synthesised by the reaction between $[(C_5H_4\text{-}^tBu)_2SmCl]_2$ and the free carbene.[181] Structural analysis revealed a Sm-$C_{carbene}$ bond length of 2.62(2) Å and complex **CXXXI** was evaluated as a catalyst for isoprene polymerisation, but was found to be almost inactive. The complex was found to be unstable in benzene solution with respect to

ligand redistribution, resulting in an equilibrium mixture of $Sm(C_5H_4\text{-}^tBu)_3$ and $[(C_5H_4\text{-}^tBu)SmCl_2(C\{N^iPrCMe\}_2)]$.

A computational analysis on the nature of the samarium-NHC bond has also been reported,[182] in which it was concluded that NHC to metal σ-donation was the main component involved in bonding, with a negligible π-component.

The amido-functionalised NHC samarium complex, **CXXXII** in Scheme 15, is synthesised in an analogous fashion to that of the yttium, cerium and neodymium congeners, **C** in Scheme 11, **CXII** in Figure 28 and **CXVIII** in Scheme 14, from a reaction between $SmN"_3$ and the lithium bromide amino-carbene adduct **LXXI**, see Scheme 11.[136] A single crystal X-ray diffraction study showed a distorted tetrahedral geometry at the samarium centre with a $Sm\text{-}C_{carbene}$ bond length of 2.588(2) Å, which is shorter than those in the examples described above. The outcome of reactions of **CXXXII** with reductants was dependent on the reductant employed.[169] With KC_8 reduction, a dark purple oil readily formed, characteristic of the formation of a divalent samarium species, although repeated attempts to crystallise the purple product from this failed and only decomposition products were isolated.

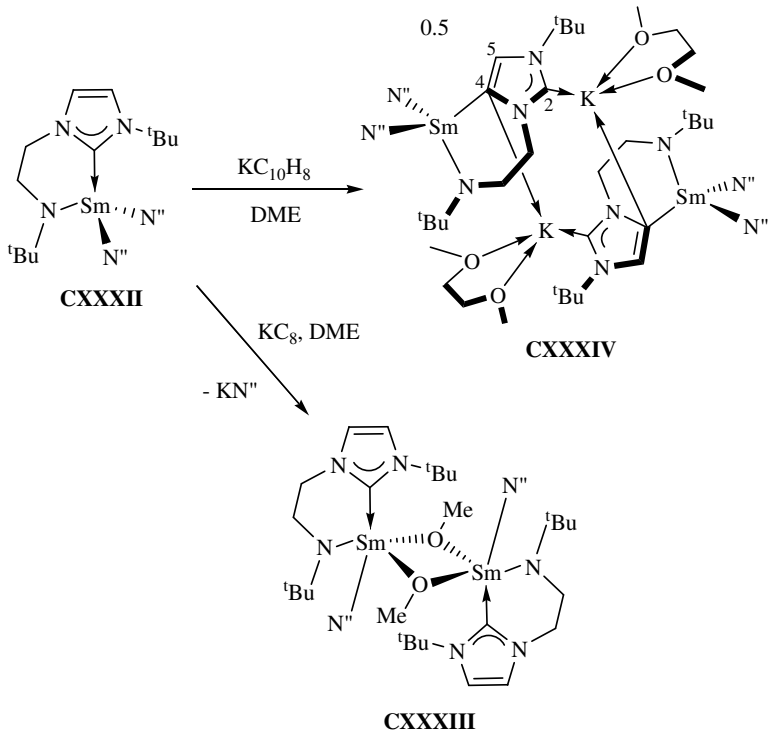

Scheme 15. Samarium amido-NHC complexes.

Brief heating of the purple reaction mixture resulted in a colour change to dark red, from which **CXXXIII** was crystallised as the ether cleavage product. The solid state structure is dimeric, constructed around a *transoid* Sm_2O_2 four-membered core, which is strictly planar as a consequence of residing over a crystallographic inversion centre. The samarium centre adopts a distorted trigonal bipyramidal geometry and displays a Sm-$C_{carbene}$ bond length of 2.682(3) Å, which is longer than that observed in **CXXXII**, a result of the higher coordination number.

Treatment of **CXXXII** with potassium naphthalenide in DME (1,2-dimethoxyethane) affords the bimetallic complex **CXXXIV**, Scheme 15, which is analogous to the yttrium congener **CI** in Scheme 12. Both complexes are isostructural in the solid state, with **CXXXIV** displaying a Sm-C4 bond length of 2.509(3) Å.

The samarium analogue of L_2NdBr, see **CXXVI** in Eq. 11, **CXXXV**, (L = [3,5-^{t}Bu$_2$-2-(O)C_6H_2CH=NCH_2CH_2(C{NCHCHN^{i}Pr})] was reported in the same paper, is isostructural in the solid state and displays a Sm-$C_{carbene}$ bond length of 2.685(6) Å.[177]

1.7.5 Europium(III) NHC complexes

There are only two examples of europium NHC complexes. The first is the analogue of the yttrium complex **XCVI**, see Figure 24, $[Eu(thd)_3(C\{NMeCMe\}_2)]$ **CXXXVI**, (where thd = $Bu^tC(O)CHC(O)^tBu$), in which the europium centre adopts a trigonal bipyramidal geometry and displays a Eu-$C_{carbene}$ bond length of 2.663(4) Å.[167] The second example is the europium analogue of **CXXXII** in Scheme 15, **CXXXVII**, and is recorded as a private communication in the Cambridge crystallographic database (#605446). In this complex the Eu-$C_{carbene}$ bond length is 2.562(3) Å.

1.7.6 Mid-lanthanide NHC complexes

There are no reported gadolinium, terbium or dysprosium NHC complexes.

1.7.7 Holmium(III) NHC complexes

The only examples of holmium NHC complexes are the *bis*(alkyl) analogues of complexes **XCIII** and **XCIV**, bearing indenyl- and fluorenyl-functionalised NHC ligands.[165, 166] The indenyl-functionalised complex $[(Ind\text{-}NHC)Ho(CH_2SiMe_3)_2]$ **CXXXVIII**, and the fluorenyl-functionalised complex $[(Flu\text{-}NHC)Ho(CH_2SiMe_3)_2]$ **CXXXIX**, were synthesised by *in-situ* deprotonation of the corresponding imidazolium bromide precursor with $LiCH_2SiMe_3$, followed by addition of $[Ho(CH_2SiMe_3)_3(THF)_2]$, Figure 31.

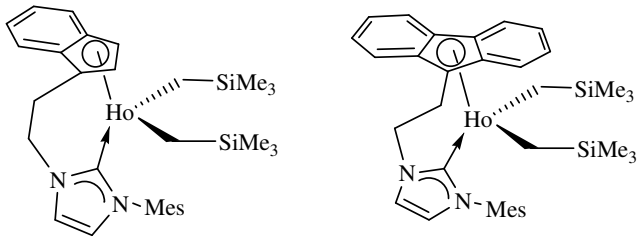

CXXXVIII **CXXXIX**

Figure 31. Holmium indenyl- and fluorenyl-NHC complexes.

The solid state structures of both complexes were determined and showed Ho-$C_{carbene}$ bond lengths of 2.490(2) and 2.484(3) Å, respectively, where both holmium metal centres adopt a tetrahedral geometry.

1.7.8 Erbium(III) NHC complexes

Anwander *et. al*. reported the first erbium NHC complex in 1997 as the adduct of erbium trichloride, $[ErCl_3(C\{NMeCH\}_2)_3]$, **CXL** in Figure 32, although the solid state structure was not obtained.[168] Ten years later, Schumann *et. al*. reported mono- and *bis*(NHC) adducts of erbium *tris*(alkyls), formed by solvent displacement reactions, $[(Me_3SiCH_2)_3Er(THF)(C\{N^iPrCMe\}_2)]$ **CXLI**, and $[(Me_3SiCH_2)_3Er(C\{N^iPrCMe\}_2)_2]$ **CXLII** in Figure 32.[183] Although suitable single crystals of **CXLII** could not be grown, the solid state structure of **CXLI** was determined and the erbium ion was found to adopt a distorted bipyramidal geometry and displayed an Er-$C_{carbene}$ bond length of 2.520(6) Å.

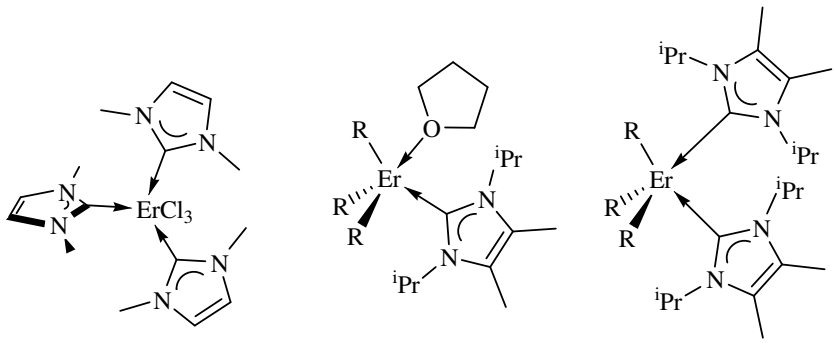

CXL **CXLI** **CXLII**

R = CH_2SiMe_3 R = CH_2SiMe_3

Figure 32. Erbium NHC adducts.

The erbium analogue of L_2NdBr, **CXXVI** in Eq. 11, **CXLIII** (L = [3,5-^{t}Bu$_2$-2-(O)C_6H_2CH=NCH_2CH_2(C{NCHCHN^{i}Pr})] was reported in the same paper. It is isostructural in the solid state and the Er-$C_{carbene}$ bond length is 2.568(7) Å.[177]

1.7.9 Ytterbium(II) NHC complexes

As well as the samarium NHC examples, NHC adducts of substituted ytterbocenes were amongst the first lanthanide NHC complexes reported by Schumann *et. al.* in 1994.[22, 180, 184, 185] A series of complexes were reported with differing substitution patterns on the cyclopentadienyl ligands or NHC N-substituents, Figure 33.

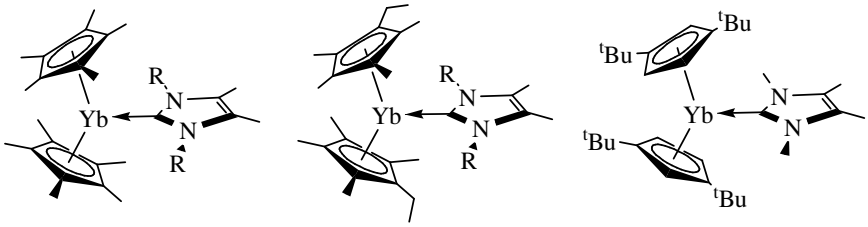

CXLIV, R = Me **CXLVI**, R = Me **CXLVIII**

CXLV, R = ^{i}Pr **CXLVII**, R = ^{i}Pr

Figure 33. Ytterbium NHC complexes.

Due to the diamagnetic nature of divalent ytterbium complexes, it is possible to obtain ^{13}C NMR spectral data and these, along with the Yb-$C_{carbene}$ bond lengths for the various complexes, are summarized in Table 3.

Table 3. Ytterbium NHC complex metal-NHC bond length and ^{13}C NMR carbene chemical shifts.

Compound	M-$C_{carbene}$ bond length (Å)	δ ^{13}C $C_{carbene}$ (ppm)	Reference
CXLIV	-	205.0	[180]
CXLV	-	200.7	[180]
CXLVI	2.552(4)	205.0	[184]
CXLVII	-	198.1	[184]
CXLVIII	2.598(3)	201.8	[180]

The NHC adducts of substituted *tris*-pyrazolyl-borate ($Tp^{tBu, Me}$) supported ytterbium(II) complexes, **CIL** and **CL** were reported by Takats *et. al*., *via* solvent displacement reactions, Figure 34.[186] Thus, **CIL** was formed by treatment of the corresponding THF solvate, ($Tp^{tBu, Me}$)YbI(THF) with one equivalent of free carbene, whereas **CL** was synthesised from the reaction of the THF-solvated ytterbium alkyl ($Tp^{tBu, Me}$)Yb(CH_2SiMe_3)(THF) and an excess of free carbene. The product is the result of both solvent displacement by the NHC and metallation of one N-Me substituent of the NHC. Both complexes were structurally characterised and **CIL** has a five coordinate ytterbium centre, but with a geometry closer to square pyramidal than trigonal bipyramidal, as a consequence of the distortion imposed by the tridentate Tp ligand. The Yb-$C_{carbene}$ bond distance of 2.641(6) Å is longer than other divalent ytterbium examples, due to the higher degree of steric crowding at the metal centre, suggesting a weaker Yb-NHC bonding interaction. The solid state structure of **CL** reveals a six coordinate ytterbium centre in a distorted octahedral geometry. The Yb-$C_{carbene}$ bond lengths of 2.710(5) Å for the monodentate NHC ligand, longer than in **CIL** due to the higher coordination

number, and 2.609(5) Å for the hydrocarbyl tethered bidentate NHC ligand, which is shorter despite this. The Yb-hydrocarbyl bond length of 2.589(5) Å is comparable to that in the ytterbium alkyl starting material, when corrected for the increase in coordination number.

The ^{13}C NMR spectrum of **CIL** displays a $C_{carbene}$ resonance at δ = 199.8 ppm, whereas the two $C_{carbene}$ resonances in **CL** are observed at δ = 208.3 and 201.7 ppm.

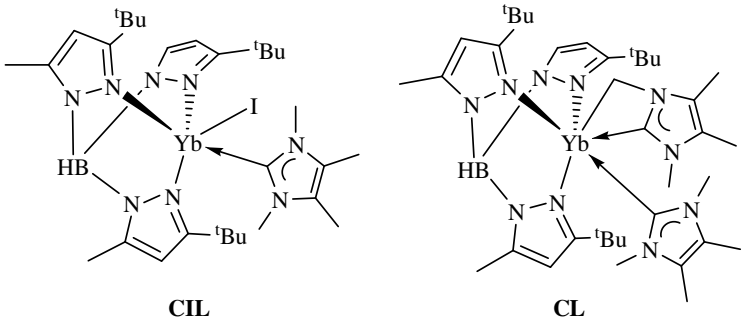

CIL **CL**

Figure 34. *Tris*-pyrazolyl-borate ytterbium complexes.

1.7.10 Ytterbium(III) NHC complexes

Ytterbium amide complexes bearing aryloxy-functionalised NHC ligands have been reported. A reaction between $[LiYb(NPr^{i}_{2})_4]$, two equivalents of the corresponding imidazolium chloride salt and one equivalent of $Li^{n}Bu$ affords the *bis*(NHC) complexes **CLI** and **CLII** in Figure 35, respectively.[130] Attempts to synthesise the mono(NHC) compounds failed due to the apparent instability of the product complexes. Both complexes were structurally characterised by single crystal X-ray diffraction studies, and found to be isostructural, the ytterbium ion in each case adopting a distorted trigonal bipyramidal geometry. The Yb-$C_{carbene}$ bond distances in **CLI** are 2.483(4) and 2.491(4) Å, which are shorter than those observed in **CLII** of 2.526(7) and 2.543(7) Å. This is attributable to the greater steric profile of the N-iso-propyl group over the methyl variant. No ^{13}C NMR data could be obtained for these complexes due to the paramagnetic nature of trivalent ytterbium.

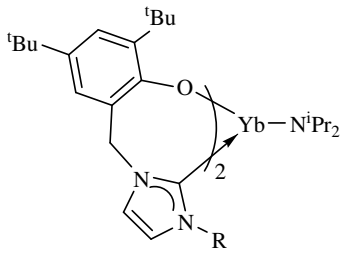

CLI, R = Me
CLII, R = ^{i}Pr

Figure 35. Anionic-tethered NHC ytterbium complexes.

1.7.11 Lutetium(III) NHC complexes

The lutetium analogues of **CXLI** and **CXLII**, see Figure 32, were reported by Schumann *et. al.* at the same time, as the mono- and *bis*(NHC) adducts of lutetium *tris*(alkyls), formed by solvent displacement reactions, $[(Me_3SiCH_2)_3Lu(THF)(C\{N^iPrCMe\}_2)]$ **CLIII**, and $[(Me_3SiCH_2)_3Lu(C\{N^iPrCMe\}_2)_2]$ **CLIV**.[183] The solid state structure of **CLIII** reveals a distorted bipyramidal geometry at the lutetium ion with a Lu-$C_{carbene}$ bond length of 2.488(3) Å, shorter than that in **CXLI** due to the decrease in size from erbium to lutetium. Complex **CLIV** is also five coordinate in the solid state, but the geometry at the lutetium centre changes to resemble a heavily distorted square pyramid, and the Lu-$C_{carbene}$ bond lengths are significantly different at 2.557(6) and 2.639(7) Å. Only the ^{13}C NMR $C_{carbene}$ resonance for **CLIII** was given, it is δ = 199.5 ppm.

The other examples of lutetium NHC complexes are the *bis*(alkyl) analogues of complexes **XCIII** and **XCIV**, Figure 23, bearing indenyl- and fluorenyl-functionalised NHC ligands.[165, 166] Thus, the indenyl-functionalised complex [(Ind-NHC)Lu($CH_2SiMe_3)_2$], **CLV**, and the fluorenyl-functionalised complex [(Flu-NHC)Lu($CH_2SiMe_3)_2$], **CLVI**, were synthesised by *in-situ* deprotonation of the corresponding imidazolium bromide precursor with $LiCH_2SiMe_3$, followed by addition

of $[Lu(CH_2SiMe_3)_3(THF)_2]$. The solid state structures of both complexes were determined and showed Lu-$C_{carbene}$ bond lengths of 2.443(3) and 2.431(3) Å, respectively, where both lutetium metal centres adopt a tetrahedral geometry. The ^{13}C NMR spectra of **CLV** and **CLVI** display $C_{carbene}$ resonances at δ = 199.9 and 199.2 ppm, respectively.

1.8 Actinide NHC complexes

In comparison to the number of NHC complexes of late transition metals, those with Lewis acidic metal centres are much more scarce. Examples of uranium NHC complexes are no exception to this trend, with the first example being reported by Oldham in 2001.[88]

No thorium NHC complexes have been reported to date.

1.8.1 Uranium(III) NHC complexes

All of the trivalent uranium NHC complexes, shown in Figure 36, are adducts of the simplest NHC, C-$(NMeCMe)_2$, which acts as a neutral two electron donor ligand. They can be synthesised by mixing the free NHC with the corresponding U^{III} starting material. Meyer *et. al*. described complexes **CLVII**, formed from the well-established U^{III} precursor $UN"_3$, and the *tris*(aryloxide)triazacyclononane **CLVIII**.[187] Both complexes have been structurally characterised and possess U-$C_{carbene}$ bond lengths of 2.672(5) and 2.789(14) Å respectively. The UV-vis-NIR spectroscopic data show a bathochromic shift of an intense charge transfer (CT) band in the electronic absorption spectra, from 478 to 594 nm in **CLVII** and from 424 to 496 nm in **CLVIII**. The larger shift observed for **CLVII** is in accordance with the shorter U-$C_{carbene}$ bond length observed from X-ray structural analysis. Computational analysis of these complexes supported the

experimental findings, and suggest that there is a significant π-back-bonding component present in the NHC coordination to the electron rich U^{III} centre.

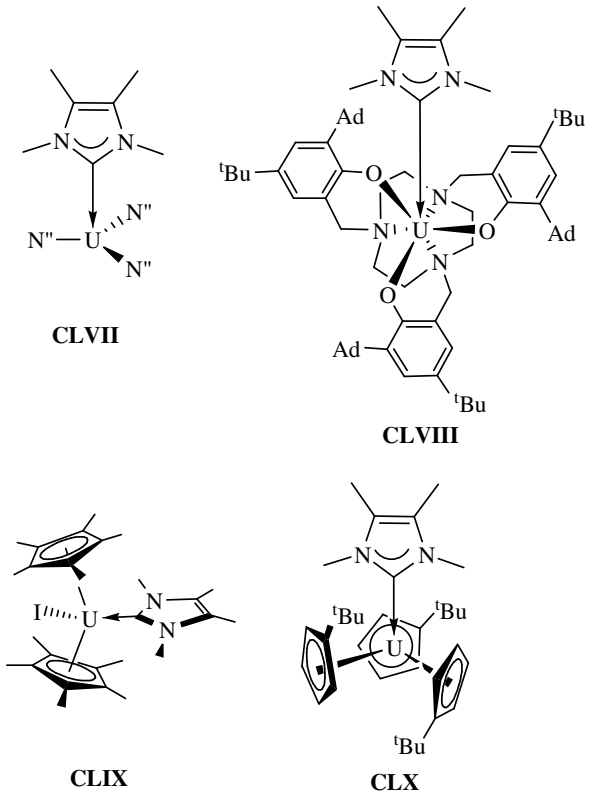

Figure 36. Trivalent uranium NHC adducts.

The indication of π-acceptor ability and softness of NHCs prompted Ephritikhine to demonstrate the stability of complexes **CLIX** and **CLX**.[171] The U-$C_{carbene}$ bond lengths in these complexes are 2.687(5) and 2.768(5) Å, respectively, and are comparable to those observed in complexes **CLVII** and **CLVIII**. This was part of an investigation into the slightly enhanced covalency of the actinide 5f orbitals compared to the lanthanide 4f orbitals. Accordingly, the U^{III} complex showed a stronger interaction with the soft NHC ligand than the analogous Ce^{III} complex **CXVI** in Figure 29. A competition reaction was used to demonstrate the preferential complexation of the carbene for U^{III} over Ce^{III}. Such demonstrations of chemical selectivity are important for the development of more effective and selective ligand sets for the partitioning of spent nuclear fuel.

1.8.2 Uranium(IV) NHC complexes

The first U^{IV}-NHC complex was reported by Evans, **CLXI** in Figure 37, and is also a rare example of a uranium mono-oxo-compound.[188] This complex was synthesised *via* the reaction between $[U(C_5Me_5)_3]$ and $C(NMeCMe)_2$, but was accompanied by unexpected oxidation, to give the mono-oxo-NHC complex. Little spectroscopic information is provided for this compound, but it was structurally characterised and possesses a U-$C_{carbene}$ bond length of 2.636(9) Å and a U=O bond length of 1.916(6) Å. This was found to be shorter than that in other U^{IV} bridging oxides or terminal hydroxides, but longer than other higher valent uranium terminal mono-oxides. Taken together, these data support the assignment of a U^{IV} terminal mono-oxide structure.

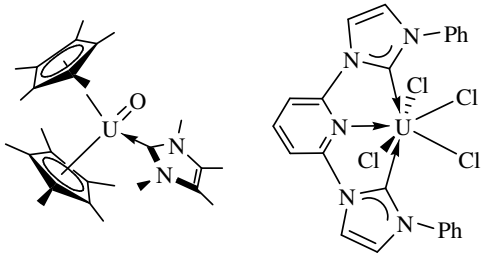

CLXI **CLXII**

Figure 37. Tetravalent uranium NHC complexes.

Danopoulos *et. al.* reported a UCl_4 adduct of a pyridine-substituted dicarbene ligand, **CLXII**.[189] Structural characterisation showed the complex had U-$C_{carbene}$ bond lengths of 2.573(5) and 2.587(5) Å, which are shorter than in any other U-NHC complex.

We have shown that treatment of uranium triiodide with 2.25 equivalents of the potassium alkoxy-NHC **LXXVII** furnishes complex **CLXIII**, Scheme 16, in high yield, although no single crystals suitable for an X-ray diffraction study could be grown and the complex was characterised by ^{1}H NMR spectroscopy and elemental analysis.[121]

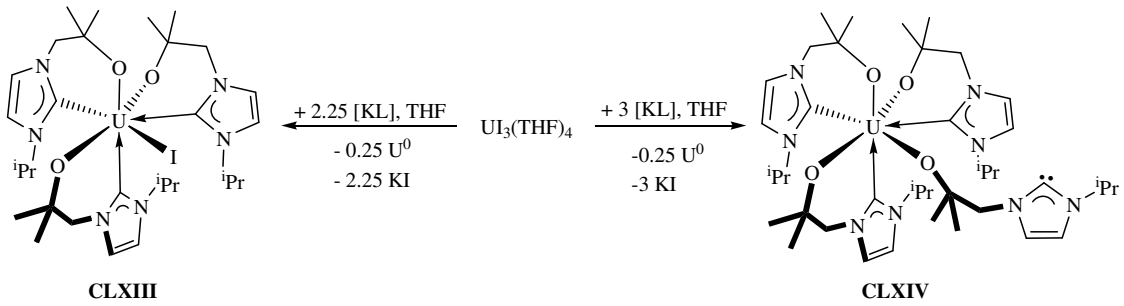

CLXIII **CLXIV**

Scheme 16. Alkoxy-NHC uranium complexes.

Treatment of uranium triiodide with three equivalents of **LXXVII** produces **CLXIV**, which was characterised in the solid state and shown to have a seven-coordinate U^{IV} centre with one unbound NHC group. The average U-$C_{carbene}$ bond length of 2.747(3) Å is long compared to other U^{IV} NHC complexes, although it has a higher coordination number. This was the first example of a metal complex containing a free NHC group which was stable towards protonation to form the imidazolium cation. The ^{1}H NMR spectrum showed only two broad singlets at δ= 17 and -6 ppm, but after cooling to 228 K revealed four different ligand environments, and suggested the presence of a dynamic equilibrium process between the free and bound NHC groups. Attempts were made to eliminate the fluxional process present in **CLXIV** by coordinating metal fragments such as [W(coe)$(CO)_5$] and [Mo(nbd)$(CO)_5$] (where coe = cyclooctene and nbd = norbornadiene), but due to the insoluble nature of the resulting complexes only IR spectroscopy and elemental analyses were used to confirm their identity. Addition of $BH_3.SMe_2$ formed the corresponding NHC-borane adduct U$(LBH_3)_4$, a single crystal X-ray diffraction structural study showed the gross features of the structure to be essentially the same as those of the starting material.

1.8.3 Uranium(VI) NHC complexes

These are all adducts of the uranyl dication, $[UO_2]^{2+}$. Whilst compounds containing a uranyl-carbon bond of any sort are scarce, and only a few uranyl-NHC complexes have been reported.

Complexes **CLXV** and **CLXVI**, Figure 38, were the first examples of an actinide-NHC and were synthesised *via* solvent displacement in $[UO_2Cl_2(THF)_3]$ with two equivalents of the corresponding free carbene.[88] X-ray structural analyses of both complexes showed the U=O bond lengths to be 1.761(4) and 1.739(3) Å for **CLXV** and **CLXVI**, respectively, which are within expected values. The U-$C_{carbene}$ bond lengths are 2.626(7) and 2.609(4) Å, which are longer than previously observed with other neutral donor ligands. The shorter U=O bond length in **CLXVI** than in **CLXV** is consistent with this NHC ligand being a comparatively weaker σ-donor, due to the σ-electron-withdrawing chlorine substituents.

The highest intensity peak in the IR spectra of **CLXV** and **CLXVI** is assigned to the asymmetric uranyl stretch, at 938 and 942 cm^{-1}, respectively; this absorption is inversely proportional to the donor strength of the equatorial ligands. These values are some of the highest reported compared to other neutral donor ligands and are consistent with the NHCs being poor donors to the UO_2 fragment.

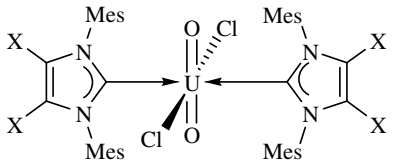

CLXV, X = H
CLXVI, X = Cl

Figure 38. Uranyl NHC adducts.

We subsequently reported the second group of uranyl-NHC complexes, **CLXVII** and **CLXVIII** in Eq. 12, with the NHC bearing an amido-functionalised arm.[151] These

complexes can be synthesised either *via* treatment of $[UO_2N"_2(THF)_2]$ with two equivalents of amine carbene (HL), L = $^tBuNHCH_2CH_2[C\{^tBuN(CHCH)N\}]$, see Eq. 12, or by a salt elimination reaction between $[UO_2Cl_2(THF)_2]$ and one equivalent of the lithium salt **LXXII**. The ^{13}C NMR spectra of **CLXVII** shows a very high-frequency $C_{carbene}$ shift of δ = 262.8 ppm, the highest so far recorded for an unsaturated-NHC-metal complex. Both **CLXVII** and **CLXVIII** were characterised in the solid state and showed the U=O bond lengths to be essentially the same at 1.801(4) Å, longer than in complex **CLXV**, and U-$C_{carbene}$ bond lengths of 2.640(5) and 2.633(7) Å, respectively, which are only marginally longer than observed in complexes **CLXV** and **CLXVI**.

The uranyl asymmetric stretch was observed in the IR spectra at 929 and 933 cm^{-1} for **CLXVII** and **CLXVIII**, respectively. Each lies at a lower frequency than those observed in **CLXV** and **CLXVI**, and support the longer U=O bond length observed in these complexes. As the U-$C_{carbene}$ bond lengths between the two sets of complexes are very similar, the weakening of the U=O bond can be attributed to the stronger donor ability of the amido substituents in **CLXVII** and **CLXVIII**.

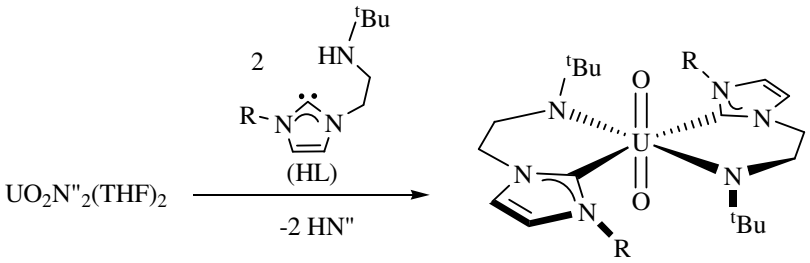

CLXVII, R = ^tBu
CLXVIII, R = Mes

Eq. 12

1.9 References

[1] D. F. Shriver, P. W. Atkins, *Inorganic Chemistry*, 3rd ed., OUP, **1999**.
[2] S. A. Cotton, *Lanthanide and Actinide Chemistry*, Wiley, **2006**.
[3] N. Kaltsoyannis, P. Scott, *The f elements*, OUP, **1999**.
[4] K. I. M. Ingram, M. J. Tassell, A. J. Gaunt, N. Kaltsoyannis, *Inorg. Chem.* **2008**, *47*, 7824.
[5] Z. Kolarik, *Chem. Rev.* **2008**, *108*, 4208.
[6] M. Roger, L. Belkhiri, T. Arliguie, P. Thuery, A. Boucekkine, M. Ephritikhine, *Organometallics* **2008**, *27*, 33.
[7] M. Roger, L. Belkhiri, P. Thuery, T. Arliguie, M. Fourmigue, A. Boucekkine, M. Ephritikhine, *Organometallics* **2005**, *24*, 4940.
[8] V. Nair, L. Balagopal, R. Rajan, J. Mathew, *Acc. Chem. Res.* **2004**, *37*, 21.
[9] V. Nair, A. Deepthi, *Chem. Rev.* **2007**, *107*, 1862.
[10] A. K. Das, *Coord. Chem. Rev.* **2001**, *213*, 307.
[11] K. Tashiro, K. Konishi, T. Aida, *Angew. Chem., Int. Ed. Engl.* **1997**, *36*, 856.
[12] J. W. Buchler, T. Dippell, *Eur. J. Inorg. Chem.* **1998**, *4*, 445.
[13] R. Anwander, *Top. Curr. Chem.* **1996**, *179*, 33.
[14] A. Greco, S. Cesca, W. Bertolini, *J. Organomet. Chem.* **1976**, *113*, 321.
[15] A. Streitwieser Jr., S. A. Kinsley, J. T. Rigsbee, I. L. Fragala, E. Ciliberto, N. Roesch, *J. Am. Chem. Soc.* **1985**, *107*, 7786.
[16] A. Streitwieser, S. A. Kinsley, C. H. Jenson, J. T. Rigsbee, *Organometallics* **2004**, *23*, 5169.
[17] T. R. Boussie, D. C. Eisenberg, J. Rigsbee, A. Streitwieser, A. Zalkin, *Organometallics* **1991**, *10*, 1922.
[18] M. Dolg, P. Fulde, W. Kuechle, C.-S. Neumann, H. Stoll, *J. Chem. Phys.* **1991**, *94*, 3011.
[19] U. Kilimann, R. Herbst-Irmer, D. Stalke, F. T. Edelmann, *Angew. Chem., Int. Ed. Engl.* **1994**, *33*, 1618.
[20] F. T. Edelmann, D. M. M. Freckmann, H. Schumann, *Chem. Rev.* **2002**, *102*, 1851.
[21] N. M. Edelstein, P. G. Allen, J. J. Bucher, D. K. Shuh, C. D. Sofield, N. Kaltsoyannis, G. H. Maunder, M. R. Russo, A. Sella, *J. Am. Chem. Soc.* **1996**, *118*, 13115.
[22] R. D. Fischer, *Angew. Chem., Int. Ed. Engl.* **1994**, *33*, 2165.
[23] C. H. Booth, M. D. Walter, M. Daniel, W. W. Lukens, R. A. Anderson, *Phys. Rev. Lett.* **2005**, *95*, 267202.
[24] H.-D. Amberger, H. Reddmann, F. T. Edelmann, *J. Organomet. Chem.* **2005**, *690*, 2238.
[25] M. D. Walter, C. H. Booth, W. W. Lukens, R. A. Anderson, *Organometallics* **2009**, *DOI: 10.1021/om7012327*.
[26] A. Ashley, G. Balazs, A. Cowley, J. Green, C. H. Booth, D. O'Hare, *Chem. Commun.* **2007**, 1515.

[27] G. Balazs, F. G. N. Cloke, J. C. Green, R. M. Harker, A. Harrison, P. B. Hitchcock, C. N. Jardine, R. Walton, *Organometallics* **2007**, *26*, 3111.
[28] A. F. England, T. M. Frankcom, C. J. Burns, S. L. Buchwald, in *207th National meeting of the American Chemical Society*, San Diego, CA, **1994**.
[29] C. Morton, N. W. Alcock, M. R. Lees, I. J. Munslow, C. J. Sanders, P. Scott, *J. Am. Chem. Soc.* **1999**, *121*, 11255.
[30] O. Eisenstein, P. B. Hitchcock, A. G. Hulkes, M. F. Lappert, L. Maron, *Chem. Commun.* **2001**, 1560.
[31] P. B. Hitchcock, A. G. Hulkes, M. F. Lappert, *Inorg. Chem.* **2004**, *43*, 1031.
[32] M. C. Cassani, Y. K. Gun'ko, P. B. Hitchcock, A. G. Hulkes, A. V. Khvostov, M. F. Lappert, A. V. Protchenko, *J. Organomet. Chem.* **2002**, *647*, 71.
[33] P. B. Hitchcock, M. F. Lappert, A. V. Protchenko, *Chem. Commun.* **2006**, 3546.
[34] M. R. Russo, N. Kaltsoyannis, A. Sella, *Chem. Commun.* **2002**, 2458.
[35] T. J. Boyle, L. A. M. Ottley, *Chem. Rev.* **2008**, *108*, 1896.
[36] D. C. Bradley, A. K. Chatterjee, W. Wardlaw, *J. Chem. Soc.* **1957**, 2600.
[37] R. C. Mehrotra, P. N. Kapoor, J. M. Batwara, *Coord. Chem. Rev.* **1980**, *31*, 67.
[38] P. S. Gradeff, F. G. Schreiber, K. C. Brooks, R. E. Sievers, *Inorg. Chem.* **1985**, *24*, 1110.
[39] W. J. Evans, T. J. Deming, J. M. Olofson, J. W. Ziller, *Inorg. Chem.* **1989**, *28*, 4027.
[40] W. J. Evans, T. J. Deming, J. W. Ziller, *Organometallics* **1989**, *8*, 1581.
[41] Y. K. Gun'ko, S. D. Elliott, P. B. Hitchcock, M. F. Lappert, *J. Chem. Soc., Dalton Trans.* **2002**, 1852.
[42] P. S. Gradeff, K. Yunlu, A. Gleizes, J. Galy, *Polyhedron* **1989**, *8*, 1001.
[43] Y. K. Gun'ko, R. Reilly, F. T. Edelmann, D. Stalke, *Angew. Chem., Int. Ed. Engl.* **2001**, *40*, 1279.
[44] S. Giessmann, S. Blaurock, V. Lorenz, F. T. Edelmann, *Inorg. Chem.* **2007**, *46*, 8100.
[45] A. Sen, H. A. Stecher, A. L. Rheingold, *Inorg. Chem.* **1992**, *31*, 473.
[46] E. O. Fischer, A. Maasboel, *Angew. Chem., Int. Ed. Engl.* **1964**, *3*, 580.
[47] A. J. Arduengo, R. L. Harlow, M. Kline, *J. Am. Chem. Soc.* **1991**, *113*, 361.
[48] W. A. Herrmann, C. Köcher, *Angew. Chem., Int. Ed. Engl.* **1997**, *36*, 2162.
[49] A. J. Arduengo, *Acc. Chem. Res.* **1999**, *32*, 913.
[50] D. Bourissou, O. Guerret, F. P. Gabbai, G. Bertrand, *Chem. Rev.* **2000**, *100*, 39.
[51] W. A. Herrmann, *Angew. Chem. Int. Ed.* **2002**, *41*, 1290.
[52] C. M. Crudden, D. P. Allen, *Coord. Chem. Rev.* **2004**, *248*, 2247.
[53] F. A. Glorius, *Top. Organomet. Chem.* **2007**, *21*, 1.
[54] F. E. Hahn, M. C. Jahnke, *Angew. Chem., Int. Ed. Engl.* **2008**, *47*, 3122.
[55] J. C. Garrison, W. J. Youngs, *Chem. Rev.* **2005**, *105*, 3978.
[56] A. T. S. M. Termaten, A. Ehlers, M. Lutz, A. L. Spek, K. Lammertsma, *Chem. Eur. J.* **2003**, *9*, 3577.
[57] D. Nemcsok, K. Wichmann, G. Frenking, *Organometallics* **2004**, *23*, 3640.
[58] X. L. Hu, I. Castro-Rodriguez, K. Olsen, K. Meyer, *Organometallics* **2004**, *23*, 755.

[59] H. Jacobsen, A. Correa, C. Costabile, L. Cavallo, *J. Organomet. Chem.* **2006**, *691*, 4350.
[60] P. L. Arnold, S. Zlatogorsky, N. A. Jones, C. D. Carmichael, S. T. Liddle, A. J. Blake, C. Wilson, *Inorg. Chem.* **2008**, *47*, 9042.
[61] R. W. Alder, M. E. Blake, C. Bortolotti, S. Bufalli, C. P. Butts, E. Linehan, J. M. Oliva, A. G. Orpen, M. J. Quayle, *Chem. Commun.* **1999**, 241.
[62] D. Enders, K. Breuer, G. Raabe, J. Runsink, J. H. Teles, J.-P. Melder, K. Ebel, S. Brode, *Angew. Chem., Int. Ed. Engl.* **1995**, *34*, 1021.
[63] E. Mas-Marza, J. A. Mata, E. Peris, *Angew. Chem., Int. Ed. Engl.* **2007**, *46*, 3729.
[64] E. Despagnet-Ayoub, R. H. Grubbs, *J. Am. Chem. Soc.* **2004**, *126*, 10198.
[65] A. J. Arduengo, J. R. Goerlich, W. J. Marshall, *Liebigs Ann. Chem.* **1997**, 365.
[66] Y. Ishida, B. Donnadieu, G. Bertrand, *Proc. Natl. Acad. Sci. U. S. A.* **2006**, *103*, 13585.
[67] C. Praesang, B. Donnadieu, G. Bertrand, *J. Am. Chem. Soc.* **2005**, *127*, 10182.
[68] T. Cantat, N. Mezailles, N. Maigrot, L. Richard, P. Le-Floch, *Chem. Commun.* **2004**, 1274.
[69] D. Martin, A. Baceiredo, H. Gornitzka, W. W. Schoeller, G. Bertrand, *Angew. Chem., Int. Ed. Engl.* **2005**, *44*, 1700.
[70] V. Lavallo, Y. Canac, C. Praesang, B. Donnadieu, G. Bertrand, *Angew. Chem., Int. Ed. Engl.* **2005**, *44*, 5705.
[71] V. Lavallo, Y. Canac, A. DeHope, B. Donnadieu, G. Bertrand, *Angew. Chem., Int. Ed. Engl.* **2005**, *44*, 7236.
[72] D. A. Dixon, A. J. Arduengo III, *J. Phys. Chem.* **1991**, *95*, 4180.
[73] A. J. Arduengo III, H. Bock, H. Chen, M. Denk, D. A. Dixon, J. C. Green, W. A. Herrmann, N. L. Jones, M. Wagner, R. West, *J. Am. Chem. Soc.* **1994**, *116*, 6641.
[74] C. Heinemann, T. Mueller, Y. Apeloig, H. Schwarz, *J. Am. Chem. Soc.* **1996**, *118*, 2023.
[75] C. Boehme, G. Frenking, *J. Am. Chem. Soc.* **1996**, *118*, 2039.
[76] J. F. Lehmann, S. G. Urquhart, L. E. Ennios, A. P. Hitchcock, K. Hatano, S. Gupta, M. K. Denk, *Organometallics* **1999**, *18*, 1862.
[77] H. W. Wanzlick, *Angew. Chem., Int. Ed. Engl.* **1962**, *1*, 75.
[78] A. J. Arduengo III, J. R. Goerlich, W. J. Marshall, *J. Am. Chem. Soc.* **1995**, *117*, 11027.
[79] A. C. Hillier, W. J. Sommer, B. S. Yong, J. L. Petersen, L. Cavallo, S. P. Nolan, *Organometallics* **2003**, *22*, 4322.
[80] R. Dorta, E. D. Stevens, N. M. Scott, C. Costabile, L. Cavallo, C. D. Hoff, S. P. Nolan, *J. Am. Chem. Soc.* **2005**, *127*, 2485.
[81] S. Fantasia, J. L. Petersen, H. Jacobsen, L. Cavallo, S. P. Nolan, *Organometallics* **2007**, *26*, 5880.
[82] P. L. Arnold, S. Pearson, *Coord. Chem. Rev.* **2007**, *251*, 596.
[83] A. A. Danopoulos, D. Pugh, J. Wright, *Angew. Chem., Int. Ed. Engl.* **2008**, *47*, 9765.
[84] F. E. Hahn, L. Wittenbecher, R. Boese, D. Blaser, *Chem. Eur. J.* **1999**, *5*, 1931.
[85] F. E. Hahn, C. Radloff, T. Pape, A. Hepp, *Organometallics* **2008**, *27*, 6408.

[86] A. J. Arduengo III, J. R. Goerlich, R. Krafczyk, W. J. Marshall, *Angew. Chem., Int. Ed. Engl.* **1998**, *37*, 1963.
[87] J. W. Ogle, J. Zhang, J. H. Reibenspies, K. A. Abboud, S. A. Miller, *Org. Lett.* **2008**, *10*, 3677.
[88] W. J. Oldham, S. M. Oldham, B. L. Scott, K. D. Abney, W. H. Smith, D. A. Costa, *Chem. Commun.* **2001**, 1348.
[89] M. Viciano, E. Mas-Marza, M. Sanau, E. Peris, *Organometallics* **2006**, *25*, 3063.
[90] A. Bittermann, P. Haerter, E. Herdtweck, S. D. Hoffmann, W. A. Herrmann, *J. Organomet. Chem.* **2008**, *693*, 2079.
[91] N. Kuhn, J. Fahl, R. Fawzi, C. Maichle-Moessmer, M. Steimann, *Z. Naturforsch., B: Chem. Sci.* **1998**, *53*, 720.
[92] Y. Ohki, T. Hatanaka, K. Tatsumi, *J. Am. Chem. Soc.* **2008**, *130*, 17174.
[93] A. Furstner, M. Alcarazo, V. Cesar, C. W. Lehmann, *Chem. Commun.* **2006**, 2176.
[94] U. Siemeling, C. Faerber, C. Bruhn, *Chem. Commun.* **2009**, 98.
[95] D. M. Khramov, E. L. Rosen, V. M. Lynch, C. W. Bielawski, *Angew. Chem., Int. Ed. Engl.* **2008**, *47*, 2267.
[96] H. W. Wanzlick, H.-J. Schoenherr, *Angew. Chem., Int. Ed. Engl.* **1968**, *7*, 141.
[97] K. Oefele, *J. Organomet. Chem.* **1968**, *12*, P42.
[98] N. Kuhn, T. Kratz, *Synthesis* **1993**, 561.
[99] S. Csihony, D. A. Culkin, A. C. Sentman, A. P. Dove, R. M. Waymouth, J. L. Hedrick, *J. Am. Chem. Soc.* **2005**, *127*, 9079.
[100] B. K. M. Chan, N.-H. Chang, M. R. Grimmett, *Aust. J. Chem.* **1977**, *30*, 2005.
[101] W. A. Herrmann, L. J. Goossen, M. Spiegler, *J. Organomet. Chem.* **1997**, *547*, 357.
[102] A. Kiyomori, J.-F. Marcoux, S. L. Buchwald, *Tetrahedron Lett.* **1999**, *40*, 2657.
[103] W. A. Herrmann, C. Kocher, L. J. Goossen, G. R. J. Artus, *Chem. Eur. J.* **1996**, *2*, 1627.
[104] A. A. Gridnev, I. M. Mihaltseva, *Synth. Commun.* **1994**, *24*, 1547.
[105] A. M. Magill, D. S. McGuinness, K. J. Cavell, G. J. P. Britovsek, V. C. Gibson, A. J. P. White, D. J. Williams, A. H. White, B. W. Skelton, *J. Organomet. Chem.* **2001**, *617*, 546.
[106] H. Nakai, Y. J. Tang, P. Gantzel, K. Meyer, *Chem. Commun.* **2003**, 24.
[107] A. Paczal, A. C. Benyei, A. Kotschy, *J. Org. Chem.* **2006**, *71*, 5969.
[108] R. S. Bon, F. J. J. deKanter, M. Lutz, A. L. Spek, M. C. Jahnke, F. E. Hahn, M. B. Groen, R. V. A. Orru, *Organometallics* **2007**, *26*, 3639.
[109] S. Sole, H. Gornitzka, O. Guerret, G. Bertrand, *J. Am. Chem. Soc.* **1998**, *120*, 9100.
[110] H. W. Wanzlick, E. Schikora, *Angew. Chem., Int. Ed. Engl.* **1960**, *72*, 494.
[111] Y. T. Chen, F. Jordan, *J. Org. Chem.* **1991**, *56*, 5029.
[112] R. W. Alder, M. E. Blake, L. Chaker, J. N. Harvey, F. Paolini, J. Schutz, *Angew. Chem., Int. Ed. Engl.* **2004**, *43*, 5896.
[113] R. E. Douthwaite, *Coord. Chem. Rev.* **2007**, *251*, 702.
[114] D. Pugh, A. A. Danopoulos, *Coord. Chem. Rev.* **2007**, *251*, 610.
[115] L. H. Gade, S. Bellemin-Laponnaz, *Coord. Chem. Rev.* **2007**, *251*, 718.

[116] E. Peris, R. H. Crabtree, *Coord. Chem. Rev.* **2004**, *248*, 2239.
[117] O. Kuehl, *Chem. Soc. Rev.* **2007**, *36*, 592.
[118] S. T. Liddle, I. S. Edworthy, P. L. Arnold, *Chem. Soc. Rev.* **2007**, *36*, 1732.
[119] P. L. Arnold, M. Rodden, K. M. Davis, A. C. Scarisbrick, A. J. Blake, C. Wilson, *Chem. Commun.* **2004**, 1612.
[120] D. Patel, S. T. Liddle, S. A. Mungur, M. Rodden, A. J. Blake, P. L. Arnold, *Chem. Commun.* **2006**, 1124.
[121] P. L. Arnold, A. J. Blake, C. Wilson, *Chem. Eur. J.* **2005**, *11*, 6095.
[122] H. Clavier, L. Coutable, L. Toupet, J. C. Guillemin, M. Mauduit, *J. Organomet. Chem.* **2005**, *690*, 5237.
[123] J. Václav, M. Gilani, R. Wilhelm, *Eur. J. Org. Chem.* **2006**, *2006*, 5103.
[124] P. L. Arnold, A. C. Scarisbrick, A. J. Blake, C. Wilson, *Chem. Commun.* **2001**, 2340.
[125] P. L. Arnold, A. C. Scarisbrick, *Organometallics* **2004**, *23*, 2519.
[126] A. W. Waltman, R. H. Grubbs, *Organometallics* **2004**, *23*, 3105.
[127] A. W. Waltman, T. Ritter, R. H. Grubbs, *Organometallics* **2006**, *25*, 4238.
[128] J. J. Veldhuizen, S. B. Garber, J. S. Kingsbury, A. H. Hoveyda, *J. Am. Chem. Soc.* **2002**, *124*, 4954.
[129] J. J. Veldhuizen, D. G. Gillingham, S. B. Garber, O. Kataoka, A. H. Hoveyda, *J. Am. Chem. Soc.* **2003**, *125*, 12502.
[130] Z. G. Wang, H.-M. Sun, H.-S. Yao, Y.-M. Yao, Q. Shen, Y. Zhang, *J. Organomet. Chem.* **2006**, *691*, 3383.
[131] Z. G. Wang, H. M. Sun, H. S. Yao, Q. Shen, Y. Zhang, *Organometallics* **2006**, *25*, 4436.
[132] H. Aihara, T. Matsuo, H. Kawaguchi, *Chem. Commun.* **2003**, 2204.
[133] D. Zhang, H. Aihara, T. Watanabe, T. Matsuo, H. Kawaguchi, *J. Organomet. Chem.* **2007**, *692*, 234.
[134] W. Li, H. Sun, M. Chen, Z. Wang, D. Hu, Q. Shen, Y. Zhang, *Organometallics* **2005**, *24*, 5925.
[135] B. E. Ketz, X. G. Ottenwaelder, R. M. Waymouth, *Chem. Commun.* **2005**, 5693.
[136] P. L. Arnold, S. A. Mungur, A. J. Blake, C. Wilson, *Angew. Chem. Int. Ed.* **2003**, *42*, 5981.
[137] R. E. Douthwaite, J. Houghton, B. M. Kariuki, *Chem. Commun.* **2004**, 698.
[138] I. S. Edworthy, M. Rodden, S. A. Mungur, K. M. Davis, A. J. Blake, C. Wilson, M. Schroder, P. L. Arnold, *J. Organomet. Chem.* **2005**, *690*, 5710.
[139] L. P. Spencer, S. Winston, M. D. Fryzuk, *Organometallics* **2004**, *23*, 3372.
[140] L. P. Spencer, M. D. Fryzuk, *J. Organomet. Chem.* **2005**, *690*, 5788.
[141] L. P. Spencer, C. Beddie, M. B. Hall, M. D. Fryzuk, *J. Am. Chem. Soc.* **2006**, *128*, 12531.
[142] S. P. Downing, A. A. Danopoulos, *Organometallics* **2006**, *25*, 1337.
[143] J. Muller, I. Piotrowski, L. von Chrzanowski, *Z. Naturforsch., B: Chem. Sci.* **2007**, *62*, 467.
[144] A. P. da Costa, M. Viciano, M. Sanau, S. Merino, J. Tejeda, E. Peris, B. Royo, *Organometallics* **2008**, *27*, 1305.

[145] R. J. Rubio, G. T. S. Andavan, E. B. Bauer, T. K. Hollis, J. Cho, F. S. Tham, B. Donnadieu, *J. Organomet. Chem.* **2005**, *690*, 5353.
[146] K. Lv, D. Cui, *Organometallics* **2008**, *27*, 5438.
[147] D. Sellmann, C. Allmann, F. Heinemann, F. Knoch, J. Sutter, *J. Organomet. Chem.* **1997**, *541*, 291.
[148] A. J. ArduengoIII, M. Tamm, J. C. Calabrese, F. Davidson, W. J. Marshall, *Chem. Lett.* **1999**, 1021.
[149] R. Frankel, C. Birg, U. Kernbach, T. Habereder, H. Noth, W. P. Fehlhammer, *Angew. Chem., Int. Ed. Engl.* **2001**, *40*, 1907.
[150] A. Wacker, H. Pritzkow, W. Siebert, *Eur. J. Inorg. Chem.* **1998**, 843.
[151] S. A. Mungur, S. T. Liddle, C. Wilson, M. J. Sarsfield, P. L. Arnold, *Chem. Commun.* **2004**, 2738.
[152] I. S. Edworthy, A. J. Blake, C. Wilson, P. L. Arnold, *Organometallics* **2007**, *26*, 3684.
[153] P. L. Arnold, C. Wilson, *Inorg. Chim. Acta* **2007**, *360*, 190.
[154] P. L. Arnold, M. Rodden, C. Wilson, *Chem. Commun.* **2005**, 1743.
[155] S. P. Downing, S. C. Guadano, D. Pugh, A. A. Danopoulos, R. M. Bellabarba, M. Hanton, D. Smith, R. P. Tooze, *Organometallics* **2007**, *26*, 3762.
[156] W. A. Herrmann, O. Runte, G. R. J. Artus, *J. Organomet. Chem.* **1995**, *501*, C1.
[157] J. Gottfriedsen, S. Blaurock, *Organometallics* **2006**, *25*, 3784.
[158] A. J. Arduengo-III, H. V. Rasika-Dias, R. Davidson, R. L. Harlow, *J. Organomet. Chem.* **1993**, *462*, 13.
[159] A. J. Arduengo, F. Davidson, R. Krafczyk, W. J. Marshall, M. Tamm, *Organometallics* **1998**, *17*, 3375.
[160] H. Schumann, J. Gottfriedsen, M. Glanz, S. Dechert, J. Demtschuk, *J. Organomet. Chem.* **2001**, *617*, 588.
[161] D. Zhang, H. Kawaguchi, *Organometallics* **2006**, *25*, 5506.
[162] I. Nieto, F. Cervantes-Lee, J. M. Smith, *Chem. Commun.* **2005**, 3811.
[163] P. L. Arnold, I. S. Edworthy, C. D. Carmichael, A. J. Blake, C. Wilson, *Dalton Trans.* **2008**, 3739.
[164] A. G. M. Barrett, M. R. Crimmin, M. S. Hill, G. K. Kociok, D. J. MacDougall, M. F. Mahon, P. A. Procopiou, *Organometallics* **2008**, *27*, 3939.
[165] B. L. Wang, D. Wang, D. M. Cui, W. Gao, T. Tang, X. S. Chen, X. B. Jing, *Organometallics* **2007**, *26*, 3167.
[166] B. Wang, D. Cui, K. Lv, *Macromolecules* **2008**, *41*, 1983.
[167] A. J. ArduengoIII, M. Tamm, S. J. McLain, J. C. Calabrese, F. Davidson, W. J. Marshall, *J. Am. Chem. Soc.* **1994**, *116*, 7927.
[168] W. A. Herrmann, F. C. Munck, G. R. J. Artus, O. Runte, R. Anwander, *Organometallics* **1997**, *16*, 682.
[169] P. L. Arnold, S. T. Liddle, *Organometallics* **2006**, *25*, 1485.
[170] S. T. Liddle, P. L. Arnold, *Organometallics* **2005**, *24*, 2597.
[171] T. Mehdoui, J. C. Berthet, P. Thuery, M. Ephritikhine, *Chem. Commun.* **2005**, 2860.
[172] P. L. Arnold, S. T. Liddle, *Chem. Commun.* **2005**, 5638.

[173] P. L. Arnold, S. T. Liddle, J. McMaster, C. Jones, D. P. Mills, *J. Am. Chem. Soc.* **2007**, *129*, 5360.
[174] P. L. Arnold, J. McMaster, S. T. Liddle, *Chem. Commun.* **2009**, 818.
[175] S. Friedrich, H. Memmler, L. H. Gade, W. S. Li, I. J. Scowen, M. McPartlin, C. E. Housecroft, *Inorg. Chem.* **1996**, *35*, 2433.
[176] P. L. Arnold, S. T. Liddle, *Comp. Rend. Chim.* **2008**, *11*, 603.
[177] J. Zhang, H. Yao, Y. Zhang, H. Sun, Q. Shen, *Organometallics* **2008**, *27*, 2672.
[178] A. J. Arduengo, M. Tamm, S. J. McLain, J. C. Calabrese, F. Davidson, W. J. Marshall, *J. Am. Chem. Soc.* **1994**, *116*, 7927.
[179] M. Glanz, S. Dechert, H. Schumann, D. Wolff, J. Springer, *Z. Anorg. Allg. Chem.* **2000**, *626*, 2467.
[180] H. Schumann, M. Glanz, J. Winterfeld, H. Hemling, N. Kuhn, T. Kratz, *Chem. Ber.* **1994**, *127*, 2369.
[181] D. Baudry-Barbier, N. Andre, A. Dormond, C. Pardes, P. Richard, M. Visseaux, C. J. Zhu, *Eur. J. Inorg. Chem.* **1998**, 1721.
[182] L. Maron, D. Bourissou, *Organometallics* **2007**, *26*, 1100.
[183] H. Schumann, D. M. M. Freckmann, S. Schutte, S. Dechert, M. Hummert, *Z. Anorg. Allg. Chem.* **2007**, *633*, 888.
[184] H. Schumann, M. Glanz, J. Winterfeld, H. Hemling, N. Kuhn, T. Kratz, *Angew. Chem., Int. Ed. Engl.* **1994**, *33*, 1733.
[185] H. Schumann, M. Glanz, J. Gottfriedsen, S. Dechert, D. Wolff, *Pure Appl. Chem.* **2001**, *73*, 279.
[186] G. M. Ferrence, A. J. Arduengo, A. Jockisch, H. J. Kim, R. McDonald, J. Takats, *J. Alloys Compd.* **2006**, *418*, 184.
[187] H. Nakai, X. L. Hu, L. N. Zakharov, A. L. Rheingold, K. Meyer, *Inorg. Chem.* **2004**, *43*, 855.
[188] W. J. Evans, S. A. Kozimor, J. W. Ziller, *Polyhedron* **2004**, 2689.
[189] D. Pugh, J. A. Wright, S. Freeman, A. A. Danopoulos, *Dalton Trans.* **2006**, 775.

Chapter 2

Ligand Development

2. Ligand Development

Aspects of the work for this section were performed in collaboration with Miss Zoe R. Turner, a fellow PhD student, therefore complexes prepared by her are included as part of the discussion. Brief synthetic details for these complexes are described in the text, where relevant, and the compounds are given a letter, separate from the main numbering scheme.

2.1 Introduction

NHCs either incorporate an unsaturated backbone, as structurally characterised by Arduengo,[1] **CLXIX** in Figure 39, or a saturated backbone, **CLXX** in Figure 39, as initially reported by Wanzlick[2, 3] and studied in Lappert's original work on the synthesis of metal carbene complexes from electron-rich olefins.[4] NHCs are undisputed as extremely strong σ-donor ligands, as a result of the strong stabilising effect of the two nitrogen substituents on the carbene carbon, and more increasingly as π-acceptors in certain situations.[5-7]

Nolan has extensively examined the differences between saturated and unsaturated NHCs in group 10 metal complexes, by analysing the CO stretching frequency in $[(NHC)Ni(CO)_3]$ adducts. He concluded that within the group, the σ-donor properties of saturated and unsaturated NHCs are almost the same.[8] Another study showed that saturated NHCs are better acceptors of π-back-donation than the unsaturated analogues in Pt(II) complexes, which contain a bonding contribution of about 10 % from back-bonding.[9] Most recently, studies on an iridium system allowed for a direct comparison of a wide range of monodentate carbenes, $[Ir(NHC)(CO)_2Cl]$, which concluded that there were negligible differences between the two types of NHC, with the differences in ligand sterics probably providing the greatest contribution to variations in the complexes formed.[10]

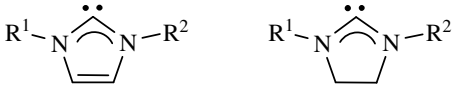

CLXIX **CLXX**

R^1, R^2 = alkyl or aryl

Figure 39. N-Heterocyclic carbenes (NHCs)

One of the limitations of using unsaturated NHCs as ligands in complexes of early or f-block metals is the acidity of the protons of the carbene heterocyclic backbone, which can lead to unanticipated and occasionally undesirable ligand rearrangement reactions, potentially resulting in the formation of abnormal NHC complexes.[11, 12]

2.2 Synthetic routes to imidazolinium proligands

There are a number of synthetic routes to substituted imidazolinium proligands that have been developed over recent years. These include a modular substituted diamine synthesis with subsequent ring closure,[13] multi-component synthesis using a combination of amine, aldehyde, isocyanide and alkyl halide,[14] the intramolecular 'hydroamidiniumation' of alkenes,[15] and a template synthesis with an azido isocyanide at a tungsten metal centre.[16] Although examples of anionic tethered NHCs are less common than their neutral counterparts, late metal complexes containing alcohol and phenol-functionalised saturated NHC ligands have been reported, Figure 40. Seeking an analogy with salicylaldimine ligands, Grubbs reported the synthesis of *o*-hydroxyaryl-substituted NHCs and showed that the palladium adducts **CLXXI** were stable.[17] Hoveyda has used the BINOL-derived proligand **CLXXII** to make ruthenium catalysts for asymmetric alkene metathesis,[18] Mauduit reported a five step route from β-aminoalcohols to chiral alkoxy-imidazolinium salts **CLXXIII** which were highly active for copper-catalysed conjugate addition,[19] and Wilhelm has shown that **CLXXIV** is a good proligand for the enantioselective addition of $ZnEt_2$ to aldehydes.[20]

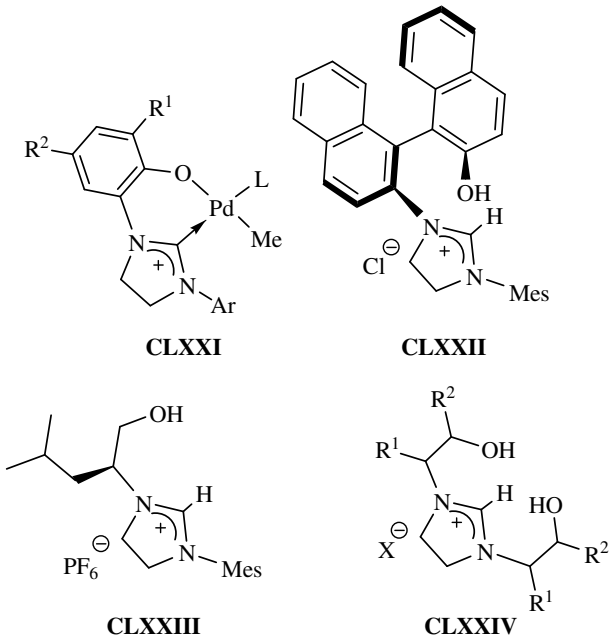

Figure 40. A functionalised, saturated NHC complex and imidazolinium salts

2.3 Synthesis of proligands

Our previous synthesis of unsaturated alkoxy-carbene ligands proceeded by means of the ring opening of a substituted epoxide with either imidazole, followed by subsequent quaternisation of the second imidazole nitrogen with an alkyl halide, **CLXXV**, or with a substituted imidazole to give a zwitterionic compound, Scheme 17.[21, 22]

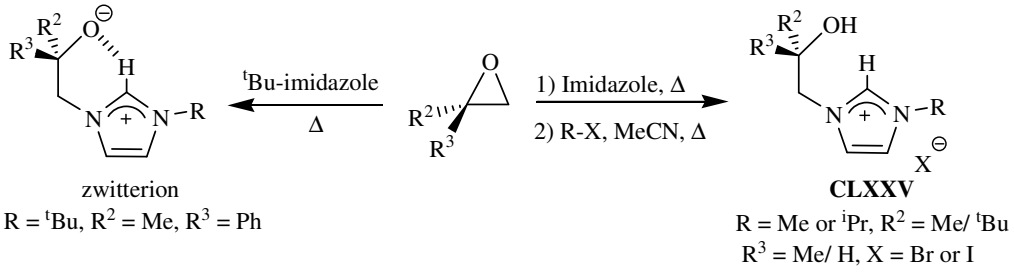

Scheme 17. Synthesis of unsaturated alkoxy-carbene proligands

Hancock previously reported that a primary amine can selectively ring open an epoxide in the presence of a secondary amine, during the synthesis of hydroxyl-substituted polyamine ligands.[23] We were interested in this result as it presented an opportunity for us to extend our straightforward modular unsaturated ligand synthesis to a range of saturated variants. Thus, alcohol-substituted imidazolinium salts of the general formula $[H_2L^R]X$, $[HOCR^2R^3CH_2(1\text{-}CH\{NCH_2CH_2NR\})]X$ (R = ^{i}Pr, denoted as P; R = Mes, denoted as M; R = Dipp, denoted as D, X = Cl, I) are synthesised according to Scheme 18, through nucleophilic attack by a mono N-substituted ethylene diamine on a substituted epoxide. Subsequent acidification and heating in trimethyl orthoformate furnishes the ring-closed alcohol-*N*-functionalised imidazolinium chloride salts, **1-R**, in good yields. A subsequent anion exchange reaction *via* treatment with sodium iodide in acetone yielded the analogous iodide salts, **2-R**. Proligands **1-P** and **2-P** were isolated as viscous brown oils, whereas **1-M/ 2-M** and **AA/ AB** were isolated as pale-coloured solids. This simple modular approach allows for the incorporation of three different substituents, each close to a ligand donor atom, to yield proligands with a variety of steric and electronic profiles.

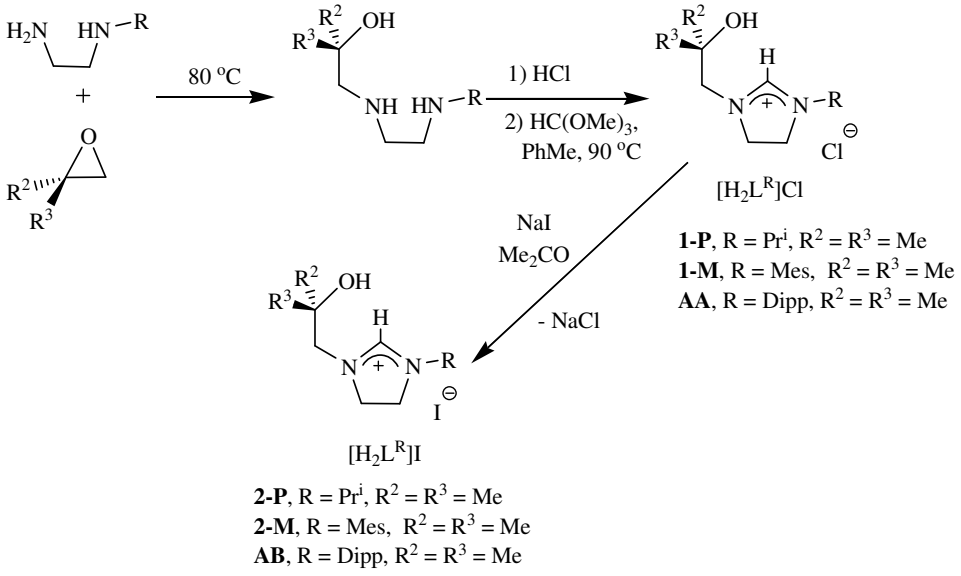

Scheme 18. Synthesis of saturated alkoxy-carbene proligands $[H_2L^R]X$ (X = Cl, I).

These proligands were characterised by multinuclear NMR studies and elemental analyses (except for **1-P**), and the ^{1}H NMR spectra of both the chloride and iodide salts display the characteristic high-frequency imidazolinium resonance between δ = 8 and 10 ppm, in the same spectral region as the unsaturated analogues. In the ^{13}C NMR spectra, the imidazolinium CH resonance in each proligand lies within the range δ = 155–160 ppm, as expected for the cationic heterocycle, and at approximately 20 ppm higher frequency than in the unsaturated examples, range δ = 135–141 ppm. X-ray quality single crystals of **2-P** and **AA** were grown from the isolated product oil and an acetone solution, respectively. The molecular structures are drawn in Figure 41 and selected bond distances and angles are collated in Table 4.

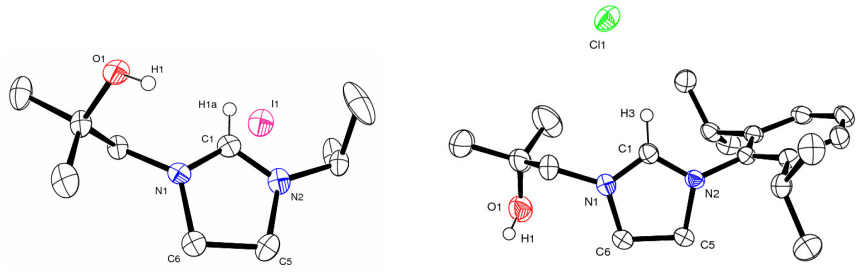

2-P **AA**

Figure 41. Displacement ellipsoid drawings of the molecular structures of a) **2-P** and b) **AA** (50 % probability ellipsoids). Hydrogen atoms omitted for clarity (except on C1 and O1).

The structures of **2-P** and **AA** display no unusual metrical parameters. The imidazolinium N-C(H)-N unit is characterised by C-N bond lengths of 1.305(3) to 1.402(6) Å, consistent with the sp^{2} character of each atom. There is a significant asymmetry within the ring, with the C1-N1 bond, adjacent to the alcohol arm, being shorter than the C1-N2 bond in both cases. The N-C-N bond angles of 110.6(4) and 113.7(2)°, respectively, are up to seven degrees wider than observed in imidazolium salts. The alcohol and imidazolinium groups in **2-P** are orientated towards the iodide counter ions in the lattice, suggesting the presence of hydrogen bonding interactions. These distances are, however, long with bond lengths O-I of 3.771 Å and C-I of 4.306 Å, respectively. The alcohol and imidazolinium groups in **AA** both participate in

intermolecular hydrogen bonding networks within the structure, and involve the chloride counter ion and a partial (60 % present) molecule of water in the lattice. Therefore, the OH forms hydrogen bonds with a lattice water molecule and the imidazolinium group forms a hydrogen bond with a chloride.

Table 4. Selected distances (Å) and angles (°) for the molecular structures of proligands **2-P** and **AA**.

	2-P	**AA**
C1-N1	1.352(6)	1.305(3)
C1-N2	1.402(6)	1.317(3)
C2-N2	1.525(6)	1.438(3)
C5-N2	1.653(7)	1.481(3)
C5-C6	1.611(7)	1.527(3)
C1-Hal1*	3.462	3.438
O1-Hal1'*	3.771	3.100
O1---O1w'	-	2.853
N1-C1-N2	110.6(4)	113.7(2)
N2-C5-C6	98.7(4)	102.9(2)

* Hal = I (**2-P**), Cl (**AA**).

2.4 Deprotonation Chemistry

2.4.1 Mono-deprotonation: Bicyclic adduct formation

Treatment of the imidazolinium proligands **2-P** and **1-M** with one equivalent of benzyl potassium in THF, or of **AA** with Li^{n}Bu in hexane/ toluene, affords the bicyclic products **3-R**, Scheme 19, in good yield. Compounds **3-P** and **3-M** are colourless, distillable oils (40 ºC at 10^{-1} mbar and 85 ºC at 10^{-1} mbar, respectively) whereas **AC** was isolated as a colourless powder and washed with hexanes.

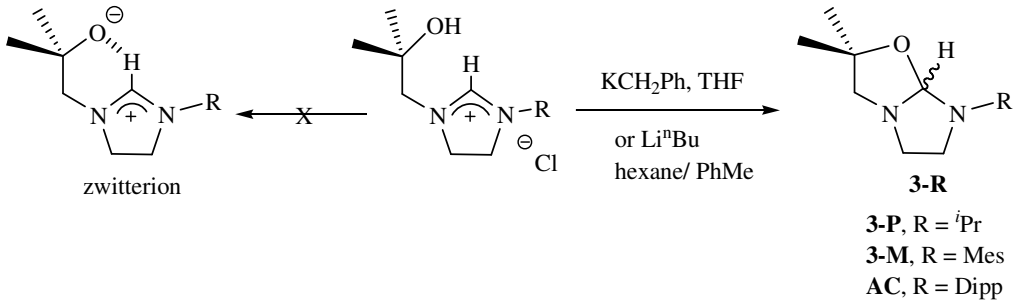

Scheme 19. Bicyclic structure adopted by HL^R adducts **3-R**.

The ^{1}H NMR spectra of these adducts verify the loss of the imidazolinium CH resonance of the starting materials between δ = 8 and 10 ppm, and confirm the presence of a single remaining acidic imidazolidine proton between δ = 5.4 and 5.7 ppm. The spectra also reveal diastereotopic *gem*-dimethyl groups, as well as inequivalent arm CH_2 resonances, which now display geminal coupling as a pair of doublets between δ = 2.4 and 2.9 ppm, $^2J_{HH}$ = 10.5 Hz. All four backbone protons are inequivalent, giving rise to a series of multiplets between δ = 2.5 and 3.5 ppm, and it is apparent that the nitrogen substituents (^{i}Pr, Mes and Dipp) also contain diastereotopic methyl groups, as the resonances assigned to these groups are also split. The ^{13}C NMR spectra are commensurate with an asymmetric structure for these adducts and display a resonance between δ = 107 and 109 ppm, attributed to the imidazolidine carbon. A similar bicyclic structure was recently reported, **CLXXVIII** in Figure 42, from the annelation of a 1-substituted benzimidazole using α,β-acetylenic-γ-hydroxyacidnitriles.[24] This compound exhibits characteristic CH resonances in the ^{1}H and ^{13}C NMR spectra as a singlet at δ = 6.28 and 109.0 ppm, respectively, which are comparable to the chemical shifts observed for adducts **3-R**.

The bicyclic adduct structures formed by **3-R** are single molecule analogues of the pentafluorophenyl (**CLXXVI**),[25] Cl_3C (**CLXXVII**)[25-27] and MeO/ ^{t}BuO (**CLXXIX** and **CLXXX**),[26, 28] all in Figure 42, adducts that have been used with great success as masked carbenes. The methanol adduct **CLXXIX** was formed from the reaction between the free imidazolin-2-ylidene and methanol, and the ^{1}H and ^{13}C NMR spectra exhibit chemical shifts for the imidazolidine CH of δ = 5.48 and 104.0 ppm, respectively.

These data are consistent with an asymmetric structure for **3-R**, as drawn in Scheme 19, which is maintained in solution, and not a zwitterionic structure as adopted by the unsaturated analogue, Scheme 17. This zwitterion displays ^{1}H and ^{13}C NMR resonances at δ = 7.77 and 199.0 ppm, respectively, for the imidazolium CH, which differ significantly from those observed in adducts **3-R**.

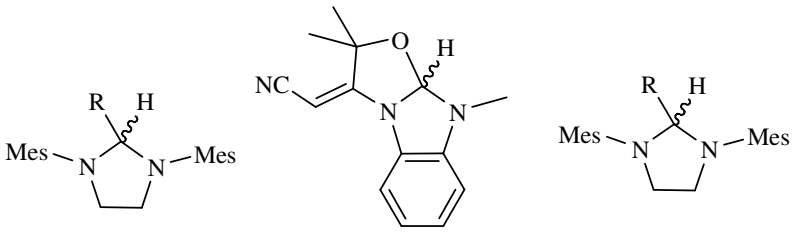

CLXXVI, R = C_6F_5
CLXXVII, R = CCl_3

CLXXVIII

CLXXIX, R = OMe
CLXXX, R = O^{t}Bu

Figure 42. Substituted imidazolidines as examples of masked carbenes.

The solid state structure of **3-M** was ascertained from X-ray quality single crystals which grew over time from the product oil. The molecular structure is drawn in Figure 43. The expected asymmetric, bicyclic adduct structure is confirmed in the solid state and can be compared with the methanol adduct **CLXXIX**, Figure 42. The imidazolidine carbon C1 has a *pseudo*-tetrahedral geometry in both cases, as expected for a sp^3 carbon, with a range of angles in **3-M** between 105.71(14) and 114.08(14)º; the N-C-N bond angle of 105.71(14)º lies closer to that of a carbene than an imidazolinium proligand starting material (110–114º). The heterocyclic C-N bond lengths are marginally asymmetric at 1.459(2) and 1.438(2) Å, and the C-O bond length is 1.432(2) Å. These bond lengths are similar to those observed in **CLXXIX**, with C-N and C-O bond lengths of 1.443(4), 1.428(5) and 1.437(4) Å, respectively.[28]

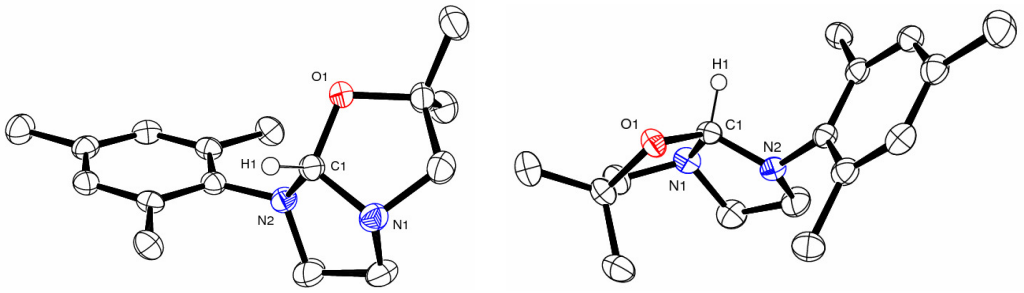

Figure 43. Displacement ellipsoid drawing of the molecular structure of **3-M** (50 % probability ellipsoids). Hydrogen atoms omitted for clarity (except on C1). Selected bond lengths (Å) and angles (º); C1-O1 1.432(2), C1-N1 1.459(2), C1-N2 1.438(2), N1-C1-N2 105.71(14), N1-C1-O1 108.23(13), N2-C1-O1 114.08(14).

2.4.2 Attempted synthesis of Group 1 NHC complexes

Our attention then turned to isolating Group One salts of these saturated-backbone ligands, as we had previously for the unsaturated analogues,[22, 29] which have shown great utility in subsequent salt metathesis chemistry.

From the reaction of **2-P** with two equivalents of KN" in THF, and subsequent extraction into hexane, was isolated a brown powder, **4** in Eq. 13.

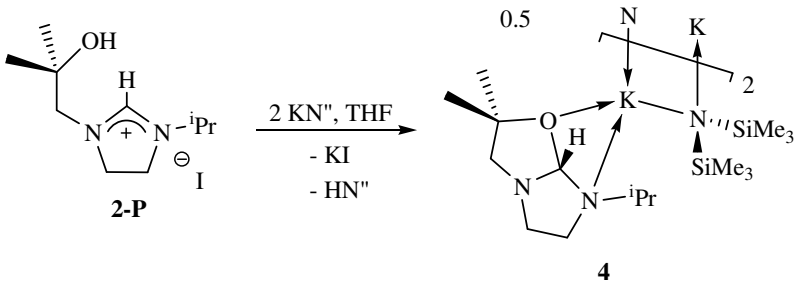

Eq. 13

The ^{1}H NMR spectrum revealed the absence of the imidazolinium CH resonance at δ = 9.00 ppm, and the rest of the spectrum is asymmetric and reminiscent of the bicyclic adduct **3-P**. The ^{13}C NMR spectrum is coonsistent with this, and no evidence for the

formation of a carbene in the high-frequency spectral region is seen. X-ray quality single crystals were isolated from a concentrated hexane solution stored at −30 ºC and proved to be very thermally sensitive. The molecular structure of **4** is drawn in Figure 44, but unfortunately the poor quality of the data does not permit a detailed discussion of the structural features. Additionally, elemental analysis proved low in carbon, hydrogen and nitrogen, indicating the purity of the bulk material was lacking.

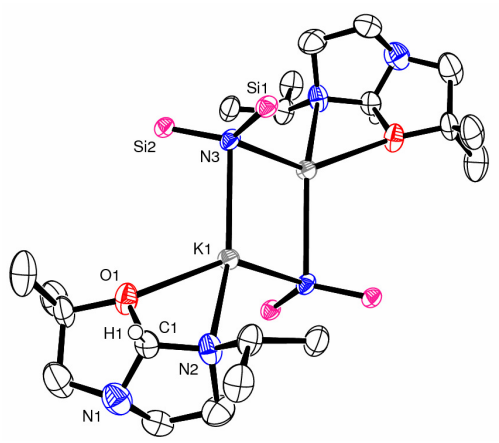

Figure 44. Displacement ellipsoid drawing of the molecular structure of **4** (50 % probability ellipsoids). Silicon bound carbon atoms and hydrogen atoms omitted for clarity (except on C1).

The structure is dimeric in the solid state, based around two bridging KN" groups forming a K_2N_2 core residing over a crystallographic inversion centre, with the coordination sphere of each potassium being completed through coordination to the oxygen and one of the nitrogen atoms of the ligand. The imidazolinium iodide starting material has been singly deprotonated, with no inclusion of any iodide containing residues, and the resulting ligand intermediate forms a bicyclic adduct structure, with the formerly imidazolinium CH now forming the central imidazolidine unit.

These results demonstrate that the mono-deprotonation of the imidazolinium proligands **1-R** or **2-R** occurs readily, with the resulting products **3-R** being isolated cleanly in good yield and adopting a bicyclic adduct structure in solution and the solid state. This bicyclic adduct appears to be quite stable, either to the extent that group one bases do not

deprotonate the imidazolidine CH, or that the subsequent metal complexes are unstable, precluding their isolation.

It was therefore desirable to probe the reactivity of these adducts, in an attempt to ascertain their potential application as ligand precursors.

2.5 Reactivity studies

The addition products of a free carbene and molecules such as pentafluorobenzene **CLXXVI**, chloroform **CLXXVII**, methanol **CLXXIX** and *tert*-butanol **CLXXX**, Figure 42, have been used successfully by others as masked carbenes which can be thermally converted to the free carbenes. For example, **CLXXX** spontaneously decomposes at room temperature[26] and the methanol adduct **CLXXIX** reversibly eliminates methanol at 25 ºC.[28] Further evidence for the generation of the free carbene at room temperature from **CLXXIX** was provided by treatment with a 10-fold excess of $CDCl_3$, Scheme 20. The new addition product **CLXXXI** was formed quantitatively after ten minutes at room temperature, with concomitant formation of methanol as identified by NMR spectroscopy.

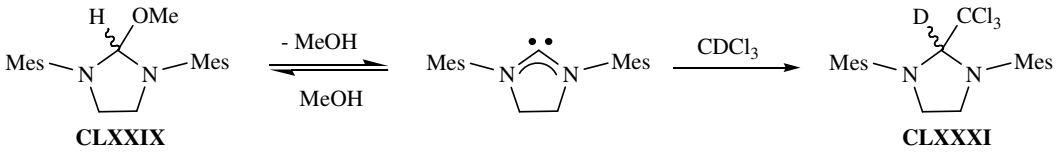

CLXXIX **CLXXXI**

Scheme 20. Reactivity of **CLXXIX** with $CDCl_3$.

Here, heating a C_6D_6 solution of adducts **3-R** to 70 ºC in the NMR spectrometer does not show any evidence of a dissociated carbene-alcohol, depicted in Scheme 21.

The reaction of adducts **3-R** with substrates bearing an acidic hydrogen, such as phenyl acetylene, pentafluorobenzene or 2,6-di-*tert*-butylphenol, in an attempt to form the corresponding ring opened addition products with an alcohol tether, were unsuccessful even at elevated temperatures up to 95 ºC. This suggests that the bicyclic structure is

significantly more thermally robust than the intermolecular adducts mentioned previously. This could be due to greater stability of the five-membered chelate in the starting material and the relative pKa of the resulting alcohol favouring the ring closed starting material.

Treatment of a C_6D_6 solution of **3-P** or **3-M** with a 10-fold excess of $CDCl_3$, followed by heating at 60 ºC, furnished the bicyclic deuterium exchange products **5-P** and **5-M**, represented as **5-R** in Scheme 21, accompanied by concomitant production of $CHCl_3$, as opposed to the anticipated ring opened addition products similar to **CLXXXI**, Scheme 20.

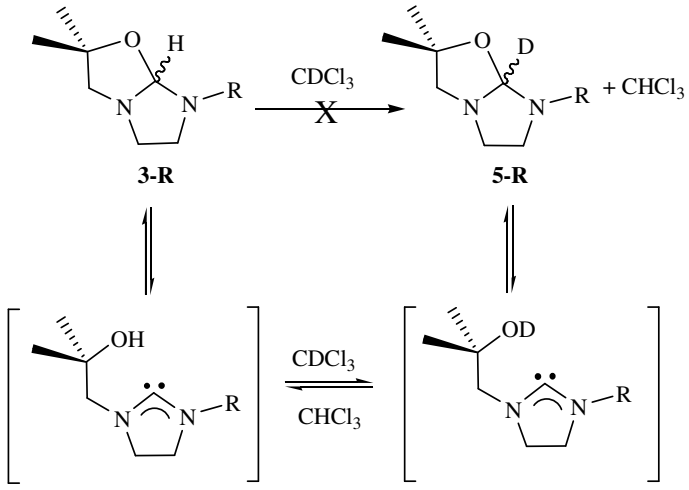

Scheme 21. Transient formation of an alcohol-carbene and reaction with $CDCl_3$.

For both reactions, the ^1H NMR spectra show the absence of the characteristic imidazolidine CH resonance at δ = 5.47 and 5.79 ppm, respectively, and a large increase in the integral of $CHCl_3$. The rest of the spectrum remains unchanged. A comparison of the imidazolidine and chloroform regions of the ^{13}C NMR spectrum are made in Figure 45. The left hand pair of spectra show the imidazolidine CH singlet of **3-R** decreasing in intensity and being replaced by a triplet, which is consistent with exchange by a quadrupolar deuterium atom. This process is accompanied by concomitant production of

$CHCl_3$, as shown by the right hand pair of spectra, through the large increase of the singlet associated with this.

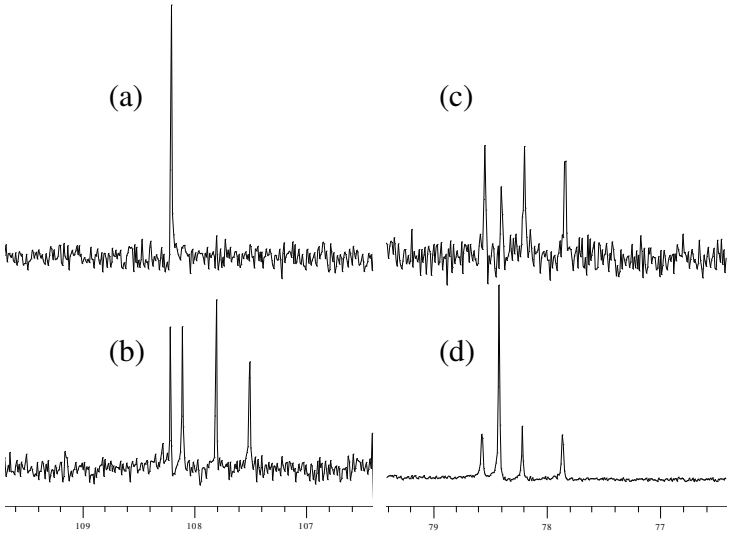

Figure 45. Comparison of ^{13}C NMR spectra for **5-R** (ppm); (a) Imidazolidine CH resonance in starting materials **3-R**; (b) Residual **3-R** and new triplet imidazolidine CD resonance; (c) Initial $CDCl_3$ triplet and small residual $CHCl_3$ singlet; (d) $CHCl_3$ singlet is considerably larger in spectra of **5-R**.

These data support the premise of a H/D exchange between the imidazolinium proton and chloroform in solution. Since a direct H/D exchange of the proton in the bicyclic structure is presumed to be not possible under these reaction conditions, the simplest exchange mechanism would involve the transient generation of the free carbene-alcohol in an equilibrium with the inter- and intra-molecular addition product, Scheme 21, to finally yield compounds **5-R**.

2.5.1 Adduct functionalisation reactions

The suggestion of transient carbene formation in these systems led us to probe further the reactivity and potential nucleophilicity of the bicyclic adducts by functionalising with a suitable electrophile. Thus, treatment of **3-P** or **3-M** with a small excess of

Me_3SiI, in hexane, furnished **6-P** and **6-M**, respectively, as colourless solids in good yield, Eq. 14.

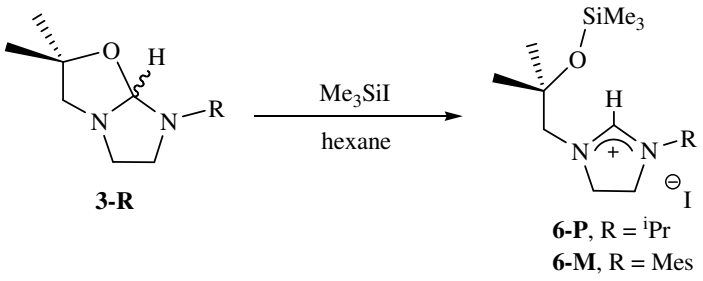

3-R

6-P, R = ^{i}Pr
6-M, R = Mes

Eq. 14

The ^{1}H NMR spectrum revealed a simplified set of ligand resonances, when compared to that of adducts **3-P** and **3-M**, indicating that the asymmetric bicyclic adduct structure has been broken. The imidazolidine CH resonance at δ = 5.47 and 5.79 ppm, respectively, is no longer present, whereas there is now a characteristic imidazolinium resonance at δ = 9.85 and 9.54 ppm, respectively, indicating the presence of a cationic ring system. The backbone CH_2 groups now appear as two simplified multiplets, and the arm CH_2 group as a singlet, between δ = 3.6 and 4.1 ppm, due to the presence of a mirror plane through the molecule. The arm methyl groups now appear as a singlet in both compounds, and the *iso*-propyl and mesityl substituents are symmetric, showing one and two methyl group resonances, respectively, in accordance with a non-chiral, sterically unconstrained system. The O-$SiMe_3$ group resonates at δ = 0.15 ppm, which is within the expected region. The ^{13}C NMR spectra are in agreement with this, and display an imidazolinium CH resonance at δ = 158.4 and 160.4 ppm, respectively, and no imidazolidine resonance between δ = 107 and 109 ppm.

X-ray quality single crystals of **6-P** were grown from a benzene solution, and the molecular structure is drawn in Figure 46.

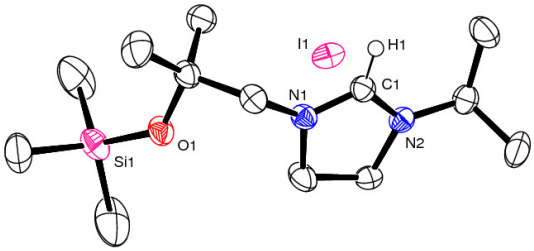

Figure 46. Displacement ellipsoid drawing of the molecular structure of **6-P** (50 % probability ellipsoids). Hydrogen atoms omitted for clarity (except on C1). Selected bond lengths (Å) and angles (º); C1-N1 1.331(4), C1-N2 1.306(4), O1-Si1 1.635(3), N1-C1-N2 114.3(3).

The loss of the bicyclic structure of **3-P** is confirmed, along with the silylation of the alcohol oxygen. The C-N bond lengths of 1.331(4) and 1.306(4) Å are similar within standard e.s.ds, unlike the asymmetry seen in the two C-N bond lengths of proligand **2-P**, Table 4. The N-C-N bond angle is 114.3(3)º, typical of the more trigonally symmetric sp^2 carbon character of the cationic imidazolinium group, and is 1.5º wider than the angle of 110.6(4)º observed in **2-P**. The O-Si bond length of 1.635(3) Å is typical of a silyl-ether group (1.63–1.67 Å).

2.6 Magnesium and Zinc complexes

We were encouraged by the formation of the silylated products **6-R**, as they demonstrated that the bicyclic adduct structure of precursors **3-R** could be opened by coordination of a suitably oxophilic element to the oxygen atom. Therefore, the protonolysis chemistry of precursors **3-R** with magnesium and zinc silylamides was investigated as a route to saturated alkoxy-carbene metal complexes.

2.6.1 Mono-alkoxy-carbene complexes

Treatment of $MgN"_2(THF)_2$ with one equivalent of the bicyclic adducts **3-P** or **3-M** in hexane, or toluene with **AC**, readily affords the corresponding mono-NHC metal

silylamide complexes **7-P**, **7-M** and **AD**, respectively, Eq. 15, in good yield as colourless powders after filtration and drying under reduced pressure. Similarly, an analogous procedure using $ZnN"_2$ and **3-P** in hexane, or **AC** in toluene, furnishes complexes **8-P** or **AE** in good yield.

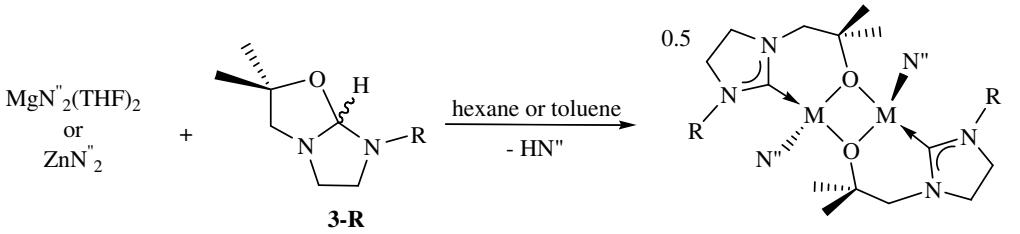

M = Mg **7-P**, R = ^{i}Pr **7-M**, R = Mes **AD**, R = Dipp

M = Zn **8-P**, R = ^{i}Pr **AE**, R = Dipp

Eq. 15

The ^{1}H NMR spectra of **7-P** and **8-P**, *iso*-propyl ligand bearing magnesium and zinc analogues, show an asymmetric set of ligand resonances, reminiscent of the diastereotopic methyl groups in the bicyclic starting material **3-R**. Crucially, however, the characteristic imidazolidine CH resonance between δ = 5.4 and 5.7 ppm is now absent. The *iso*-propyl CH septet has shifted ~1.5 ppm downfield of that in **3-P**, to δ = 4.28 and 4.35 ppm, respectively, in accordance with the heterocylic ring system becoming more electron deficient with coordination to the electropositive metal centre. The methylene arm protons again appear as a pair of doublets, one of which is shifted almost 1 ppm downfield, from δ = 2.45 and 2.91 ppm in **3-P**, to δ = 2.45 and 3.70 ppm in **7-P** and δ = 2.45 and 3.63 ppm in **8-P**. The $^2J_{HH}$ coupling constant for these doublets has increased, from 10.5 Hz to 14.4 and 13.8 Hz, respectively. The ^{13}C NMR spectra confirm that the ligand is metal-bound, by the presence of a high-frequency carbene resonance at δ = 210.2 (Mg) and 204.8 ppm (Zn).

The ^{1}H NMR spectra of the magnesium and zinc complexes bearing a Dipp group, **AD** and **AE**, surprisingly show a set of symmetric ligand resonances despite the more sterically demanding substituent, compared to **7-R** and **8-P**, possibly indicating achiral

complexes and therefore a different structure in solution. Both ^{13}C NMR spectra possess a carbene carbon resonance at δ = 207.9 and 196.1 ppm, respectively, which are similar to those observed in **7-P** and **8-P**.

The mesityl analogue **7-M** displays a broadened, poorly resolved symmetric set of ligand resonances in the ^{1}H NMR spectrum. At room temperature, the mesityl substituent experiences hindered rotation around the N-C bond, as evidenced by two broad *ortho*-methyl resonances at δ = 2.33 and 2.23 ppm. The ^{13}C NMR spectrum displays a carbene carbon resonance at δ = 213.2 ppm, although a number of other ligand resonances are very poorly resolved, so as to be almost indiscernible from the baseline. A variable temperature NMR study up to 70 ºC shows a coalescence of the *ortho*-methyl resonances to a singlet at δ = 2.27 ppm in the ^{1}H NMR spectrum, as well as the sharpening of all other ligand resonances. This implies that free rotation around the C-N bond is now possible, borne out by examination of the ^{13}C NMR spectrum which displays a complete set of well resolved symmetric ligand resonances, and a carbene resonance at δ = 214.0 ppm.

In a further NMR scale reaction, $MgN"_2(THF)_2$ was treated with one equivalent of the unsaturated analogue of **3-P**, the zwitterion **HL**, in benzene at room temperature. The reaction produced products containing three ligand environments in an approximate 2:1:1 ratio, as identified by ^{1}H NMR spectroscopy. Only the resonances due to the main component could be assigned, as the mono-alkoxy-carbene magnesium amide complex **9**, analogous to **7-P**. The ^{13}C NMR spectrum also displays a $Mg\text{-}C_{carbene}$ resonance at δ = 185.9 ppm.

X-ray quality single crystals of magnesium complexes **7-P** and **9**, and zinc complexes **8-P** and **AE**, were grown from benzene solutions at room temperature. Thermal ellipsoid drawings of the molecular structures are shown in Figure 47, with selected bond lengths and angles displayed in Table 5.

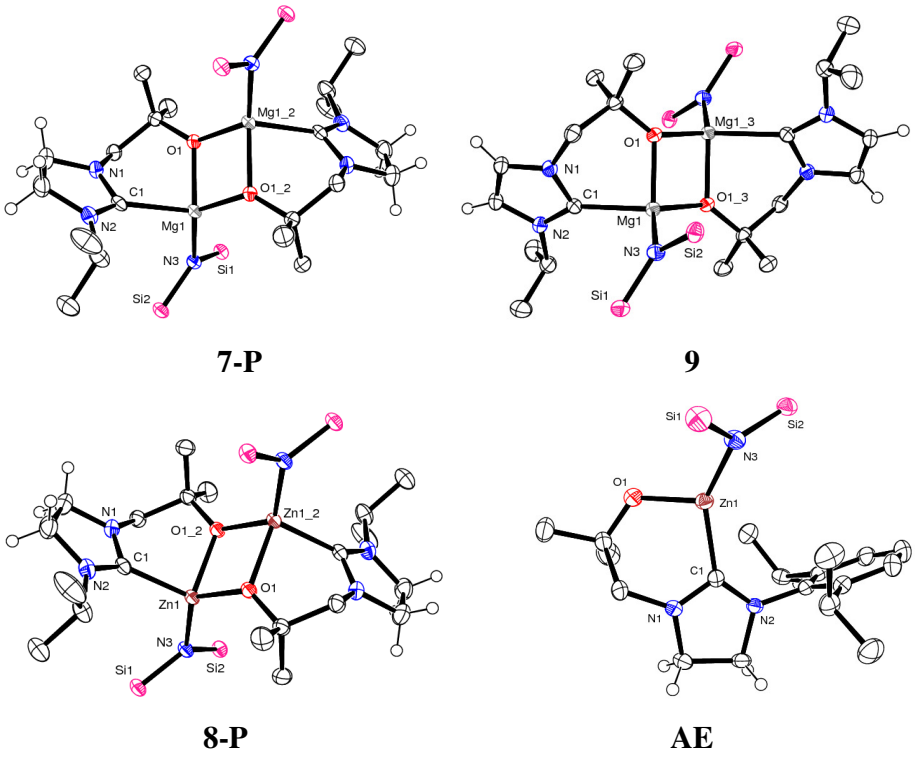

Figure 47. Displacement ellipsoid drawings of the molecular structures of **7-P**, **9**, **8-P** and **AE** (50 % probability ellipsoids). Solvent molecules, silicon bound methyl groups and hydrogen atoms omitted for clarity (except on the NHC backbone carbons).

Complexes **7-P**, **9** and **8-P**, bearing an *iso*-propyl substituent, all adopt a dimeric structure in the solid state, with the central M_2O_2 core positioned at a crystallographic inversion centre and containing a μ_2-O ligand alkoxide, with a distorted tetrahedral geometry at the metal centre. Zinc complex **AE**, however, adopts a monomeric structure in the solid state, likely due to the more sterically demanding Dipp substituent preventing dimerisation, Figure 47. The geometry at zinc is distorted trigonal planar due to the constrained bite angle of the alkoxy-carbene ligand. Thus, the C1-Zn1-O1 angle is 97.73(7)º, whereas the C1-Zn1-N3 and O1-Zn1-N3 angles are 142.79(8) and 118.16(8)º, respectively, and the angle sum is 358.7º.

As the magnesium complexes **7-P** and **9** are identical other than in the saturated/ unsaturated backbone of the NHC, respectively, any differences in the observed metrical parameters can be attributed to differences in the metal-carbene bonding interaction. The

Mg1-O1 and Mg1-N3 bond lengths in both complexes are essentially the same at 1.95 and 2.03 Å, respectively. The Mg1-C1 bond length of 2.2615(18) Å in **7-P** is *ca.* 0.021 Å longer than that in **9** of 2.2403(18) Å and well outside the 3σ criteria. This suggests that whilst the Mg-NHC bond appears stronger in the unsaturated complex than the saturated, in agreement with Nolan's previous studies,[8, 10] the overall difference is marginal. The average NHC N-C bond lengths in **7-P** and **9** of 1.339(2) and 1.365(2) Å, respectively, as well as the N-C-N bond angles of 107.22(15) and 103.16(14)º respectively, all lie within the ranges expected for saturated (1.32–1.36 Å, 106–111º) and unsaturated (1.36–1.38 Å, 101–103º) NHCs.

The magnesium and zinc complexes **7-P** and **8-P** are isostructural, and so any metrical deviations can be ascribed to differences between the divalent cations. The Zn1-O1_2 bond length of 2.0565(9) Å in **8-P** is significantly longer than the Mg1-O1 bond length of 1.9566(13) Å in **7-P**. Conversely, the Zn1-C1 and Zn1-N3 bond lengths are 2.1017(13) and 1.9712(11) Å, respectively, which are much shorter than the Mg1-C1 and Mg1-N3 bond lengths of 2.2615(18) and 2.0324(15) Å, respectively. These data are commensurate with the harder, more oxophilic magnesium cation forming stronger Mg-O bonds, at the expense of longer Mg-C and Mg-N bond lengths, whereas the more polarisable zinc cation accommodates the softer carbene and nitrogen groups more effectively through shorter bonds, resulting in a longer Zn-O bond length. The NHC bond lengths and angles in both complexes are within expected ranges.

The differences in steric profile of the ligand substituents has a profound effect on the molecular structures of dimeric zinc complex **8-P** and monomeric **AE**, which results in large differences in the metrical parameters between the two complexes. The zinc-ligand bond lengths in **AE** are all much shorter than those observed in **8-P**, Zn1-C1 2.024(2) vs. 2.1017(13) Å, Zn1-N3 1.8991(18) vs. 1.9712(11) Å, Zn1-O1 1.8878(16) vs. Zn1-O1_2 2.0565(9) Å, respectively. The NHC N-C-N bond angle and N-C bond lengths in **AE** are comparable to those in **8-P**, although there is a small degree of asymmetry in the N-C bond lengths seen in **AE** of 1.317(3) and 1.336(2) Å. The *iso*-propyl substituent in **8-P** does not sterically protect the metal centre sufficiently, allowing the zinc to achieve coordinative saturation *via* dimerisation and formation of a sterically crowded complex,

whereas the Dipp substituent in **AE** is too bulky to allow dimer formation, and so the coordinatively unsaturated zinc cation interacts more strongly with its ligand set. If these solid state structures are maintained in solution, which is reasonable to assume in the absence of a coordinating solvent, it is now evident why the chiral dimer **8-P** produces a complex, asymmetric ^{1}H NMR spectrum, whereas the achiral monomer **AE** yields a simplified, symmetric spectrum.

Table 5. Selected distances (Å) and angles (°) for the molecular structures of **7-P**, **9**, **8-P** and **AE**.

	7-P (M = Mg)	**9** (M = Mg)	**8-P** (M = Zn)	**AE** (M = Zn)
M1-C1	2.2615(18)	2.2403(18)	2.1017(13)	2.024(2)
M1-O1	1.9566(13)	1.9476(14)	2.0565(9)	1.8878(16)
M1-N3	2.0324(15)	2.0332(15)	1.9712(11)	1.8991(18)
N1-C1-N2	107.22(15)	103.16(14)	108.25(12)	108.93(18)
N1-C1	1.343(2)	1.366(2)	1.3348(18)	1.317(3)
N2-C1	1.335(2)	1.363(2)	1.3361(17)	1.336(2)
M1-M_$1	2.9553(12)	2.9549(12)	3.0755(3)	–

2.6.2 Bis-alkoxy-carbene complexes

Treatment of ZnN"$_2$ with two equivalents of **3-P** or **3-M** in hexane, or **AC** in toluene, at 70 ºC overnight furnishes complexes **10-P**, **10-M** or **AF**, respectively, in good yield, Scheme 22. All attempts to synthesise the corresponding magnesium analogues, even after prolonged heating up to 100 ºC, resulted only in an equal mixture of the mono-alkoxy-carbene complexes **7-P**, **7-M** and **AD** and the corresponding ligand adduct **3-R**.

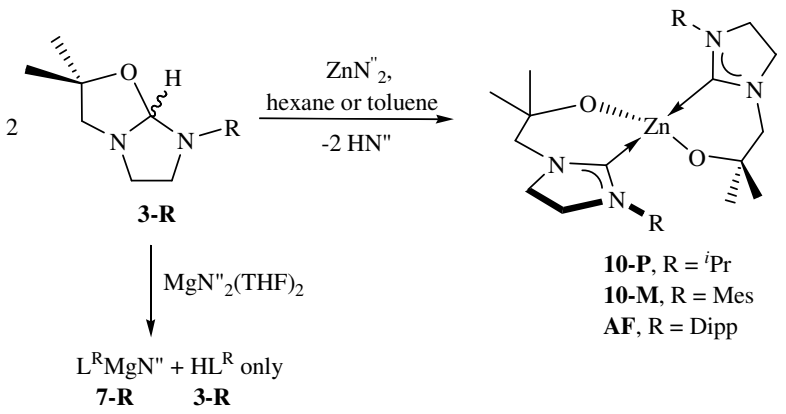

Scheme 22. Synthesis of *bis*-alkoxy-carbene zinc complexes.

All three zinc complexes exhibit distinctly asymmetric ^{1}H NMR spectra. Complex **10-P** exhibits an *iso*-propyl septet at δ = 4.65 ppm, as opposed to δ = 4.35 ppm seen in **8-P**, and a pair of roofed doublets at δ = 3.12 and 3.05 ppm with a coupling constant $^{2}J_{HH}$ = 12.6 Hz, attributable to the diastereotopic methylene arm protons. The mesityl analogue **10-M** displays similar methylene arm doublets at δ = 2.78 and 2.33 ppm, with a coupling constant $^{2}J_{HH}$ = 12.4 Hz, and three aromatic methyl groups at δ = 2.61, 2.20 and 2.04 ppm. Complex **AF** displays two septets at δ = 3.16 and 2.97 ppm and four doublets at δ = 1.39, 1.35, 1.25 and 1.14 ppm, all with a coupling constant $^{3}J_{HH}$ = 7.0 Hz, resulting from the asymmetric Dipp group. A pair of methylene arm doublets are also present at δ = 2.73 and 2.08 ppm, coupling constant $^{2}J_{HH}$ = 14.0 Hz. The ^{13}C NMR spectra of **10-P**, **10-M** and **AF** each display a high-frequency carbene carbon resonance at δ = 203.6, 205.7 and 201.3 ppm, which are similar to those seen for the mono-ligand complexes.

In a comparison study with the unsaturated backbone zwitterion **HL**, Scheme 17, on an NMR scale, the reaction between ZnN"$_2$ and two equivalents of **HL** in C_6D_6 proceeded smoothly at ambient temperature within 30 min to yield **11**, ZnL_2, in quantitative yield. The methylene arm protons are equivalent and appear as a singlet at δ = 3.74 ppm, although the arm methyl groups are asymmetric and show two singlets at δ = 1.50 and 1.31 ppm, the diastereotopic *iso*-propyl methyl groups appear as a pair of doublets at δ = 1.26 and 1.14 ppm, with a coupling constant of $^{3}J_{HH}$ = 6.7 Hz. The ^{13}C NMR spectrum displays a high-frequency carbene carbon resonance at δ = 179.0 ppm, within the

expected region for unsaturated metal-bound NHCs, and is typically 20–30 ppm lower frequency from the saturated analogues.

An X-ray structural analysis was performed on single crystals of **10-M**, the molecular structure of which is drawn in Figure 48. Unfortunately, the quality of the dataset obtained was not sufficient for publication and only allows connectivity to be ascertained.

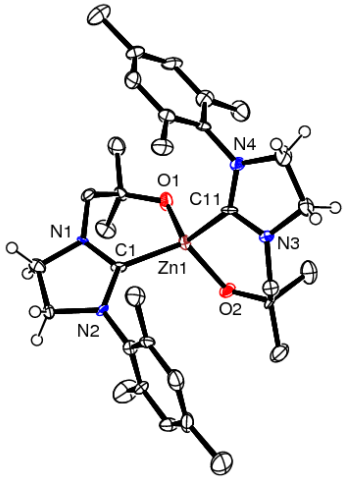

Figure 48. Displacement ellipsoid drawing of the molecular structure of **10-M** (50 % probability ellipsoids). Hydrogen atoms omitted for clarity (except on the NHC backbone carbons).

The complex consists of two bidentate alkoxy-carbene ligands bound to the zinc centre, and the geometry at the four coordinate metal is distorted-tetrahedral.

2.6.3 NMR-scale Reactivity Studies

The reactivity of the mono-ligand magnesium **7-P** and zinc **8-P** complexes were investigated through NMR spectroscopic studies, *via* treatment of a benzene solution with one equivalent of Me_3SiI, Scheme 23. No reaction was observed at room temperature for **7-P**, but subsequent heating at 80 °C overnight produced **12**. The ^1H NMR spectrum is simpler than that of the starting material, indicative of a monodentate alkoxy-NHC ligand, with the *iso*-propyl septet now resonating at δ = 3.74 ppm and the

methylene arm group as a singlet at δ = 3.42 ppm, suggesting a symmetric ligand environment. The carbene carbon resonance in the ^{13}C NMR spectrum at δ = 210.2 ppm is no longer present, although there is a resonance at δ = 174.6 ppm, which implies that the Mg-C bond has been broken and the carbene silylated, resulting in a cationic ring system. This is at approximately 20 ppm higher-frequency than a protonated imidazolinium carbon, which resonates at δ = 155–160 ppm. In comparison, treatment of the zinc analogue **8-P** with Me_3SiI proceeds smoothly at room temperature within 30 mins to afford **13**. The ^{1}H NMR spectrum is simplified and shows the *iso*-propyl septet at δ = 4.64 ppm, similar to complexes containing a metal-bound NHC, and the methylene arm group is present as a singlet at δ = 3.46 ppm, again suggesting a monodentate alkoxy-NHC ligand. The ^{13}C NMR spectrum confirms the presence of a metal-bound carbene at δ = 196.8 ppm, which is shifted 8 ppm upfield of the starting material.

These reactivity differences highlight and complement those differences in the metrical data observed in the solid state structures of **7-P** and **8-P**, Figure 47, which showed a shorter Mg-O vs. Zn-O bond length and conversely a shorter Zn-C vs. Mg-C bond length. Hence, the Mg-C and Zn-O in **12** and **13**, respectively, have been broken and silylated.

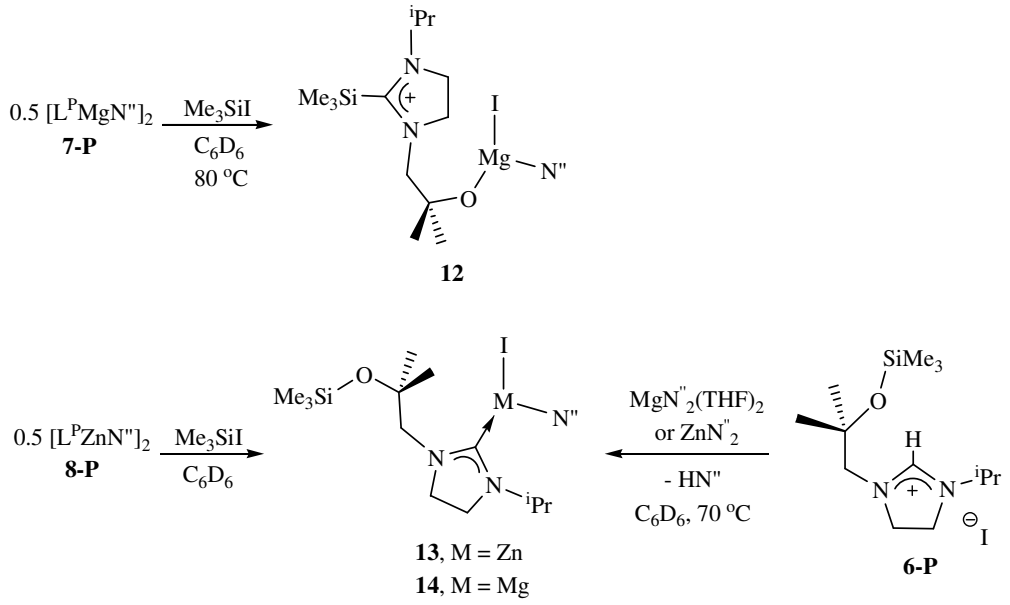

Scheme 23. NMR-scale reactivity studies.

Bearing in mind these differences, an attempt was made to affect the resulting product by treatment of $MgN"_2(THF)_2$ or $ZnN"_2$ with one equivalent of the pre-silylated imidazolinium proligand **6-P**. Predictably, the reaction with $ZnN"_2$ yielded **13**, albeit in ~40 % yield by NMR, and a second unidentified compound which contains a monodentate silylated-alkoxy-NHC ligand, as evidenced by a similar ^{1}H NMR spectrum and carbene carbon resonance at δ = 198.3 ppm, in an estimated 60 % yield. Contrastingly, the reaction with $MgN"_2(THF)_2$ affords **14**, which is analogous to the zinc congener **13** and different from the first magnesium compound **12**. The main difference between these two magnesium complexes is that **14** displays a carbene carbon resonance in the ^{13}C NMR spectrum at δ = 207.2 ppm, as opposed to the silylated imidazolinium carbon resonance at δ = 176.4 ppm, suggesting the ligand is now carbene bound.

2.7 Lactide polymerisation studies

In recent years, NHC ligands have been applied in numerous ways, particularly in homogeneous catalysis for effecting organic transformations,[22, 30-32] in stabilising more Lewis acidic metal centres[33-35] and as active polymerisation catalysts.[36, 37]

One such process, the ring opening polymerisation (ROP) of *rac*-lactide, to form polylactide (PLA), has become one of the most important ROP processes of all the cyclic esters, Eq. 16.[38-41] This is due to the inexpensive, renewable sources of the starting monomer and the biodegradable[42] and biocompatible nature of the resulting PLA, which in recent times has found many uses in biomedical and packaging applications.[43-45]

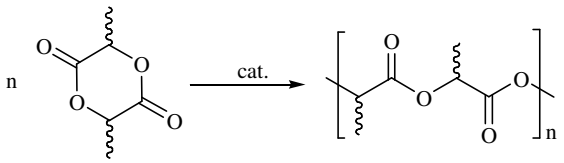

rac-lactide PLA

Eq. 16

Incorporation of metal residues from the catalyst into the product PLA is an important consideration with medical applications. In light of this, although innumerable metal complexes have been utilised for the ROP of lactide,[38, 40, 41, 46, 47] the low toxicity of magnesium and zinc, coupled with their low cost and the lack of colour associated with these metal ions, has led to numerous examples of their use in producing PLA for this field. The range of supporting ligands reported for these complexes include amidinate,[48] ketiminate[49] and β-diiminate,[50-58] Salen type ligands,[59, 60] pyrazolyl derived scorpionates,[58, 61-63] oxazolinate,[64] and phenolates.[65-68]

Of the reported zinc-NHC complexes,[69-73] only a few have been applied to lactide polymerisation. Tolman and Hillmeyer reported substituted- zinc-NHC complexes, **CLXXXII**, **CLXXXIII**, **CLXXXIV** and **CLXXXV** in Figure 49, that are readily

synthesised from diethyl zinc and the free carbene or imidazolium salts and have been shown to be very active lactide polymerisation catalysts.[74, 75]

Magnesium-NHC complexes are rare, as discussed in Chapter 1, and to date there are no examples of magnesium NHC complexes being utilised as homogeneous polymerisation catalysts.

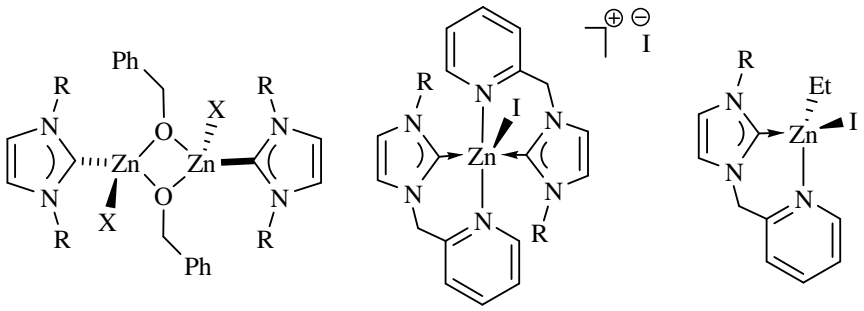

CLXXXII, X = OCH_2Ph
CLXXXIII, X = Cl

R = Mes

CLXXXIV

CLXXXV

Figure 49. Zinc NHC complexes applied to lactide polymerisation.

2.7.1 Polymerisation Studies

The data for a series of reactions between a range of magnesium and zinc alkoxy-NHC complexes and *rac*-lactide are displayed in Table 6. A typical reaction was conducted at room temperature by the addition of THF solutions of the catalyst (3.0 mg) to a solution of the monomer (300 mg), total THF volume of 3.0 ml, with vigorous stirring. It was not necessary to include an initiator, such as benzyl alcohol, to effect polymerisation. As expected, magnesium complexes **7-P** and **AD** are more active catalysts than the zinc complexes **8-P**, **AE**, **10-M** and **AF**, in accordance with the published literature.[50] The more sterically hindered Dipp bearing magnesium complex **AD** is slower than the *iso*-propyl analogue **7-P**, attaining 27 % and 98 % conversion, respectively, after 0.75 h, Table 6 entries 1 and 2. With the exception of entries 2 and 8 in Table 6, all of the experimental polymer molecular weights ($M_{n, exp}$) are less than the theoretical molecular

weights ($M_{n,\ theo}$), with the zinc complexes producing polymers of lower PDI than the magnesium analogues. Of these, the zinc mono-NHC complexes **8-P** and **AE** produce polymer with the lowest PDIs at 1.30 and 1.32, respectively, Table 6 entries 3 and 4, with a conversion of 78 % in 16 h and $M_{n,\ exp}$ of 27 500 g/ mol for **8-P** and 92 % conversion in 17 h and a lower $M_{n,\ exp}$ of 16 000 g/ mol for **AE**. The mesityl and Dipp *bis*-NHC zinc complexes **10-M** and **AF,** Table 6 entries 5 and 6, show a similarly high conversion of ~92 % after 16 and 17 h, respectively, producing polymers with $M_{n,\ exp}$ and PDIs of 20 500 g/ mol and 1.48 and 35 500 g/ mol and 1.40, respectively.

The free NHCs liberated from the pentafluorophenyl **CLXXVI** and methanol **CLXXIX** adducts, Figure 42, as well as a number of other NHCs, have been shown to be potent organocatalysts for the ROP of lactide.[25, 28, 36, 76-79] Similarly, the *iso*-propyl substituted bicyclic adduct **3-P**, Scheme 19, is active towards *rac*-lactide polymerisation, Table 6 entry 7, albeit in low conversion of 30 % after 16 h and low $M_{n,\ exp}$ of 2 000 g/ mol although with good PDI, 1.31. This activity and selectivity is less than that observed with other literature compounds, confirming the inherent stability of these bicyclic adducts when compared to other masked carbenes, and inclusion of an equivalent of benzyl alcohol initiator, Table 6 entry 8, increases the polymerisation rate.

The bicyclic adduct **3-P** could act as a bifunctional catalyst for the ring opening of *rac*-lactide, Scheme 24. If a transient carbene is formed during the polymerisation process it could act as a nucleophilic initiator (path a), whereas formation of an alkoxide could also initiate polymerisation *via* another route (path b). This bifunctional behaviour has been seen previously with the zwitterion **HL**.[36] Attempts to gain insight into the mechanism by which **3-P** initiates the polymerisation of *rac*-lactide, by examination of the ^{13}C NMR spectrum to determine whether the imidazolinium carbon was proton or lactide bound, proved inconclusive.

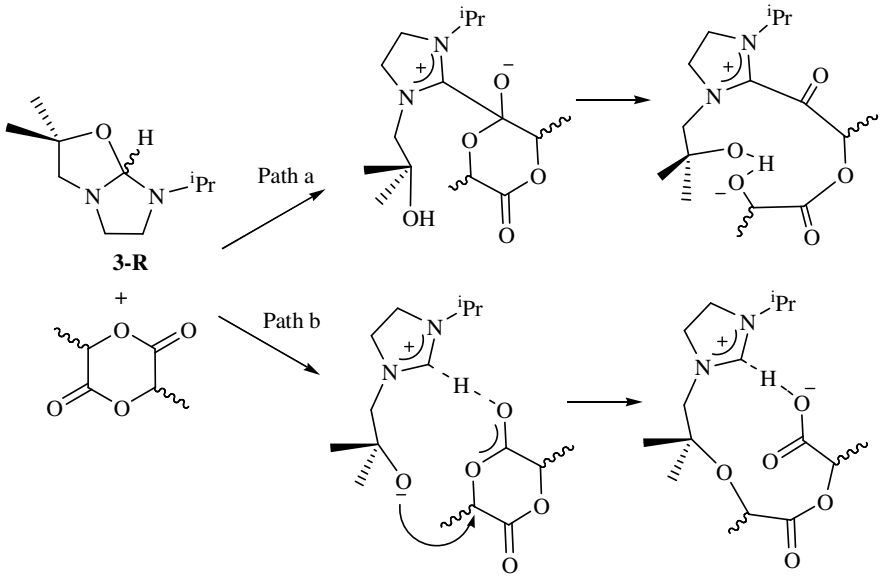

Scheme 24. Possible initiation reactions of *rac*-lactide.

Closer examination of the mono-ligand magnesium and zinc complexes, entries 1–4 in Table 6, may provide some information on the mechanism of polymerisation. The *iso*-propyl bearing magnesium complex **7-P**, entry 1, shows a conversion of 98 % after 0.75 h, and the Dipp bearing analogue **AD**, entry 2, a conversion of 27 % in the same reaction time. This suggests the ligand plays an important role, as the more sterically demanding substituent slows the rate of polymerisation. However, the conversion rates of the *iso*-propyl zinc complex **8-P**, entry 3, and the Dipp analogue **AE**, entry 4, are approximately the same. The initial results for these zinc complexes suggest that the ligand may exert little influence over the rate of polymerisation, and that the metal centre is the dominant factor. This disparity in the rate of polymerisation could indicate a different mechanism to be present between these two pairs of complexes.

Under catalytically relevant conditions, the presence of the strong donor lactide will likely cleave the dimeric structure most of these catalysts adopt in the solid state, thereby mitigating any polymerisation effects due to differences in their solid state structures.

It is established that *rac*-lactide can be polymerised by both metal alkoxide and metal carbene complexes,[36] so it is likely in a complex containing both functionalities that both mechanisms are present. The differences in the rates of polymerisation observed for

complexes **7-P** and **AD**–**AE** can be rationalised by considering the differences between the solid state metrical parameters, Table 4, and reactivity, Scheme 23, of the analogous complexes **7-P** and **8-P**. The magnesium complex **7-P** possesses stronger Mg-O and weaker Mg-C bonds than the zinc analogue **8-P**, as shown in Table 5. Therefore for magnesium, the favoured insertion mechanism is probably into the Mg-C bond. Hence, increasing the steric profile of the *N*-substituent from *iso*-propyl to Dipp restricts the accessibility of the Mg-C bond, and therefore the favoured insertion mechanism, resulting in the observed decrease in polymerisation rate. In the context of the polymerisation by the zinc catalyst, this implies that the dominant insertion mechanism is into the Zn-O bond, which is remote from the ligand N-substituents. Hence, increasing the steric profile of this substituent has negligible effect upon the rate of polymerisation.

Table 6. *Rac*-lactide polymerisation data for Mg and Zn alkoxy-NHC and amide complexes

Entry	Catalyst	Cat:Mono:Sol ratio (wt%)[a]	T (°C)	Time (h)	Conv.[b] (%)	$M_{n\ Theory}$[c] (g/ mol)	$M_{n\ Expt}$[d] (g/ mol)	PDI (M_w/M_n)
1	**7-P**, L^PMgN''	1:100:1000	25	0.75	97.7	36327	26000	1.57
2	**AD**, L^DMgN''	1:100:1000	25	0.75	26.9	13564	18000	1.32
3	**8-P**, L^PZnN''	1:100:1000	25	16	78.3	32444	27500	1.30
4	**AE**, L^DZnN''	1:100:1000	25	17	91.8	48928	16000	1.32
5	**10-M**, ZnL^M_2	1:100:1000	25	16	92.5	54620	20500	1.48
6	**AF**, ZnL^D_2	1:100:1000	25	17	91.9	62085	35500	1.40
7	**3-P**, HL^P	1:100:1000	25	16	29.5	5622	2000	1.31
8	**3-P** + BnOH	1:1[f]:100:1000	25	16	84.0	15667	19500	1.54
9	$MgN''_2(THF)_2$	1:100:1000	25	16	94.6	46788	24500	1.79

a) Solvent = THF; b) Conversion of LA monomer (($[LA]_0$-[LA])/$[LA]_0$); c) ({[LA]/[Cat]}.conversion.RMM(LA))-RMM(Cat) d) measured by GPC, values based on polystyrene standards, weight corrected by multiplication by 0.58 [Mark-Houwink equation] e) polydispersity index (Mw/Mn), PDI, measured by GPC. f) includes one equivalent of benzyl alcohol initiator.

2.8 Conclusions

A new synthetic route to alcohol-functionalised saturated backbone imidazolinium proligands has been developed, *via* a simple modular approach of the ring opening of an epoxide by a substituted diamine with subsequent ring closure. Although deprotonation of these proligands to form the group one metal salts proved unsuccessful, mono-deprotonation furnished a bicyclic imidazolidine intermediate, which subsequent reactivity studies showed could act as a 'masked' carbene. Protonolysis routes to effect ligand transfer with magnesium and zinc silylamides proved facile, with a number of complexes being isolated and characterised. A selection of these complexes proved to be effective for the ROP of *rac*-lactide, at room temperature and without the need for an initiator, to yield polymers of reasonable molecular weight and with good PDI. These are the first magnesium and zinc complexes bearing saturated-backbone alkoxy-NHC ligands, and this is the first time that a magnesium NHC complex has been demonstrated to effect lactide polymerisation.

2.9 References

[1] A. J. Arduengo, *Acc. Chem. Res.* **1999**, *32*, 913.
[2] H. W. Wanzlick, H. J. Kleiner, *Angew. Chem.* **1961**, *73*, 493.
[3] H. W. Wanzlick, *Angew. Chem., Int. Ed. Engl.* **1962**, *1*, 75.
[4] D. J. Cardin, B. Cetinkaya, M. F. Lappert, L. J. Manojlovic-Muir, K. W. Muir, *Chem. Commun.* **1971**, 400.
[5] D. M. Khramov, V. M. Lynch, C. W. Bielawski, *Organometallics* **2007**, *26*, 6042.
[6] S. Díez-González, S. P. Nolan, *Coord. Chem. Rev.* **2007**, *251*, 874.
[7] P. L. Arnold, S. Zlatogorsky, N. A. Jones, C. D. Carmichael, S. T. Liddle, A. J. Blake, C. Wilson, *Inorg. Chem.* **2008**, *47*, 9042.
[8] R. Dorta, E. D. Stevens, N. M. Scott, C. Costabile, L. Cavallo, C. D. Hoff, S. P. Nolan, *J. Am. Chem. Soc.* **2005**, *127*, 2485.
[9] S. Fantasia, J. L. Petersen, H. Jacobsen, L. Cavallo, S. P. Nolan, *Organometallics* **2007**, *26*, 5880.
[10] R. A. Kelly III, H. Clavier, S. Giudice, N. M. Scott, E. D. Stevens, J. Bordner, I. Samardjiev, C. D. Hoff, L. Cavallo, S. P. Nolan, *Organometallics* **2008**, *27*, 202.
[11] P. L. Arnold, S. Pearson, *Coord. Chem. Rev.* **2007**, *251*, 596.
[12] P. L. Arnold, S. T. Liddle, *Chem. Commun.* **2005**, 5638.
[13] A. Paczal, A. C. Benyei, A. Kotschy, *J. Org. Chem.* **2006**, *71*, 5969.
[14] R. S. Bon, F. J. J. deKanter, M. Lutz, A. L. Spek, M. C. Jahnke, F. E. Hahn, M. B. Groen, R. V. A. Orru, *Organometallics* **2007**, *26*, 3639.
[15] R. Jazzar, J. B. Bourg, R. D. Dewhurst, B. Donnadieu, G. Bertrand, *J. Org. Chem.* **2007**, *72*, 3492.
[16] F. E. Hahn, V. Langenhahn, T. Pape, *Chem. Commun.* **2005**, 5390.
[17] A. W. Waltman, R. H. Grubbs, *Organometallics* **2004**, *23*, 3105.
[18] A. O. Larsen, W. Leu, C. N. Oberhuber, J. E. Campbell, A. H. Hoveyda, *J. Am. Chem. Soc.* **2004**, *126*, 11130.
[19] H. Clavier, L. Coutable, L. Toupet, J. C. Guillemin, M. Mauduit, *J. Organomet. Chem.* **2005**, *690*, 5237.
[20] J. Václav, M. Gilani, R. Wilhelm, *Eur. J. Org. Chem.* **2006**, *2006*, 5103.
[21] P. L. Arnold, A. C. Scarisbrick, A. J. Blake, C. Wilson, *Chem. Commun.* **2001**, 2340.
[22] P. L. Arnold, M. Rodden, K. M. Davis, A. C. Scarisbrick, A. J. Blake, C. Wilson, *Chem. Commun.* **2004**, 1612.
[23] C. B. de Koning, R. D. Hancock, W. A. L. van Otterlo, *Tetrahedron Lett.* **1997**, *38*, 1261.
[24] B. A. Trofimov, L. V. Andriyankova, A. G. Mal'kina, K. V. Belyaeva, L. P. Nikitina, O. A. Dyachenko, O. N. Kazheva, A. N. Chekhlov, G. V. Shilov, A. V. Afonin, I. A. Ushakov, L. V. Baikalova, *Eur. J. Org. Chem.* **2007**, *2007*, 1018.
[25] G. W. Nyce, S. Csihony, R. M. Waymouth, J. L. Hedrick, *Chem. Eur. J.* **2004**, *10*, 4073.

[26] T. M. Trnka, J. P. Morgan, M. S. Sanford, T. E. Wilhelm, M. Scholl, T. L. Choi, S. Ding, M. W. Day, R. H. Grubbs, *J. Am. Chem. Soc.* **2003**, *125*, 2546.
[27] A. J. Arduengo III, J. C. Calabrese, F. Davidson, H. V. Rasika Dias, J. R. Goerlich, R. Krafczyk, W. J. Marshall, M. Tamm, R. Schmutzler, *Helv. Chim. Acta* **1999**, *82*, 2348.
[28] S. Csihony, D. A. Culkin, A. C. Sentman, A. P. Dove, R. M. Waymouth, J. L. Hedrick, *J. Am. Chem. Soc.* **2005**, *127*, 9079.
[29] P. L. Arnold, M. Rodden, C. Wilson, *Chem. Commun.* **2005**, 1743.
[30] F. E. Hahn, M. C. Jahnke, *Angew. Chem., Int. Ed. Engl.* **2008**, *47*, 3122.
[31] W. A. Herrmann, *Angew. Chem., Int. Ed. Engl.* **2002**, *41*, 1291.
[32] D. Bourissou, O. Guerret, F. P. Gabbai, G. Bertrand, *Chem. Rev.* **2000**, *100*, 39.
[33] P. L. Arnold, S. T. Liddle, *Chem. Commun.* **2006**, 3959.
[34] P. L. Arnold, S. T. Liddle, J. McMaster, C. Jones, D. P. Mills, *J. Am. Chem. Soc.* **2007**, *129*, 5360.
[35] I. J. Casely, S. T. Liddle, A. J. Blake, C. Wilson, P. L. Arnold, *Chem. Commun.* **2007**, 5037.
[36] D. Patel, S. T. Liddle, S. A. Mungur, M. Rodden, A. J. Blake, P. L. Arnold, *Chem. Commun.* **2006**, 1124.
[37] M. K. Samantaray, V. Katiyar, K. Pang, H. Nanavati, P. Ghosh, *J. Organomet. Chem.* **2007**, *692*, 1672.
[38] B. J. O'Keefe, M. A. Hillmyer, W. B. Tolman, *Dalton Trans.* **2001**, 2215.
[39] A. Sodergard, M. Stolt, *Progress in Polymer Science* **2002**, *27*, 1123.
[40] O. Dechy-Cabaret, B. Martin-Vaca, D. Bourissou, *Chem. Rev.* **2004**, *104*, 6147.
[41] K. Nakano, N. Kosaka, T. Hiyama, K. Nozaki, *Dalton Trans.* **2003**, 4039.
[42] G. Swift, *Acc. Chem. Res.* **1993**, *26*, 105.
[43] H. Sawalha, K. Schroën, R. Boom, *J. Appl. Polym. Sci.* **2008**, *107*, 82.
[44] E. Chiellini, R. Solaro, *Advanced Materials* **1996**, *8*, 305.
[45] R. E. Drumright, P. R. Gruber, D. E. Henton, *Advanced Materials* **2000**, *12*, 1841.
[46] J. Wu, T.-L. Yu, C.-T. Chen, C.-C. Lin, *Coord. Chem. Rev.* **2006**, *250*, 602.
[47] P. L. Arnold, J.-C. Buffet, R. P. Blaudeck, S. Sujecki, A. J. Blake, C. Wilson, *Angew. Chem., Int. Ed. Engl.* **2008**, *47*, 6033.
[48] T. Chivers, C. Fedorchuk, M. Parvez, *Organometallics* **2005**, *24*, 580.
[49] H. Y. Tang, H. Y. Chen, J. H. Huang, C. C. Lin, *Macromolecules* **2007**, *40*, 8855.
[50] M. H. Chisholm, J. Gallucci, K. Phomphrai, *Inorg. Chem.* **2002**, *41*, 2785.
[51] M. H. Chisholm, J. C. Huffman, K. Phomphrai, *Dalton Trans.* **2001**, 222.
[52] L. F. Sanchez-Barba, D. L. Hughes, S. M. Humphrey, M. Bochmann, *Organometallics* **2006**, *25*, 1012.
[53] M. H. Chisholm, K. Phomphrai, *Inorg. Chim. Acta* **2003**, *350*, 121.
[54] A. P. Dove, V. C. Gibson, E. L. Marshall, A. J. P. White, D. J. Williams, *Dalton Trans.* **2004**, 570.
[55] M. H. Chisholm, J. C. Gallucci, K. Phomphrai, *Inorg. Chem.* **2005**, *44*, 8004.
[56] E. L. Marshall, V. C. Gibson, H. S. Rzepa, *J. Am. Chem. Soc.* **2005**, *127*, 6048.
[57] B. M. Chamberlain, M. Cheng, D. R. Moore, T. M. Ovitt, E. B. Lobkovsky, G. W. Coates, *J. Am. Chem. Soc.* **2001**, *123*, 3229.
[58] M. H. Chisholm, J. Gallucci, K. Phomphrai, *Chem. Commun.* **2003**, 48.

[59] J.-C. Wu, B.-H. Huang, M.-L. Hsueh, S.-L. Lai, C.-C. Lin, *Polymer* **2005**, *46*, 9784.
[60] S. Range, D. F.-J. Piesik, S. Harder, *Eur. J. Inorg. Chem.* **2008**, *2008*, 3442.
[61] M. H. Chisholm, N. W. Eilerts, J. C. Huffman, S. S. Iyer, M. Pacold, K. Phomphrai, *J. Am. Chem. Soc.* **2000**, *122*, 11845.
[62] B. Lian, C. M. Thomas, O. L. Casagrande Jr, T. Roisnel, J.-F. Carpentier, *Polyhedron* **2007**, *26*, 3817.
[63] L. F. Sanchez-Barba, A. Garces, M. Fajardo, C. Alonso-Moreno, J. Fernandez-Baeza, A. Otero, A. Antinolo, J. Tejeda, A. Lara-Sanchez, M. I. Lopez-Solera, *Organometallics* **2007**, *26*, 6403.
[64] C.-T. Chen, C.-Y. Chan, C.-A. Huang, M.-T. Chen, K.-F. Peng, *Dalton Trans.* **2007**, 4073.
[65] Q. Dong, X. Ma, J. Guo, X. Wei, M. Zhou, D. Liu, *Inorganic Chemistry Communications* **2008**, *11*, 608.
[66] T.-L. Yu, C.-C. Wu, C.-C. Chen, B.-H. Huang, J. Wu, C.-C. Lin, *Polymer* **2005**, *46*, 5909.
[67] J. Ejfler, M. Kobylka, L. B. Jerzykiewicz, P. Sobota, *Dalton Trans.* **2005**, 2047.
[68] J. Wu, Y.-Z. Chen, W.-C. Hung, C.-C. Lin, *Organometallics* **2008**.
[69] G. Anantharaman, K. Elango, *Organometallics* **2007**, *26*, 1089.
[70] C. D. Abernethy, R. J. Baker, M. L. Cole, A. J. Davies, C. Jones, *Transition Metal Chemistry* **2003**, *28*, 296.
[71] A. J. Arduengo, F. Davidson, R. Krafczyk, W. J. Marshall, M. Tamm, *Organometallics* **1998**, *17*, 3375.
[72] A. J. Arduengo-III, H. V. Rasika-Dias, R. Davidson, R. L. Harlow, *J. Organomet. Chem.* **1993**, *462*, 13.
[73] D. R. Wang, K. Wurst, M. R. Buchmeiser, *J. Organomet. Chem.* **2004**, *689*, 2123.
[74] T. R. Jensen, C. P. Schaller, M. A. Hillmyer, W. B. Tolman, *J. Organomet. Chem.* **2005**, *690*, 5881.
[75] T. Jensen, L. Breyfogle, M. Hillmyer, W. Tolman, *Chem. Commun.* **2004**, 2504.
[76] A. P. Dove, H. Li, R. C. Pratt, B. G. G. Lohmeijer, D. A. Culkin, R. M. Waymouth, J. L. Hedrick, *Chem. Commun.* **2006**, 2881.
[77] G. W. Nyce, T. Glauser, E. F. Connor, A. Mock, R. M. Waymouth, J. L. Hedrick, *J. Am. Chem. Soc.* **2003**, *125*, 3046.
[78] E. F. Connor, G. W. Nyce, M. Myers, A. Mock, J. L. Hedrick, *J. Am. Chem. Soc.* **2002**, *124*, 914.
[79] O. Coulembier, B. G. G. Lohmeijer, A. P. Dove, R. C. Pratt, L. Mespouille, D. A. Culkin, S. J. Benight, P. Dubois, R. M. Waymouth, J. L. Hedrick, *Macromolecules* **2006**, *39*, 5617.

Chapter 3

Cerium Chemistry

3. Cerium Chemistry

Aspects of the work for this section were performed in collaboration with Miss Zoe R. Turner, a fellow PhD student, therefore complexes prepared by her are included as part of the discussion. Brief synthetic details for these complexes are described in the text, where relevant, and the compounds are given a letter, separate from the main numbering scheme.

3.1 Aims

The aim of this work was to expand the known chemistry of tetravalent cerium complexes and starting materials, and to isolate the first Ce^{IV}-NHC complexes.
In general, there are two possible routes to access tetravalent cerium complexes; a) use of a Ce^{IV} starting material or, b) oxidation of a suitable Ce^{III} precursor. Both routes have been investigated.

3.2 Tetravalent Cerium Starting materials

The tetravalent cerium halides would be ideal starting materials, but only CeF_4 is thermally stable and not a synthetically viable compound.[1] Although $CeCl_4$ is thermally unstable, a series of complexes with neutral donor ligands, of the form $CeCl_4L_2$, L = arsine- and phosphine-oxides, sulfoxides and amides, have been reported.[2] Despite this, there are other readily available alternative tetravalent cerium coordination compounds. The most common are ceric ammonium nitrate $(NH_4)_2Ce(NO_3)_6$ (CAN), ceric ammonium sulphate $(NH_4)_4Ce(SO_4)_4$ (CAS), cerium sulphate $Ce(SO_4)_4$, cerium acetate $Ce(OAc)_4$ (OAc = OC(O)Me) and cerium triflate $Ce(OTf)_4$ (OTf = O_3SCF_3). A more comprehensive appraisal of the available complexes and their synthetic utility was

presented by Binnemans in 2006.[3] Of these reagents, CAN is by far the most synthetically useful as a precursor to other more soluble tetravalent cerium starting materials, particularly the alkoxides.

3.2.1 CAN derived alkoxides

This area was pioneered by Evans *et. al*. in 1989 with the use of CAN in the synthesis of a series of soluble Ce^{IV}-alkoxide and alkoxide-nitrate complexes, *via* careful control of reagent stoichiometry.[4] We considered that the reported high yielding route to $Ce(O^tBu)_4(THF)_2$, **CLXXXVI** in Eq. 17, would provide an entry point into Ce^{IV}-NHC chemistry.

$$(NH_4)_2Ce(NO_3)_6 + 6\ NaO^tBu \xrightarrow[\begin{array}{l}-\ 6\ NaNO_3\\ -\ 2\ HO^tBu\\ -\ 2\ NH_3\end{array}]{THF,\ 25\ ^oC,\ 2\text{-}16\ h} \underset{\textbf{CLXXXVI}}{Ce(O^tBu)_4(THF)_2}$$

Eq. 17

However, in our hands this reaction proved difficult to reproduce. Despite numerous attempts to synthesise **CLXXXVI**, complex product mixtures were always obtained, with many reaction mixtures becoming green or brown after a few hours. Sublimation of the crude material (120 ºC, 10^{-5} mbar) yielded a yellow crystalline solid, in very low yield (<10 %), and complex **CLXXXVI** is reported to be a yellow solid. The ^1H NMR spectrum contained a singlet at δ = 1.58 ppm, consistent for the formation of an unsolvated complex $Ce(O^tBu)_4$, **15**. However, elemental analysis of the material is significantly low in both carbon and hydrogen.

On one occasion, the green-brown solution which formed during the reaction was isolated by filtration, and dried. A dark green solution was obtained by hot hexane

extraction, from which single crystals suitable for an X-ray diffraction study could be grown *via* slow cooling, Eq. 18.

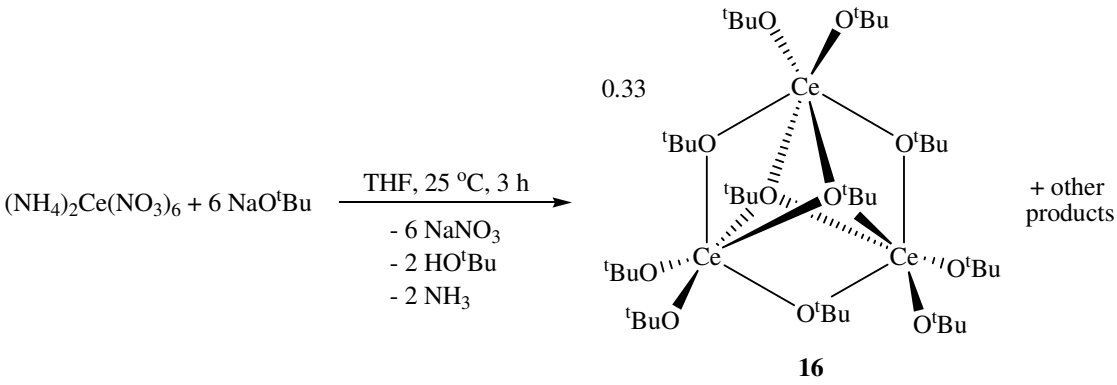

16

Eq. 18

The solid state structure of **16** is revealed to be $Ce_3(\mu_3\text{-}O^tBu)_2(\mu\text{-}O^tBu)_3(O^tBu)_6$ and is shown in Figure 50 as a PLUTO drawing; due to the low quality of the data only connectivity can be ascertained. This complex is also drawn and compared to similar examples in Figure 51. Two crystal morphologies were observed, as emerald blocks and semi-crystalline green needles, present in an approximate 1:1 ratio. Manual separation of these two components and ^{1}H NMR spectroscopic analysis of each showed that they are essentially the same material, although the needles contain a higher proportion of an unidentified diamagnetic product, observed in each sample. Both components revealed three broad singlets at δ = 3.58, 0.54 and -5.09 ppm, which based on the integral ratios of 6:2:3 can be assigned as terminal (O^tBu), triply-bridging (μ_3-O^tBu) and bridging (μ-O^tBu), respectively. The product **16** can be isolated pure by washing the blocks with hexane.

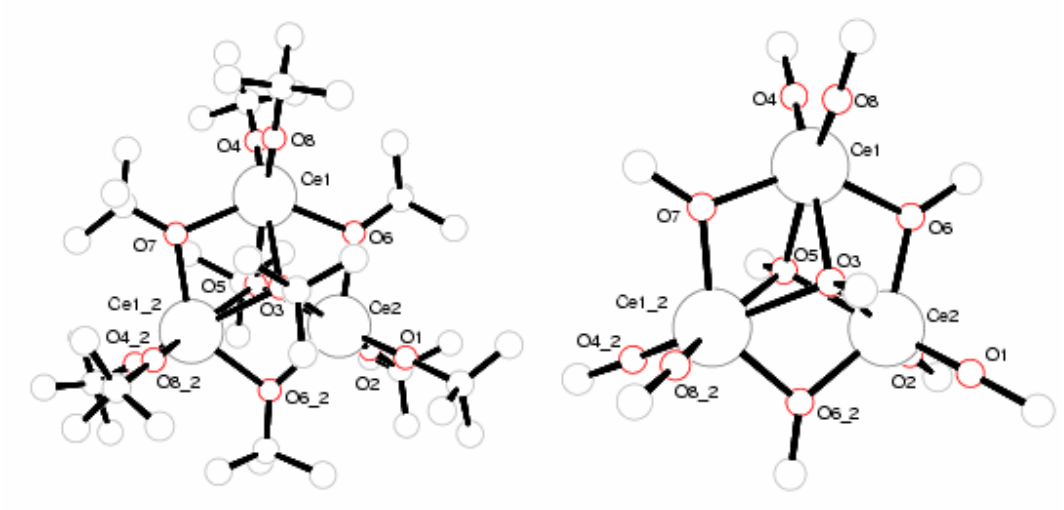

Figure 50. PLUTO drawing of **16**, left, with hydrogens omitted and right, with methyl groups omitted.

The cluster **16** has D_{3h} symmetry, and contains a trinuclear central core consisting of three cerium atoms, arranged in an almost equilateral triangle. Each cerium atom is six-coordinate with distorted octahedral geometry, a consequence of the bridging alkoxide ligands forming the central Ce_3O_3 core, and is bound by two terminal, two bridging and two triply bridging *tert*-butoxide ligands. Lewis base solvated analogues of this trinuclear cluster are the most commonly structurally characterised species isolated for trivalent lanthanide alkoxides, including $Ce_3(\mu_3\text{-}O^tBu)_2(\mu\text{-}O^tBu)_3(O^tBu)_4(HO^tBu)_2$, **CLXXXVII** in Figure 51, recently reported by Boyle and co-workers,[5] as well as the Y, La, Nd, Dy and Er congeners.[6] Complex **CLXXXVII** was synthesised by treatment of $CeN"_3$ with an excess of HO^tBu, and although coordinated HO^tBu was not identified in the solid state, its presence was inferred by charge balance with the three Ce^{III} cations. Another related structurally characterised complex is the mixed valence trinuclear cluster $Ce_3(O^tBu)_{11}NO_3$, **XVII** in Figure 51, reported by Lappert *et. al.*.[7] Complex **XVII** was synthesised from the reaction between a mixture of $Ce(O^tBu)_3(NO_3)(THF)_2$, **XIV**, two equivalents of **CLXXXVI** and three equivalents of $Sn(C_5H_3{}^tBu_2\text{-}1,3)$. Structural characterisation and a computational analysis of model compounds revealed the oxidation states of the three metal centres to be $Ce^{III}Ce^{IV}Ce^{IV}$, in which the single f-electron is found to be localised on the NO_3-bearing cerium atom.

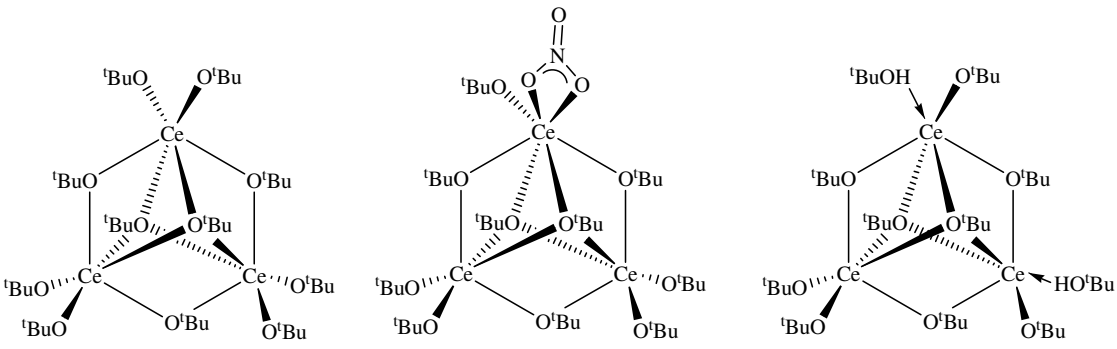

Figure 51. Trimetallic cerium *tert*-butoxide clusters.

In his original work, Evans states that over 2–3 days in toluene at room temperature, complex **CLXXXVI** converts into the yellow trimetallic Ce^{IV} oxo-alkoxide $Ce_3(O)(O^tBu)_{10}$, **CLXXXVIII**, formed by an unknown reaction pathway but maintaining the tetravalent oxidation state of each metal. The uranium analogue was reported by Cotton *et. al.* in 1984, and the authors discuss that the reaction conditions, and in particular the temperature during the work-up procedure, strongly influences the nature of the products isolated.[8] Conversely, the solvated cluster **CLXXXVII** contains exclusively trivalent cerium atoms, and was isolated as a colourless crystalline solid. Complex **16** does not contain an oxo group, and so therefore cannot have formed by the same reaction/ decomposition pathway as **CLXXXVIII**, and was isolated as dark green crystals, suggesting that it is not the same compound as solvated **CLXXXVII**. After consideration of the paramagnetic ^1H NMR spectrum displayed by **16**, the cluster most likely contains mixed valence metals, either one or two Ce^{IV} cations, similar to Lappert's $Ce^{III}Ce^{IV}Ce^{IV}$ cluster **XVII**, Figure 51, also isolated as a green-brown crystalline solid. The IR spectra of **16** did not show an alcohol OH stretch, which may suggest the cluster is not solvated. The EI-MS spectrum contained a lower intensity peak than observed in **XVII** at *m/z* = 1093 (15 %), assigned to $[\{Ce(O^tBu)_3\}_3O]^+$, and showed a different fragmentation pattern. The UV-vis spectrum in toluene displayed strong absorptions at λ = 219, 229, 241, 258 and 278 nm, comparable to those reported by Lappert.

For **16** to contain any trivalent cerium centres, reduction of the tetravalent CAN starting material will have had to occur during the reaction. As the second reagent in the reaction, NaO^{t}Bu, is not an obvious reductant, the precise mechanism by which **16** is formed remains unclear. It would seem that the reaction conditions and work-up procedure, as observed by Cotton, are likely to play a pivotal role in the product isolated from this reaction.

3.2.2 Ce(OTf)$_4$ derived alkoxides

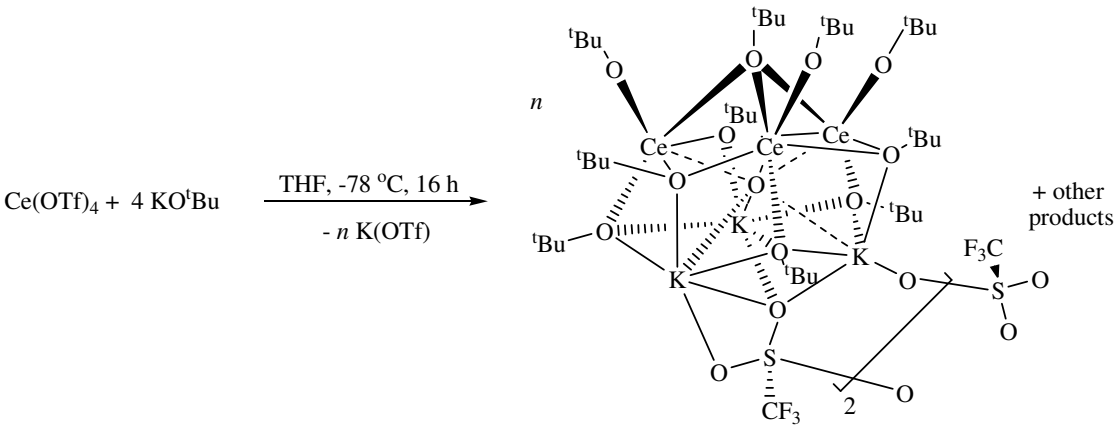

17

Eq. 19

We also evaluated Ce(OTf)$_4$ as a potential starting material, by treatment with four equivalents of KO^{t}Bu in THF at -78 ºC, and subsequent stirring at room temperature overnight, Eq. 19. This reaction did not afford **CLXXXVI**, but an almost colourless cerium 'ate' complex with incorporated potassium ions and KOTf, [K$_3${Ce$_3$(O)(O^{t}Bu)$_{10}$(OTf)}]$_2$ **17**. Single crystals of **17** suitable for an X-ray diffraction study were grown from a benzene solution in an NMR tube at room temperature, and the molecular structure is shown in Figure 52.

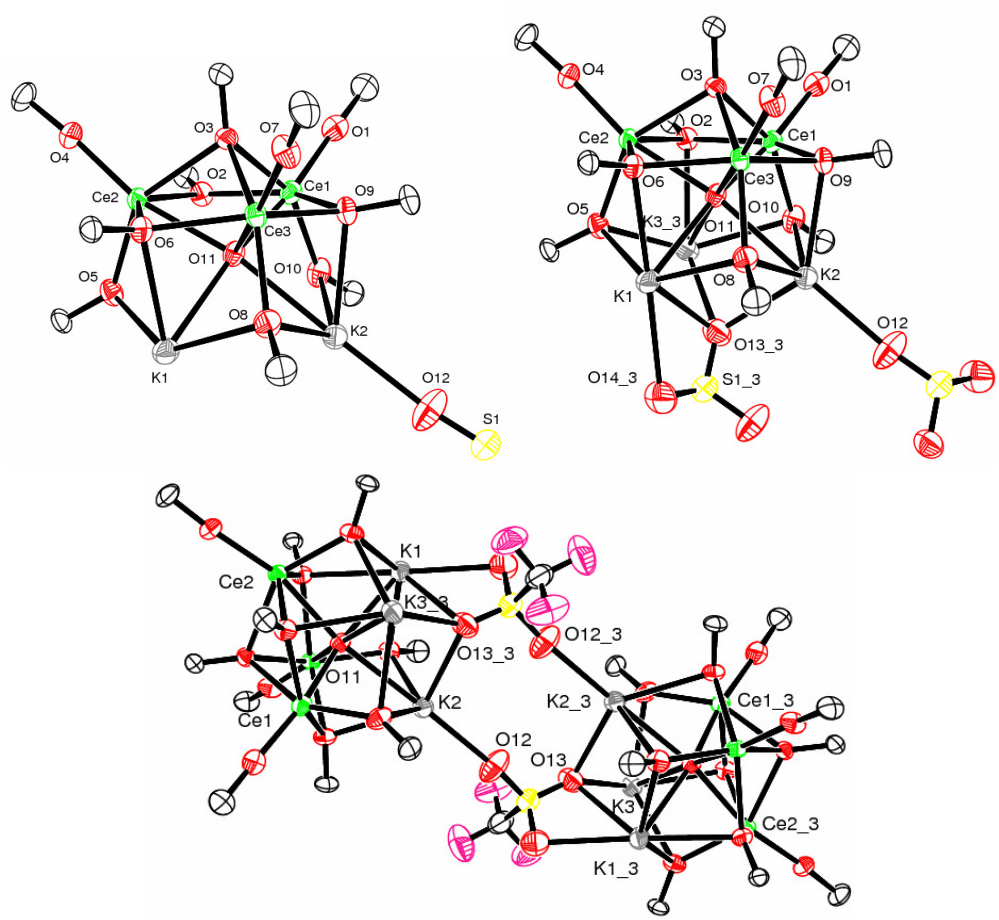

Figure 52. ORTEP drawing of **17**. Top left, contents of asymmetric unit; Top right, asymmetric unit plus symmetry generated KOTf; Bottom, contents of unit cell. Solvents and Me groups omitted for clarity, as well as CF_3 groups and some OTf oxygen atoms in the top two examples.

The centre of the dimer lies on a crystallographic inversion centre, and each six-coordinate *pseudo*-octahedral cerium centre is bound to one terminal O^{t}Bu ligand, two μ-O^{t}Bu ligands, forming a six-membered Ce_3O_3 ring, and all three cerium cations are capped by one μ_3-O^{t}Bu ligand. The Ce-μ-O^{t}Bu groups are each additionally bound to one potassium cation, therefore overall binding as Ce_2K-μ_3-O^{t}Bu ligands, and the remaining three alkoxide groups act as triply bridging CeK_2-μ_3-O^{t}Bu ligands. All six metal centres are additionally bridged by an oxo-group located in the centre of the cluster. Two potassium cations are six-coordinate, with the remaining five-coordinate potassium cation and one triflate group being symmetry generated from the other half of

the dimer. The triflate group binds through the oxygen atoms to the potassium cations with terminal and μ_3-bridging interactions, and additionally acts as a bidentate ligand to one of these potassium cations. It is common for triflate anions to bridge multiple metal centres. Average bond length data for **17** are displayed in Table 7. The terminal Ce-O bond lengths of 2.159(3) Å are within the standard range for Ce^{III}-alkoxides, although the complex is not neutral with this assignment from charge balance. The cerium starting material used in this reaction contained Ce^{IV} and would balance the charges if the complex contained $Ce^{IV}Ce^{III}Ce^{III}$ centres, which would seem most probable as no coordinating HO^{t}Bu by-product is formed from this reaction. There are no Ce-K-alkoxide clusters similar to **17** in the literature, although the metal-μ_3-alkoxide bond lengths in Table 7 are generally within the standard range for triply bridging alkoxides, 2.32–2.81 Å.[6]

The ^{1}H NMR spectrum of **17** displays numerous resonances between δ = 8 and -8 ppm, and could not be readily assigned.

Table 7. Average Ce-O and K-O bond distances in **17**.

Distance (Å)	**17**
Ce-$O_{(av)}$ (terminal)	2.159(3)
Ce-$O_{(av)}$ (μ_3)	2.563(3)
Ce-$O_{(av)}$ (Ce_2K-μ_3)	2.461(3)
K-$O_{(av)}$ (Ce_2K-μ_3)	2.848(3)
Ce-$O_{(av)}$ (CeK_2-μ_3)	2.300(3)
K-$O_{(av)}$ (CeK_2-μ_3)	2.814(3)
Ce-(O) (oxide)	2.442(3)
K-(O) (oxide)	2.908(3)

3.2.3 Oxidation of Ce^{III} coordination complexes

As discussed at the beginning of the introduction, Lappert reported the oxidation of $CeN"_3$ with $TeCl_4$ or PBr_2Ph_3, yielding dark purple $CeN"_3(Cl)$ **VIII** and $CeN"_3(Br)$ **IX**, respectively, albeit in yields of <30 %. Complex **VIII** is potentially a very useful tetravalent cerium starting material, as it contains chloride and amide functionalities. Unfortunately, the low isolated yields and poor scalability of this reaction have precluded further investigations.

In an attempt to find another route to **VIII**, we treated a toluene solution of $CeN"_3$ with an excess of $PhICl_2$ at room temperature, Eq. 20. An immediate colour change to dark purple was observed, and following stirring for 16 h, the reaction mixture was filtered. The solution was layered with hexane and stored at -78 °C overnight, to afford **VIII** as purple-black crystals in 12 % yield. The product colour and singlet observed at $\delta = 0.44$ ppm in the ^1H NMR spectrum were in agreement with the data reported by Lappert, although use of $PhICl_2$ as the oxidant does not seem to offer any improvements to the yield of the isolated product.

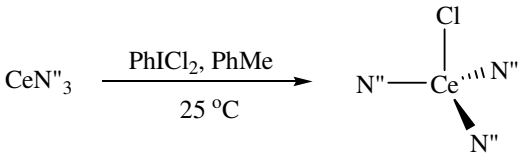

VIII

Eq. 20

3.3 Attempted synthesis of Ce^{IV}-NHC complexes

3.3.1 Protonolysis reactions

Treatment of **15**, the compound tentatively assigned as $Ce(O^tBu)_4$, with one equivalent of the unsaturated zwitterion, **HL**, in THF at -78 °C afforded a yellow solution which was allowed to stir at room temperature overnight. Following concentration and storage of the now brown reaction mixture at -30 °C, a brown solid was isolated in 24 % yield, and formulated as the dinuclear cerium *tert*-butoxide imidazolium tethered complex **18**. The synthesis was subsequently repeated with the correct stoichiometry, affording a similar yield of 25 %, as shown in Eq. 21.

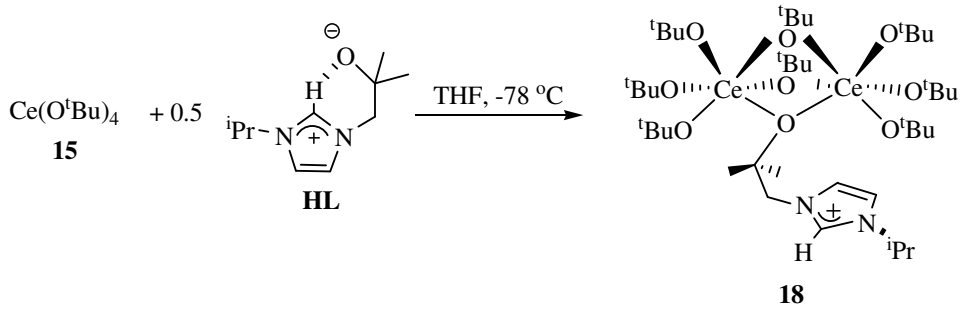

Eq. 21

The ^1H NMR spectrum of **18** displays a clean set of ligand resonances with the characteristic imidazolium CH resonance at δ = 9.84 ppm. There are three *tert*-butoxide resonances at δ = 2.05, 1.75 and 1.53 ppm, which integrate in a 1:1:2 ratio and can be assigned to the two bridging alkoxides, two terminal alkoxides on the same face as the alkoxy-imidazolium ligand and the remaining four terminal alkoxides. The ^{13}C NMR spectrum is commensurate with this and displays an imidazolium carbon resonance at δ = 137.3 ppm. As with the starting material **15**, the elemental analysis results for **18** were significantly low in both carbon and hydrogen, although the value for nitrogen was correct.

Single crystals suitable for an X-ray diffraction study were grown from a THF solution stored at -30 °C, although the data was of poor quality and so it was only possible to establish connectivity. A PLUTO drawing of **18** is shown in Figure 53.

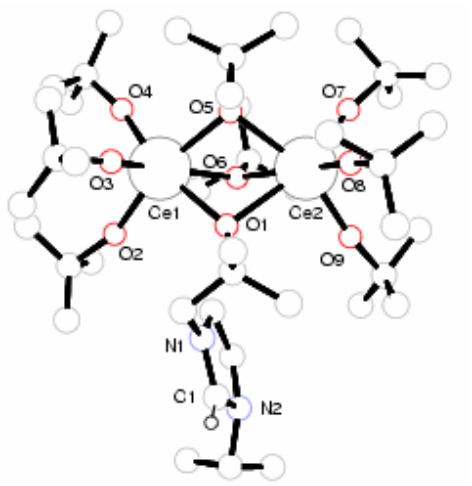

Figure 53. PLUTO drawing of **18**. Hydrogen atoms (except on C1) are omitted for clarity.

The molecule is dimeric in the solid state, with each six-coordinate cerium cation supporting three terminal and two bridging *tert*-butoxide ligands. The coordination sphere of each cerium is completed by the bridging alkoxide of the zwitterionic ligand, HL, bearing the cationic imidazolium group, which hydrogen bonds to a lattice THF molecule. From charge balance, both metals are Ce^{IV} cations, as evidenced by the diamagnetic NMR spectra, and the structure of **18** lends support to the formulation of the starting material **15** as $Ce(O^tBu)_4$.

The saturated backbone imidazolinium complex **19**, see Eq. 22, analogous to **18**, was synthesised by treatment of a hexane solution of **15** with half an equivalent of the bicyclic ligand adduct **3-P** in hexane. A pale yellow precipitate formed from the yellow solution after standing at room temperature overnight, and following filtration was isolated in 20 % yield. The ^{1}H NMR spectrum displays an imidazolinium CH resonance at δ = 9.22 ppm, as well as a simplified set of ligand resonances which are reminiscent of breaking the bicyclic ring structure. As observed for **18**, three *tert*-butoxide resonances are present at δ = 2.02, 1.76 and 1.63 ppm in a ratio of 1:1:2. The ^{13}C NMR

spectrum is in agreement with these assignments, and displays an imidazolinium CH resonance at δ = 159.0 ppm.

The isolation of **18** and **19** indicate that the elimination of *tert*-butanol from these complexes, to form the corresponding Ce^{IV}-NHC complexes, is not a favourable process. In an attempt to force elimination of HO^tBu, a sample of **19** was heated under vacuum (80 °C, 10^{-5} mbar), as shown in Eq. 22. The ^1H NMR spectrum of the resulting pale yellow solid contains predominantly starting material **19** with decomposition products that could not be assigned.

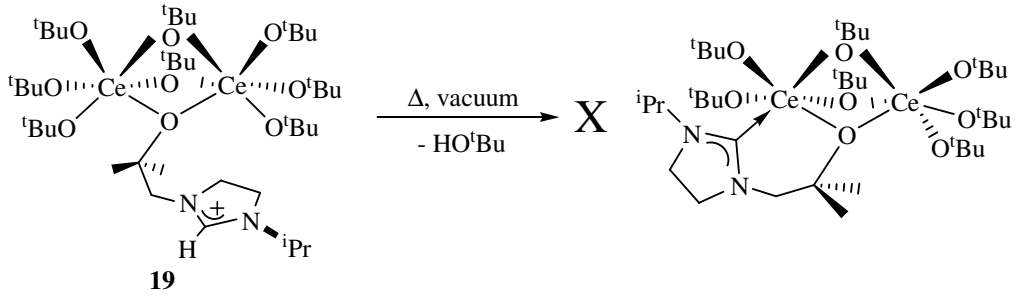

19

Eq. 22

3.3.2 Ligand salt metathesis reactions

The direct synthesis of mixed Ce^{IV}-NHC-nitrate complexes was attempted *via* treatment of CAN with three or five equivalents of KL, **LXXVII**, in THF at room temperature, Eq. 23. The evolution of ammonia and precipitation of potassium nitrate were observed, although the resulting yellow and brown residues, respectively, proved intractable to all attempts at further analysis.

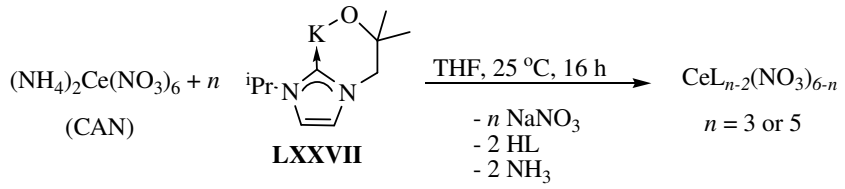

Eq. 23

In contrast, treatment of $Ce(OTf)_4$ with four equivalents of KL, **LXXVII**, in THF resulted in the formation of a dark orange solution which afforded an orange solid after filtration and removal of the volatiles, Eq. 24. The ^1H NMR spectrum revealed a mixture of paramagnetic CeL_3, **20**, and diamagnetic CeL_4, **21**, in a 3:1 ratio, for which full characterisation and a detailed discussion is given in the following section. Complex **20** was originally synthesised by Dr. Stephen Liddle in our group.

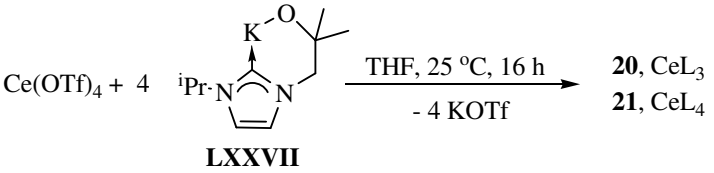

LXXVII

Eq. 24

3.4 Cerium unsaturated backbone NHC complexes

3.4.1 Synthesis of CeL_3

Treatment of cerium triiodide with three equivalents of KL, **LXXVII,** in THF at -78 ºC, followed by stirring at room temperature for 16 h, afforded **20** as an orange microcrystalline solid in good yield, Eq. 25. The ^1H NMR spectrum of **20**, Figure 54, displays a set of paramagnetically shifted ligand resonances, as expected for a Ce^{III} $4f^1$ complex, which lie between δ = 12 and -6 ppm. These are sharp (and spread over a relatively small chemical shift range) which is suggestive of a high symmetry structure. Although no X-ray quality single crystals have so far been obtained, the Ti^{III} (TiL_3) and Y^{III} (YL_3) congeners have been isolated and structurally characterised.[9, 10] These both contain *meridionally*-aligned ligands, with one alkoxide and one NHC being mutually *trans* in each molecule. The room temperature ^1H NMR spectrum of YL_3 contains one set of ligand resonances, suggesting the complex has overall C_3 symmetry in solution, or

that the ligands are sufficiently mobile to equilibrate the resonances on the NMR time-scale. A low temperature VT NMR experiment at 218 K initially revealed two resonances assigned to the now diastereotopic methylene arm protons, and subsequently that one of these split into a further two resonances, consistent with a lower symmetry *mer*-conformation.

The solution magnetic susceptibility of **20**, determined by an Evans' method NMR experiment in C_6D_6 at 300 K, is 2.21 μ_B, within the expected range for Ce^{III} complexes, 1.8-2.5 μ_B. As **20** contains a Ce^{III} $4f^1$ metal centre, a sample was dissolved in methyl-THF and an EPR spectrum run at 77 K. No spectrum was obtained, which is presumably due to rapid relaxation effects, and is consistent with other lanthanide containing complexes only yielding spectra at very low temperature, typically 4.2 K.[11]

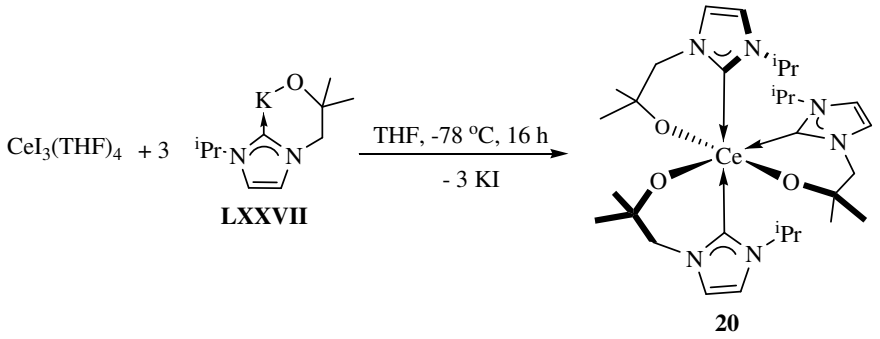

Eq. 25

3.4.2 Oxidation reactions; Isolation of CeL_4

Initially, oxidants that had previously proven successful for the oxidation of Ce^{III} amides to give molecular Ce^{IV} products were investigated. For example, iodine, which was successful in the oxidation of $Ce(NN'_3)$ (NN'_3 = $N(CH_2CH_2NSiMe_2{}^tBu)_3$) to give $CeI(NN'_3)$, **VII**,[12] or $TeCl_4$ and PBr_2Ph_3 which were successfully used by Lappert *et. al.* in the oxidation of CeN''_3 to give $Ce(N'')_3X$ (where X = Cl, **VIII** and Br, **IX**), respectively.[13, 14]

However, the reaction of **20** with oxidants such as I_2, Br_2, $TeCl_4$, PBr_2Ph_3, TEMPO, TlCp, silver salts and $SPPh_3$, all in THF at -78 °C, followed by stirring at room temperature for 16 h, afforded only intractable products.

Sen *et. al.* have previously reported the oxidation of a Ce^{III}-alkoxide with benzoquinone, and structurally characterised the product as a Ce^{IV}-alkoxide dimer containing a bridging hydroquinonediolate unit, $[\{Ce(OC^tBu_3)_3\}_2(\mu\text{-}OC_6H_4O)]$ **XIX**.[15]

However, treatment of **20** with half an equivalent of benzoquinone in Et_2O at ambient temperature, Eq. 26, afforded tetravalent **21** in poor yield, due to the precipitation of a polymeric Ce-*bis*(phenolate) by-product. Subsequently, inclusion of an equivalent of KL in the reaction mixture afforded an excellent yield of **21**, by providing a source of extra ligand and incorporating the potassium cation in the polymeric by-product, thereby no longer sacrificing any of the cerium from the starting material.

The oxidation of **20** can also be effected by XeF_2 or $[Fe(Cp)_2][OTf]$, yielding **21**, albeit in poor yield.

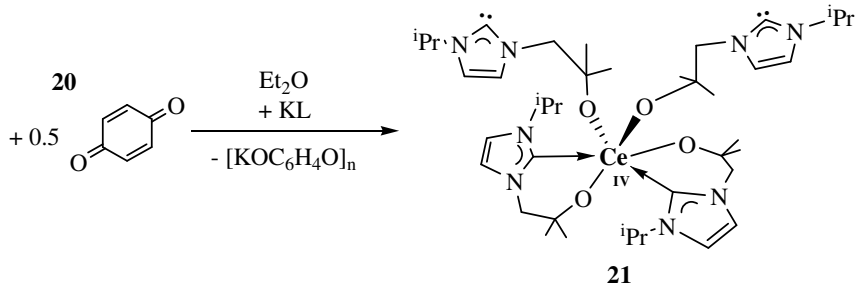

Eq. 26

The ^1H NMR spectrum of **21** is diamagnetic, as expected for a Ce^{IV} $4f^0$ complex, with a sharp set of ligand resonances between δ = 8 and 0 ppm, Figure 54. The ^{13}C NMR spectrum now displays the high-frequency carbene carbon resonance at δ = 212.6 ppm. Only one set of ligand resonances is visible in the NMR spectra, which is commensurate with the presence of a fast fluxional process between the free and bound carbenes on the NMR timescale.

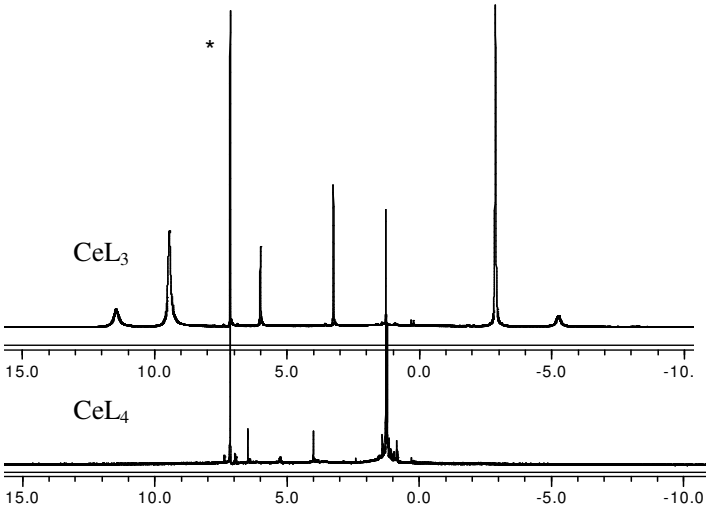

Figure 54. ^{1}H NMR spectra (ppm) of **20** (upper trace) and **21** (lower) (* = solvent H resonance)

Thus, a low temperature VT NMR experiment was conducted in d_8-THF solution, and the part of the NMR spectrum containing the backbone CH resonances is shown in Figure 55 at different temperatures. For example, in the ^{1}H NMR spectrum, these two resonances are broadened at 231 K, with further cooling to 192 K resulting in three sets of ligand resonances being observed in a 2:1:1 ratio. Two pendent carbenes are equivalent, even at 192 K, and the two rigid, bound bidentate ligands are sterically congested around the small Ce^{IV} centre, resulting in different environments. This observation suggests that the rate of the fast fluxional process observed at 298 K has been slowed enough so that different ligand environments are visible. It was not possible to obtain spectra at lower temperatures, due to precipitation of the complex from solution.

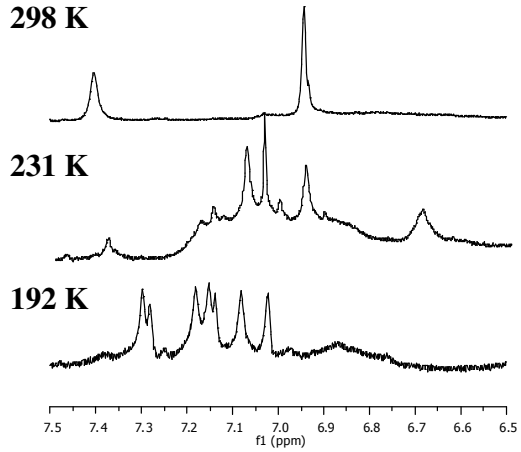

Figure 55. NHC backbone region of low temperature ^{1}H NMR experiments for **21**.

X-ray quality single crystals of **21** were grown from a THF solution and the molecular structure is drawn in Figure 56. The geometry at the cerium cation is *pseudo*-octahedral, and it is coordinated by two bidentate ligands and two monodentate ligands, in which the NHC groups are unbound. The Ce-O distances are standard for tetravalent cerium (av. 2.135 Å; range 2.02-2.15 Å) and the Ce-C1 and Ce-C11 bond lengths are 2.693(6) and 2.652(7) Å respectively. There are no tetravalent Ce-C single bonds with which to compare these Ce^{IV}-C bond lengths, but the shortest Ce^{III}-$C_{carbene}$ distance reported is 2.670(2) Å in $Ce(L)N''_2$ (L = $C\{N(Bu^t)CHCHN\}CH_2CH_2NBu^t$,[16] whilst in $Ce(CH\{SiMe_3\}_2)_3$, the Ce^{III}-alkyl bond length is 2.475 Å.[17]

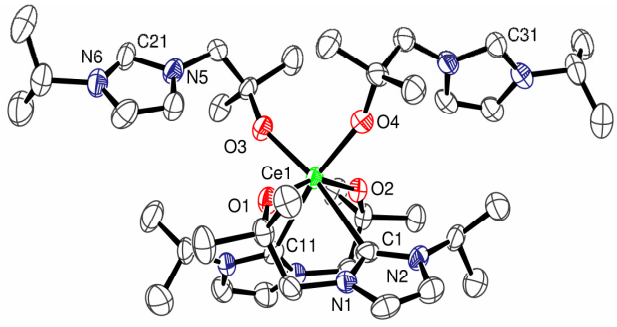

Figure 56. Displacement ellipsoid drawing of the molecular structure of **21** (50 % probability ellipsoids). Solvent and hydrogens omitted.

It is important to confirm that the two free NHC groups in **21** are neutral, free carbenes and not protonated, cationic imidazolium groups, as this would change the assignment of the cerium oxidation state. The N-C-N bond angles and N-C bond lengths of the heterocyclic rings in carbene and protonated imidazolium groups are significantly different. A summary of average bond distances and angles found in **21** is displayed in Table 8. Examination of the N-C bond lengths of the heterocyclic rings in **21** shows that the free and bound NHC groups possess average N-C bond lengths of 1.367(8) and 1.377(9) Å, respectively, which lie within the range of 1.36-1.38 Å expected for neutral NHC groups. The N-C-N bond angles for the bound and free groups are 102.3(6) and 100.9(6)º, respectively, which lie within the range expected for neutral NHC groups of 101-103º, and are significantly smaller than the angle typically observed in protonated imidazolium groups of 108-109º. The N-C-N bond angle decreases upon formation of a free carbene from the corresponding imidazolium salt, as the lone pair located in the carbene σ-orbital occupies more space than the original hydrogen atom. Upon metal complexation, the N-C-N bond angle increases slightly as a consequence of lone pair donation to the metal centre. These data support the premise that all the heterocyclic rings in **21** are neutral NHC groups, supporting the assignment of the tetravalent oxidation state.

Table 8. Comparison of bond distances and angles in **21**, **22** and **24**.

Distance (Å)/angle(º)	**21**	**22**	**24**
Ce-$O_{(av)}$	2.135(5)	2.309(2)	2.138(1)
Ce-$C_{(av)}$	2.674(7)	2.802(3)	2.704(2)
N-$C_{(av)}$ (M-NHC)	1.367(8)	1.363(4)	1.359(3)
N-$C_{(av)}$ (NHC)	1.377(9)	-	1.358(2)*
N-$C_{(av)}$ (Im)	-	1.332(4)	-
N-C-$N_{(av)}$ (M-NHC)	102.3(6)	103.0(2)	103.0(2)
N-C-$N_{(av)}$ (NHC)	100.9(6)	-	104.2(2)*
N-C-$N_{(av)}$ (Im)	-	108.5(2)	-

* denotes borane bound NHC groups.

3.4.3 Isolation of a Ce^{III} analogue $[Ce(L)_2(HL)_2]I$

From one oxidation reaction, where an insufficient quantity of benzoquinone oxidant was added, a small number of crystals of a Ce^{III} compound, **22**, Eq. 27, were isolated and structurally characterised. It is believed that the very crystalline **22** is formed due to the presence of a small amount of iodide impurities incorporated into the starting material, **20**. Although the isolation of such a small quantity of material precluded further characterisation, the structural characterisation of **22** provided a direct comparison to **21** of a protonated Ce^{III} analogue.

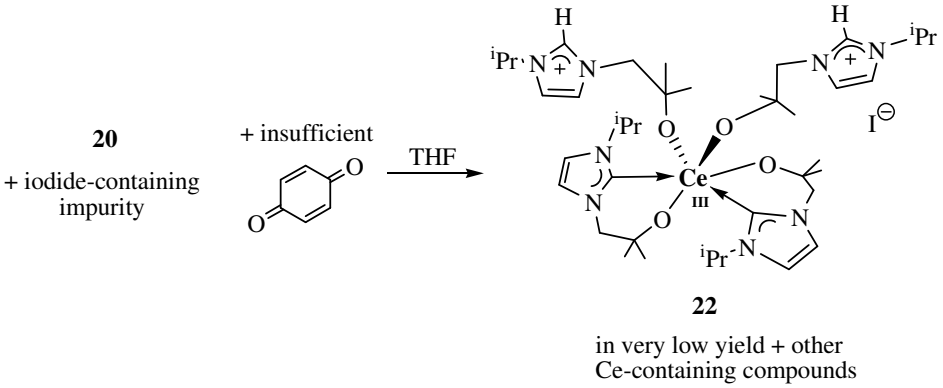

Eq. 27

The molecular structure of **22** is drawn in Figure 57, and pertinent metrical data are listed in Table 8. As observed in **21**, the geometry at the six coordinate Ce^{III} centre is *pseudo*-octahedral, and comprises two bidentate alkoxy carbene ligands and two alkoxide tethered, protonated imidazolium cations. The presence of an iodide counterion confirms the oxidation state as Ce^{III} after balancing of the charges. The average Ce-O bond lengths are 2.390(2) Å (range 2.12-2.41 Å) which are significantly longer than those observed in **21**, due to the larger ionic radii of the Ce^{III} cation, whilst the average Ce-C bond lengths of 2.802(3) Å are similarly elongated and now compare more favourably to other Ce^{III}-NHC complexes (range 2.67-2.77 Å). The average Ce-C bond

lengths in **22** are longer than in other reported complexes due to its higher coordination number. The average N-C bond lengths and N-C-N bond angles of the metal bound NHC ligands are commensurate with those observed in **21**, whilst the same bond lengths and angles in the protonated imidazolium cations lie within the ranges expected for imidazolium groups (typical N-C bond lengths are <1.33 Å and N-C-N bond angles are 108-109º).

Taken together, these data provide credible evidence for the assignment of **21** as a Ce^{IV} complex containing two free NHC groups.

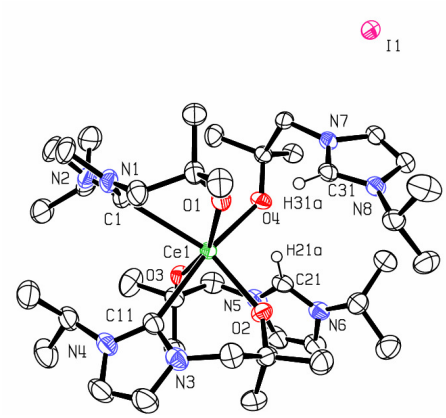

Figure 57. Displacement ellipsoid drawing of the molecular structure of **22** (50 % probability ellipsoids).

3.4.4 Borane functionalisation of CeL_4

Another method to prove unequivocally the presence of the two free NHC groups in **21** is the reaction with a Lewis acid, to form an acid-base adduct. This would rule out the presence of any protonated imidazolium salt and also freeze out the dynamic equilibria observed in the ^{1}H NMR spectrum of **21** between free and bound carbenes.

Other simple carbene-borane adducts have been reported and structurally characterised; Yamaguchi reported the complexes $Et_3B\{C(NRCH)_2\}$, where R = *iso*-propyl and Mes, respectively, which showed carbene carbon resonances at δ = 174.0 and 180.4 ppm, respectively, in the ^{13}C NMR spectrum. The solid state structures revealed these complexes to possess $C_{carbene}$-B bond lengths of 1.683(5) and 1.678(6) Å,

respectively.[18] The BH_3-adducts $H_3B\{C(NMesCH)_2\}$ and $H_3B\{C(NEtCMe)_2\}$ exhibit shorter $C_{carbene}$-B bond lengths of 1.596(4) and 1.603(3) Å, respectively,[19, 20] as, to a lesser extent, do BF_3-adducts $F_3B\{C(NMesCH)_2\}$ and $F_3B\{C(NMesCCl)_2\}$, of 1.635(5) and 1.669(6) Å, respectively.[21]

Treatment of **21** with two equivalents of $BH_3.SMe_2$ furnished **23** as a brown powder in quantitative yield, Scheme 25. Although no single crystals of **23** could be grown, elemental analysis supported the formulation as the carbene-borane adduct. The ^1H NMR spectrum displays two distinct ligand sets in a 1:1 ratio, metal coordinated and borane coordinated, which implies that the dynamic equilibrium observed in **21** has been suppressed. The ^{13}C NMR spectrum shows only one $C_{carbene}$ resonance at $\delta = 211.2$ ppm, attributed to the metal coordinated ligands, as the carbene carbon bound to the quadrupolar boron centre is not observed.

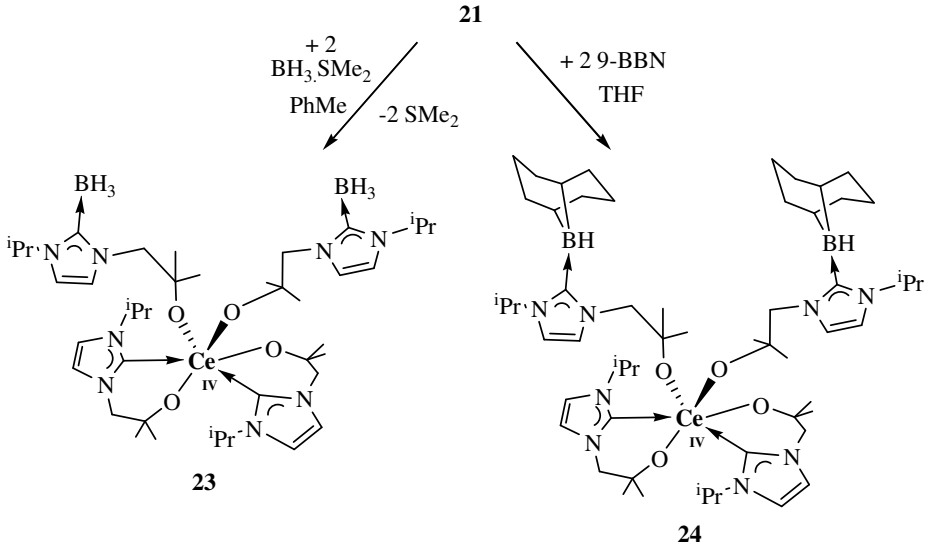

Scheme 25. Borane functionalisation of **21**.

Due to the lack of crystallinity of **23**, complex **21** was treated with two equivalents of 9-BBN, 9-borabicyclo[3.3.1]nonane, to yield **24** in Scheme 25. The ^1H NMR spectrum displays three ligand environments in a 2:1:1 ratio, assignable as two equivalent borane coordinated ligands and two inequivalent metal coordinated ligands. This difference to

23 could be attributed to the large steric profile of the two 9-BBN groups reducing the steric freedom of the two metal bound ligands, forcing them into different environments. The $C_{carbene}$ resonances in the ^{13}C NMR spectrum are, however, similar enough that only one resonance is observed at δ = 212.5 ppm, although the remaining ligand resonances are split and the boron coupled carbene resonances are again not observed. The ^{11}B NMR spectrum contains a single resonance at δ = -15.4 ppm.

X-ray quality single crystals of **24** were grown from a benzene solution, and the molecular structure is drawn in Figure 58. The geometry at the Ce^{IV} centre is *pseudo*-octahedral for the six coordinate metal. The average Ce-O, Ce-C and heterocycle N-C bond lengths are 2.138(1), 2.704(2) and 1.359(3) Å, respectively, whilst the average N-C-N bond angles for metal bound and borane bound NHC groups are 103.0(2) and 104.2(2)°, respectively. These data are displayed in Table 8 with the metrical data for **21**, and are in agreement with **21** and **24** both being Ce^{IV}-NHC complexes. The average $C_{carbene}$-B bond lengths of 1.639(3) Å are comparable to those in other simple carbene-borane adducts; 1.667 Å in $Et_3BC(NMesCH)_2$[18] and 1.653(2) Å in **25**.

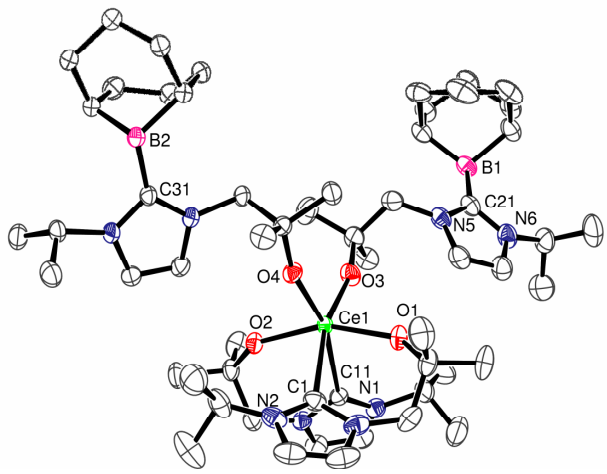

Figure 58. Displacement ellipsoid drawing of the molecular structure of **24** (50 % probability ellipsoids). Solvent and hydrogens omitted.

3.4.5 Crystal structure of an alkoxy carbene-borane complex

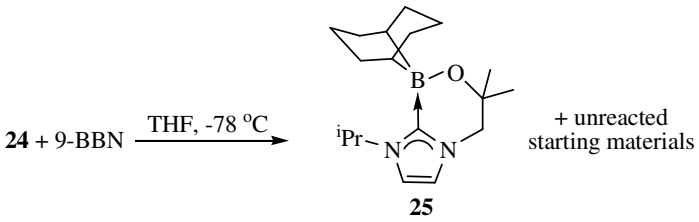

Eq. 28

Treatment of **24** with an extra equivalent of 9-BBN in THF at -78 ºC furnished a yellow solid after filtration and removal of the solvent under reduced pressure. The ^{1}H NMR spectrum resembled that of the starting material **24** with a number of unidentified resonances. From this NMR sample, a small number of colourless single crystals formed, **25**, and the solid state structure is drawn in Figure 59. Elemental analysis of the bulk material was significantly low in C, H and N, and insufficient quantity of the recrystallised material could be isolated for further characterisation. The molecular structure does provide a useful comparison for the carbene-borane bond length in **24**. The geometry at the four coordinate boron centre is *pseudo*-tetrahedral, with a $C_{carbene}$-B bond length of 1.653(2) Å, comparable to both **24** and the literature complexes already discussed. The B-O bond length is 1.524(2) Å and, at 1.356(2), 1.359(2) Å and 104.42(14)º, the two N-C bond lengths and N-C-N bond angle are unremarkable for a bound NHC group.

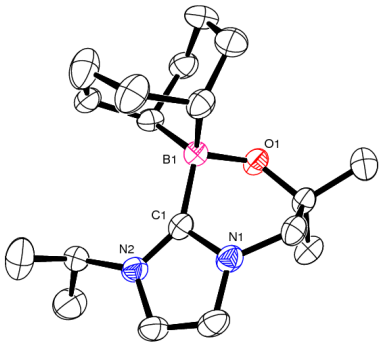

Figure 59. Displacement ellipsoid drawing of the molecular structure of **25** (50 % probability ellipsoids). Hydrogen atoms omitted for clarity. Selected distances (Å) and angles (°); C1-B1 1.653(2); N1-C1 1.356(2); N2-C1 1.359(2); B1-O1 1.524(2); N1-C1-N2 104.42(14).

3.4.6 Further functionalisation of 21

After the successful isolation of borane functionalised products **23** and **24**, we made attempts to coordinate the free NHC groups in **21** to other metal fragments. Thus, treatment of **21** with two equivalents of $AlMe_3$ in THF at -78 °C, followed by stirring at room temperature for 12 h, afforded crude **26** as a brown solid, Eq. 29.

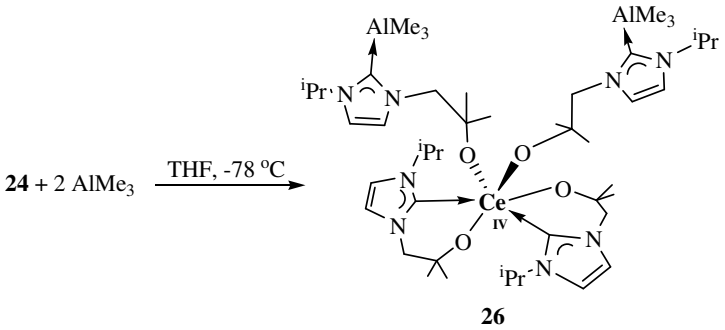

Eq. 29

The ^{1}H NMR spectrum of **26** was reminiscent of **23**, with two ligand environments giving rise to four NHC backbone CH resonances between δ = 8.86 and 6.20 ppm. The ^{13}C NMR spectrum displayed a Ce-$C_{carbene}$ resonance at δ = 211.0 ppm and a broad

aluminium coupled Al-$C_{carbene}$ resonance at δ = 172.2 ppm, which is comparable to that observed by Ong *et. al.* in amido-NHC-$AlMe_3$ adduct [$Me_3AlNH(^tBu)CH_2CH_2[C\{NCHCHN(Mes)\}]$] of δ = 177.0 ppm.[22]

Similarly, the reactions with other metal compounds, typically on an NMR scale, furnished ^1H NMR spectra that showed differing sets of ligand environments, suggesting free carbene coordination to the metal fragment, although definitive assignment did not prove possible. Treatment of **21** with one equivalent of $CaN"_2(THF)_2$ in benzene at room temperature produced ^1H NMR spectra with only two backbone CH resonances, instead of the anticipated minimum of four, or in THF at -78 °C afforded ^1H NMR spectra with eight backbone CH resonances between δ = 7.4 and 6.2 ppm, suggesting NHC coordination to the calcium centre. The reaction of **21** with one or two equivalents of $UN"_3$ resulted in loss of the starting material resonances in the ^1H NMR spectra of both reactions, and the appearance of a number of paramagnetically shifted resonances between δ = 85 and -40 ppm. This may imply NHC coordination to the uranium metal centre in both cases, and potentially that a one electron redox process has occurred between the two metal centres to form a more stable Ce^{III}-U^{IV} containing bimetallic system. Treatment of **21** with $YN"_3$ resulted in a ^1H NMR spectrum containing a series of diamagnetic and paramagnetic resonances between δ = 13 and -8 ppm, indicating a Ce^{III} complex has been formed, which is curious as Y^{III} cannot act as a reductant. The reaction of **21** with one equivalent of P_4 produced pale brown material with limited solubility, although it was possible to obtain a ^{31}P NMR spectrum which contained a series of complex multiplets between δ = 80 and -175 ppm, suggesting NHC coordination and activation of the P_4 moiety, in a similar manner to that of Bertrand and co-workers.[23]

Other reactions between **21** and $NiCl_2$, $SnCl_2$, $UI_3(THF)_4$, SmI_2, $UO_2N"_2(THF)_2$ and $MgMe_2$ afforded intractable materials which were resistant to further characterisation.

3.5 Comparison of CeL_4 21 to the 5f UL_4

With structural characterisation of the Ce^{IV}-NHC complex **21**, it is possible to make a comparison to the U^{IV} analogue $\mathbf{UL_4}$, Figure 60, to highlight the differences between the bonding in the 4f and 5f metals.[24] Although the sizes of the Ce^{IV} (1.01 Å) and U^{IV} (1.09 Å) cations are very similar, it is apparent that the softer carbene groups favour coordination to the more polarisable 5f metal centre than the harder 4f metal. This results in significant differences between the two complexes, as **21** has a six-coordinate cerium centre with distorted-octahedral geometry with two bound and two free NHC groups, whereas $\mathbf{UL_4}$ has a pentagonal bi-pyramidal geometry at the seven-coordinate uranium centre with three bound and one free NHC group. The higher coordination number forms at the expense of forming longer U-O and U-C bonds, Table 9.

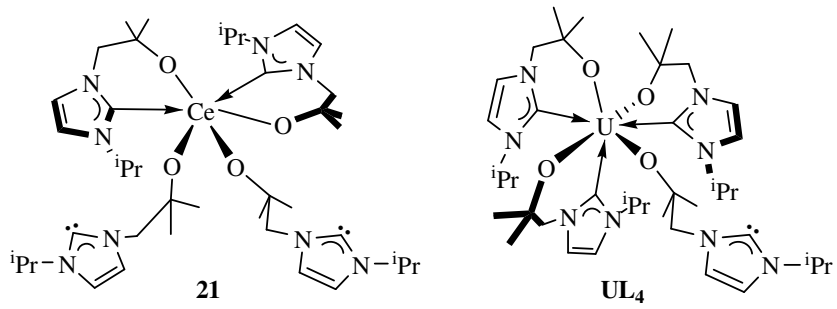

Figure 60. Analogous Ce^{IV} and U^{IV} complexes.

Table 9. Comparison of metrical data for **21** and $\mathbf{UL_4}$.

Distance (Å)/angle(°)	M = Ce	M = U	Δ (U-Ce)	Δ (U-Ce)corr[a]
$M\text{-}O_{(av)}$	2.135(5)	2.203(3)	0.068	-0.012
$M\text{-}C_{(av)}$	2.674(7)	2.747(3)	0.073	-0.007
$N\text{-}C_{car(coord, av)}$	1.367(8)	1.365(4)	–	–
$N\text{-}C_{car(free, av)}$	1.377(9)	1.373(4)	–	–
$NCN_{(coord, av)}$	102.3(6)°	102.1(2)°	–	–
$NCN_{(free, av)}$	100.9(6)°	101.3(2)°	–	–

[a] corrected for 6- and 7-coordinate radii of Ce^{IV} (1.01 Å) and U^{IV} (1.09 Å) respectively.[25]

3.6 Cerium saturated backbone NHC complexes

3.6.1 Reactions with a Ce^{IV} starting material; CeN''_3Cl

Work on cerium complexes bearing saturated backbone NHC complexes began by treatment of CeN''_3Cl, **VIII**, with one equivalent of **3-M** in benzene on an NMR scale, Eq. 30, resulting in a colour change from dark purple to orange. Unfortunately this reaction did not yield the desired mesityl substituted alkoxy-carbene Ce^{IV} complex. The ^1H NMR spectrum contained a set of paramagnetic ligand resonances, assigned as $L^MCeN''_2$, formed from small amounts of CeN''_3 impurity in the cerium starting material, and a host of diamagnetic resonances that could not be assigned.

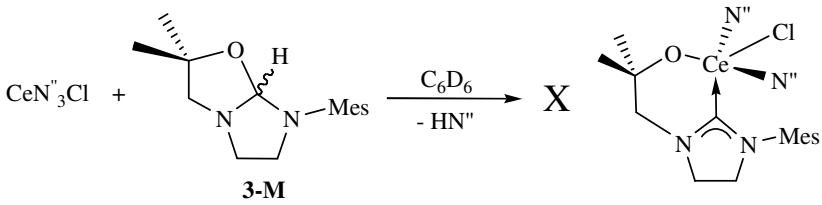

Eq. 30

Attempts to synthesise the *bis*-ligand analogue of the compound shown in Eq. 30, on an NMR scale, resulted in a mixture of multiple products which could not be identified.

3.6.2 Synthesis of Ce^{III}-NHC complexes

Treatment of a toluene solution of $CeN"_3$ with a toluene solution of **3-M** for 12 h, after filtration and removal of the volatiles, afforded a crude yellow solid **27**, Eq. 31. Following removal of the impurities *via* sublimation (85 °C, 10^{-5} mbar), **27** was isolated as an orange solid in good yield, displaying a set of paramagnetically shifted ligand resonances between δ = 14 and -7 ppm in the ^{1}H NMR spectrum, although the elemental analysis results were low in carbon, hydrogen and nitrogen.

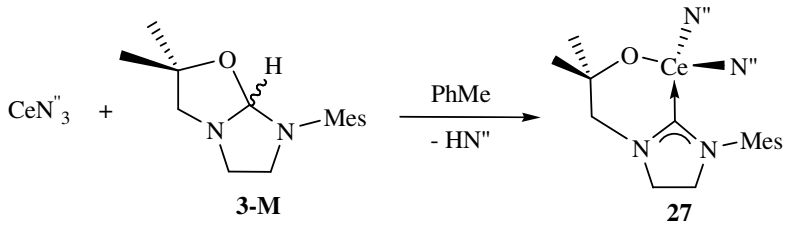

Eq. 31

Subsequently, the *bis*-NHC cerium analogue was synthesised *via* treatment of $CeN"_3$ with two equivalents of **3-M** in toluene, Eq. 32. The mesityl-substituted complex **28** crystallised as single crystals from the reaction mixture after standing at room temperature for ten minutes. Isolation and hexane washing after 12 h afforded the product in good yield.

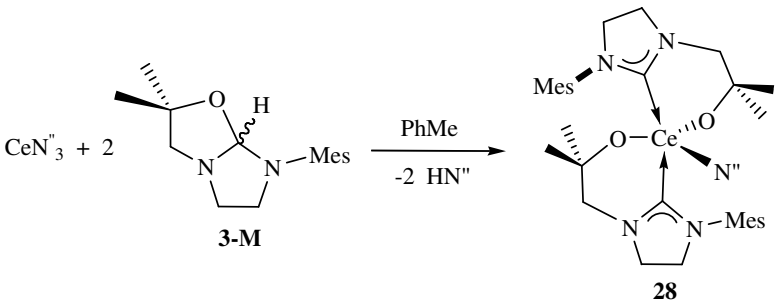

Eq. 32

The ^{1}H NMR spectrum of **28** displays a very broad set of ligand resonances compared to the spectra observed for **27**, most likely due to the presence of a fluxional process in solution at room temperature. At room temperature the ^{1}H NMR spectrum of **28** displays five broadened resonances almost indistinguishable from the baseline, with the remaining three resonances observed as better resolved broad singlets, all within the range δ = 23 to -10 ppm. Despite the uninformative NMR spectra, **28** was characterised by elemental analysis and a single crystal X-ray diffraction study. The molecular structure is drawn in Figure 61, and selected bond lengths and angles displayed in Table 10.

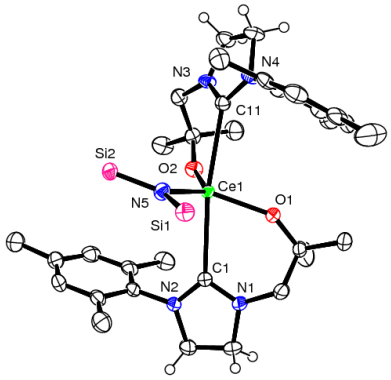

Figure 61. Displacement ellipsoid drawing of the molecular structure of **28** (50 % probability ellipsoids). Solvent, silicon bound methyl groups and hydrogens omitted for clarity, except on the NHC backbone.

The cerium centre is five coordinate, and in **28** adopts a distorted trigonal bipyramidal geometry, with an axial C1-Ce1-C11 angle of 167.55(10)° and equatorial angles O1-

Ce1-O2, O1-Ce1-N5 and O2-Ce1-N5 of 105.00(10), 124.33(13) and 130.65(12)°, respectively, with an angle sum of 359.98°. The average ligand bite angle is 71.68(12)° in **28**, which contributes in part to the observed distortion, and the average Ce-O and Ce-C bond lengths are 2.178(3) and 2.792(4) Å, respectively. There are no structurally characterised Ce^{III} saturated backbone NHC complexes with which to compare the Ce-C bond lengths of **28**, but the five-coordinate Ce^{III}-amido-NHC complex $[Ce(L)N''(\mu\text{-}I)_2]_2$ (L = $^{t}BuNHCH_2CH_2[C\{^{t}BuNCHCHN\}]$), **CXIV**, has a Ce-$C_{carbene}$ bond length of 2.700(3) Å and the six-coordinate Ce^{III}-alkoxy-NHC complex discussed earlier, $[Ce(L)_2(HL)_2]I$ **22**, possesses a Ce-$C_{carbene}$ bond length of 2.802(3) Å, longer than that observed in **28** as expected with the larger coordination number. The NHC heterocycle metrical data are consistent with metal bound carbene groups.

Table 10. Summary of metrical data for **28**.

Distance (Å)/angle(°)	**28**
Ce1-O1, -O2	2.172(3), 2.184(3)
Ce1-C1, -C11	2.786(4), 2.798(4)
Ce1-N5	2.442(3)
N-$C_{(av)}$	1.336(5)
N-C-$N_{(av)}$	107.1(4)

3.6.3 Oxidation reactions

In an NMR tube, to a pale yellow solution of two equivalents of **27** in benzene was added a one half equivalent of benzoquinone, resulting in the immediate formation of a dark purple solution, Eq. 33, formulated as the hydroquinonediolate-bridged di-cerium complex **29**. This is reminiscent of the bridged Ce^{IV}-alkoxide **XIX**, reported by Sen and

discussed in Chapter 1. The ^{1}H NMR spectrum of **29** showed a set of diamagnetic ligand resonances between δ = 7 and 0 ppm, and displayed a Ce-$C_{carbene}$ resonance in the ^{13}C NMR spectrum at δ = 238.3 ppm.

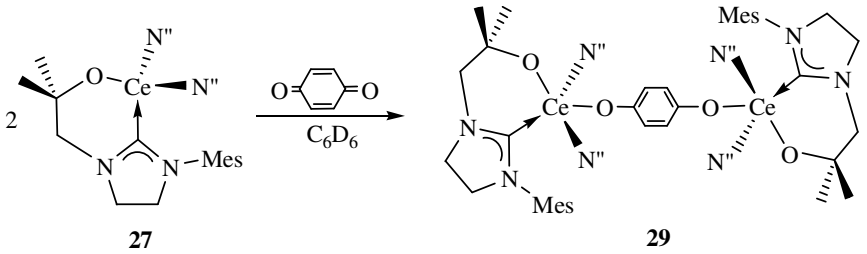

27 **29**

Eq. 33

Subsequent benzoquinone oxidation of the Ce^{III}-*bis*(NHC) complex **28** was investigated on a preparative scale. A dark purple colouration formed immediately upon addition of benzoquinone to a yellow toluene solution of **28** in a 1:2 ratio, and after stirring for 12 h furnished the product **30** as a dark purple precipitate from the now colourless solution, Eq. 34. This product is insoluble in most hydrocarbon solvents, although **30** is partially soluble in d_5-pyridine, such that a poorly resolved ^{1}H NMR spectrum could be obtained. This complex exhibits a symmetric set of diamagnetic ligand resonances over the range δ = 7 to 0 ppm, and displays a singlet at δ = 5.78 ppm, assigned to the hydroquinonediolate linker. No ^{13}C NMR spectrum could be obtained due to insufficient solubility. Elemental analysis of **30** was in agreement with the formulation shown in Eq. 34.

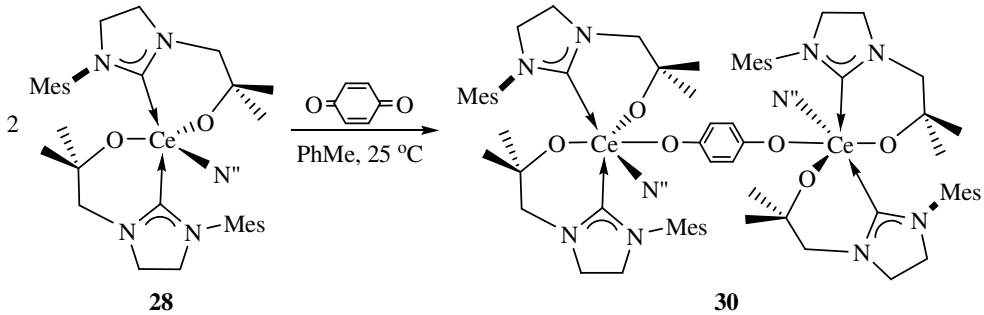

28 **30**

Eq. 34

Other attempted reactions utilising XeF_2 and $PhICl_2$ as oxidants did not result in clean oxidation, and gave ^1H NMR spectra consisting of complex mixtures of paramagnetic and diamagnetic products. The purple colour observed in these complexes could arise from a ligand-to-metal-charge-transfer (LMCT) process from the amide ligands or quinine-diolate linker onto the Ce^{IV} metal centre. The lack of observed purple colour in CeL_4, **21**, could be due to the absence of the amide ligands and hence such a LMCT process, or that the transition is shifted to another part of the visible spectrum.

3.6.4 Preliminary reactivity studies.

Reactivity studies of the Ce^{III}-mono-NHC complex **27** was undertaken on an NMR scale, by treatment with one equivalent of Me_3SiI in benzene at room temperature, to afford **31**, Eq. 35. The ^1H NMR spectrum of **31** indicated that all of the starting material had been converted into a new paramagnetic compound, displaying resonances between δ = 17 and -4 ppm. These resonances can be tentatively assigned to the structure of **31** drawn in Eq. 35, although a preparative scale reaction is needed to characterise this compound fully.

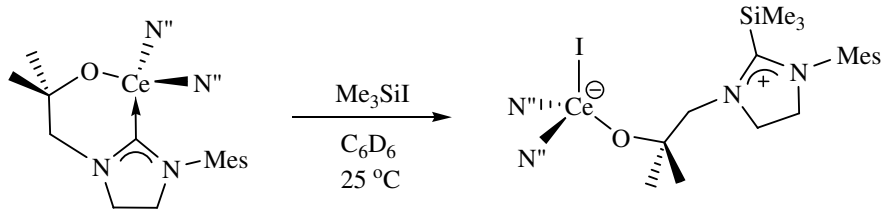

27 **31**

Eq. 35

The Dipp substituted analogue of **31** was synthesised in an analogous manner and colourless crystals grew from the pale yellow NMR scale reaction mixture over 2-3 days. The molecular structure supports the formulation of **31** drawn in Eq. 35. It is

apparent that the Me_3SiI reagent has added across the weak Ce-$C_{carbene}$ bond, resulting in a zwitterionic complex containing a four-coordinate cerium centre with distorted tetrahedral geometry, and an alkoxide tethered silylated NHC ligand.

Treatment of the Ce^{III}-*bis*-NHC complex **28** with Me_3SiI in an analogous fashion to the synthesis of **31** furnished a similar pale yellow solution, although the ^1H NMR spectrum showed a large number of resonances that could not be assigned.

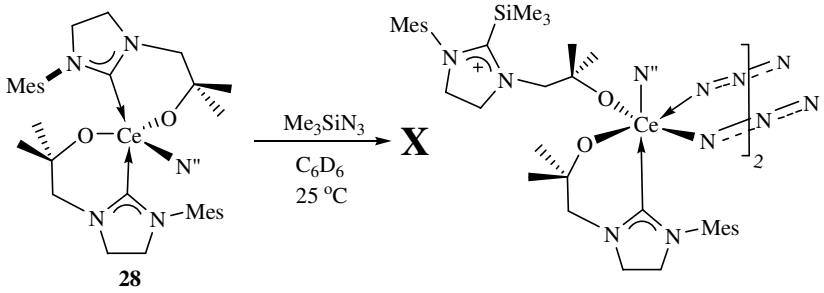

Eq. 36

Treatment of the Ce^{III}-*bis*(NHC) complex **28** with one equivalent of Me_3SiN_3 in benzene on an NMR scale produced a pale yellow solution, Eq. 36, although the formulation of the product could not be definitively confirmed. This reaction gave a ^1H NMR spectrum containing a set of small paramagnetic ligand resonances, assigned as **27**, and one sharp set of diamagnetic ligand resonances between δ = 7 and 0 ppm. In addition to this, the ^{13}C NMR spectrum also shows a high-frequency resonance at δ = 244 ppm. These diamagnetic spectra would suggest that the Ce^{III}-azide bridged dimer, as drawn in Eq. 36, is not the major product. This would imply that either the ligand is no longer bound to the Ce^{III} metal centre, or that oxidation has occurred to afford a diamagnetic Ce^{IV} complex. Reactions of NHCs with Me_3SiN_3 are known to form the corresponding 2-iminoimidazoline derivatives, such as $Me_3SiN=\{C(^iPrNCH)_2\}$ reported by Tamm *et. al.*, and an Al^{III} adduct $AlCl_3.Me_3SiN=\{C(^iPrNCH)_2\}$ reported by Kuhn and co-workers, although both of these display a N-C-N resonance in the ^{13}C NMR spectrum at δ = 153 and 148 ppm, respectively.[26, 27] That leaves the possibility of a Ce^{IV} complex, which

would explain the diamagnetic ligand resonances observed in the NMR spectra and a high-frequency Ce^{IV}-$C_{carbene}$ resonance at δ = 244 ppm, which compares well to that observed at δ = 238.3 ppm in **29**. One way in which substituted azides can react is *via* elimination of dinitrogen and formation of a metal imido bond. Could this reaction have formed an unprecedented Ce-imido complex, with a concomitant ligand redistribution reaction? Based on one NMR scale reaction, it is impossible to say, but clearly further investigation is merited.

3.7 Conclusions

This chapter began with the attempted repeat of a literature procedure for tetravalent cerium alkoxide complexes from CAN, for use as potential sources of Ce^{IV} starting materials in targeting Ce^{IV}-NHC complexes. Instead of the desired cerium alkoxides, trinuclear cerium alkoxide clusters containing mixed valence metal centres were isolated. After the poor yielding oxidation of $CeN"_3$ with a hypervalent iodide reagent, attention turned to the oxidation of a Ce^{III}-NHC complex, CeL_3, which had been recently synthesised within the group. A range of oxidants were evaluated, the majority of which were unsuccessful, but benzoquinone proved suitable for this oxidation. The reaction was accompanied by ligand redistribution, and by inclusion of an extra equivalent of KL with the reaction mixture, afforded CeL_4 in excellent yield, as well as a polymeric potassium phenolate by-product. This complex was structurally characterised as containing two bidentate and two alkoxy-bound monodentate ligands with free NHC groups. Subsequent functionalisation with 9-BBN proved that the free NHC groups were not protonated, and that the assignment of the Ce^{IV} oxidation state was correct. Functionalisation of CeL_4 with other metal fragments offered some promising preliminary results, which need further investigation. Using the saturated backbone alkoxy-NHC ligands, mono- and *bis*-NHC Ce^{III} complexes were synthesised and the latter of these was structurally characterised. Initial reactivity studies of these complexes with benzoquinone and trimethylsilyl iodide and azide provided a range of structurally diverse products.

3.8 References

[1] N. Kaltsoyannis, P. Scott, *The f elements*, OUP, **1999**.
[2] J. Barry, J. G. H. du Preez, T. I. Gerber, A. Litthauer, H. E. Rohwer, B. J. van Brecht, *J. Chem. Soc., Dalton Trans.* **1983**, 1265.
[3] K. Binnemans, *Applications of Tetravalent Cerium Compounds, Vol. 36, Chapter 229*, Elsevier, Amsterdam, **2006**.
[4] W. J. Evans, T. J. Deming, J. M. Olofson, J. W. Ziller, *Inorg. Chem.* **1989**, *28*, 4027.
[5] T. J. Boyle, L. J. Tribby, S. D. Bunge, *Eur. J. Inorg. Chem.* **2006**, 4553.
[6] T. J. Boyle, L. A. M. Ottley, *Chem. Rev.* **2008**, *108*, 1896.
[7] Y. K. Gun'ko, S. D. Elliott, P. B. Hitchcock, M. F. Lappert, *J. Chem. Soc., Dalton Trans.* **2002**, 1852.
[8] F. A. Cotton, D. O. Marler, W. Schwotzer, *Inorg. Chim. Acta* **1984**, *95*, 207.
[9] N. A. Jones, S. T. Liddle, C. Wilson, P. L. Arnold, *Organometallics* **2007**, *26*, 755.
[10] P. L. Arnold, S. Zlatogorsky, N. A. Jones, C. D. Carmichael, S. T. Liddle, A. J. Blake, C. Wilson, *Inorg. Chem.* **2008**, *47*, 9042.
[11] S. A. Cotton, *Lanthanide and Actinide Chemistry*, Wiley, **2006**.
[12] C. Morton, N. W. Alcock, M. R. Lees, I. J. Munslow, C. J. Sanders, P. Scott, *J. Am. Chem. Soc.* **1999**, *121*, 11255.
[13] O. Eisenstein, P. B. Hitchcock, A. G. Hulkes, M. F. Lappert, L. Maron, *Chem. Commun.* **2001**, 1560.
[14] P. B. Hitchcock, A. G. Hulkes, M. F. Lappert, *Inorg. Chem.* **2004**, *43*, 1031.
[15] A. Sen, H. A. Stecher, A. L. Rheingold, *Inorg. Chem.* **1992**, *31*, 473.
[16] S. T. Liddle, P. L. Arnold, *Organometallics* **2005**, *24*, 2597.
[17] A. G. Avent, C. F. Caro, P. B. Hitchcock, M. F. Lappert, Z. N. Li, X. H. Wei, *Dalton Trans.* **2004**, 1567.
[18] Y. Yamaguchi, T. Kashiwabara, K. Ogata, Y. Miura, Y. Nakamura, K. Kobayashi, T. Ito, *Chem. Commun.* **2004**, 2160.
[19] T. Ramnial, H. Jong, I. D. McKenzie, M. Jennings, J. A. C. Clyburne, *Chem. Commun.* **2003**, 1722.
[20] N. Kuhn, G. Henkel, T. Kratz, J. Kreutzberg, R. Boese, A. H. Maulitz, *Chem. Ber.* **1993**, *126*, 2041.
[21] A. J. Arduengo III, F. Davidson, R. Krafczyk, W. J. Marshall, R. Schmutzler, *Monatsh. Chem.* **2000**, *131*, 251.
[22] W.-C. Shih, C.-H. Wang, Y.-T. Chang, G. P. A. Yap, T.-G. Ong, *Organometallics* **2009**, *doi: 10.1021/om800917j*.
[23] J. D. Masuda, W. W. Schoeller, B. Donnadieu, G. Bertrand, *J. Am. Chem. Soc.* **2007**, *129*, 14180.
[24] P. L. Arnold, A. J. Blake, C. Wilson, *Chem. Eur. J.* **2005**, *11*, 6095.
[25] R. D. Shannon, *Acta Cryst. A.* **1976**, *32*, 751.

[26] M. Tamm, D. Petrovic, S. Randoll, S. Beer, T. Bannenberg, P. G. Jones, J. Grunenberg, *Org. Biomol. Chem.* **2007**, *5*, 523.
[27] N. Kuhn, R. Fawzi, M. Steimann, J. Wiethoff, *Z. Anorg. Allg. Chem.* **1997**, *623*, 554.

Chapter 4

Yttrium and Uranium saturated NHC complexes

4. Yttrium and uranium saturated NHC complexes.

Aspects of the work for this section were performed in collaboration with Miss Zoe R. Turner, a fellow PhD student, therefore complexes prepared by her are included as part of the discussion. Brief synthetic details for these complexes are described in the text, where relevant, and the compounds are given a letter, separate from the main numbering scheme.

4.1 Yttrium Complexes

4.1.1 Mono-alkoxy-NHC complexes

Treatment of $YN"_3$ with one equivalent of **3-P** or **3-M** on an NMR scale in benzene, affords yellow NMR solutions of **32-P**, after heating at 85 °C for 12 h, and **32-M** after standing at ambient temperature for 12 h, respectively, Eq. 37.

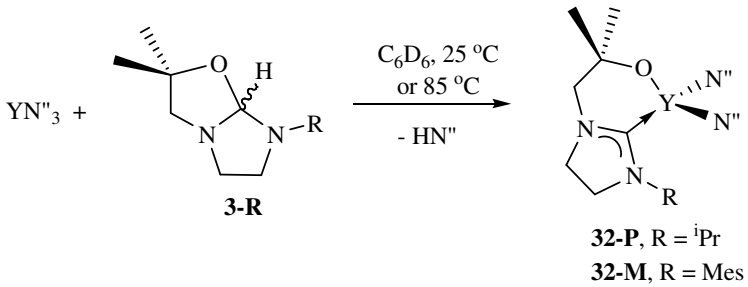

Eq. 37

Complexes **32-P** and **32-M** are immediately identifiable by the yttrium-carbene $^1J_{YC}$ coupling constants of 46 and 44 Hz, respectively, for the carbene carbon resonance at δ = 213.3 and 215.5 ppm, respectively. As previously observed for other diamagnetic saturated NHC complexes, these chemical shift values are at higher frequencies than those observed for unsaturated yttrium-carbene complexes, and compare with chemical

shifts of 186.3 ($^1J_{YC}$ = 53 Hz) in Y(L)N"$_2$, L = NBu^t{CH_2CH_2(1-C[NCHCHNBu^t])},[1] 194.3 ppm ($^1J_{YC}$ = 48 Hz) in Y(L)N"Cl, L = N[CH_2CH_2{1-C(NCHCHNMes)}]$_2$,[2] and 194.0 ppm in [Y{N($SiHMe_2$)$_2$}$_3${C($NMeCH$)$_2$}$_2$].[3] The ^{1}H NMR spectra of **32-P** and **32-M** are simplified upon breaking the doubly five-membered bicyclic ring system of **3-R** into the six-membered metallacyclic yttrium-alkoxide carbene, and the alkoxide arm CH_2 protons are now observed as a singlet between δ = 3.3 and 2.9 ppm.

An X-ray diffraction study of the *N*-Dipp substituted analogue supports the formulation of **32-P** and **32-M** drawn in Eq. 37.

4.1.2 Sequential ligand additions

The sequential addition of one equivalent of **3-P** to the NMR tube initially containing **32-P**, followed by heating at 85 °C for 12 h, cleanly afforded the *bis*- and *tris*-NHC yttrium complexes **33** and **34**, respectively, monitored by NMR spectroscopy, Scheme 26. The identity of **33** and **34** were verified on an NMR scale by independent treatment of YN"$_3$ with two and three equivalents of **3-P**, respectively, which after heating at 85 °C for 12 h provided identical NMR spectra. The ^{1}H NMR spectra of **32-P**, **33** and **34** display distinct *iso*-propyl septets at δ = 4.37, 5.05 and 5.56 ppm, respectively, and an yttrium-coupled carbene doublet in the ^{13}C NMR spectra at δ = 212.3, 216.5 and 220.2 ppm ($^1J_{YC}$ = 46.4, 35.8 and 29.1 Hz), respectively. The magnitude of the $^1J_{YC}$ coupling constants are an indication of the degree of σ-character in the Y-C bond. The decreasing trend observed across **32-P**, **33** and **34** suggests that the carbenes act as progressively worse σ-donors to the yttrium centre with the addition of each extra alkoxy-NHC ligand, due to the yttrium centre becoming more electron rich with each successive donor. The magnitude of these coupling constants is moderate compared to other examples, which displayed coupling constants up to 62 Hz.[4]

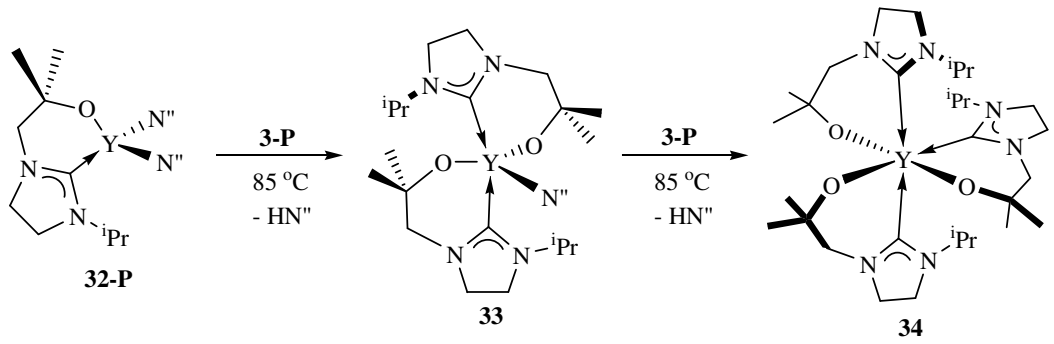

Scheme 26. Sequential NMR scale syntheses of Y^{III}-NHC complexes.

It proved necessary to heat reactions of **32-P**, **33** and **34** at 85 °C for 12 h to cleanly afford these products, as mixtures were formed at room temperature regardless of the reaction stoichiometry used.

4.1.3 Preliminary reactivity studies

Treatment of the *bis*-ligand complex **33** with one equivalent of Me_3SiI in benzene on an NMR scale, in an attempt to exchange the amide ligand for an iodide, afforded an insoluble orange oil after one hour, Eq. 38. Removal of the volatiles and dissolution in pyridine provided a ^1H NMR spectrum indicative of a mixture of products, one of which suggested the formation of **35**. The ^{13}C NMR spectrum of **35** no longer displays a high-frequency yttrium-coupled carbene resonance as observed for **33**, but instead possesses a resonance between δ = 175 and 180 ppm, commensurate with silylation of the C2-carbon. This trend was in agreement with the NMR data obtained for the product arising from treatment of the mono-*N*-Dipp complex $L^{Dipp}YN"_2$ with one equivalent of Me_3SiI. This reaction afforded $[Me_3Si\{C(NDippCH_2CH_2N)\}CH_2C(CH_3)_2O]YN"_2I$, for which a solid state structure was also obtained.

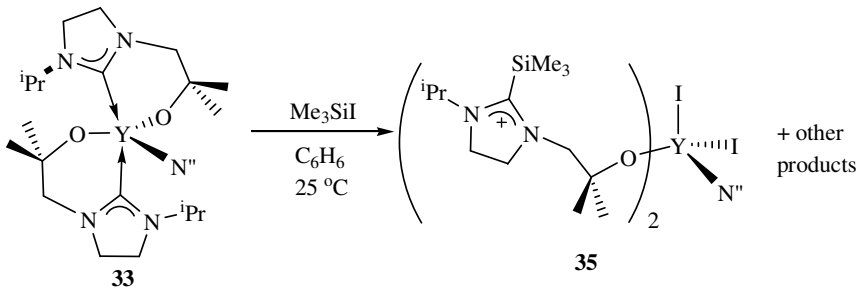

Eq. 38

4.2 Uranium Complexes

Treatment of a dark purple solution of $UN"_3$ with one equivalent of **3-M** in hexane at room temperature immediately affords a dark blue solution, accompanied by the formation of a small amount of an unidentified brown residue, Eq. 39. Crude **36** is very soluble in hexane, but can be isolated as a dark blue glassy solid in good yield.

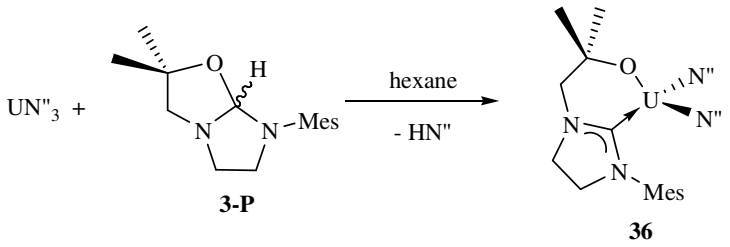

Eq. 39

The ^{1}H NMR spectra of **36** shows a broadened, paramagnetically shifted set of ligand resonances between δ = 30 and -20 ppm, and was also characterised by elemental analysis. Dissolution in d_5-pyridine immediately yields a brown solution and brown-pink precipitate, and the ^{1}H NMR spectrum reveals no resonances attributable to **36** and numerous new resonances between δ = 42 and -24 ppm. The UV-vis-NIR spectrum of **36** in toluene displayed a series of bands between 320 and 1313 (nm), with ε values of between 2296 and 131 (M^{-1} cm^{-1}), which are indicative of allowed d-f and forbidden f-f transitions in U^{III} ions.[5, 6] The *N*-Dipp substituted analogue of **36** was synthesised in a

similar manner, and a single crystal X-ray diffraction study confirmed a structure in agreement with that drawn for **36** in Eq. 39.

4.2.1 Reactivity studies

Treatment of a dark blue hexane solution of **36** with one equivalent of Me_3SiI in hexane at room temperature immediately produces a brown solution, from which a brown precipitate forms over 12 h. Following filtration, **37** can be isolated in 52 % yield, Eq. 40.

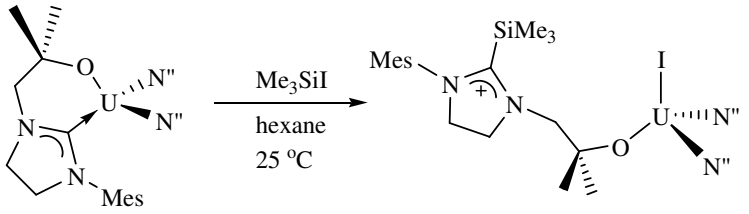

36 **37**

Eq. 40

Beautiful trapezoid-shaped pale brown single crystals of **37** were grown from a benzene solution at room temperature, although this compound has not been structurally characterised since it is assumed to be isostructural with the *N*-Dipp analogue, which was synthesised in an identical fashion. These crystals were used to characterise **37**, and the ^{1}H NMR spectrum contained a set of ligand resonances shifted between δ = 77 and -11 ppm. The UV-vis-NIR spectrum of **37** in toluene displayed a series of bands between 319 and 1051 (nm), with ε values of between 2431 and 39 (M^{-1} cm^{-1}), indicating that the metal centre is still U^{III}. Elemental analysis was also in agreement with the formulation of **37** shown in Eq. 40

Complex **37** is only moderately stable in solution, such that heating a benzene solution to 70 °C overnight, or standing a hexane solution at room temperature for up to four

weeks, results in the formation of dark pink-orange single crystals of **38**, accompanied by concomitant deposition of a pale brown precipitate, Eq. 41.

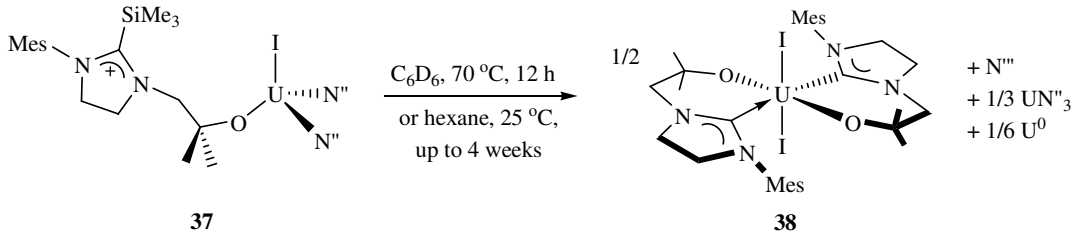

37 **38**

Eq. 41

To afford **38** from **37**, de-silylation of the imidazolinium group needs to occur, with one feasible route proceeding *via* coupling with N" to eliminate N"' ($N\{SiMe_3\}_3$). This would enable the formation of half an equivalent of **38**, with concomitant disproportionation, to produce a one third equivalent of $UN"_3$ and a one sixth equivalent of metallic uranium, accounting for the necessary redox process. Attempts to identify the N"' by-product by analysis of the mother liquor from this reaction with electrospray mass spectrometry proved unsuccessful. The spectra obtained showed a peak assigned as HL^M, **3-M**, which may have originated from hydrolysis of the product **38** present in solution. No peaks corresponding to N"', HN" or even the coupled $Me_3SiSiMe_3$ could be identified.

A sample of the pink crystals of **38** were isolated by decanting as much of the mother liquor and brown precipitate as possible, followed by washing with toluene and hexane and drying under reduced pressure. Satisfactory elemental analysis of this material was obtained, but it proved insoluble in aromatic NMR solvents. A ^1H NMR spectrum was obtained in d_5-pyridine but contained myriad paramagnetic resonances between δ = 100 and -32 ppm, which combined with the yellow colour of the solution probably indicates that **38** has reacted with the solvent to afford one or more new unidentified products.

Dark pink-orange single crystals of **38** were deposited from the reaction mixture anywhere between 12 h and four weeks after the reaction was conducted. The molecular structure is drawn in Figure 62, and selected metrical data displayed in Table 11.

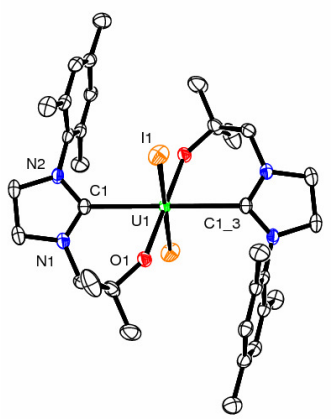

Figure 62. Displacement ellipsoid drawing of **38** (50 % probability ellipsoids). Hydrogens omitted for clarity.

Complex **38** possesses a crystallographic C_2 axis along the I-U-I vector, which enforces octahedral geometry and results in one iodide and one ligand being symmetry generated. The U^{IV}-I bond length of 3.0784(3) Å is shorter than in the five-coordinate [U{(Me_2^{t}BuSiNCH$_2$CH$_2$)N}I] (3.11 Å),[7] but longer than in four-coordinate IU(OAr)$_3$ (3.011(2) Å, Ar = 2, 6-^{t}BuC$_6$H$_3$)[8] and six-coordinate UI$_4$(tmu)$_2$ (3.011(3) Å, tmu = tetramethyl urea).[9] There are very few tetravalent uranium NHC complexes with which to compare the U-$C_{carbene}$ bond length of 2.647(4) Å found in **38**. This value is comparable to the U-$C_{carbene}$ bond length of 2.636(9) Å found in the U^{IV} terminal mono-oxide Cp*U(O){C(NMeCMe)$_2$}, **CLXI** in Chapter 1, and unsurprisingly shorter than the average U-$C_{carbene}$ bond length of 2.747(3) Å found in the seven-coordinate U^{IV}-alkoxy-NHC complex **CLXIV** in Chapter 1. The ligand bite angle in **38** is 73.47(11)°, and the heterocycle parameters are standard for metal bound NHCs of this type. The *N*-Dipp analogue forms in a similar manner, and the solid state structure is isostructural with **38**.

Table 11. Selected metrical data for **38**.

Distance (Å)/angle(º)	**38**
U1-I1	3.0784(3)
U1-O1	2.061(3)
U1-C1	2.647(4)
N-$C_{(av)}$	1.336(5)
N-C-N	107.6(3)

Similarly, treatment of a benzene solution of **36** with one equivalent of *iso*-propyl iodide, on an NMR scale, immediately formed a dark brown solution from which a pale brown precipitate and dark pink single crystals formed at room temperature over one month.

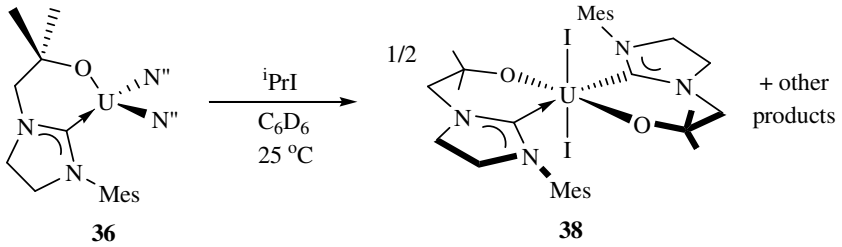

Eq. 42

The ^{1}H NMR spectrum revealed that the starting **36** had been completely transformed into an unknown brown compound. The ^{1}H NMR spectrum contains resonances between δ = 70 and -30 ppm. A cell check of the pink crystalline material confirmed the formation of **38**. Addition of *iso*-propyl iodide across the U-C bond forms an unstable intermediate product, which subsequently decomposes and disproportionates to **38** and other uranium containing by-products.

Treatment of a vigorously stirred dark blue hexane solution of **36** with an atmosphere of carbon dioxide results in the immediate formation of a pale green solution, accompanied by precipitation of very pale green solid in 70 % yield, **39** in Eq. 43.

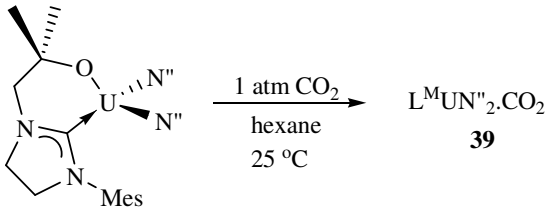

36 **39**

Eq. 43

The solubility of **39** is greatly reduced in hydrocarbon solvents compared to **36**, although it does dissolve readily in coordinating solvents such as THF and pyridine. The ^{1}H NMR spectrum in d_5-pyridine shows a set of paramagnetically shifted ligand resonances between δ = 53 and 10 ppm, but the silylamido resonance is not apparent, although there is a very broad feature in the baseline which merges with a number of other resonances. The UV-vis-NIR spectrum of **39** in THF contains weak bands between 601 and 1654 (nm), with ε values of between 9 and 26 (M^{-1} cm^{-1}), which are indicative of forbidden f-f transitions in U^{IV} ions.[7] Elemental analysis of **39** agrees with a product arising from the addition of one equivalent of CO_2 to **36**. There are a number of possible ways in which CO_2 could be incorporated in **39**, including coordination to the metal centre,[10-13] or insertion into the U-N, U-C, or U-O bonds to afford a uranium carbamate,[14-16] carboxylate[17-20] or carbonate[21] complex, respectively, see Figure 63. IR spectroscopy provides a method to identify these functional groups and probe their binding mode. A range of mono-metallic possibilities with the anticipated stretching frequencies are displayed in Figure 63. Complex **39** displays a very distinctive stretch at 2185 cm^{-1}, which closely matches that reported by Meyer *et. al.* for the linear η^1-**O**CO bound uranium complex [1,4,7-*tris*(3-adamantyl-5-^{t}Bu-2-hydroxybenzyl)1,4,7-triazacyclononane]$U^{IV}(CO_2)$ of 2188 cm^{-1}. Without a solid state X-ray diffraction analysis of **39**, it is difficult to verify this binding mode. The IR spectrum of **39** also displays three bands at 1687, 1646 and 1583 cm^{-1}, which are close to those detailed in Figure 63 for the products of insertion into U-N, U-C and U-O bonds. As the quantity of CO_2 added to the reaction mixture was not measured, it could be feasible that more than

one insertion product could have been formed during the reaction, but elemental analysis agrees with a product containing only one equivalent of CO_2.

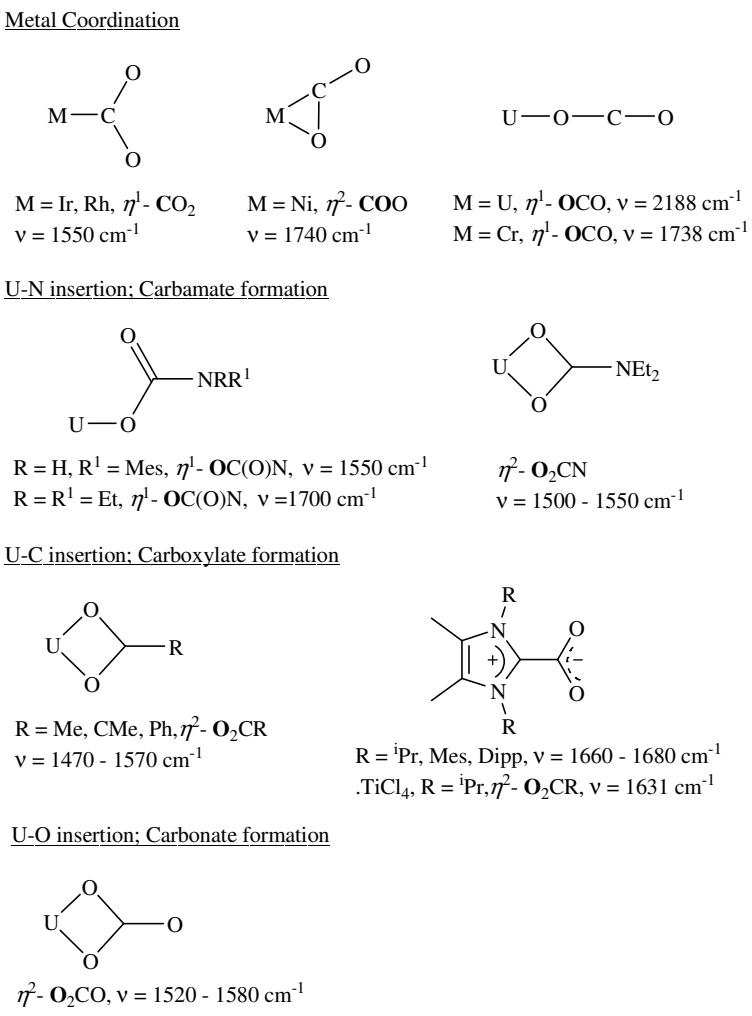

Figure 63. Possible formulations for **39** and reported IR stretching frequencies.

It has subsequently become apparent, through comparison with the work of Gambarotta and Budzelaar, that treatment of a metal amide complex with carbon dioxide results in the formation of an isocyanate complex.[22] Following chemical decomposition and treatment with $AgNO_3$, Ag(NCO) was isolated and displayed a characteristic intense resonance at 2176 cm^{-1} in the IR spectrum, which matches very closely with the stretch observed at 2188 cm^{-1} in **39**.

4.3 Uranyl Complexes

Miss Zoe Turner is thanked for the gift of HL^D, **AC**.

Mixing benzene solutions of $UO_2N"_2(THF)_2$ and two equivalents of **3-M** results in the deposition of pale yellow crystals of a new compound over a period of minutes, Eq. 44. The compound was identified as the poorly benzene-soluble *trans-bis*(L^M) adduct $UO_2(L^M)_2$ **40-M**, by elemental analysis, multinuclear NMR spectroscopy and a single crystal X-ray diffraction study, and isolated in 52 % yield.

An NMR spectroscopic-scale reaction between two equivalents of **3-D** and $UO_2N"_2(THF)_2$ shows that the analogous uranyl complex **40-D** is also straightforwardly accessible, Eq. 44.

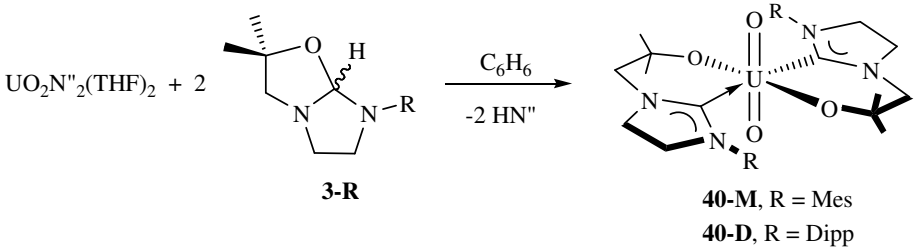

3-R

40-M, R = Mes
40-D, R = Dipp

Eq. 44

The most interesting feature of complexes **40-M** and **40-D** is the extraordinarily high chemical shift exhibited by the carbenic carbon in the ^{13}C NMR spectrum, of δ = 281.6 and 283.6 ppm, respectively. To our knowledge, these are the highest frequency carbene resonances exhibited by a metal NHC compound.

A particularly high carbene chemical shift of δ = 255.5 ppm was reported for the open-chain *bis*(di*iso*-propyl)carbene (N,N,N', N'-tetra *iso*-propylformamidinylidene), and the high value attributed to the wide NCN bond angle. Likewise, its complexes exhibit chemical shifts at values δ = 30–40 ppm higher frequency than the corresponding unsaturated NHC analogues.[23] Transition metal Fischer carbene complexes also exhibit

high frequency carbene chemical shifts, such as δ = 260.1 ppm in $(CO)_5Cr\{2\text{-}C(OC(OEt)CHC(Ph)CH)\}$[24] and δ = 300.9 ppm in $(CO)_5W\{C(OMe)CHC(Ph)OMe\}$.[25]

In NHC complexes, the highest chemical shifts yet reported have also been in uranyl systems. For example $\delta_{carbene}$ = 262.8 ppm for *trans*-$UO_2(L^N)_2$ (L^N = $NBu^tCH_2CH_2\{1\text{-}C(NCHCHNBu^t)\}$.[26]

The asymmetric OUO stretch, ν_{asymm}(OUO), is observed in the FTIR spectrum at 851 cm^{-1}, indicating a relatively strong binding of the two alkoxy-carbene ligands in the equatorial plane, which serves to weaken the UO_2 stretching energy. For comparison, ν_{asymm}(OUO) in the analogous uranyl complex *cis*-$UO_2(OBu^t)_2(OPPh_3)_2$ is 861 cm^{-1}, and in $UO_2N''_2(OPPh_3)_2$ it is 901 cm^{-1}.[27] This ligand set also weakens the UO_2 bonding more than in the complexes $UO_2(L^N)_2$, in which the average ν_{asymm}(OUO) is 931 cm^{-1}. We can conclude from these comparisons that the alkoxides are the dominating factor in the ability of the equatorial donor set to weaken the UO_2 stretch, but that the carbenes are stronger ligands than phosphine oxides here.

The molecular structures of **40-M** and **40-D** were determined by single crystal X-ray diffraction and are shown in Figure 64. Selected distances and angles are collated in Table 12.

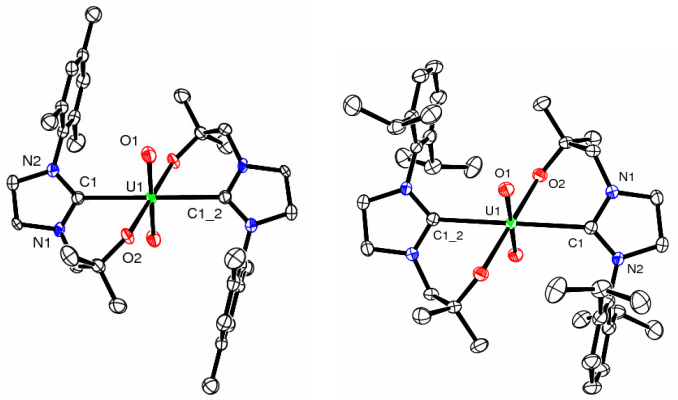

40-M **40-D**

Figure 64. Displacement ellipsoid drawings of **40-M** and **40-D** (50 % probability ellipsoids). Solvent molecules and hydrogens omitted for clarity.

The UO_2^{2+} uranyl unit in each is rigorously linear as expected, and the compounds are four-coordinate in the equatorial plane, in which the two bidentate OC ligands adopt a perfectly symmetrical *trans*-geometry about the metal, enforced by a crystallographic C_2 axis. Most uranyl compounds are between five and seven-coordinate in the equatorial plane. Additionally, in **40-M** there is a disorder in the crystal which superimposes two crystallographically independent molecules; only one is shown in Figure 64.

In both structures, the alkoxycarbene ligands twist out of the equatorial plane to accommodate the bulky aryl groups, with a ligand bite angle of 72°. The carbene ring is tilted with respect to the UC_2O_2 equatorial plane by 11° in **40-M** and 22° in **40-D**; this brings the arene rings out of the ligand plane in the same direction as the substituents on the alkoxide of the opposite ligand.

The U-$C_{carbene}$ distances of 2.580(4) Å in **40-M** and 2.612(2) Å in **40-D** are shorter than in the six-coordinate UO_2L_2, L = $NBu^t\{CH_2CH_2(1\text{-}C[NCHCHNBu^t])\}$(2.640(5) Å) and L = $NBu^t\{CH_2CH_2(1\text{-}C[NCHCHNMes])\}$(2.633(7) Å),[26] and $[UO_2Cl_2\{C(NMesCH)_2\}_2]$ (2.626(7) Å).[28] The U-OC distances of 2.161(3) Å in **40-M** and 2.154(2) Å in **40-D** are comparable to those in *cis*-$UO_2(OBu^t)_2(OPPh_3)_2$, in which the average is 2.149 Å.[27] The N-C-N angle of the coordinated carbene group is now 108.9(7)° in **40-M** and 108.0(2)° in **40-M**. Other distances and angles are within standard ranges.

Table 12. Selected metrical data for **40-M** and **40-D**.

Distance (Å)/angle(°)	**40-M**	**40-D**
U1-O1	1.7978(18)	1.7984(16)
U1-O2	2.161(3)	2.1538(16)
U1-C1	2.580(4)	2.612(2)
N1-C1	1.298(17)	1.336(3)
N2-C1	1.343(6)	1.338(3)
N-C-N	108.9(7)	108.0(2)

4.4 Conclusions

A series of yttrium alkoxy-NHC complexes have been synthesised. They show distinctive NMR spectra, dependent upon the degree of ligand substitution. The first examples of uranium complexes bearing saturated backbone alkoxy-NHC ligands have been synthesised, *via* metal-amide protonolysis chemistry and a mono-alkoxy-NHC substituted uranium amide has been synthesised and fully characterised, and some of its reaction chemistry investigated. Treatment of this complex with trimethylsilyl iodide furnishes a trivalent silylated-imidazolinium uranium iodide-amide complex. Alternatively, treatment of the uranium-NHC complex with carbon dioxide in hexane affords a pale green precipitate in good yield. This displays a stretch in the IR spectrum suggestive of an end-on bound linear CO_2 molecule, although there is no other evidence to corroborate this. This stretching frequency has subsequently been found to match well for the formation of a metal-bound isocyanate complex. UV-vis-NIR spectroscopy suggests that the uranium centre has been oxidised in this complex. Finally, two uranyl-NHC complexes have been synthesised and structurally characterised. Both of these complexes exhibit extremely high carbene carbon chemical shifts in the ^{13}C NMR spectrum.

4.5 References

[1] P. L. Arnold, S. A. Mungur, A. J. Blake, C. Wilson, *Angew. Chem. Int. Ed.* **2003**, *42*, 5981.

[2] I. S. Edworthy, A. J. Blake, C. Wilson, P. L. Arnold, *Organometallics* **2007**, *26*, 3684.

[3] W. A. Herrmann, F. C. Munck, G. R. J. Artus, O. Runte, R. Anwander, *Organometallics* **1997**, *16*, 682.

[4] P. L. Arnold, S. T. Liddle, *Organometallics* **2006**, *25*, 1485.

[5] P. Roussel, R. Boaretto, J. S. Kingsbury, N. W. Alcock, P. Scott, *J. Chem. Soc., Dalton Trans.* **2002**, 1423.

[6] J. E. Nelson, D. L. Clark, C. J. Burns, A. P. Sattelberger, *Inorg. Chem.* **1992**, *31*, 1973.

[7] P. Roussel, N. W. Alcock, R. Boaretto, A. J. Kingsley, I. J. Munslow, C. J. Sanders, P. Scott, *Inorg. Chem.* **1999**, *38*, 3651.

[8] L. R. Avens, D. M. Barnhart, C. J. Burns, S. D. McKee, W. H. Smith, *Inorg. Chem.* **1994**, *33*, 4245.

[9] J. G. H. du Preez, B. Zeelie, U. Casellato, R. Graziani, *Inorg. Chim. Acta* **1987**, *129*, 289.

[10] T. Herskovitz, *J. Am. Chem. Soc.* **1977**, *99*, 2391.

[11] M. Aresta, C. F. Nobile, V. G. Albano, E. Forni, M. Manassero, *J. Chem. Soc., Chem. Commun.* **1975**, 636.

[12] I. Castro-Rodriguez, H. Nakai, L. N. Zakharov, A. L. Rheingold, K. Meyer, *Science* **2004**, *305*, 1757.

[13] P. F. Souter, L. Andrews, *J. Am. Chem. Soc.* **1997**, *119*, 7350.

[14] S. C. Bart, C. Anthon, F. W. Heinemann, E. Bill, N. M. Edelstein, K. Meyer, *J. Am. Chem. Soc.* **2008**, *130*, 12536.

[15] F. Calderazzo, G. Dell'Amico, R. Netti, M. Pasquali, *Inorg. Chem.* **1978**, *17*, 471.

[16] A. L. Arduini, J. D. Jamerson, J. Takats, *Inorg. Chem.* **1981**, *20*, 2474.

[17] K. G. Moloy, T. J. Marks, *Inorg. Chim. Acta* **1985**, *110*, 127.

[18] A. L. Arduini, J. Takats, *Inorg. Chem.* **1981**, *20*, 2480.

[19] H. A. Duong, T. N. Tekavec, A. M. Arif, J. Louie, *Chem. Commun.* **2004**, 112.

[20] N. Kuhn, C. Maichle-Moessmer, G. Weyes, *Z. Anorg. Allg. Chem.* **1999**, *625*, 851.

[21] S. Amayri, T. Arnold, T. Reich, H. Foerstendorf, G. Geipel, G. Bernhard, A. Massanek, *Environ. Sci. Technol.* **2004**, *38*, 6032.

[22] H. Phull, D. Alberti, I. Korobkov, S. Gambarotta, P. H. M. Budzelaar, *Angew. Chem. Int. Ed.*, **2006**, *45*, 5331.

[23] K. Denk, P. Sirsch, W. A. Herrmann, *J. Organomet. Chem.* **2002**, *649*, 219.

[24] L. Jordi, F. Camps, S. Ricart, J. M. Vinas, J. M. Moreto, M. Mejias, E. Molins, *J. Organomet. Chem.* **1995**, *494*, 53.

[25] A. Llebaria, J. M. Moreto, S. Ricart, J. Ros, J. M. Vinas, R. Yanez, *J. Organomet. Chem.* **1992**, *440*, 79.

[26] S. A. Mungur, S. T. Liddle, C. Wilson, M. J. Sarsfield, P. L. Arnold, *Chem. Commun.* **2004**, 2738.
[27] C. J. Burns, D. C. Smith, A. P. Sattelberger, H. B. Gray, *Inorg. Chem.* **1992**, *31*, 3724.
[28] W. J. Oldham, S. M. Oldham, B. L. Scott, K. D. Abney, W. H. Smith, D. A. Costa, *Chem. Commun.* **2001**, 1348.

Chapter 5

Experimental Details

5. Experimental Procedures

All manipulations were carried out under a dry, oxygen-free dinitrogen atmosphere using standard Schlenk techniques, or in an MBraun Unilab or Vacuum Atmospheres OMNI-lab glovebox unless otherwise stated. The solvents used were degassed and dried either by refluxing over potassium or by passage through activated alumina towers prior to use. All deuterated solvents were refluxed over potassium, vacuum transferred and freeze-pump-thaw degassed three times prior to use. Me_3SiI and Me_3SiN_3 were vacuum transferred prior to use. Benzoquinone, NaO^tBu and KO^tBu were sublimed prior to use. The solutions of HCl (2 M in diethyl ether), $BH_3.SMe_2$ (2 M in toluene), 9-BBN (0.5 M in THF) and $AlMe_3$ (1.87 M solution in hexanes) were stored in a sealed ampoule and used as received from Aldrich. $CeCl_3(THF)_3$ was dried with Me_3SiCl in THF over three days, followed by filtration, washing with THF and drying under reduced pressure. *Rac*-lactide was recrystallised from toluene and sublimed prior to use. Phosphorous was recrystallised from toluene prior to use. The compounds KN",[1] $MgN"_2(THF)_2$, $ZnN"_2$,[2] $CaN"_2(THF)_2$,[3] $CeN"_3$, $YN"_3$,[4] $UN"_3$,[5] $UO_2N"_2(THF)_2$,[6] HL,[7] KL,[8] $CeI_3(THF)_4$,[9] KCH_2Ph,[10] *N*-Mesityl- and *N*-Dipp-ethylene diamines[11], $PhICl_2$[12] and [Fc][OTf][13] were synthesised according to literature procedures. All other reagents were used as received without further purification.

5.1 Instrumentation

^1H NMR spectra were recorded on Bruker arx250 MHz, avance360 MHz or av500 MHz spectrometers, and ^{13}C-{^1H} on the same spectrometers at 63, 90 and 125 MHz, respectively, at 300 K unless otherwise stated, and referenced internally to residual protio solvent. Chemical shift values are quoted in ppm. Elemental analyses were determined by Mr. Stephen Boyer at London Metropolitan University. IR spectra were recorded on Nicolet 210 and Jasco 410 spectrophotometers. UV-vis-nIR measurements

were recorded on a Perkin Elmer Lambda 900 UV/VIS/ NIR spectrometer, and the solutions were made in the glovebox and recorded in a Young's tap topped 10 mm quartz cell. Mass spectra were run on a VG autospec instrument or an Agilent 1100 series LCMS instrument. Molecular weight and molecular weight distribution of polymers were obtained by Gel Permeation Chromatography (1100 series, Hewlett Packard) with an RI detector. The columns (30 cm PLgel Mixed-C, 2 in series) were eluted with THF and calibrated with polystyrene standards. All calibration and analysis were performed at 35 °C and a flow rate of 0.5 mL/min.

5.2 Synthetic Procedures for Chapter 2

5.2.1 Proligand synthesis: General procedure

Proligands were synthesised via a combination and modification of literature procedures[14, 15] in air. In a typical reaction, an *N*-substituted ethylenediamine was heated with an epoxide in a melt reaction in a sealed ampoule at 90 ºC for two days. The resulting oil was dissolved in diethyl ether and cooled to 0 ºC, acidified with a solution of anhydrous 2 M HCl in diethyl ether and stirred for 1 h at ambient temperature. Following filtration and drying under reduced pressure, the resulting yellow solid was combined with trimethylorthoformate in toluene and refluxed at 90 ºC for 2 h. The final workup procedure varied for each proligand.

5.2.2 Synthesis of 1-P ($[H_2L^P]Cl$)

N-iso-propylethylenediamine (3.00 g, 29.35 mmol) and isobutylene oxide (2.12 g, 29.35 mmol) produced a yellow oil to which was added diethyl ether (50 ml) and HCl (2 M in ether, 14.60 ml, 29.35 mmol), furnishing a yellow solid. Toluene (50 ml) and $(MeO)_3CH$ (13.01 g, 122.60 mmol) were added and after reflux, a brown oil settled from solution. The solvent was decanted and **1-P** dried under reduced pressure to yield a viscous brown oil. (3.92 g, 60 %).

^{1}H NMR ($CDCl_3$); δ 9.71 (s, 1H, N-C*H*-N), 5.25 (s, 1H, O*H*), 4.33 (bm, 2H, N-CH_2-CH_2-N), 4.05 (bm, 2H, N-CH_2-CH_2-N), 4.05 (bm, 1H, N-C*H*-$(CH_3)_2$), 3.74 (s, 2H, N-CH_2-C), 1.46 (d, 6H, $^3J_{HH}$ = 6 Hz, N-CH-(CH_3)$_2$), 1.36 (s, 6H, C(CH_3)$_2$). ^{13}C; 158.5 (N-*C*H-N), 70.3 (*C*-$(CH_3)_2$), 58.1 51.5 46.3 (N-*C*H_2), 50.8 (N-*C*H-$(CH_3)_2$), 27.7 (C-(*C*H_3)$_2$), 21.3 (CH-(*C*H_3)$_2$). MS (EI) m/z: 185 (M-Cl, 100 %).

5.2.3 Synthesis of 2-P ($[H_2L^P]I$)

To a stirred solution of **1-P** (3.92 g, 17.75 mmol) in acetone (30 ml) at ambient temperature was added portionwise a solution of NaI (1.5 eq, 3.99 g, 26.63 mmol) in acetone (30 ml). A colourless precipitate formed immediately and the reaction was

stirred for 2 h. Following filtration and removal of the volatiles, the residue was extracted into DCM (40 ml), filtered and the volatiles removed to yield **2-P** as a viscous brown oil (5.07 g, 93 %).

Colourless crystals suitable for an X-ray diffraction study grew from the product oil after standing at room temperature for a number of weeks.

Found: C 38.18, H 6.10, N 8.18. Calc. for $C_{10}H_{21}IN_2O$: C 38.47, H 6.79, N 8.97 %. ^{1}H NMR ($CDCl_3$); δ 9.00 (s, 1H, N-C*H*-N), 4.22 (bm, 2H, N-CH_2-CH_2-N), 4.00 (bm, 2H, N-CH_2-CH_2-N), 4.00 (bm, 1H, N-C*H*-$(CH_3)_2$), 3.68 (s, 2H, N-CH_2-C), 1.42 (d, 6H, $^3J_{HH}$ = 6 Hz, N-CH-(CH_3)$_2$), 1.31 (s, 6H, C(CH_3)$_2$). ^{13}C; 157.5 (N-*C*H-N), 71.1 (*C*-$(CH_3)_2$), 58.4 52.0 46.9 (N-*C*H_2), 51.2 (N-*C*H-$(CH_3)_2$), 28.0 (C-(*C*H_3)$_2$), 21.5 (CH-(*C*H_3)$_2$).

5.2.4 Synthesis of 1-M ([H_2L^M]Cl)

N-mesitylethylenediamine (4.00 g, 22.44 mmol) and isobutylene oxide (1.78 g, 24.68 mmol) produced a yellow oil to which was added diethyl ether (60 ml) and HCl (2 M in ether, 11.22 ml, 22.44 mmol), furnishing a yellow solid. Toluene (50 ml) and trimethylorthoformate (11.91 g, 112.20 mmol) were added and after reflux a yellow/ brown oil settled from solution. The volatiles were removed under reduced pressure giving a yellow solid which was suspended in acetone (50 ml) and sonicated briefly; filtration and drying yielded **1-M** as a cream solid (4.94 g, 74 %).

Found: C 64.84, H 8.57, N 9.41. Calc. for $C_{16}H_{25}ClN_2O$: C 64.73, H 8.51, N 9.44 %. ^{1}H NMR ($CDCl_3$); δ 9.33 (s, 1H, N-C*H*-N), 6.89 (s, 2H, Ar-C*H*), 5.20 (s, 1H, O*H*), 4.42 (bm, 2H, N-CH_2-CH_2-N), 4.13 (bm, 2H, N-CH_2-CH_2-N), 3.89 (bs, 2H, N-CH_2-C), 2.26 (bs, 9H, Ar-CH_3), 1.27 (s, 6H, C(CH_3)$_2$). ^{13}C; 160.8 (N-*C*H-N), 140.6 135.6 131.2 (quaternary Ar-*C*), 130.4 (Ar-*C*H), 70.1 (*C*-$(CH_3)_2$), 57.9 52.4 51.4 (N-*C*H_2), 27.7 (C-(*C*H_3)$_2$), 21.4 18.4 (Ar-*C*H_3). MS (EI) m/z: 261 (M-Cl, 100 %).

5.2.5 Synthesis of 2-M ([H_2L^M]I)

A similar anion exchange procedure to that already described was used. **1-M** (0.28 g, 0.94 mmol) and NaI (0.21 g, 1.42 mmol) in acetone (5 ml each) yielded **2-M** as a yellow solid (0.33 g, 90 %).

Found: C 50.17, H 6.81, N 7.96. Calc. for $C_{16}H_{25}IN_2O$: C 49.49, H 6.50, N 7.22 %. ^{1}H NMR ($CDCl_3$); δ 8.94 (s, 1H, N-C*H*-N), 6.89 (s, 2H, Ar-C*H*), 4.50 (m, 2H, N-C*H*$_2$-CH$_2$-N), 4.16 (m, 2H, N-CH$_2$-C*H*$_2$-N), 3.92 (s, 2H, N-C*H*$_2$-C), 3.63 (s, 1H, O*H*), 2.28 (s, 6H, Ar-ortho-C*H*$_3$), 2.25 (s, 3H, Ar-para-C*H*$_3$), 1.31 (s, 6H, C(C*H*$_3$)$_2$). ^{13}C; 159.5 (N-*C*H-N), 140.7 135.6 130.9 (quaternary Ar-*C*), 130.4 (Ar-*C*H), 71.0 (*C*-(CH$_3$)$_2$), 58.2 52.9 51.4 (N-*C*H$_2$), 27.8 (C-(*C*H$_3$)$_2$), 21.4 18.8 (Ar-*C*H$_3$).

5.2.6 Bicyclic carbene-alcohol adduct synthesis: General procedure.

To a Schlenk charged with a stirred mixture of KCH_2Ph and one equivalent of the appropriate proligand, at −78 °C, was added THF. The resulting dark orange solution/ suspension was allowed to warm slowly to ambient temperature overnight, furnishing a yellow/ green solution and fine precipitate. After filtration, the volatiles were removed and, in the case of **3-P** and **3-M**, the residue was purified *via* short path distillation and the product isolated as a colourless oil. Compound **3-D** was isolated as a green oily solid after removal of the volatiles, from which a small amount of colourless crystalline solid could be sublimed.

Alternatively, one equivalent of Li^{n}Bu was added to a cooled (−78 °C) suspension of the proligand in hexanes or toluene, and the mixture allowed to warm to ambient temperature slowly overnight. The subsequent workup was the same as that just described for **3-P** and **3-M**, although no green colour was observed for **3-D** and the product could be isolated as a colourless solid after hexane washing.

5.2.7 Synthesis of 3-P (HL^P)

2-P (3.00 g, 9.61 mmol) and KCH_2Ph (1.25 g, 9.61 mmol) with THF (30 ml) produced a pale yellow solution and colourless precipitate. After filtration and removal of the volatiles, the resulting yellow oil was distilled (10^{-1} mbar at 35-40 ºC) to yield **3-P** as a colourless oil (0.91 g, 51 %).

Found: C 65.13, H 11.06, N 15.19. Calc. for $C_{10}H_{20}N_2O$: C 65.16, H 10.96, N 15.20 %. ^{1}H NMR (C_6D_6); δ 5.47 (s, 1H, N-C(O)*H*-N), 3.13 2.85 2.64 2.63 (m, 1H each, N-C*H*$_2$-

CH_2-N), 2.91 2.45 (d, 1H each, $^2J_{HH}$ = 10.5 Hz N-CH_2-C), 2.85 (m, 1H, N-CH-(CH_3)$_2$), 1.24 1.16 (s, 3H each, C(CH_3)$_2$), 1.14 1.09 (d, 3H each, $^3J_{HH}$ = 6.0 Hz, N-CH-(CH_3)$_2$). ^{13}C; 107.8 (N-C(O)H-N), 78.6 (C-(CH_3)$_2$), 65.6 54.4 47.9 (N-CH$_2$), 50.4 (N-CH-(CH_3)$_2$), 28.4 27.8 (C-(CH_3)$_2$), 22.6 21.6 (CH-(CH_3)$_2$).

5.2.8 Synthesis of 3-M (HL^M)

1-M (4.79 g, 16.14 mmol) and KCH_2Ph (2.10 g, 16.14 mmol) with THF (30 ml) produced a yellow/ green solution and fine colourless precipitate. After filtration and removal of the volatiles, the resulting yellow oil was distilled (10^{-1} mbar at 85 ºC) to yield **3-M** as a colourless oil (3.08 g, 73 %).

Colourless crystals suitable for an X-ray diffraction study grew from the product oil after standing at room temperature for a number of months.

Found: C 73.90, H 9.36, N 10.63. Calc. for $C_{16}H_{24}N_2O$: C 73.79, H 9.31, N 10.76 %. ^{1}H NMR (C_6D_6); δ 6.80 (s, 2H, Ar-CH), 5.79 (s, 1H, N-C(O)H-N), 3.42 3.21 3.02 2.94 (m, 1H each, N-CH_2-CH_2-N), 2.90 2.52 (d, 1H each, $^2J_{HH}$ = 10.5 Hz N-CH_2-C), 2.39 (bs, 6H, Ar-ortho-CH_3), 2.14 (s, 3H, Ar-para-CH_3), 1.30 1.11 (s, 3H each, C(CH_3)$_2$). ^{13}C; 140.3 138.8 135.8 (quaternary Ar-C), 129.7 (Ar-CH), 108.6 (N-C(O)H-N), 77.5 (C-(CH_3)$_2$), 64.2 54.8 49.9 (N-CH$_2$), 29.4 28.0 (C-(CH$_3$)$_2$), 21.0 18.8 (Ar-CH$_3$).

5.2.9 Synthesis of 4 ([HL^P.KN"])

To a mixture of **2-P** (0.50 g, 1.60 mmol) in THF (10 ml) cooled to −60 ºC was added a solution of KN" (0.64 g, 3.20 mmol) in THF (10 ml) with stirring. The reaction mixture was allowed to warm to room temperature slowly over 16 h. The resulting orange solution was filtered from a white precipitate and had the solvent removed under reduced pressure to furnish crude **4** as a pale brown solid (0.52 g, 84.7 %).

X-ray quality single crystals were grown from a hexane solution cooled to −30 ºC over 4 weeks. These crystals proved to be very thermally sensitive.

Found: C 33.81, H 6.68, N 6.80. Calc. for $C_{16}H_{38}KN_3OSi_2$: C 50.06, H 10.00, N 10.95 %. ^{1}H NMR (C_6D_6); δ 5.36 (s, 1H, N-C(O)H-N), 3.04 2.87 2.61 2.60 (m, 1H each, N-CH_2-CH_2-N), 2.86 2.43 (d, 1H each, $^2J_{HH}$ = 10.8 Hz N-CH_2-C), 2.81 (m, 1H, N-CH-

$(CH_3)_2$), 1.26 1.13 (s, 3H each, C(CH_3)$_2$), 1.09 1.06 (d, 3H each, $^3J_{HH}$ = 6.8 Hz, N-CH-(CH_3)$_2$), 0.27 (s, 18H, N(Si{CH_3}$_3$)$_2$. ^{13}C; 108.4 (N-*C*(O)H-N), 79.1 (*C*-$(CH_3)_2$), 65.6 54.8 48.7 (N-*C*H_2), 51.4 (N-*C*H-$(CH_3)_2$), 29.4 28.2 (C-(*C*H_3)$_2$), 22.9 22.0 (CH-(*C*H_3)$_2$), 8.0 N(Si{*C*H_3}$_3$)$_2$.

5.2.10 NMR H/D exchange studies of 5-R (DL^R)

5-P (DL^P); To a J-Youngs NMR tube containing a solution of **3-P** (35 mg, 0.19 mmol) in C_6D_6 (0.5 ml) was added $CDCl_3$ (227 mg, 1.90 mmol) and then shaken well. The reaction was monitored by proton and carbon NMR spectroscopy and, after heating at 60 ºC for 1.5 h was found to be >90 % complete.

^{1}H NMR (C_6D_6); δ 6.54 (s, $CHCl_3$), 3.13 2.85 2.64 2.63 (m, 1H each, N-CH_2-CH_2-N), 2.91 2.45 (d, 1H each, $^2J_{HH}$ = 10.5 Hz N-CH_2-C), 2.85 (m, 1H, N-C*H*-$(CH_3)_2$), 1.24 1.16 (s, 3H each, C(CH_3)$_2$), 1.14 1.09 (d, 3H each, $^3J_{HH}$ = 6.0 Hz, N-CH-(CH_3)$_2$). ^{13}C; 107.8 (t, $^1J_{CD}$ = 27.2 Hz, N-*C*(O)D-N), 78.6 (*C*-$(CH_3)_2$), 78.3 (*C*HCl_3), 65.6 54.4 47.9 (N-*C*H_2), 50.4 (N-*C*H-$(CH_3)_2$), 28.4 27.8 (C-(*C*H_3)$_2$), 22.6 21.6 (CH-(*C*H_3)$_2$).

5-M (DL^M); To a J-Youngs NMR tube containing a solution of **3-M** (50 mg, 0.19 mmol) in C_6D_6 (0.5 ml) was added $CDCl_3$ (227 mg, 1.90 mmol) and then shaken well. The reaction was monitored by proton and carbon NMR spectroscopy and, after heating at 60 ºC for 12 h was found to be >90 % complete.

^{1}H NMR (C_6D_6); δ 6.80 (s, 2H, Ar-C*H*), 6.54 (s, $CHCl_3$), 3.42 3.21 3.02 2.94 (m, 1H each, N-CH_2-CH_2-N), 2.90 2.52 (d, 1H each, $^2J_{HH}$ = 10.5 Hz N-CH_2-C), 2.39 (bs, 6H, Ar-ortho-CH_3), 2.14 (s, 3H, Ar-para-CH_3), 1.30 1.11 (s, 3H each, C(CH_3)$_2$). ^{13}C; 140.3 138.8 135.8 (quaternary Ar-*C*), 129.7 (Ar-*C*H), 108.6 (t, $^1J_{CD}$ = 27.2 Hz, N-*C*(O)D-N), 78.3 (*C*HCl_3), 77.5 (*C*-$(CH_3)_2$), 64.2 54.8 49.9 (N-*C*H_2), 29.4 28.0 (C-(*C*H_3)$_2$), 21.0 18.8 (Ar-*C*H_3).

5.2.11 Synthesis of 6-P ([$HL^{P, OSiMe_3}$]I)

To a solution of **3-P** (150.0 mg, 0.81 mmol) in hexane (10 ml) was added a solution of TMSI (166.1 mg, 0.83 mmol, 118 µl) in hexane (5 ml) at room temperature with stirring.

A white precipitate formed immediately and the reaction mixture was stirred for 1.5 h. The solid was filtered, washed with hexane (10 ml) and dried under reduced pressure to yield **6-P** as a colourless solid (260.0 mg, 83.6 %).

Colourless crystals suitable for an X-ray diffraction study were grown from a benzene solution at room temperature.

Found: C 40.53, H 7.75, N 7.21. Calc. for $C_{10}H_{29}IN_2OSi$: C 40.61, H 7.62, N 7.29 %. ^{1}H NMR (C_6D_6); δ 9.85 (s, 1H, N-C*H*-N), 3.91 (bm, 2H, N-CH_2-CH_2-N), 3.84 (sept, 1H, $^3J_{HH}$ = 7.2 Hz, N-C*H*-$(CH_3)_2$), 3.77 (s, 2H, N-CH_2-C), 3.64 (bm, 2H, N-CH_2-CH_2-N), 1.32 (s, 6H, C(CH_3)$_2$), 1.22 (d, 6H, $^3J_{HH}$ = 7.2 Hz, N-CH-(CH_3)$_2$), 0.15 (s, 9H, O-Si-(CH_3)$_3$). ^{13}C; 158.4 (N-*C*H-N), 75.1 (*C*-$(CH_3)_2$), 60.2 51.9 48.0 (N-*C*H_2), 51.2 (N-*C*H-$(CH_3)_2$), 28.5 (C-(*C*H_3)$_2$), 22.0 (CH-(*C*H_3)$_2$), 3.4 (O-Si-(*C*H_3)$_3$).

5.2.12 Synthesis of 6-M ([$HL^{M, OSiMe_3}$]I)

To a solution of **3-M** (200.0 mg, 0.77 mmol) in hexane (10 ml) was added a solution of TMSI (156.8 mg, 0.78 mmol, 111.5 µl) in hexane (5 ml) at room temperature with stirring. A white precipitate formed immediately and the reaction mixture was stirred for 1.5 h. The solid was filtered, washed with hexane (10 ml) and dried under reduced pressure to yield **6-M** as a colourless solid (277.0 mg, 78.1 %).

Found: C 49.60, H 7.12, N 6.02. Calc. for $C_{19}H_{33}IN_2OSi$: C 49.56, H 7.24, N 6.08 %. ^{1}H NMR (C_6D_6); δ 9.54 (s, 1H, N-C*H*-N), 6.67 (s, 2H, Ar-C*H*), 4.06 (m, 2H, N-CH_2-CH_2-N), 3.86 (s, 2H, N-CH_2-C), 3.64 (m, 2H, N-CH_2-CH_2-N), 2.21 (s, 6H, Ar-ortho-CH_3), 2.06 (s, 3H, Ar-para-CH_3), 1.28 (s, 6H, C(CH_3)$_2$), 0.09 (s, 9H, O-Si-(CH_3)$_3$). ^{13}C; 160.4 (N-*C*H-N), 140.6 136.3 129.2 (quaternary Ar-*C*), 130.7 (Ar-*C*H), 74.9 (*C*-$(CH_3)_2$), 60.1 52.5 51.4 (N-*C*H_2), 28.1 (C-(*C*H_3)$_2$), 21.5 19.0 (Ar-*C*H_3), 3.0 (O-Si-(*C*H_3)$_3$).

5.2.13 Synthesis of 7-P ([L^PMgN"]$_2$)

To a solution of MgN"$_2$(THF)$_2$ (398.2 mg, 0.81 mmol) in hexane (10 ml) was added a solution of **3-P** (150.0 mg, 0.81 mmol) in hexane (10 ml) with stirring. A colourless precipitate formed from the colourless solution after approximately one minute at room temperature. Stirring was continued for a further 16 h. Following filtration to remove the

mother liquor the solid was washed with hexanes (2 x 5 ml), and dried under reduced pressure to yield **7-P** as a colourless solid (230.0 mg, 77.0 %).

X-ray quality single crystals were grown from a benzene solution at room temperature over 2-3 days.

Found: C 52.10, H 9.95, N 11.19. Calc. for $C_{16}H_{37}MgN_3OSi_2$: C 52.21, H 10.15, 11.42 %. ^{1}H NMR (C_6D_6); δ 4.28 (sept, 1H, $^3J_{HH}$ = 7.0 Hz, N-C*H*-$(CH_3)_2$), 3.70 2.45 (d, 1H each, $^2J_{HH}$ = 14.0 Hz, N-CH_2-C), 2.88 2.78 2.64 2.63 (m, 1H each, N-CH_2-CH_2-N), 1.37 1.32 (s, 3H each, C(CH_3)$_2$), 1.04 1.02 (d, 3H each, $^3J_{HH}$ = 7.0 Hz, N-CH-(CH_3)$_2$), 0.43 (s, 18H, N(Si{CH_3}$_3$)$_2$. ^{13}C; 210.2 ($C_{carbene}$), 71.4 (*C*-$(CH_3)_2$), 61.1 53.1 42.2 (N-*C*H$_2$), 51.3 (N-*C*H-$(CH_3)_2$), 32.1 30.1 (C-(*C*H$_3$)$_2$), 22.1 21.4 (CH-(*C*H$_3$)$_2$), 8.4 N(Si{*C*H$_3$}$_3$)$_2$.

5.2.14 Synthesis of 7-M ([L^{M}MgN'']$_2$)

To a solution of MgN"$_2$(THF)$_2$ (260.0 mg, 0.53 mmol) in hexane (10 ml) was added a solution of **3-M** (138.3 mg, 0.53 mmol) in hexane (10 ml) with stirring. A colourless precipitate formed from the colourless solution after approximately one minute at room temperature. Stirring was continued for a further 16 h. Following filtration to remove the mother liquor the solid was washed with hexanes (2 x 5 ml), and dried under reduced pressure to yield **7-M** as a colourless solid (180 mg, 76.5 %).

Found: C 59.43, H 9.21, N 9.59. Calc. for $C_{22}H_{41}MgN_3OSi_2$: C 59.49, H 9.32, N 9.46 %. ^{1}H NMR (C_6D_6); δ 6.83 (bs, 2H, Ar-C*H*), 3.60 (bs, 2H, N-CH_2-C), 2.91 (bs, 4H, N-CH_2-CH_2-N), 2.33 2.23 (bs, 3H each, Ar-ortho-CH_3), 2.11 (s, 3H, Ar-para-CH_3), 1.34 (bs, 6H, C(CH_3)$_2$), 0.38 (s, 18H, N(Si{CH_3}$_3$)$_2$). ^{13}C; 213.2 ($C_{carbene}$), 138.4 128.0 (quaternary Ar-*C*), the third quaternary carbon and Ar-*C*H cannot be identified, 70.9 (*C*-$(CH_3)_2$), 53.8 51.1 (N-*C*H$_2$), the third methylene resonance cannot be identified, 31.0 (C-(*C*H$_3$)$_2$), 21.6 (Ar-*C*H$_3$), the third methyl resonance cannot be identified, 8.3 N(Si{*C*H$_3$}$_3$)$_2$.

At 70 ºC; ^{1}H NMR (C_6D_6); δ 6.83 (s, 2H, Ar-C*H*), 3.26 (bs, 2H, N-CH_2-C), 3.03 (bs, 4H, N-CH_2-CH_2-N), 2.27 (s, 6H, Ar-ortho-CH_3), 2.12 (s, 3H, Ar-para-CH_3), 1.29 (s, 6H, C(CH_3)$_2$), 0.31 (s, 18H, N(Si{CH_3}$_3$)$_2$). ^{13}C; 214.0 ($C_{carbene}$), 138.5 137.0 128.3

(quaternary Ar-*C*), 130.5 (Ar-*C*H), 70.9 (*C*-(CH_3)$_2$), 62.4 53.9 51.3 (N-*C*H_2), 31.0 (C-(*C*H_3)$_2$), 21.4 20.2 (Ar-*C*H_3), 8.1 N(Si{*C*H_3}$_3$)$_2$.

5.2.15 Synthesis of 8-P ([L^{P}ZnN"]$_2$)

To a solution of ZnN"$_2$ (386.3 mg, 1.00 mmol) in hexane (10 ml) was added a solution of **3-P** (184.3 mg, 1.00 mmol) in hexane (10 ml) with stirring. A colourless precipitate formed from the colourless solution after approximately one minute at room temperature. Stirring was continued for a further 16 h. Following filtration to remove the mother liquor the solid was washed with hexanes (2 x 5 ml), and dried under reduced pressure to yield **8-P** as a colourless solid (309.0 mg, 75.5 %).

X-ray quality single crystals were grown from a benzene solution at room temperature overnight.

Found: C 46.89, H 9.08, N 10.19. Calc. for $C_{16}H_{37}N_3OSi_2Zn$: C 46.97, H 9.13, N 10.27 %. ^{1}H NMR (C_6D_6); δ 4.34 (sept, 1H, $^3J_{HH}$ = 7.0 Hz, N-C*H*-(CH_3)$_2$), 3.63 2.45 (d, 1H each, $^2J_{HH}$ = 14.0 Hz, N-CH_2-C), 2.90 2.72 2.64 2.62 (m, 1H each, N-CH_2-CH_2-N), 1.41 1.39 (s, 3H each, C(*CH*$_3$)$_2$), 1.07 1.02 (d, 3H each, $^3J_{HH}$ = 7.0 Hz, N-CH-(C*H*$_3$)$_2$), 0.44 (s, 18H, N(Si{C*H*$_3$}$_3$)$_2$. ^{13}C; 204.8 ($C_{carbene}$), 72.5 (*C*-(CH_3)$_2$), 61.5 52.8 42.1 (N-*C*H_2), 51.1 (N-*C*H-(CH_3)$_2$), 32.0 30.2 (C-(*C*H_3)$_2$), 22.3 21.2 (CH-(*C*H_3)$_2$), 8.3 N(Si{*C*H_3}$_3$)$_2$.

5.2.16 NMR scale synthesis of 9 ([LMgN"]$_2$)

To a J-Youngs NMR tube containing a solution of MgN"$_2$(THF)$_2$ (26.9 mg, 0.06 mmol) in C_6D_6 (0.5 ml) was added a solution of **HL** (10.0 mg, 0.06 mmol) in C_6D_6 (0.5 ml) and then shaken well. A pale yellow solution formed immediately, followed by an off white precipitate over approximately 2 h, which redissolved upon warming. Three components were present in the NMR spectra in an approximate 2:1:1 ratio. Only the main component could be convincingly assigned.

X-ray quality single crystals were grown from this benzene solution at room temperature overnight.

Main component: ^{1}H NMR (C_6D_6); δ 6.26 6.12 (s, 1H each, N-C*H*-C*H*-N), 4.64 (sept, 1H, $^3J_{HH}$ = 6.6 Hz, N-C*H*-(CH_3)$_2$), 4.17 3.13 (d, 1H each, $^2J_{HH}$ = 13.8 Hz, N-CH_2-C),

1.49 (s, 3H each, C(CH_3)$_2$) second methyl resonance obscured by THF resonance, 1.22 (d, 6H, $^3J_{HH}$ = 6.6 Hz, N-CH-(CH_3)$_2$), 0.37 (s, 18H, N(Si{CH_3}$_3$)$_2$. ^{13}C; 185.9 ($C_{carbene}$), 123.7 114.8 (N-*C*H-*C*H-N), 70.5 (*C*-(CH$_3$)$_2$), 63.3 (N-*C*H$_2$), 53.1 (N-*C*H-(CH$_3$)$_2$), 32.1 (CH-(*C*H$_3$)$_2$), 25.5 23.7 (C-(*C*H$_3$)$_2$), 7.0 N(Si{*C*H$_3$}$_3$)$_2$.

5.2.17 Synthesis of 10-P (ZnL^P_2)

To a solution of ZnN"$_2$ (100.0 mg, 0.26 mmol) in hexane (10 ml) was added a solution of **3-P** (95.4 mg, 0.52 mmol) in hexane (10 ml) with stirring. The solution turned yellow immediately and colourless crystals of **8-P** formed after 5 min. The reaction mixture was heated at 70 ºC for 16 h. A brown precipitate formed and, following filtration of the mother liquor and washing of the solid with hexanes (2 x 5 ml), the product was dried under reduced pressure to yield **10-P** as a pale brown solid (70.0 mg, 62.0 %).

Found: C 55.53, H 8.82, N 12.88. Calc. for $C_{20}H_{38}N_4O_2Zn$: C 55.60, H 8.88, N 12.97 %. ^{1}H NMR (C_6D_6); δ 4.65 (sept, 1H, $^3J_{HH}$ = 6.8 Hz, N-C*H*-(CH$_3$)$_2$), 3.12 3.05 (d, 1H each, $^2J_{HH}$ = 12.6 Hz, N-C*H*$_2$-C), 2.80 2.46–2.64 (m, 2H each, N-C*H*$_2$-C*H*$_2$-N), 1.54 1.53 (s, 6H, C(C*H*$_3$)$_2$), 1.15 0.96 (d, 3H each, $^3J_{HH}$ = 6.8 Hz, N-CH-(C*H*$_3$)$_2$). ^{13}C; 203.6 ($C_{carbene}$), 71.7 (*C*-(CH$_3$)$_2$), 64.0 53.2 41.7 (N-*C*H$_2$), 50.4 (N-*C*H-(CH$_3$)$_2$), 33.4 32.0 (C-(*C*H$_3$)$_2$), 21.8 (CH-(*C*H$_3$)$_2$).

5.2.18 Synthesis of 10-M (ZnL^M_2)

To a solution of ZnN"$_2$ (111.2 mg, 0.29 mmol) in hexane (10 ml) was added a solution of **3-M** (150.0 mg, 0.58 mmol) in hexane (10 ml) with stirring. The solution turned yellow immediately and was heated at 70 ºC for 16 h. A pale yellow precipitate formed and, following filtration of the mother liquor and washing of the solid with hexanes (2 x 5 ml), the product was dried under reduced pressure to yield **10-M** as a yellow solid (140.0 mg, 83.0 %).

X-ray quality single crystals were grown from a benzene solution at room temperature over 2-3 days.

Found: C 65.82, H 7.14, N 8.85. Calc. for $C_{32}H_{46}N_4O_2Zn$: C 65.78, H 7.95, N 9.59 %. ^{1}H NMR (C_6D_6); δ 6.95 6.76 (s, 1H each, Ar-C*H*), 2.80-2.89 (m, 4H, N-C*H*$_2$-C*H*$_2$-N),

2.78 2.33 (d, 1H each, $^{2}J_{HH}$ = 12.0 Hz, N-C*H*$_2$-C), 2.61 2.19 2.03 (s, 3H each, Ar-C*H*$_3$), 1.37 1.17 (s, 3H each, C(C*H*$_3$)$_2$). ^{13}C; 205.7 ($C_{carbene}$), 140.3 137.7 135.7 (quaternary Ar-*C*), 130.7 (Ar-*C*H), 71.1 (*C*-(CH$_3$)$_2$), 63.7 53.5 49.4 (N-*C*H$_2$), 32.3 31.5 (C-(*C*H$_3$)$_2$), 21.7 20.1 18.6 (Ar-*C*H$_3$).

5.2.19 NMR scale synthesis of 11 (ZnL_2)

To a J-Youngs NMR tube containing a solution of ZnN"$_2$ (15.9 mg, 0.04 mmol) in C_6D_6 (0.5 ml) was added a solution of **HL** (15.0 mg, 0.08 mmol) in C_6D_6 (0.5 ml) and then shaken well, forming a pale yellow solution after 30 min.

^{1}H NMR (C_6D_6); δ 6.39 6.33 (s, 1H each, N-C*H*-C*H*-N), 4.94 (sept, 1H, $^{3}J_{HH}$ = 6.7 Hz, N-C*H*-(CH$_3$)$_2$), 3.74 (s, 2H, N-C*H*$_2$-C), 1.50 1.31 (s, 3H each, C(C*H*$_3$)$_2$), 1.26 1.14 (d, 3H each, $^{3}J_{HH}$ = 6.7 Hz, N-CH-(C*H*$_3$)$_2$). ^{13}C; 179.0 ($C_{carbene}$), 71.1 (*C*-(CH$_3$)$_2$), 66.1 (N-*C*H$_2$), 52.6 (N-*C*H-(CH$_3$)$_2$), 33.2 31.2 (C-(*C*H$_3$)$_2$), 24.4 24.1 (CH-(*C*H$_3$)$_2$).

5.2.20 NMR-scale synthesis of 12 (L^{P}-(SiMe$_3$)MgIN")

To a J-Youngs NMR tube containing a solution of **7-P** (20.0 mg, 0.05 mmol) in C_6D_6 (0.5 ml) was added a solution of Me$_3$SiI (10.9 mg, 0.05 mmol, 7.7 µl) in C_6D_6 (0.5 ml) and then shaken well, forming a colourless solution after heating at 80 °C for 16 h.

^{1}H NMR (C_6D_6); δ 3.90 (m, 2H, N-C*H*$_2$-CH$_2$-N), 3.74 (sept, 1H, $^{3}J_{HH}$ = 6.6 Hz, N-C*H*-(CH$_3$)$_2$), 3.42 (s, 2H, N-C*H*$_2$-C), 3.24 (m, 2H, N-CH$_2$-C*H*$_2$-N), 1.05 (s, 6H, C(C*H*$_3$)$_2$), 0.92 (d, 6H, $^{3}J_{HH}$ = 6.6 Hz, N-CH-(C*H*$_3$)$_2$), 0.64 (s, 18H, N(Si{C*H*$_3$}$_3$)$_2$, 0.23 (s, 9H, C-Si-(C*H*$_3$)$_3$). ^{13}C; 174.6 (N-*C*Si-N), 74.6 (*C*-(CH$_3$)$_2$), 60.8 53.0 43.9 (N-*C*H$_2$), 50.5 (N-*C*H-(CH$_3$)$_2$), 28.9 (C-(*C*H$_3$)$_2$), 21.0 (CH-(*C*H$_3$)$_2$), 7.6 N(Si{*C*H$_3$}$_3$)$_2$, 3.4 (C-Si-(*C*H$_3$)$_3$).

5.2.21 NMR-scale synthesis of 13 ($L^{P, OSiMe_3}$ZnIN")

To a J-Youngs NMR tube containing a solution of **8-P** (20.0 mg, 0.05 mmol) in C_6D_6 (0.5 ml) was added a solution of Me$_3$SiI (9.8 mg, 0.05 mmol, 7.0 µl) in C_6D_6 (0.5 ml) and then shaken well, forming a colourless solution.

^{1}H NMR (C_6D_6); δ 4.64 (sept, 1H, $^{3}J_{HH}$ = 6.6 Hz, N-C*H*-(CH$_3$)$_2$), 3.46 (s, 2H, N-C*H*$_2$-C), 3.11 (m, 2H, N-C*H*$_2$-CH$_2$-N), 2.55 (m, 2H, N-CH$_2$-C*H*$_2$-N), 1.17 (s, 6H, C(C*H*$_3$)$_2$), 0.87

(d, 6H, $^{3}J_{HH}$ = 6.6 Hz, N-CH-(CH_3)$_2$), 0.43 (s, 18H, N(Si{CH_3}$_3$)$_2$, 0.05 (s, 9H, O-Si-(CH_3)$_3$). ^{13}C; 196.8 ($C_{carbene}$), 75.5 (*C*-(CH$_3$)$_2$), 62.3 50.6 43.1 (N-*C*H$_2$), 50.9 (N-*C*H-(CH$_3$)$_2$), 28.3 (C-(*C*H$_3$)$_2$), 21.0 (CH-(*C*H$_3$)$_2$), 6.7 N(Si{*C*H$_3$}$_3$)$_2$, 3.3 (O-Si-(*C*H$_3$)$_3$).

5.2.22 Alternative synthesis of 13 (L$^{P, OSiMe_3}$ZnIN'')

To a J-Youngs NMR tube containing a solution of ZnN"$_2$ (42.0 mg, 0.11 mmol) in C_6D_6 (0.5 ml) was added a solution of **6-P** (41.8 mg, 0.11 mmol) in C_6D_6 (0.5 ml) and then shaken well, forming a colourless solution after heating at 70 °C for 16 h. Two components were indentified by ^{1}H NMR spectroscopy, in a 2:3 ratio. The data for the first compound formed confirm that it is **13**, and the data for the second is given below.

^{1}H NMR (C_6D_6); δ 4.66 (sept, 1H, $^{3}J_{HH}$ = 6.6 Hz, N-C*H*-(CH$_3$)$_2$), 4.13 (s, 2H, N-C*H*$_2$-C), 3.38 (m, 2H, N-C*H*$_2$-CH$_2$-N), 2.78 (m, 2H, N-CH$_2$-C*H*$_2$-N), 1.47 (s, 6H, C(C*H*$_3$)$_2$), 1.05 (d, 6H, $^{3}J_{HH}$ = 6.6 Hz, N-CH-(CH_3)$_2$), 0.43 (s, 18H, N(Si{CH_3}$_3$)$_2$, 0.11 (s, 9H, O-Si-(CH_3)$_3$). ^{13}C; 198.3 ($C_{carbene}$), 76.6 (*C*-(CH$_3$)$_2$), 61.6 51.1 42.6 (N-*C*H$_2$), 50.6 (N-*C*H-(CH$_3$)$_2$), 28.3 (C-(*C*H$_3$)$_2$), 21.2 (CH-(*C*H$_3$)$_2$), 5.8 N(Si{*C*H$_3$}$_3$)$_2$, 3.3 (O-Si-(*C*H$_3$)$_3$).

5.2.23 NMR-scale synthesis of 14 (L$^{P, OSiMe_3}$MgIN'')

To a J-Youngs NMR tube containing a solution of MgN"$_2$(THF)$_2$ (50.9 mg, 0.10 mmol) in C_6D_6 (0.5 ml) was added a solution of **6-P** (40.0 mg, 0.10 mmol) in C_6D_6 (0.5 ml) and then shaken well, forming a pale yellow solution after 30 min. The reaction mixture was heated at 70 °C for 16 h.

^{1}H NMR (C_6D_6); δ 4.81 (sept, 1H, $^{3}J_{HH}$ = 6.7 Hz, N-C*H*-(CH$_3$)$_2$), 3.68 (s, 2H, N-C*H*$_2$-C), 3.25 (m, 2H, N-C*H*$_2$-CH$_2$-N), 2.73 (m, 2H, N-CH$_2$-C*H*$_2$-N), 1.31 (s, 6H, C(C*H*$_3$)$_2$), 1.04 (d, 6H, $^{3}J_{HH}$ = 6.7 Hz, N-CH-(CH_3)$_2$), 0.43 (s, 18H, N(Si{CH_3}$_3$)$_2$, 0.12 (s, 9H, O-Si-(CH_3)$_3$). ^{13}C; 207.2 ($C_{carbene}$), 75.9 (*C*-(CH$_3$)$_2$), 62.7 50.8 43.0 (N-*C*H$_2$), 50.2 (N-*C*H-(CH$_3$)$_2$), 28.5 (C-(*C*H$_3$)$_2$), 21.6 (CH-(*C*H$_3$)$_2$), 7.4 N(Si{*C*H$_3$}$_3$)$_2$, 3.3 (O-Si-(*C*H$_3$)$_3$).

5.2.24 General polymerisation procedure

A typical reaction was conducted at room temperature by the addition of THF solutions of the catalyst (3.0 mg) to a solution of the monomer (300 mg), total THF volume of 3.0

ml, with vigorous stirring. It was not necessary to include an initiator, such as benzyl alcohol, to effect polymerisation. The reaction was quenched by addition of bench THF and exposure to ambient atmosphere, followed by removal of the volatiles under reduced pressure.

5.3 Synthetic Procedures for Chapter 3

5.3.1 Synthesis of 15 ($Ce(O^tBu)_4$)

To a stirred slurry of CAN (2.00 g, 3.64 mmol) in THF (10 ml) was added portion wise a solution of NaO^tBu (2.10 g, 21.89 mmol) in THF (10 ml) at room temperature. A yellow solution formed immediately with concomitant production of a colourless precipitate and evolution of ammonia. The solution was stirred at room temperature for 2 h and after filtration and removal of the volatiles under reduced pressure, the crude product was isolated as a yellow solid (1.50 g). Sublimation (120 ºC at 10^{-5} mbar) yielded a yellow crystalline solid, **15**, in poor yield (150 mg, 9.5 %).

Found: C 30.06, H 5.79, N 0. Calc. for $C_{16}H_{36}CeO_4$: C 44.42, H 8.40, N 0 %. ^{1}H NMR (C_6D_6); δ 1.58 (s, O-C-$(CH_3)_3$).

5.3.2 Synthesis of 16 ($Ce_3(\mu_3\text{-}O^tBu)_2(\mu\text{-}O^tBu)_3(O^tBu)_6$)

To a Schlenk was added CAN (3.0 g, 5.47 mmol) and NaO^tBu (3.16 g, 32.83 mmol), followed by THF (50 ml) with stirring at room temperature. After 2-3 h a yellow solution and colourless precipitate formed, which was accompanied by the evolution of ammonia. The reaction mixture was stirred overnight and the green/ brown solution filtered, followed by removal of the volatiles under reduced pressure. The residue was dissolved in hexane and placed in a -30 ºC freezer, from which **16** was isolated as a green solid (1.24 g, 55.6 %).

X-ray quality single crystals were grown by slow cooling of a hot hexane solution to ambient temperature overnight, and formed as dark green blocks and light green needles. After manual separation, the blocks were washed with hexane and dried before further characterisation.

Found: C 43.12, H 8.05, N 0. Calc. for $C_{44}H_{99}Ce_3O_{11}$: C 43.15, H 8.16, N 0 %. ^{1}H NMR (C_6D_6); δ 3.58 (bs, 36H, terminal O-C-$(CH_3)_3$), 0.54 (bs, 18H, μ_3-O-C-$(CH_3)_3$), -5.09 (bs, 36H, μ-O-C-$(CH_3)_3$). IR (nujol) υ_{max}/ cm^{-1}: 1225(m), 1188(s), 1022(w), 984(m), 969(s), 942(s), 912(s), 876(m), 770(m), 747(m), 722(m), 503(m), 478(m), 417(m).

MS (EI) *m/z*: 1093 ([M-^{t}Bu]$^+$, 15 %), 1020 ([[M-^{t}Bu]– O^{t}Bu]$^+$, 30 %), 963 ([[M-^{t}Bu]– O^{t}Bu - ^{t}Bu]$^+$, 22 %), 874 ([[M-^{t}Bu]– 3 O^{t}Bu]$^+$, 9 %), 791 ([[M-^{t}Bu] – OCe(O^{t}Bu)$_2$]$^+$, 65 %), 718 ([[M-^{t}Bu]– OCe(O^{t}Bu)$_3$]$^+$, 41 %), 661 ([[M-^{t}Bu]– Ce(O^{t}Bu)$_4$]$^+$, 29 %), 588 ([[M-^{t}Bu] – Ce(O^{t}Bu)$_5$]$^+$, 21 %), 531 ([[M-^{t}Bu]– Ce(O^{t}Bu)$_5$ - ^{t}Bu]$^+$, 10 %), 359 ([Ce(O^{t}Bu)$_3$]$^+$, 78 %), 286 ([Ce(O^{t}Bu)$_2$]$^+$, 58 %), 214 ([CeO^{t}Bu]$^+$, 59 %), 156 ([CeO]$^+$, 98 %), 57 ([^{t}Bu]$^+$, 100 %).

5.3.3 Synthesis of 17 ([K$_3${Ce(O)(O^{t}Bu)$_{10}$(OTf)}]$_2$)

To a cooled (-78 ºC) mixture of Ce(OTf)$_4$ (0.75 g, 1.02 mmol) and KO^{t}Bu (0.46 g, 4.08 mmol) was added THF (20 ml) with stirring. A yellow solution and colourless precipitate formed immediately and the reaction was allowed to warm to room temperature over 12 h. The solvent was removed under reduced pressure from the resulting very pale green solution, and the residue was extracted into hexane, filtered and dried to yield crude **17** as an off white solid (0.40 g, 27.4 %). X-ray quality single crystals were grown from a benzene solution at room temperature. The ^{1}H NMR spectrum displayed numerous resonances, so as to preclude identification.

5.3.4 Oxidation of CeN"$_3$ to afford VIII

To a stirred solution of CeN"$_3$ (673 mg, 1.08 mmol) in toluene (15 ml) at room temperature was added PhICl$_2$ (447 mg, 1.62 mmol) in one portion. The pale yellow solution immediately turned dark purple, and stirring was maintained for 16 h. The solution was filtered away from a dark purple precipitate, layered with hexane (15 ml) and stored at -78 °C overnight, which afforded **VIII** as purple-black needles (98 mg, 12.0 %).

^{1}H NMR (C$_6$D$_6$); δ 0.44 (s, 54H, N(Si{C*H*$_3$}$_3$)$_2$).

5.3.5 Synthesis of 18 ([^{t}BuO)$_3$Ce(μ-O^{t}Bu)]$_2$(μ-HL))

To a mixture of **15** (0.60 g, 1.51 mmol) and HL (138 mg, 0.76 mmol) at -78 ºC was added cooled (-78 ºC) THF (15 ml) with stirring. A yellow solution formed and was allowed to slowly warm to ambient temperature with stirring for 12 h. The resulting pale

brown reaction mixture was concentrated under reduced pressure and stored at -30 ºC overnight. Filtration and removal of volatiles from the filtrate under reduced pressure afforded a brown solid **18** (198 mg, 25.0 %). X-ray quality single crystals were grown by slow cooling of a THF solution to -30 ºC.

Found: C 33.72, H 6.13, N 2.69. Calc. for $C_{42}H_{90}Ce_2N_2O_9$: C 48.15, H 8.68, N 2.67 %. ^{1}H NMR (C_6D_6); δ 9.84 (s, 1H, N-C*H*-N), 6.17 (s, 1H, N-C*H*-CH-N), 5.76 (s, 1H, N-CH-C*H*-N), 4.29 (sept, 1H, $^3J_{HH}$ = 6 Hz, N-C*H*$(CH_3)_2$), 3.97 (s, 2H, N-CH_2-C), 2.05 (s, 18H, O-C-(CH_3)$_3$), 1.75 (s, 18H, O-C-(CH_3)$_3$), 1.53 (s, 36H, O-C-(CH_3)$_3$), 0.85 (d, 6H, $^3J_{HH}$ = 6 Hz, N-CH(CH_3)$_2$). ^{13}C; 137.3 (N-*C*H-N), 124.6 (N-*C*-C-N), 114.6 (N-C-*C*-N), 81.3 79.4 75.6 (O-*C*$(CH_3)_3$), 74.1 (O-*C*$(CH_3)_2$), 64.8 (N-*C*H_2), 52.0 (N-*C*H$(CH_3)_2$), 35.9 34.8 34.6 (O-C(*C*H_3)$_3$), 30.00 (N-C(*C*H_3)$_2$), 22.5 (O-C(*C*H_3)$_2$).

5.3.6 Synthesis of 19 ([^{t}BuO)$_3$Ce(μ-O^{t}Bu)]$_2$(μ-HL^P))

To a solution of **15** (85 mg, 0.20 mmol) in hexane (5 ml) was added a solution of **3-P** (18.1 mg, 0.1 mmol) in hexane. The yellow solution was mixed well and stored under N_2 at room temperature overnight. A pale yellow precipitate formed, which was isolated by filtration, washed with hexane (2 x 2 ml) and dried under reduced pressure to afford **19** (35 mg, 19.6 %).

Found: C 27.81, H 5.05, N 1.70. Calc. for $C_{42}H_{91}Ce_2N_2O_9$: C 27.70, H 5.05, N 1.54 %. ^{1}H NMR (C_6D_6); δ 9.22 (s, 1H, N-C*H*-N), 3.85 (sept, 1H, $^3J_{HH}$ = 6.6 Hz, N-C*H*-$(CH_3)_2$), 3.25 (bs, 2H, N-CH_2-C), 2.89 (bm, 2H, N-CH_2-CH_2-N), 2.34 (m, 2H, N-CH_2-CH_2-N), 2.02 (s, 18H, O-C-(CH_3)$_3$), 1.83 (s, 6H, C(CH_3)$_2$), 1.76 (s, 18H, O-C-(CH_3)$_3$), 1.63 (s, 36H, O-C-(CH_3)$_3$), 0.71 (d, 6H, $^3J_{HH}$ = 6.6 Hz, N-CH-(CH_3)$_2$). ^{13}C; 159.0 (N-*C*H-N), 82.2 80.2 76.5 (O-*C*$(CH_3)_3$), 75.8 (*C*-$(CH_3)_2$), 62.5 51.9 41.5 (N-*C*H_2), 50.3 (N-*C*H-$(CH_3)_2$), 36.6 35.7 35.6 (O-C(*C*H_3)$_3$), 30.9 (C-(*C*H_3)$_2$), 20.8 (CH-(*C*H_3)$_2$).

5.3.7 Synthesis of 20 (CeL_3)

To a stirred, cooled mixture of $CeI_3(THF)_4$ (9.14 g, 11.29 mmol) and KL, **LXXVII**, (7.39 g, 33.54 mmol) was added cooled THF (100 ml, −78 °C). The yellow suspension was allowed to warm to room temperature over 12 h, during which time it became a

bright orange solution containing a colorless precipitate. Filtration and removal of volatiles from the filtrate under reduced pressure afforded an orange solid **20** (6.04 g, 78 %).

Found: C 52.58, H 7.60, N 12.20. Calc. for $C_{30}H_{51}CeN_6O_3$: C 52.68, H 7.53, N 12.29 %. ^{1}H NMR (C_6D_6); δ 11.71 (bs, 2H, N-C*H*$_2$-C), 9.64 (bs, 6H, N-CH-(C*H*$_3$)$_2$), 6.05 (bs, 1H, N-C*H*-CH-N), 3.22 (bs, 1H, N-CH-C*H*-N), -2.94 (bs, 6H, O-C-(C*H*$_3$)$_2$), -5.56 (bs, 1H, N-C*H*-(CH$_3$)$_2$). MS (EI) *m/z*: 683 (M^+, 10 %). μ_{eff} (Evans method, benzene, 300 K) 2.21 μ_B.

5.3.8 Synthesis of 21 (CeL_4)

To a mixture of **20** (2.40 g, 3.51 mmol), KL, **LXXVII**, (0.78 g, 3.51 mmol) and benzoquinone (0.19 g, 1.76 mmol) was added diethyl ether (40 ml). A dark brown suspension formed immediately and was stirred at room temperature for 12 h. Filtration and removal of volatiles from the filtrate under reduced pressure afforded **21** as a yellow solid (2.29 g, 75.0 %). Pale yellow crystals suitable for an X-ray diffraction study were grown from a THF solution at −30 °C.

Found: C 55.41, H 8.07, N 12.83. Calc. for $C_{40}H_{68}CeN_8O_4$: C 55.52, H 7.94, N 12.95 %. ^{1}H NMR (C_6D_6); δ 7.01 (s, 1H, N-C*H*-CH-N), 6.50 (s, 1H, N-CH-C*H*-N), 5.28 (sept, 1H, $^3J_{HH}$ = 6 Hz, N-C*H*-(CH$_3$)$_2$), 4.03 (s, 2H, N-C*H*$_2$), 1.29 (s, 6H, O-C-(C*H*$_3$)$_2$), 1.23 (d, 6H, $^3J_{HH}$ = 6 Hz, N-C*H*-(CH$_3$)$_2$). ^{13}C; 212.60 ($C_{carbene}$), 122.03 (N-*C*-C-N), 113.08 (N-C-*C*-N), 78.51 (O-*C*Me$_2$), 64.35 (N*C*H$_2$), 51.04 (N-*C*HMe$_2$), 30.00 (N-C(*C*H$_3$)$_2$), 24.13 (O-C(CH$_3$)$_2$). ^{1}H NMR (C_6D_6) at −81 °C; δ 7.31, 7.29, 7.18, 7.16, 7.15, 7.13, 7.09, 7.03 (s, 1H, N-C*H*-C*H*-N), 1.32 (bd, 24H, indistinguishable, N-C*H*-(CH$_3$)$_2$), 1.04 (bs, 24H, O-C-(C*H*$_3$)$_2$). The complex precipitates out of solution at this temperature; no further resonances could be identified. MS (EI) *m/z*: 699 (L_3CeO, 7 %), 683 (CeL_3, 95 %). μ_{eff} (Evans method, benzene, 300 K) 0.00 μ_B.

5.3.9 Oxidation of 20 with XeF_2 or $[Fe(Cp)_2][OTf]$.

Each reaction was carried out as above, but with the benzoquinone reagent replaced by XeF_2 (37.0 mg, 0.22 mmol) and **20** (300 mg, 0.44 mmol), or $[Fe(Cp)_2][OTf]$ (290 mg,

0.88 mmol) and **20** (600 mg, 0.88 mmol). Dark orange solutions formed in both cases and after an analogous work-up, **21** was isolated as a yellow solid in 32.0 %, and <10 % yield, respectively.

5.3.10 Synthesis of 22 ([Ce(L)$_2$(HL)$_2$]I

To a mixture of **20** (0.5 g, 0.73 mmol) and benzoquinone (3.9 mg, 0.04 mmol) was added THF (15 ml). An orange solution formed immediately and was stirred for 12 h. Filtration and removal of volatiles from the filtrate under reduced pressure afforded an orange solid (0.47 g). The ^{1}H NMR spectra in C_6D_6 showed predominantly **20** and **21** to be present. A small crop of **22** was isolated from the solution, and a yellow single crystal suitable for X-ray structure determination was grown from a benzene solution at 25 °C, although there was insufficient **22** to enable further characterisation. Structural characterisation confirms that complex **22** is a Ce^{III} analogue of **21**.

5.3.11 Synthesis of 23 (CeL$_2$(L-BH$_3$)$_2$)

To a cooled solution of **21** (0.75 g, 0.87 mmol) in toluene (20 ml, −78 °C), was added a solution of $BH_3.SMe_2$ (2.0 M, 0.87 ml, 1.73 mmol) dropwise. An opaque yellow-brown solution formed and was allowed to warm to room temperature with stirring for 12 h. A brown oily solid was deposited from the pale coloured solution, and the volatiles were removed under reduced pressure to yield **23** as a brown solid in quantitative yield.

Found: C 53.73, H 8.51, N 12.44. Calc. for $C_{40}H_{74}B_2CeN_8O_4$: C 53.80, H 8.37, N 12.55 %. ^{1}H NMR (C_6D_6); δ 8.60 6.39 (s, 1H each, N-C*H*-CH-N), 6.62 6.27 (s, 1H each, N-CH-C*H*-N), 5.34 5.32 (multiplet, 1H each, $^3J_{HH}$ = 6 Hz, N-C*H*$(CH_3)_2$), 4.47 3.66 (s, 2H each, N-C*H*$_2$), 1.51 1.31 (s, 6H each, O-C(C*H*$_3$)$_2$), 1.10 1.07 (d, 6H each, $^3J_{HH}$ = 6 Hz, N-C*H*$(CH_3)_2$). ^{13}C; 211.2 (N-*C*-N), 123.5 122.1 (N-*C*-C-N), 114.7 112.7 (N-C-*C*-N), 80.5 78.3 (O-*C*$(CH_3)_3$), 64.2 60.3 (N-*C*H$_2$), 51.3 49.0 (N-*C*H$(CH_3)_2$), 30.5 29.1 (N-C(*C*H$_3$)$_2$), 24.0 22.7 (O-C(*C*H$_3$)$_3$).

5.3.12 Synthesis of 24 ($(CeL_2(L\text{-}9\text{-}BBN)_2)$)

To a cooled solution of **21** (1.30 g, 1.50 mmol) in THF (30 ml, −78 °C), was added a solution of 9-BBN (0.5 M, 6.0 ml, 3.00 mmol) dropwise. A yellow-brown suspension formed and was allowed to warm to room temperature with stirring for 12 h. The volatiles were removed from the dark brown solution under reduced pressure, affording a brown solid which was recrystallised from benzene, yielding **24** as yellow crystals (1.34 g, 80 %). Crystals suitable for X-ray diffraction were grown *via* slow cooling of a hot benzene solution to room temperature.

Found: C 60.74, H 9.00, N 10.06. Calc. for $C_{56}H_{98}B_2CeN_8O_4$: C 60.03, H 8.92, N 10.10 %. ^{1}H NMR (C_5D_5N); δ 9.00, 7.37 (s, 1H, H(c), H(c')), 7.18, 7.04 (s, 1H, H(d), H(d')), 7.37 (s, 2H, H(C)), 7.20 (s, 2H, H(D)), 5.42 (broad sept, 2H, $^3J_{HH}$ = 6 Hz, H(e), H(e')), 5.19 (sept, 2H, $^3J_{HH}$ = 6 Hz, H(E)), 4.51 (bs, 2H, H(b)), 4.00 (bs, 2H, H(b')), 3.92 (s, 4H, H(B)), 2.95-3.96 (m, 28H, 9-BBN), 2.51, 2.49 (d, 12H, $^3J_{HH}$ = 6 Hz, N-C*H*-$(CH_3)_2$), 2.29, 2.25 (s, 12H, O-C-$(CH_3)_2$). ^{13}C; δ 212.53 (both Ce-bound $C_{carbene}$), 125.61, 124.0 (C(c), C(c')), 123.40 (C(C)), 116.62 (C(D)), 115.88, 115.11 (C(d), C(d')), 81.62, 80.29 (O-C), 70.65 (O-C), 65.64, 61.34 (C(b), C(b')), 59.23 (C(B)), 53.01, 49.83 (C(e), C(e')), 51.10 (C(E)), 39.67, 32.85 (C(f), C(f')), 34.08 (C(F)), 34.33 (9-BBN-CH), 30.61, 26.20, 25.95 (9-BBN-CH_2), 24.86 (C(A)), 24.86, 24.67 (C(a), C(a')). ^{11}B (C_5D_5N); δ -15.4. The boron-coordinated $C_{carbene}$ resonance is not observed due to coupling to the quadrupolar B nucleus. μ_{eff} (Evans method, pyridine, 300 K) 0.0 μ_B.

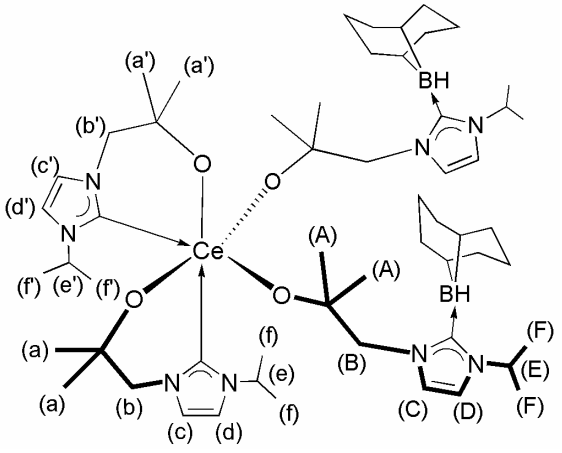

Labelling scheme for assignment of ^{1}H NMR spectra of **24**

5.3.13 Synthesis of 25 (L-9-BBN)

To a cooled solution (-78 ºC) of **24** (98 mg, 0.088 mmol) in THF (10 ml) was added a solution of 9-BBN (0.18 ml, 0.088 mmol) with stirring and the reaction was allowed to warm slowly to room temperature over 12 h. Following filtration and removal of the solvent under reduced pressure, the crude product was obtained as a yellow solid (80 mg). The crude ^{1}H NMR spectra resembled the starting material **24**.

Single crystals suitable for an X-ray diffraction study grew from this d_5-pyridine solution. There was insufficient recrystallised material for further satisfactory characterisation.

Found: C 59.23, H 8.00, N 8.78. Calc. for $C_{18}H_{31}BN_2O$: C 71.51, H 10.36, N 9.27 %.

5.3.14 Synthesis of 26 ($(CeL_2(L\text{-}AlMe_3)_2)$)

To a cooled (-78 °C) solution of **21** (0.75 g, 0.87 mmol) in THF (10 ml) was added a solution of $AlMe_3$ (1.87 M in hexane, 1.85 ml, 3.47 mmol) dropwise. After stirring at room temperature for 12 h and removal of the volatiles under reduced pressure, crude **26** was isolated as a pale brown solid in quantitative yield. Due to solubility problems, the ^{13}C NMR spectrum was run in d_5-pyridine.

^{1}H NMR (C_6D_6); δ 8.68 6.33 (s, 1H each, N-C*H*-CH-N), 6.63 6.20 (s, 1H each, N-CH-C*H*-N), 5.23 5.19 (bm, N-C*H*$(CH_3)_2$), 4.36 3.58 (s, 2H each, N-CH_2), 1.27 1.05 (d, 6H each, $^{3}J_{HH}$ = 6.0 Hz, N-C*H*$(CH_3)_2$), 1.22 1.20 (s, 6H each, O-C(CH_3)$_2$). ^{13}C (C_6D_5N); 211.0 (Ce-$C_{carbene}$), 172.2 (m, Al-$C_{carbene}$), 126.1 124.4 (N-*C*-C-N), 115.1 113.7 (N-C-*C*-N), 79.3 79.0 (O-*C*$(CH_3)_3$), 64.2 61.4 (N-*C*H_2), 51.5 50.3 (N-*C*H$(CH_3)_2$), 29.9 29.2 (N-C(*C*H_3)$_2$), 24.2 23.4 (O-C(*C*H_3)$_3$), -5.7 ($AlMe_3$).

5.3.15 Attempted NMR scale synthesis of C2-22XM ($L^{M}CeClN''_2$)

To a dark purple slurry of **VIII** (33.0 mg, 0.05 mmol) in C_6D_6 (0.5 ml) in a Youngs tap NMR tube was added a solution of **3-M** (13.1 mg, 0.05 mmol) in C_6D_6 (0.5 ml). The tube was shaken and a dark orange solution formed within ten minutes. The ^{1}H NMR spectrum revealed a small amount of $L^{M}CeN''_2$, **27**, to be present. Product resonances could not be assigned from the diamagnetic part of the spectrum.

5.3.16 Synthesis of 27 ($L^{M}CeN''_2$)

To a solution of CeN''_3 (200.0 mg, 0.32 mmol) in toluene (10 ml) was added a solution of **3-M** (83.8 mg, 0.32 mmol) in toluene (5 ml) and was stirred at room temperature for 12 h. Filtration and removal of the volatiles under reduced pressure afforded crude **27** as a yellow solid. The product was purified *via* sublimation and removal of the impurities (85 °C, 10^{-5} mbar) to leave pure **27** as an orange solid (87 mg, 44.3 %).

Found: C 38.22, H 6.23, N 5.07. Calc. for $C_{28}H_{59}CeN_4OSi_4$: C 46.68, H 8.27, N 7.78 %. ^{1}H NMR (C_6D_6); δ 14.04 -6.54 (bs, 6H each, Ar-*o*-CH_3 and C(CH_3)$_2$), 11.36 2.12 (bs, 2H each, N-CH_2-CH_2-N), 2.20 (s, 2H, N-CH_2-C), 0.75 (s, 3H, Ar-*p*-CH_3), 0.30 (bs, 2H, Ar-C*H*), -5.12 (bs, 36H, N(Si{CH_3}$_3$)$_2$).

5.3.17 Synthesis of 28 (L^{M}_2CeN'')

To a solution of CeN''_3 (0.50 g, 0.80 mmol) in toluene (10 ml) was added a solution of **3-M** (0.42 g, 1.61 mmol) in toluene (5 ml), from which crystalline yellow blocks were deposited within ten minutes. After sitting for 12 h, the product was isolated by filtration, hexane washing (2 x 5 ml) and drying under reduced pressure (0.34 g). A second crop of crystals were isolated from the toluene-hexane filtrate after one week at room temperature (0.10 g), affording **28** as a crystalline yellow solid (0.44 g, 67.1 %).

Single crystals suitable for an X-ray diffraction study grew from the toluene reaction mixture at room temperature within ten minutes.

Found: C 55.60, H 7.80, N 8.63. Calc. for $C_{38}H_{64}CeN_5O_2Si_2$: C 55.70, H 7.89, N 8.55 %. ^{1}H NMR (C_6D_6); δ 22.4 15.8 9.6 5.5 -9.9 (very broad), 6.45 (bs, 6H, Ar-*p*-CH_3), 0.81 (s, 12H, Ar-*o*-CH_3 or C(CH_3)$_2$), -0.97 (bs, 18H, N(Si{CH_3}$_3$)$_2$).

5.3.18 NMR scale synthesis of 29 ($[L^{M}CeN''_2]_2(\mu$-$OC_6H_4O)$)

To an orange solution of **27** (20 mg, 0.028 mmol) in C_6D_6 (0.50 ml) in a Youngs tap NMR tube was added a solution of benzoquinone (1.5 mg, 0.014) in C_6D_6 (0.25 ml). The reaction was shaken and a dark purple-black solution formed immediately.

^{1}H NMR (C_6D_6); δ 6.84 (s, 2H, Ar-C*H*), 5.96 (s, 2H, $OCC_3H_2C_2H_2CO$), 3.04 (bs, 2H, N-CH_2-C), 2.92 2.77 (bm, 2H each, N-CH_2-CH_2-N), 2.27 (s, 3H, Ar-*p*-CH_3), 2.26 (s, 6H, Ar-*o*-CH_3), 1.19 (s, 6H, C(CH_3)$_2$), 0.61 (s, 36H, N(Si{CH_3}$_3$)$_2$). ^{13}C; 238.3 ($C_{carbene}$), 167.4 (quaternary O*C*C$_4$H$_4$*C*O), 140.0 137.9 135.7 (quaternary Ar-*C*), 130.8 (Ar-*C*H), 118.2 (OC*C*$_4$H$_4$CO), 85.5 (*C*-(CH$_3$)$_2$), 67.7 53.7 52.5 (N-*C*H$_2$), 28.7 (C-(*C*H$_3$)$_2$), 22.2 19.4 (Ar-*C*H$_3$), 6.3 (N(Si{*C*H$_3$}$_3$)$_2$).

5.3.19 Synthesis of 30 ([L^M$_2$CeN"]$_2$(μ-OC$_6$H$_4$O))

To a solution of **28** (150 mg, 0.18 mmol) in toluene (20 ml) was added benzoquinone (9.9 mg, 0.09 mmol) in one portion, from which a dark purple solution and precipitate formed immediately. After sitting for 12 h, the product was isolated from the colourless solution by filtration, hexane washing (2 x 5 ml) and drying under reduced pressure, affording purple **30** in quantitative yield.

Found: C 56.29, H 7.54, N 7.97. Calc. for $C_{82}H_{132}Ce_2N_{10}O_6Si_4$: C 56.38, H 7.63, N 8.02 %. ^{1}H NMR (C_6D_5N); δ 6.84 (s, 4H, Ar-C*H*), 5.78 (s, 2H, $OCC_3H_2C_2H_2CO$), 3.56 3.38 3.04 2.77 (bm, 2H each, N-CH_2-CH_2-N), 3.12 (bm, 4H, N-CH_2-C), 2.35 (bs, 12H, Ar-*o*-CH_3), 2.19 (bs, 6H, Ar-*p*-CH_3), 1.38 1.18 (bs, 6H each, C(CH_3)$_2$), 0.15 (bs, 18H, N(Si{CH_3}$_3$)$_2$).

5.3.20 NMR scale synthesis of 31 ({L^M-Me$_3$Si}CeN"$_2$I)

To a yellow-orange solution of **27** (40 mg, 0.064 mmol) in C_6D_6 (0.50 ml) in a Youngs tap NMR tube was added Me_3SiI (9.1 µl, 0.064 mmol) in C_6D_6 (0.25 ml). The reaction was shaken briefly and a very pale yellow solution formed over 2 h upon standing.

^{1}H NMR (C_6D_6); δ 16.40 (bs, 4H, N-CH_2-CH_2-N), 8.94 (bs, 2H, N-CH_2-C), 6.09 (bs, 2H, Ar-C*H*), 1.73 (bs, 3H, Ar-*p*-CH_3), 1.06 (bs, 6H, C(CH_3)$_2$), 0.62 (bs, 9H, Si(CH_3)$_3$), -1.10 (bm, 6H, Ar-*o*-CH_3), -3.59 (bs, 36H, N(Si{CH_3}$_3$)$_2$).

5.3.21 NMR scale reaction of 28 with Me_3SiN_3.

To a yellow solution of **28** (20 mg, 0.024 mmol) in C_6D_6 (0.50 ml) in a Youngs tap NMR tube was added Me_3SiN_3 (3.2 μl, 0.024 mmol) in C_6D_6 (0.25 ml). The reaction was shaken and a very pale yellow solution formed over 2 h.

^{1}H NMR (C_6D_6); δ 6.82 (s, 2H, Ar-C*H*), 3.61 (s, 2H, N-CH_2-C), 3.57 3.30 (m, 2H each, N-CH_2-CH_2-N), 2.29 (s, 6H, Ar-*o*-CH_3), 2.15 (s, 3H, Ar-*p*-CH_3), 1.24 (s, 6H, C(CH_3)$_2$), 0.15 (bs, 36H, 9H, seemingly overlapping N(Si{CH_3}$_3$)$_2$ and $SiMe_3$). ^{13}C; 244.2 ($C_{carbene}$), 140.6 137.0 136.7 (quaternary Ar-*C*), 130.0 (Ar-*C*H), 76.7 (*C*-(CH$_3$)$_2$), 63.4 52.1 51.6 (N-*C*H$_2$), 28.8 (C-(*C*H$_3$)$_2$), 21.7 19.0 (Ar-*C*H$_3$), 3.4 (N(Si{*C*H$_3$}$_3$)$_2$).

5.4 Experimental details for Chapter 4

5.4.1 NMR scale synthesis of 32-P ($L^PYN''_2$)

In a Youngs tap NMR tube, C_6D_6 (0.75 ml) solutions of YN''_3 (46.4 mg, 0.08 mmol) and **3-P** (15.0 mg, 0.08 mmol) were combined and mixed well. The solution turned pale yellow and was heated to 85 ºC for 24 h.

^{1}H NMR (C_6D_6); δ 4.37 (sept, 1H, $^3J_{HH}$ = 7.0 Hz, N-C*H*-(CH_3)$_2$), 2.97 (s, 2H, N-C*H*$_2$-C), 2.74 2.53 (m, 2H, N-C*H*$_2$-C*H*$_2$-N), 1.14 (s, 6H, C(C*H*$_3$)$_2$), 0.96 (d, 6H, $^3J_{HH}$ = 7.0 Hz, N-CH-(C*H*$_3$)$_2$), 0.40 (s, 36H, N(Si{C*H*$_3$}$_3$)$_2$). ^{13}C; 212.3 (d, $^1J_{YC}$ = 46.0 Hz, $C_{carbene}$), 75.1 (*C*-(CH_3)$_2$), 63.3 53.2 42.0 (N-*C*H$_2$), 51.5 (N-*C*H-(CH_3)$_2$), 29.7 (C-(*C*H$_3$)$_2$), 21.5 (CH-(*C*H$_3$)$_2$), 5.9 (N(Si{*C*H$_3$}$_3$)$_2$).

5.4.2 NMR scale synthesis of 32-M ($L^MYN''_2$)

In a Youngs tap NMR tube, C_6D_6 (0.75 ml) solutions of YN''_3 (43.8 mg, 0.08 mmol) and **3-M** (20.0 mg, 0.08 mmol) were combined and mixed well. The solution turned pale yellow after 5-10 minutes.

^{1}H NMR (C_6D_6); δ 6.75 (s, 2H, Ar-C*H*), 3.10 (s, 2H, N-C*H*$_2$-C), 2.85 (bs, 4H, N-C*H*$_2$-C*H*$_2$-N), 2.17 (s, 6H, Ar-ortho-C*H*$_3$), 2.14 (s, 3H, Ar-para-C*H*$_3$), 1.22 (s, 6H, C(C*H*$_3$)$_2$), 0.33 (s, 36H, N(Si{C*H*$_3$}$_3$)$_2$). ^{13}C; 215.5 (d, $^1J_{YC}$ = 44.0 Hz, $C_{carbene}$), 139.0 136.6 128.3 (quaternary Ar-*C*), 130.7 (Ar-*C*H), 74.3 (*C*-(CH_3)$_2$), 63.3 53.8 50.5 (N-*C*H$_2$), 29.3 (C-(*C*H$_3$)$_2$), 21.4 19.1 (Ar-*C*H$_3$), 5.7 (N(Si{*C*H$_3$}$_3$)$_2$).

5.4.3 NMR scale synthesis of 33 (L^P_2YN'')

In a Youngs tap NMR tube, C_6D_6 (0.75 ml) solutions of YN''_3 (46.4 mg, 0.08 mmol) and **3-P** (30.0 mg, 0.16 mmol) were combined and mixed well. The solution turned pale yellow and was heated to 85 ºC for 12 h.

^{1}H NMR (C_6D_6); δ 5.05 (sept, 1H, $^3J_{HH}$ = 6.7 Hz, N-C*H*-(CH_3)$_2$), 3.12 (bs, 2H, N-C*H*$_2$-C), 2.83 2.65 (m, 2H each, N-C*H*$_2$-C*H*$_2$-N), 1.25 (s, 6H, C(C*H*$_3$)$_2$), 1.16 (d, 6H, $^3J_{HH}$ = 6.7 Hz, N-CH-(C*H*$_3$)$_2$), 0.51 (s, 9H, N(Si{C*H*$_3$}$_3$)$_2$). ^{13}C; 216.5 (d, $^1J_{YC}$ = 35.8 Hz,

$C_{carbene}$), 73.4 (C-$(CH_3)_2$), 63.5 53.4 41.6 (N-CH$_2$), 50.3 (N-CH-$(CH_3)_2$), 31.0 (C-(CH$_3$)$_2$), 21.8 (CH-(CH$_3$)$_2$), 7.0 (N(Si{CH$_3$}$_3$)$_2$).

5.4.4 NMR scale synthesis of 34 (YL^P_3)

In a Youngs tap NMR tube, C_6D_6 (0.75 ml) solutions of YN"$_3$ (25.8 mg, 0.05 mmol) and **3-P** (25.0 mg, 0.14 mmol) were combined and mixed well. The solution turned pale yellow and was heated to 85 ºC for 12 h.

^{1}H NMR (C_6D_6); δ 5.56 (sept, 1H, $^3J_{HH}$ = 6.7 Hz, N-CH-$(CH_3)_2$), 3.33 (s, 2H, N-CH_2-C), 3.04 2.79 (m, 2H each, N-CH_2-CH_2-N), 1.35 (s, 6H, C(CH_3)$_2$), 1.08 (d, 6H, $^3J_{HH}$ = 6.7 Hz, N-CH-(CH_3)$_2$). ^{13}C; 220.2 (d, $^1J_{YC}$ = 29.1 Hz, $C_{carbene}$), 72.5 (C-$(CH_3)_2$), 63.7 53.2 41.6 (N-CH$_2$), 49.0 (N-CH-$(CH_3)_2$), 31.7 (C-(CH$_3$)$_2$), 21.7 (CH-(CH$_3$)$_2$).

5.4.5 NMR scale synthesis of 35 ({L^P-$SiMe_3$}$_2$$YI_2$N")

In a Youngs tap NMR tube, C_6D_6 (0.75 ml) solutions of YN"$_3$ (46.4 mg, 0.08 mmol) and **3-P** (30.0 mg, 0.16 mmol) were combined and mixed well. The solution turned pale yellow and was heated to 85 ºC for 12 h. Subsequently, Me_3SiI (11.6 µl, 0.08 mmol) was added and the NMR tube shaken well. After one hour, an orange oil settled from solution and, following removal of the volatiles under reduced pressure, the resulting solid was redissolved in pyridine, yielding a mixture of compounds.

^{1}H NMR (C_6D_5N); δ 4.27 (sept, 1H, $^3J_{HH}$ = 6.8 Hz, N-CH-$(CH_3)_2$), 4.23 3.94 (m, 2H each, N-CH_2-CH_2-N), 3.63 (bs, 2H, N-CH_2-C), 1.26 (d, 6H, $^3J_{HH}$ = 6.8 Hz, N-CH-(CH_3)$_2$), 1.24 (s, 6H, C(CH_3)$_2$), 0.60 (s, 9H, N(Si{CH_3}$_3$)$_2$), 0.22 (s, 9H, Si(CH_3)$_3$). ^{13}C; 176.6 (s, CSi(CH$_3$)$_3$), 76.4 (C-$(CH_3)_2$), 62.5 54.9 46.1 (N-CH$_2$), 52.3 (N-CH-$(CH_3)_2$), 30.2 (C-(CH$_3$)$_2$), 22.5 (CH-(CH$_3$)$_2$), 8.6 (N(Si{CH$_3$}$_3$)$_2$), 4.8 (Si(CH$_3$)$_3$).

5.4.6 Synthesis of 36 ($L^MUN"_2$)

To a solution of UN"$_3$ (500 mg, 0.70 mmol) in hexane (10 ml) was added a solution of **3-M** (181 mg, 0.70 mg) in hexane (10 ml) in one portion at room temperature with stirring. The solution immediately turned dark blue, and after standing for 12 h, was

filtered from a small amount of brown residue. Removal of the volatiles and drying at 90 °C at 10^{-5} mbar afforded crude **36** as a dark blue glassy solid (510 mg, 89.7 %).

Found: C 40.97, H 7.36, N 6.78. Calc. for $C_{28}H_{59}N_4OSi_4U$: C 41.09, H 7.28, N 6.85 %. ^{1}H NMR (C_6D_6); δ 28.20 0.62 (bs, 6H each, Ar-*o*-C*H*$_3$, C(C*H*$_3$)$_2$), 26.24 0.67 -5.69 -19.38 (bs, 2H each, N-C*H*$_2$-C*H*$_2$-N, N-C*H*$_2$-C, Ar-C*H*), -9.80 (bs, 3H, Ar-*p*-C*H*$_3$), -10.55 (bs, 36H, N(Si{C*H*$_3$}$_3$)$_2$). IR (nujol) υ_{max}/ cm^{-1}: 1421(w), 1252(s), 1170(w), 999(s), 837(s), 768(m), 666(m), 598(m), 553(w). UV λ_{max}/ nm (ε/ M^{-1} cm^{-1}) toluene: 320 (2296), 379 (1091), 607 (574), 804 (344), 950 (205), 1313 (131).

5.4.7 Synthesis of 37 ({L^{M}SiMe$_3$}UIN''$_2$)

To a dark blue solution of **36** (520 mg, 0.64 mmol) in hexane (5 ml) was added a solution of Me_3SiI (127 mg, 0.64 mmol) in hexane (5 ml) at room temperature, which immediately formed a dark brown solution. A dark brown precipitate formed after standing for 12 h, which following isolation by filtration and washing with hexane (2 x 5 ml), was dried under reduced pressure to afford **37** as a brown solid (379 mg, 52 %). X-ray quality single crystals were grown from a benzene solution at room temperature, although the structure was not obtained. They were subsequently used to obtain characterising data.

Found: C 36.45, H 6.66, N 5.56. Calc. for $C_{31}H_{68}IN_4OSi_5U$: C 36.56, H 6.74, N 5.50 %. ^{1}H NMR (C_6D_6); δ 76.79 8.09 2.93 -10.17 (bs, 2H each, N-C*H*$_2$-C*H*$_2$-N, N-C*H*$_2$-C, Ar-C*H*), 42.59 6.40 (bs, 6H each, Ar-*o*-C*H*$_3$, C(C*H*$_3$)$_2$), 11.81 (bs, 3H, Ar-*p*-C*H*$_3$), 8.55 (bs, 9H, Si(C*H*$_3$)$_3$), -4.37 (bs, 36H, N(Si{C*H*$_3$}$_3$)$_2$). IR (nujol) υ_{max}/ cm^{-1}: 1608(w), 1529(m), 1277(s), 1246(s), 1192(m), 1167(m), 1132(m), 991(s), 960(s), 903(s), 843(s), 771(s), 663(m), 611(m), 536(w), 488(w). UV λ_{max}/ nm (ε/ M^{-1} cm^{-1}) toluene: 319 (2431), 352 (1695), 474 (513), 505 (484), 631 (252), 753 (82), 931 (48), 1051 (39).

5.4.8 Formation of 38 *via* a decomposition pathway; (UI$_2$L$^M_2$)

From a heated NMR tube containing **37** in benzene at 70 °C for 12 h, or hexane solutions of **37** stored at room temperature for up to four weeks, formed dark pink single crystals of **38** and a pale brown precipitate. The preparative scale hexane reaction had as

much mother liquor and brown precipitate decanted as possible, and **38** as the majority remaining pink crystalline material was washed with toluene, hexane and dried under reduced pressure. No yield was recorded. Complex **38** is insoluble in aromatic NMR solvents, and although did prove to be soluble in d_5-pyridine, reacted with the solvent to provide a yellow solution with a mass of unassignable paramagnetically shifted ligand resonances between δ = 100 and -32 ppm.

Found: C 37.98, H 4.71, N 5.46. Calc. for $C_{32}H_{46}I_2N_4O_2U$: C 38.03, H 4.60, N 5.54 %.

5.4.9 NMR-scale treatment of $L^MUN''_2$ with ^iPrI

To a dark blue solution of **36** (57 mg, 0.07 mmol) in d_6-benzene (0.75 ml) was added *iso*-propyl iodide (6.9 µl, 0.07 mmol) in an NMR tube at room temperature, with subsequent mixing. A dark brown solution formed immediately, from which a pale brown precipitate and large dark pink crystals slowly formed over four weeks. The ^{1}H NMR spectrum revealed that the starting **36** had been completely transformed into an unknown compound, which displayed resonances between δ = 70 and -30 ppm. A cell check of the pink crystalline material confirmed the eventual formation of **38**.

5.4.10 Synthesis of 39 ($L^MUN''_2.CO_2$)

A dark blue solution of **36** (540 mg, 0.66 mmol) in hexane (15 ml) was freeze-pump-thaw degassed three times before an atmosphere of CO_2 was introduced at room temperature with vigorous stirring. A pale brown solution and precipitate formed immediately, which after 0.5 h changed to a pale green solution and almost colourless precipitate. Following filtration, the solid was washed with hexane (2 x 5 ml) and dried under reduced pressure, affording **39** as a very pale green solid (401 mg, 70.3 %).

Found: C 40.29, H 6.79, N 6.41. Calc. for $C_{29}H_{59}N_4O_3Si_4U$: C 40.39, H 6.91, N 6.50 %. ^{1}H NMR (C_6D_5N); δ 52.92 43.52 26.17 15.59 (bs, 2H each, N-CH_2-CH_2-N, N-CH_2-C, Ar-C*H*), 22.35 10.11 (bs, 6H each, Ar-*o*-CH_3, C(CH_3)$_2$), 20.40 (bs, 3H, Ar-*p*-CH_3), the N" is not observed, although there is a very broad feature in the baseline between δ = 6 and -2 ppm. IR (nujol) υ_{max}/ cm^{-1}: 2278(w), 2185(m), 1687(m), 1646(m), 1583(m),

1288(m), 1244(m), 1172(w), 904(m), 836(m), 749(m), 722(m), 680(w). UV λ_{max}/ nm (ε/ M^{-1} cm^{-1}) THF: 601 (20), 809 (9), 999 (22), 1113 (26), 1505 (10) and 1654 (12).

5.4.11 Synthesis of 40-M ($UO_2L^M_2$)

A solution of **3-M** (30.0 mg, 0.12 mmol) in benzene (2 ml) was carefully layered onto a red solution of $UO_2N"_2(THF)_2$ (42.3 mg, 0.06 mmol) in benzene (2 ml) and allowed to diffuse slowly overnight at room temperature. The solution turned yellow and **40-M** formed as yellow needles which were washed with benzene (3 x 1 ml) and dried under reduced pressure (24.0 mg, 52 %).

Bi-refringent yellow/ green crystals suitable for an X-ray diffraction study were grown from a 5:1 pyridine/benzene mixture via slow cooling of a hot solution to room temperature overnight.

Found: C 48.74, H 6.55, N 6.52. Calc. for $C_{32}H_{46}N_4O_4U$: C 48.72, H 5.89, N 7.10 %. ^{1}H NMR (C_5D_5N); δ 6.82 (s, 2H, Ar-C*H*), 3.84 (bs, 2H, N-CH_2-C), 3.75 3.64 (bm, 2H each, N-CH_2-CH_2-N), 2.29 (bs, 6H, Ar-ortho-CH_3), 2.25 (s, 3H, Ar-para-CH_3), 1.45 (s, 6H, C(CH_3)$_2$). ^{13}C; 281.6 ($C_{carbene}$), 140.6 135.6 131.2 (quaternary Ar-*C*), 130.4 (Ar-*C*H), 83.7 (*C*-(CH_3)$_2$), 64.8 57.4 54.6 (N-*C*H_2), 33.1 (C-(*C*H_3)$_2$), 23.4 20.8 (Ar-*C*H_3). IR(nujol); $\nu_{(asymm)}$ cm^{-1}: 1260(m), 1169(w), 981(w), 958(w), 948(w), 852(m), 722(w).

5.4.12 NMR scale synthesis of 40-D ($UO_2L^D_2$)

A solution of **3-D** (32.9 mg, 0.10 mmol) in benzene (2 ml) was carefully layered onto a red solution of $UO_2N_2"(THF)_2$ (40.0 mg, 0.05 mmol) in benzene (2 ml) and allowed to slowly diffuse overnight at room temperature in the glovebox. The solution turned yellow and single crystals of **40-D** suitable for an X-ray diffraction study formed from the reaction mixture.

^{1}H NMR (C_5D_5N); δ 7.43 (t, $^3J_{HH}$ = 8.0 Hz, 1H, 4-Ar-C*H*), 7.27 (d, $^3J_{HH}$ = 8.0 Hz, 2H, 3,5-Ar-C*H*), 3.94 3.87 (m, 2H each, N-CH_2-CH_2-N), 3.87 (s, 2H, N-CH_2-C), 3.43 (sept, $^3J_{HH}$ = 7.0 Hz, 2H, Ar-C*H*(CH_3)$_2$), 1.31 (s, 6H, C(CH_3)$_2$), 1.28 1.17 (d, $^3J_{HH}$ = 7.0 Hz, 6H each, Ar-CH(CH_3)$_2$). ^{13}C; 283.6 ($C_{carbene}$), 150.0 139.2 (quaternary Ar-*C*), 130.8 (4-Ar-*C*H), 126.4 (3,5-Ar-*C*H), 83.6 (*C*-(CH_3)$_2$), 64.6 (N-*C*H_2-C)), 57.3 57.0 (N-*C*H_2-*C*H_2-N),

32.4 (C-(CH_3)$_2$), 30.4 (Ar-$CH(CH_3)_2$), 27.6 26.2 (Ar-CH(CH_3)$_2$). IR(nujol); $\nu_{(asymm)}$ cm^{-1}: 1257(m), 1176(w), 1056(w), 984(w), 957(w), 853(m), 804(w), 758(w), 675(w), 548(w).

5.5 X-ray Crystallography

Crystallographic X-ray data were collected using Mo-Kα radiation (λ = 0.71073 Å) on a Bruker Smart APEX CCD area detector diffractometer using ω, or ω and φ scans. Structure solution and refinement was carried out using the SIR program and the SHELXTL suite of programs and graphics generated using Ortep-3.

The ADPs for C(3) and C(4) (on the *iso*-propyl group) in **2-P** were restrained to account for an unmodelled disorder, which results in close contacts between the hydrogen atoms placed upon these carbons. This is independent of the method used to place them (geometrically or by electron density). The hydroxyl hydrogen in **2-P** was found in the electron difference map and restrained to lie approximately on the O(1)-I(1) axis.

Compound **AA** contains 0.6 molecules of water in the lattice.

Compound **40-M** crystallised as a racemic mixture of the two enantiomers, with half of the molecule, and one molecule of benzene, present in the asymmetric unit. There is a superpositional disorder of the two enantiomers, which appear superimposed in the asymmetric unit; no higher symmetry or cell-doubling was found. The superpositional disorder has been modelled with a *trans*-L^{D}_{2} geometry. Several anisotropic displacement parameter restraints, both spatial and rigid-rotor, were required to account for the superpositional disorder and also a disorder in the mesityl groups and co-crystallised benzene. There are several close crystallographic contacts between some hydrogen atoms as a result, and several carbon atoms still retain higher than desired thermal displacement parameters.

Complex **40-D** contains two molecules of benzene in the unit cell, disordered about a special position. This disorder was not modelled, however, resulting in short C-C bonds across the special position.

Computer programs: *SMART (Siemens, 1993*; *SMART* (Siemens, 1993); *SMART* (Siemens, 1993); *SAINT* (Siemens, 1995); *SAINT* (Siemens, 1995); *SIR-92* (Giacovazzo, 1994); *SHELXL-97* (Sheldrick, 1997); *ORTEP* (Farrugia, 1997); *enCIFer* (Allen et al., 2004).

Experimental Tables

Chapter 2

	2-P	3-M
Crystal data		
Chemical formula	$C_{10}H_{21}IN_2O$	$C_{16}H_{24}N_2O$
M_r	312.19	260.38
Cell setting, space group	Orthorhombic, $Pna2_1$	Monoclinic, $P2_1/n$
Temperature (K)	150 (2)	150 (2)
a, b, c (Å)	9.916 (3), 11.780 (3), 11.387 (3)	8.5230 (2), 17.2780 (5), 10.0850 (3)
α, β, γ (Å)		91.125 (2)
V (Å^3)	1330.1 (6)	1484.83 (7)
Z	4	4
D_x (Mg m^{-3})	1.559	1.165
Radiation type	Mo $K\alpha$	Mo $K\alpha$
μ (mm^{-1})	2.38	0.07
Crystal form, colour	Cube, colourless	Block, colourless
Crystal size (mm)	0.61 × 0.54 × 0.50	0.3 × 0.27 × 0.16
Data collection		
Diffractometer	Brucker SMART APEX CCD area detector	Brucker SMART APEX CCD area detector
Data collection method	ω scans	ω scans
Absorption correction	Multi-scan (based on symmetry-related measurements)	Multi-scan (based on symmetry-related measurements)
T_{min}	0.584	0.832
T_{max}	1.000	0.992
No. of measured, independent and observed reflections	15127, 3263, 3223	18663, 3951, 3387
Criterion for observed reflections	$I > 2\sigma(I)$	$I > 2\sigma(I)$
R_{int}	0.037	0.041
θ_{max} (°)	34.0	29.7
Refinement		

Refinement on	F^2	F^2
$R[F^2 > 2\sigma(F^2)]$, $wR(F^2)$, S	0.031, 0.078, 1.12	0.068, 0.159, 1.12
No. of relections	3263 reflections	3951 reflections
No. of parameters	132	177
H-atom treatment	Riding	Riding
Weighting scheme	Calculated $w = 1/[\sigma^2(F_o^2) + (0.0351P)^2 + 1.682P]$ where $P = (F_o^2 + 2F_c^2)/3$	Calculated $w = 1/[\sigma^2(F_o^2) + (0.0485P)^2 + 1.1529P]$ where $P = (F_o^2 + 2F_c^2)/3$
$(\Delta/\sigma)_{max}$	0.001	<0.0001
$\Delta\rho_{max}$, $\Delta\rho_{min}$ (e Å^{-3})	0.99, –1.40	0.30, –0.25
Absolute structure	Flack H D (1983), Acta Cryst. A39, 876-881	
Flack parameter	0.03 (3)	

	4	**6-P**
Crystal data		
Chemical formula	$C_{16}H_{38}KN_3OSi_2$	$C_{13}H_{29}N_2OSi.I$
M_r	383.77	384.37
Cell setting, space group	Triclinic, *P*-1	Monoclinic, *P*2(1)/*c*
Temperature (K)	150 (2)	150 (2)
a, *b*, *c* (Å)	9.9490 (4), 10.9970 (5), 12.2370 (5)	13.0263 (5), 12.5089 (5), 11.8971 (5)
α, β, γ (Å)	95.194 (2), 111.793 (2), 108.661 (2)	103.656 (2)
V (Å^3)	1143.97 (8)	1883.77 (13)
Z	2	4
D_x (Mg m^{-3})	1.114	1.355
Radiation type	Mo *K*α	Mo *K*α
μ (mm^{-1})	0.34	1.76
Crystal form, colour	Block, colourless	Block, colourless
Crystal size (mm)	0.65 × 0.45 × 0.30	0.45 × 0.43 × 0.16
Data collection		
Diffractometer	Brucker SMART APEX CCD area detector	Bruker SMART APEX CCD area detector
Data collection method	ω–scans	ω scans
Absorption correction	Multi-scan (based on symmetry-	Multi-scan (based on symmetry-

	related measurements)	related measurements)
T_{min}	0.584	0.465
T_{max}	0.746	0.75
No. of measured, independent and observed reflections	13380, 5406, 4732	5197, 5197, 5053
Criterion for observed reflections	$I > 2\sigma(I)$	$I > 2\sigma(I)$
R_{int}	0.042	0.000
θ_{max} (°)	29.0	28.6
Refinement		
Refinement on	F^2	F^2
$R[F^2 > 2\sigma(F^2)]$, $wR(F^2)$, S	0.108, 0.240, 1.29	0.042, 0.111, 1.28
No. of relections	5406 reflections	5197 reflections
No. of parameters	209	182
H-atom treatment	Riding	Riding
Weighting scheme	Calculated $w = 1/[\sigma^2(F_o^2) + (0.0529P)^2 + 4.806P]$ where $P = (F_o^2 + 2F_c^2)/3$	Calculated $w = 1/[\sigma^2(F_o^2) + (0.0421P)^2 + 3.2124P]$ where $P = (F_o^2 + 2F_c^2)/3$
$(\Delta/\sigma)_{max}$	2.836	0.001
$\Delta\rho_{max}$, $\Delta\rho_{min}$ (e Å^{-3})	1.11, –0.63	0.87, –0.54

	7-P	**8-P**
Crystal data		
Chemical formula	$C_{32}H_{74}Mg_2N_6O_2Si_4.C_6H_6$	$C_{32}H_{74}N_6O_2Si_4Zn_2.C_6H_6$
M_r	814.06	896.18
Cell setting, space group	Triclinic, *P*-1	Triclinic, *P*-1
Temperature (K)	93 (2)	150 (2)
a, *b*, *c* (Å)	10.0920 (18), 11.541 (2), 11.960 (3)	10.0409 (2), 11.4568 (3), 11.9216 (3)
α, β, γ (Å)	111.934 (3), 103.197 (3), 96.862 (3)	112.0690 (10), 102.6990 (10), 96.5540 (10)
V (Å^3)	1225.3 (4)	1210.14 (5)
Z	1	1
D_x (Mg m^{-3})	1.103	1.230
Radiation type	Mo $K\alpha$	Mo $K\alpha$
μ (mm^{-1})	0.18	1.13

Crystal form, colour	Prism, colourless	Shard, colourless
Crystal size (mm)	0.1 × 0.1 × 0.1	0.45 × 0.32 × 0.18
Data collection		
Diffractometer	Brucker SMART APEX CCD area detector	Brucker SMART APEX CCD area detector
Data collection method	dtprofit.ref	ω scans
Absorption correction	Multi-scan	Multi-scan (based on symmetry-related measurements)
T_{min}	0.893	0.716
T_{max}	0.98	0.82
No. of measured, independent and observed reflections	7882, 4343, 3675	19801, 6759, 6435
Criterion for observed reflections	$I > 2\sigma(I)$	$I > 2\sigma(I)$
R_{int}	0.032	0.025
θ_{max} (°)	25.4	30.6
Refinement		
Refinement on	F^2	F^2
$R[F^2 > 2\sigma(F^2)]$, $wR(F^2)$, S	0.043, 0.108, 1.07	0.028, 0.074, 1.10
No. of relections	4343 reflections	6759 reflections
No. of parameters	245	245
H-atom treatment	Riding	Riding
Weighting scheme	Calculated $w = 1/[\sigma^2(F_o^2) + (0.0507P)^2 + 0.0423P]$ where $P = (F_o^2 + 2F_c^2)/3$	Calculated $w = 1/[\sigma^2(F_o^2) + (0.0324P)^2 + 0.4032P]$ where $P = (F_o^2 + 2F_c^2)/3$
$(\Delta/\sigma)_{max}$	0.001	0.002
$\Delta\rho_{max}$, $\Delta\rho_{min}$ (e Å^{-3})	0.25, –0.32	0.40, –0.29

	9	**10-M**
Crystal data		
Chemical formula	$C_{32}H_{70}Mg_2N_6O_2Si_4$	$C_{32}H_{46}N_4O_2Zn$
M_r	731.92	584.10
Cell setting, space group	Monoclinic, $P2_1/n$	Monoclinic, $C2/c$
Temperature (K)	93 (2)	93 (2)
a, b, c (Å)	10.537 (2), 11.495 (2), 18.056 (4)	45.089 (4), 11.2093 (9), 12.7221 (11)
α, β, γ (Å)	96.067 (6)	104.578 (2)

V (Å^3)	2174.7 (8)	6222.9 (9)
Z	2	8
D_x (Mg m^{-3})	1.118	1.247
Radiation type	Mo $K\alpha$	Mo $K\alpha$
μ (mm^{-1})	0.20	0.82
Crystal form, colour	Prism, colorless	Block, colourless
Crystal size (mm)	0.20 × 0.15 × 0.05	0.19 × 0.13 × 0.06
Data collection		
Diffractometer	Mercury (2x2 bin mode) CCD area detector	Brucker SMART APEX CCD area detector
Data collection method	dtprofit.ref	ω–scans
Absorption correction	Multi-scan (based on symmetry-related measurements)	Multi-scan (based on symmetry-related measurements)
T_{min}	0.833	?
T_{max}	1.000	?
No. of measured, independent and observed reflections	13350, 3951, 3390	19344, 4017, 2934
Criterion for observed reflections	$I > 2\sigma(I)$	$I > 2\sigma(I)$
R_{int}	0.040	0.134
θ_{max} (°)	25.3	25.4
Refinement		
Refinement on	F^2	F^2
$R[F^2 > 2\sigma(F^2)]$, $wR(F^2)$, S	0.041, 0.103, 1.05	0.071, 0.188, 0.86
No. of relections	3951 reflections	4017 reflections
No. of parameters	218	352
H-atom treatment	Riding	Mixture of independent and constrained refinement
Weighting scheme	Calculated $w = 1/[\sigma^2(F_o^2) + (0.0499P)^2 + 0.537P]$ where $P = (F_o^2 + 2F_c^2)/3$	Calculated $w = 1/[\sigma^2(F_o^2) + (0.1063P)^2 + 78.112P]$ where $P = (F_o^2 + 2F_c^2)/3$
$(\Delta/\sigma)_{max}$	0.001	0.042
$\Delta\rho_{max}$, $\Delta\rho_{min}$ (e Å^{-3})	0.25, –0.29	0.56, –0.45

Chapter 3

	16	**17**
Crystal data		
Chemical formula	$C_{44}H_{96}Ce_3O_{11}$	$C_{41}H_{90}Ce_3F_3K_3O_{14}S.C_6H_6$
M_r	1221.57	1511.96
Cell setting, space group	Orthorhombic, $Cmc2_1$	Monoclinic, $P2(1)/n$
Temperature (K)	125 (2)	150 (2)
a, b, c (Å)	17.807, 32.196, 10.902	13.9022 (7), 20.4589 (11), 22.8617 (12)
α, β, γ (Å)		90.2740 (10)
V (Å^3)	6250.3	6502.3 (6)
Z	4	4
D_x (Mg m^{-3})	1.298	1.544
Radiation type	Mo $K\alpha$	Mo $K\alpha$
μ (mm^{-1})	2.19	2.35
Crystal form, colour	Block, green	Plate, colourless
Crystal size (mm)	0.20 × 0.20 × 0.20	0.42 × 0.17 × 0.01
Data collection		
Diffractometer	Brucker SMART APEX CCD area detector	Brucker SMART APEX CCD area detector
Data collection method	ω scans	ω scans
Absorption correction	Multi-scan (based on symmetry-related measurements)	Multi-scan (based on symmetry-related measurements)
T_{min}	0.668	0.439
T_{max}	0.668	0.977
No. of measured, independent and observed reflections	4885, 4885, 4703	75624, 14942, 10281
Criterion for observed reflections	$I > 2\sigma(I)$	$I > 2\sigma(I)$
R_{int}	0.000	0.090
θ_{max} (°)	25.0	27.5
Refinement		
Refinement on	F^2	F^2
$R[F^2 > 2\sigma(F^2)]$, $wR(F^2)$, S	0.041, 0.103, 1.05	0.037, 0.092, 0.92
No. of relections	3951 reflections	14942 reflections

No. of parameters	218	711
H-atom treatment	Riding	Riding
Weighting scheme	Calculated $w = 1/[\sigma^2(F_o^2) + (0.0499P)^2 + 0.537P]$ where $P = (F_o^2 + 2F_c^2)/3$	Calculated $w = 1/[\sigma^2(F_o^2) + (0.0406P)^2]$ where $P = (F_o^2 + 2F_c^2)/3$
$(\Delta/\sigma)_{max}$	0.001	0.002
$\Delta\rho_{max}$, $\Delta\rho_{min}$ (e Å^{-3})	0.25, –0.29	1.53, –0.93
Absolute structure	Flack H D (1983), Acta Cryst. A39, 876-881	
Flack parameter	0.18 (6)	

	18	**21**
Crystal data		
Chemical formula	$C_{22}H_{44}CeN_2O_4$	$C_{52}H_{92}CeN_8O_7$
M_r	540.71	1081.46
Cell setting, space group	Monoclinic, *P*2(1)	Monoclinic, $P2_1/n$
Temperature (K)	293 (2)	150 (2)
a, *b*, *c* (Å)	15.014 (2), 17.587 (2), 15.158 (2)	23.188 (3), 11.1458 (14), 24.392 (3)
α, β, γ (Å)	118.502 (2)	99.709 (2)
V (Å^3)	3517.3 (8)	6213.8 (14)
Z	8	4
D_x (Mg m^{-3})	2.042	1.156
Radiation type	Mo *K*α	Mo *K*α
μ (mm^{-1})	2.63	0.78
Crystal form, colour	Block, colourless	Tablet, colourless
Crystal size (mm)	0.26 × 0.11 × 0.05	0.26 × 0.17 × 0.05
Data collection		
Diffractometer	Brucker SMART APEX CCD area detector	Bruker SMART APEX CCD area detector
Data collection method	ω–scans	ω
Absorption correction	Multi-scan (based on symmetry-related measurements)	Multi-scan (based on symmetry-related measurements)
T_{min}	?	0.333
T_{max}	?	1.000
No. of measured, independent and observed reflections	13073, 9429, 6648	38792, 10920, 6660

Criterion for observed reflections	$I > 2\sigma(I)$	$I > 2\sigma(I)$
R_{int}	0.061	0.11
θ_{max} (°)	25.0	25.0
Refinement		
Refinement on	F^2	F^2
$R[F^2 > 2\sigma(F^2)]$, $wR(F^2)$, S	0.113, 0.322, 1.08	0.067, 0.182, 0.96
No. of relections	9429 reflections	10920 reflections
No. of parameters	252	640
H-atom treatment	Mixture of independent and constrained refinement	Constrained to parent site
Weighting scheme	Calculated $w = 1/[\sigma^2(F_o^2) + (0.1927P)^2 + 3.3158P]$ where $P = (F_o^2 + 2F_c^2)/3$	Calculated $w = 1/[\sigma^2(F_o^2) + (0.1019P)^2]$ where $P = (F_o^2 + 2F_c^2)/3$
$(\Delta/\sigma)_{max}$	0.054	0.001
$\Delta\rho_{max}$, $\Delta\rho_{min}$ (e Å^{-3})	2.36, –1.50	1.18, –1.64
Absolute structure	Flack H D (1983), Acta Cryst. A39, 876-881	
Flack parameter	0.44 (9)	

	22	**24**
Crystal data		
Chemical formula	$C_{61}H_{91}CeIN_8O_4$	$C_{74}H_{116}B_2CeN_8O_4$
M_r	1267.44	1343.49
Cell setting, space group	Triclinic, *P*-1	Triclinic, *P*-1
Temperature (K)	150 (2)	150 (2)
a, *b*, *c* (Å)	11.371 (2), 16.609 (3), 19.615 (3)	13.6344 (5), 15.6439 (6), 19.9007 (7)
α, β, γ (Å)	70.250 (3), 74.282 (3), 74.021 (3)	78.468 (2), 74.110 (2), 66.660 (2)
V (Å^3)	3286.5 (10)	3728.3 (2)
Z	2	2
D_x (Mg m^{-3})	1.281	1.197
Radiation type	Mo $K\alpha$	Mo $K\alpha$
μ (mm^{-1})	1.21	0.66
Crystal form, colour	Block, pale yellow	Block, yellow
Crystal size (mm)	0.33 × 0.24 × 0.15	0.64 × 0.50 × 0.35

Data collection		
Diffractometer	Bruker SMART APEX CCD diffractometer	Bruker SMART APEX CCD diffractometer
Data collection method	ω	ω
Absorption correction	Multi-scan (based on symmetry-related measurements)	Multi-scan (based on symmetry-related measurements)
T_{min}	0.701	0.661
T_{max}	0.834	0.793
No. of measured, independent and observed reflections	29604, 14551, 11968	34250, 16851, 15594
Criterion for observed reflections	$I > 2\sigma(I)$	$I > 2\sigma(I)$
R_{int}	0.019	0.013
θ_{max} (°)	27.5	27.5
Refinement		
Refinement on	F^2	F^2
$R[F^2 > 2\sigma(F^2)]$, $wR(F^2)$, S	0.030, 0.075, 1.02	0.032, 0.086, 1.06
No. of relections	14551 reflections	16848 reflections
No. of parameters	676	826
H-atom treatment	Constrained to parent site	Constrained, HB Refined independently
Weighting scheme	Calculated $w = 1/[\sigma^2(F_o^2) + (0.0308P)^2 + 3.3194P]$ where $P = (F_o^2 + 2F_c^2)/3$	Calculated $w = 1/[\sigma^2(F_o^2) + (0.0503P)^2 + 0.7231P]$ where $P = (F_o^2 + 2F_c^2)/3$
$(\Delta/\sigma)_{max}$	0.002	0.012
$\Delta\rho_{max}$, $\Delta\rho_{min}$ (e Å^{-3})	0.83, –0.70	1.46, –0.98
Absolute structure		
Flack parameter		

	25	**28**
Crystal data		
Chemical formula	$C_{18}H_{31}BN_2O$	$C_{38}H_{64}CeN_5O_2Si_2$
M_r	302.26	819.24
Cell setting, space group	Orthorhombic, $P2_12_12_1$	Triclinic, P-1
Temperature (K)	150 (2)	150 (2)
a, b, c (Å)	10.181 (3), 10.724 (3), 15.819 (4)	11.1139 (4), 18.0530 (6), 11.5188 (4)

α, β, γ (Å)		89.924 (2), 112.910 (2), 89.187 (2)
V (Å^3)	1727.1 (8)	2128.54 (13)
Z	4	2
D_x (Mg m^{-3})	1.162	1.278
Radiation type	Mo $K\alpha$	Mo $K\alpha$
μ (mm^{-1})	0.07	1.16
Crystal form, colour	Trapezoid tablet, colourless	Block, yellow
Crystal size (mm)	0.32 × 0.21 × 0.09	0.4 × 0.2 × 0.17
Data collection		
Diffractometer	Bruker SMART1000 CCD area detector	Brucker SMART APEX CCD area detector
Data collection method	ω	ω scans
Absorption correction	Multi-scan (based on symmetry-related measurements)	Multi-scan (based on symmetry-related measurements)
T_{min}	0.982	0.627
T_{max}	0.994	0.820
No. of measured, independent and observed reflections	15459, 3973, 2783	17055, 17055, 15887
Criterion for observed reflections	$I > 2\sigma(I)$	$I > 2\sigma(I)$
R_{int}	0.041	0.000
θ_{max} (°)	27.6	28.4
Refinement		
Refinement on	F^2	F^2
$R[F^2 > 2\sigma(F^2)]$, $wR(F^2)$, S	0.040, 0.090, 0.95	0.056, 0.132, 1.15
No. of relections	3973 reflections	17055 reflections
No. of parameters	203	449
H-atom treatment	Riding	Riding
Weighting scheme	Calculated $w = 1/[\sigma^2(F_o^2) + (0.0442P)^2]$ where $P = (F_o^2 + 2F_c^2)/3$	Calculated $w = 1/[\sigma^2(F_o^2) + (0.0352P)^2 + 5.4025P]$ where $P = (F_o^2 + 2F_c^2)/3$
$(\Delta/\sigma)_{max}$	<0.0001	0.001
$\Delta\rho_{max}$, $\Delta\rho_{min}$ (e Å^{-3})	0.32, –0.22	1.51, –1.83
Absolute structure	Flack H D (1983), Acta Cryst. A39, 876-881	
Flack parameter	2.1 (13)	

Chapter 4

	38	**40-M**
Crystal data		
Chemical formula	$C_{32}H_{46}I_2N_4O_2U$	$C_{44}H_{58}N_4O_4U$
M_r	1010.56	944.97
Cell setting, space group	Monoclinic, $P2_1/n$	Triclinic, P-1
Temperature (K)	150 (2)	150 (2)
a, b, c (Å)	12.1805 (4), 12.0395 (4), 12.3962 (4)	7.7547 (2), 12.0229 (3), 12.3593 (3)
α, β, γ (Å)	101.881 (2)	68.6800 (10), 75.4660 (10), 83.0090 (10)
V (Å^3)	1778.92 (10)	1038.50 (4)
Z	2	1
D_x (Mg m^{-3})	1.887	1.511
Radiation type	Mo $K\alpha$	Mo $K\alpha$
μ (mm^{-1})	6.33	3.95
Crystal form, colour	Prism, dark pink	Block, yellow
Crystal size (mm)	0.67 × 0.45 × 0.42	0.50 × 0.26 × 0.25
Data collection		
Diffractometer	Brucker SMART APEX CCD area detector	Brucker SMART APEX CCD area detector
Data collection method	ω scans	ω scans
Absorption correction	Multi scan	Multi-scan (based on symmetry-related measurements)
T_{min}	0.041	0.804
T_{max}	0.069	1.000
No. of measured, independent and observed reflections	18933, 4693, 4138	14300, 5762, 5762
Criterion for observed reflections	$I > 2\sigma(I)$	$I > 2\sigma(I)$
R_{int}	0.034	0.031
θ_{max} (°)	29.6	30.6
Refinement		
Refinement on	F^2	F^2
$R[F^2 > 2\sigma(F^2)]$, $wR(F^2)$, S	0.033, 0.075, 1.16	0.023, 0.054, 1.09

No. of relections	4693 reflections	5762 reflections
No. of parameters	192	479
H-atom treatment	Riding	Riding
Weighting scheme	Calculated $w = 1/[\sigma^2(F_o^2) + (0.0299P)^2 + 3.093P]$ where $P = (F_o^2 + 2F_c^2)/3$	Calculated $w = 1/[\sigma^2(F_o^2) + (0.0314P)^2]$ where $P = (F_o^2 + 2F_c^2)/3$
$(\Delta/\sigma)_{max}$	<0.0001	0.013
$\Delta\rho_{max}$, $\Delta\rho_{min}$ (e Å^{-3})	2.23, –0.83	1.97, –1.29

40-D

Crystal data	
Chemical formula	$C_{38}H_{58}N_4O_4U.C_{12}H_{12}$
M_r	1029.13
Cell setting, space group	Triclinic, *P*-1
Temperature (K)	150 (2)
a, *b*, *c* (Å)	10.1261 (7), 10.4437 (7), 11.7599 (8)
α, β, γ (°)	93.023 (3), 92.881 (4), 101.057 (3)
V (Å^3)	1216.56 (14)
Z	1
D_x (Mg m^{-3})	1.405
Radiation type	Mo *K*α
μ (mm^{-1})	3.38
Crystal form, colour	Irregular, colourless
Crystal size (mm)	0.41 × 0.38 × 0.29
Data collection	
Diffractometer	Bruker SMART APEX CCD area detector
Data collection method	phi and ω scans
Absorption correction	Multi-scan (based on symmetry-related measurements)
T_{min}	0.779
T_{max}	1.000
No. of measured, independent and observed reflections	17211, 6730, 6725
Criterion for observed reflections	$I > 2\sigma(I)$
R_{int}	0.032

θ_{max} (°)	30.5
Refinement	
Refinement on	F^2
$R[F^2 > 2\sigma(F^2)]$, $wR(F^2)$, S	0.025, 0.061, 1.07
No. of relections	6730 reflections
No. of parameters	274
H-atom treatment	Riding
Weighting scheme	Calculated $w = 1/[\sigma^2(F_o^2) + (0.0346P)^2]$ where $P = (F_o^2 + 2F_c^2)/3$
$(\Delta/\sigma)_{max}$	<0.0001
$\Delta\rho_{max}$, $\Delta\rho_{min}$ (e Å^{-3})	1.88, –0.99

5.6 References

[1] W. J. Evans, D. B. Rego, J. W. Ziller, *Inorg. Chem.* **2006**, *45*, 3437.
[2] H. Burger, W. Sawodny, U. Wannagat, *J. Organomet. Chem.* **1965**, *3*, 113.
[3] M. Westerhausen, *Inorg. Chem.*, **1991**, *30*, 96.
[4] D. C. Bradley, J. S. Ghotra, F. A. Hart, *J. Chem. Soc., Dalton Trans.* **1973**, 1021.
[5] L. R. Avens, S. G. Bott, D. L. Clark, A. P. Sattelberger, J. G. Watkin, B. D. Zwick, *Inorg. Chem.* **1994**, *33*, 2248.
[6] R. A. Anderson, *Inorg. Chem.* **1979**, *18*, 209.
[7] P. L. Arnold, M. Rodden, K. M. Davis, A. C. Scarisbrick, A. J. Blake, C. Wilson, *Chem. Commun.* **2004**, 1612.
[8] P. L. Arnold, M. Rodden, C. Wilson, *Chem. Commun.* **2005**, 1743.
[9] K. Izod, S. T. Liddle, W. Clegg, *Inorg. Chem.* **2004**, *43*, 214.
[10] L. Lochmann, J. Trekoval, *J. Organomet. Chem.* **1987**, *326*, 1.
[11] A. Paczal, A. C. Benyei, A. Kotschy, *J. Org. Chem.* **2006**, *71*, 5969.
[12] X.-F. Zhao, C. Zhang, *Synthesis* **2007**, *4*, 551.
[13] R. R. Schrock, L. G. Sturgeoff, P. R. Sharp, *Inorg. Chem.*, **1983**, *22*, 2801.
[14] C. B. de Koning, R. D. Hancock, W. A. L. van Otterlo, *Tetrahedron Lett.* **1997**, *38*, 1261.
[15] H. Clavier, L. Coutable, L. Toupet, J. C. Guillemin, M. Mauduit, *J. Organomet. Chem.* **2005**, *690*, 5237.